OPTIMISATION AND IMPLEMENTATION OF FUZZY CONTROLLERS FOR POWER SYSTEM STABILISATION

by

Ms Juan Shi, B.E.

A thesis submitted for the degree of

Doctor of Philosophy

in the

Department of Electrical and Electronic Engineering

Faculty of Engineering

Victoria University of Technology

P.O.Box 14428, MMC, Melbourne

Victoria 3000, Australia

May, 1994

To my family

Contents

Contents i

List of Figures ix

List of Tables xxiii

List of Principal Symbols and Abbreviations xxvi

Abstract xxxiv

Statement of Originality xxxvii

Preface xxxviii

Acknowledgements xl

1 Introduction 1

1.1 Excitation Control and Its Role on Power System Stability 1

1.2 The Definition of Power System Stability 4

1.3 The Application of Power System Stabilisers (PSSs) 5

1.4 Conventional Power System Stabilisers (CPSSs) 7

1.5 Adaptive Power System Stabilisers 8

1.6 Fuzzy Logic and Fuzzy Control 10

1.7 The Application of Fuzzy Controllers as PSSs 13

1.8 Motivation for the Thesis 14

1.9 Contributions of the Thesis 16

1.10 Organisation of the Thesis 17

2 Experimental Systems Used in the Power Laboratory **20**

2.1 Introduction 20

2.2 Single-machine Infinite Bus Power System 20

2.3 Two-machine Infinite Bus Power System 23

3 Excitation Control System Design **26**

3.1 Introduction 26

3.2 Mathematical Modelling of the Experimental System 27

3.3 Discrete-time Analytical Design Method 31

3.4 Digital Automatic Voltage Regulator (AVR) Design 34

3.5 Experimental Test Results 37

3.6 Concluding Remarks 39

4 Proposed Design of Two Fuzzy Control Schemes **45**

4.1 Introduction 45

4.2 Introduction to Fuzzy Logic Controller (FLC) 45

4.2.1 Structure of the FLC 45

4.2.2 Data Base 48

4.2.3 Rule Base 51

4.2.4 Defuzzification Strategies 53

4.2.5 Design Parameters of the FLC 55

4.3 Design of a FLC as a PSS 55

4.4 Design of the Proposed Fuzzy Logic Based PSS (FLBPSS) 64

4.5 Concluding Remarks 69

5 Optimisation of the Fuzzy Control Strategy **70**

5.1 Introduction 70

5.2 Optimisation of the FLC by Observation of Model Behaviour 71

5.2.1 Optimisation of the FLC using Whole Overlap Ratio (WOR) . 71

5.2.2 Sensitivity to Nominal Parameter Variations and Robustness to Operating Condition Variations 75

5.3 Optimal Setting of the FLBPSS Parameters and Sensitivity Analysis 80

5.3.1 Optimal Setting of the FLBPSS Parameters 80

5.3.2 Robustness to Operating Condition Variations and Sensitivity to Nominal Parameter Variations 93

5.4 Comparison of the Proposed FLBPSS and Hassan's Self-tuned FLBPSS 96

5.4.1 Review of Hassan's Self-tuned FLBPSS (STFLBPSS) 96

5.4.2 Optimal Setting of the STFLBPSS Parameters 98

5.4.3 Comparison of the Performance Index 98

5.4.4 Comparison of the Dynamic Response 99

5.5 Comparison Study of the Two Fuzzy Control Schemes 101

5.5.1 Comparison of the Performance Index 101

5.5.2 Comparison of the Dynamic Response 102

5.6 Concluding Remarks 102

6 Implementation Study **112**

6.1 Introduction 112

6.2 Hardware Development 113

6.2.1 Sensor 113

6.2.2 A/D and D/A Adapter 114

6.2.3 Field Drive Unit 114

6.2.4 Rotor Position Measurement by Using an Optical Shaft Encoder 114

6.3 Software Development 115

6.3.1 The **Main** Program 115

6.3.2 The Driver Routines 116

6.3.3 The Interrupt Set up and Handling Routines 116

6.3.4 The FLBPSS Routine 116

6.3.5 The AVR Routine 117

6.3.6 Screen Graphics 117

6.3.7 Other Features 117

6.3.8 The Block Diagram of the Software 117

6.4 Implementation Tests 117

6.4.1 Step Change in the Reference Voltage 119

6.4.2 Sudden Load Change 119

6.4.3 Three-phase to Ground Fault 121

6.5 Concluding Remarks 127

7 Application of the FLBPSS to Multi-machine Systems 131

7.1 Introduction 131

7.2 AVR Design 133

7.2.1 Design of the AVR for Generator 1 133

7.2.2 Design of the AVR for Generator 2 133

7.2.3 Practical Evaluation of the Designed AVRs 135

7.3 The Design and Optimisation of the FLBPSS 136

7.4 Simulation Results for the FLBPSS 136

7.5 Implementation and Test Results for the FLBPSS 137

7.5.1 Step Change in the Reference Voltage at Generator 1 Side . . 137

7.5.2 Rated Load Change 137

7.5.3 Test Results Under Different Operating Conditions 148

7.5.4 Three-phase to Ground Fault 148

7.5.5 Transmission Line Loss Between Generators 1 and 2 157

7.6 Concluding Remarks 159

8 Rules Reduction for the FLC Using Neural Networks **161**

8.1 Introduction 161

8.2 Rules Reduction for the FLC Using Neural Networks 163

8.3 Comparison Study 166

8.4 Concluding Remarks 170

9 Conclusions **171**

9.1 A Retrospective Overview of the Thesis 171

9.2 Avenues to be Explored in Further Work 178

A Mathematical Model of the Synchronous Machine **181**

A.1 Mathematical Model of the Synchronous Machine 181

A.1.1 Flux Linkage Equations 182

A.1.2 Voltage Equations 184

A.1.3 Torque and Power Equations 185

A.1.4 Swing Equation 186

A.1.5 Load Equation 186

A.1.6 Formulation of State-Space Equations 187

A.1.7 Current Model 188

A.2 Linearisation of the Non-linear Power System Model 191

A.2.1 Linearisation of the Generator State-Space Current Model . . 191

A.2.2 Linearisation of the Load Equation for the Single-machine Infinite Bus Power System 192

A.3 Simplified Linear Model 194

B Introduction to Fuzzy Set Theory **201**

B.1 Fuzzy Sets and Terminology 201

B.2 Fuzzy Set Theoretical Operations 203

B.3 Linguistic Variables and Linguistic Hedges 206

B.4 Fuzzy Inference and Composition 208

B.5 Fuzzy Logic and Approximate Reasoning 212

C The Whole Overlap Ratio (WOR) **214**

C.1 The WOR for Linear Membership Functions 214

C.2 The WOR for Quadratic Membership Functions 216

C.3 The WOR for Gaussian Membership Functions 219

D Mathematical Model for Multi-machine Power System **222**

D.1 Statement of the Problem 222

D.2 Conversion to a Common Reference Frame 224

D.3 Conversion of Machine Coordinates to System Reference 226

D.4 Linearised Model for the Network 228

D.5 Generator Equations 231

E The Input FPL File and the Generated Rule Base **232**

E.1 The Input FPL File 232

E.2 The Generated Rule Base 235

F Bibliography **241**

G Turbo Pascal Source Code For Single-Machine Infinite Bus Power System **258**

List of Figures

2.1 The overall view of the single-machine infinite bus experimental power system 22

2.2 Experimental circuit configuration of single-machine infinite bus power system 23

2.3 The overall view of the two-machine infinite bus experimental power system 24

2.4 Two-machine infinite bus power system 25

3.1 Block diagram of the simplified linear model. 29

3.2 The voltage regulator loop 30

3.3 Unit step response of the voltage regulator loop 37

3.4 Terminal voltage corresponding to 1/2 sudden inductive load change without and with the AVR, (a)-without AVR, (b)-with the designed AVR 38

3.5 Terminal voltage corresponding to 3/4 sudden inductive load change without and with the AVR, (a)-without AVR, (b)-with the designed AVR 40

3.6 Terminal voltage corresponding to 1/2 sudden capacitive load change without and with the AVR, (a)-without AVR, (b)-with the designed AVR 40

3.7 Terminal voltage corresponding to 3/4 sudden capacitive load change without and with the AVR, (a)-without AVR, (b)-with the designed AVR 41

3.8 Terminal voltage corresponding to 1/2 sudden resistive load change without and with the AVR, (a)-without AVR, (b)-with the designed AVR 41

3.9 Terminal voltage corresponding to 3/4 sudden resistive load change without and with the AVR, (a)-without AVR, (b)-with the designed AVR 42

3.10 Control signals corresponding to 1/2 and 3/4 sudden inductive load changes with the AVR, (a)-1/2 rated inductive load change, (b)-3/4 rated inductive load change 42

3.11 Control signals corresponding to 1/2 and 3/4 sudden capacitive load changes with the AVR, (a)-1/2 rated capacitive load change, (b)-3/4 rated capacitive load change 43

3.12 Control signals corresponding to 1/2 and 3/4 sudden resistive load changes with the AVR, (a)-1/2 rated resistive load change, (b)-3/4 rated resistive load change 43

3.13 Terminal voltage and control signal corresponding to a 10% step increase in the reference voltage sustained for 7.5 seconds, (a)-terminal voltage, (b)-control signal 44

3.14 Terminal voltage and control signal corresponding to a three-phase to ground fault at A (Figure 2.2) sustained for 125 milliseconds, (a)-terminal voltage, (b)-control signal 44

4.1 Schematic diagram of a FLC 46

4.2 Inappropriate universe of discourse 57

4.3 Inappropriate output universe of discourse 58

4.4 Disproportionately large output membership function 59

4.5 Membership functions for both condition parts and consequent parts 60

4.6 Two sectors in the phase plane 65

4.7 The proposed non-linear membership functions 67

4.8 Gain factor related to distance $D(k)$ 68

5.1 Membership functions after tuning 72

5.2 Performance index corresponding to α changes $J = f(\alpha)$ with different D_r values under the nominal operating condition for a 20% step change in mechanical torque ($\beta = -35$) 81

5.3 Performance index corresponding to α changes $J = f(\alpha)$ with different D_r values under the nominal operating condition for a 20% step change in mechanical torque ($\beta = -38$) 81

5.4 Performance index corresponding to α changes $J = f(\alpha)$ with different D_r values under the nominal operating condition for a 20% step change in mechanical torque ($\beta = -40$) 82

5.5 Performance index corresponding to α changes $J = f(\alpha)$ with different D_r values under the nominal operating condition for a 20% step change in mechanical torque ($\beta = -42$) 82

5.6 Performance index corresponding to α changes $J = f(\alpha)$ with different D_r values under the nominal operating condition in response to a three-phase to ground fault ($\beta = -35$) 83

5.7 Performance index corresponding to α changes $J = f(\alpha)$ with different D_r values under the nominal operating condition in response to a three-phase to ground fault ($\beta = -38$) 83

5.8 Performance index corresponding to α changes $J = f(\alpha)$ with different D_r values under the nominal operating condition in response to a three-phase to ground fault ($\beta = -40$) 84

5.9 Performance index corresponding to α changes $J = f(\alpha)$ with different D_r values under the nominal operating condition in response to a three-phase to ground fault ($\beta = -42$) 84

5.10 Performance index corresponding to α changes $J = f(\alpha)$ with different D_r values and +20% variation in inertia constant H for a 20% step change in mechanical torque ($H = 1.2s, \beta = -35$) 85

5.11 Performance index corresponding to α changes $J = f(\alpha)$ with different D_r values and +20% variation in inertia constant H for a 20% step change in mechanical torque ($H = 1.2s, \beta = -38$) 86

5.12 Performance index corresponding to α changes $J = f(\alpha)$ with different D_r values and +20% variation in inertia constant H for a 20% step change in mechanical torque ($H = 1.2s, \beta = -40$) 86

5.13 Performance index corresponding to α changes $J = f(\alpha)$ with different D_r values and +20% variation in inertia constant H for a 20% step change in mechanical torque ($H = 1.2s, \beta = -42$) 87

5.14 Performance index corresponding to α changes $J = f(\alpha)$ with different D_r values and -20% variation in inertia constant H for a 20% step change in mechanical torque ($H = 0.8s, \beta = -35$) 87

5.15 Performance index corresponding to α changes $J = f(\alpha)$ with different D_r values and -20% variation in inertia constant H for a 20% step change in mechanical torque ($H = 0.8s, \beta = -38$) 88

5.16 Performance index corresponding to α changes $J = f(\alpha)$ with different D_r values and -20% variation in inertia constant H for a 20% step change in mechanical torque ($H = 0.8s, \beta = -40$) 88

5.17 Performance index corresponding to α changes $J = f(\alpha)$ with different D_r values and -20% variation in inertia constant H for a 20% step change in mechanical torque ($H = 0.8s, \beta = -42$) 89

5.18 Minimum performance index corresponding to changes in β values $J_{min} = f(\beta)$ (20 % step increase in mechanical torque) 89

5.19 Minimum performance index corresponding to changes in β values $J_{min} = f(\beta)$ (three-phase to ground fault) 90

5.20 System response corresponding to a 20% step change in T_m under two optimal settings 91

5.21 System response corresponding to a 20% step change in T_m and a three-phase to ground fault, (a)-20% step increase in mechanical torque, (b)-three-phase to ground fault 92

5.22 Performance index corresponding to changes in α $J = f(\alpha)$ with different D_r values in response to a 20% step increase in T_m under operating condition P1 ($\beta = -40$) 93

5.23 Performance index corresponding to changes in α $J = f(\alpha)$ with different D_r values in response to a three-phase fault under operating condition P1 ($\beta = -40$) 94

5.24 Performance index corresponding to changes in α $J = f(\alpha)$ with different D_r values in response to a 20% step increase in T_m under operating condition P4 ($\beta = -40$) 94

5.25 Performance index corresponding to changes in α $J = f(\alpha)$ with different D_r values in response to a three-phase fault under operating condition P4 ($\beta = -40$) 95

5.26 System responses at operating condition P4 with the corresponding optimal settings (COS) and the nominal optimal settings (NOS), (a)-20% step increase in mechanical torque, (b)-three-phase to ground fault 105

5.27 System responses at P0 with inertia constant parameter variation $H = 1.2s$ with the corresponding optimal settings (COS) and the nominal optimal settings (NOS), (a)-20% step increase in mechanical torque, (b)-three-phase to ground fault 105

5.28 System response corresponding to three-phase to ground fault under different operating conditions with the nominal optimal settings (NOS), (a)-operating conditions P0, P1, P2 and P4, (b)-operating condition P3 106

5.29 System response corresponding to a 20% step increase in mechanical torque with the nominal optimal settings (NOS) for different system parameter changes, (a)-±20% variation in H, (b)-±20% variation in τ'_{d0} 106

5.30 Membership functions used for the STFLBPSS 107

5.31 System response corresponding to a 20% step change in mechanical torque and a three-phase fault under the nominal operating condition, (a)-20% step increase in mechanical torque, (b)-three-phase fault . . 107

5.32 System response corresponding to a 20% step change in mechanical torque under different operating conditions, (a)-(d) provide the speed deviation responses under operating conditions P1-P4 respectively . . 108

5.33 System response corresponding to a three-phase to ground fault under different operating conditions, (a)-(d) provide the speed deviation responses under operating conditions P1-P4 respectively 108

5.34 System response corresponding to a 20% step change in mechanical torque with ±20% variation in inertia constant H, (a)-$H = 1.2s$, (b)-$H = 1s$, (c)-$H = 0.8s$ 109

5.35 System response corresponding to a 20% step change in mechanical torque with ±20% variation in τ'_{d0}, (a)-$\tau'_{d0} = 0.414s$, (b)-$\tau'_{d0} = 0.345s$, (c)-$\tau'_{d0} = 0.276s$ 109

5.36 System response corresponding to a 20% step change in mechanical torque with ±20% variation in X_e, (a)-$X_e = 0.48pu$, (b)-$X_e = 0.4pu$, (c)-$X_e = 0.32pu$ 110

5.37 System response corresponding to a 20% step change in mechanical torque and reference voltage change (without PSS) 110

5.38 System response corresponding to a 20% step change in mechanical torque and reference voltage change (with the FLC) 111

5.39 System response corresponding to a 20% step change in mechanical torque and reference voltage change (with the FLBPSS) 111

6.1 Sensor circuit of rectifier, potential divider and filter circuit 113

6.2 Software diagram (Part I) 118

6.3 Software diagram (Part II) 118

6.4 Rotor angle and speed deviation corresponding to a 10% step increase in the reference voltage sustained for 7.5 seconds (without the FLBPSS), (a)-rotor angle, (b)-speed deviation 120

6.5 Rotor angle and speed deviation corresponding to a 10% step increase in the reference voltage sustained for 7.5 seconds (with the FLBPSS), (a)-rotor angle, (b)-speed deviation 121

6.6 Control signal corresponding to a 10% step increase in the reference voltage sustained for 7.5 seconds, (a)-without the FLBPSS and (b)-with the FLBPSS 122

6.7 Rotor angle and speed deviation corresponding to sudden resistive load change without the FLBPSS (operating condition OC1), (a)-rotor angle, (b)-speed deviation 123

6.8 Rotor angle and speed deviation corresponding to sudden resistive load change with the FLBPSS (operating condition OC1), (a)-rotor angle, (b)-speed deviation 123

6.9 Rotor angle and speed deviation corresponding to sudden inductive load change without the FLBPSS (operating condition OC1), (a)-rotor angle, (b)-speed deviation 124

6.10 Rotor angle and speed deviation corresponding to sudden inductive load change with the FLBPSS (operating condition OC1), (a)-rotor angle, (b)-speed deviation 124

6.11 Rotor angle and speed deviation corresponding to sudden capacitive load change without the FLBPSS (operating condition OC1), (a)-rotor angle, (b)-speed deviation 125

6.12 Rotor angle and speed deviation corresponding to sudden capacitive load change with the FLBPSS (operating condition OC1), (a)-rotor angle, (b)-speed deviation 125

6.13 Rotor angle and speed deviation corresponding to sudden resistive load change without the FLBPSS (operating condition OC2), (a)-rotor angle, (b)-speed deviation 126

6.14 Rotor angle and speed deviation corresponding to sudden resistive load change with the FLBPSS (operating condition OC2), (a)-rotor angle, (b)-speed deviation 126

6.15 Rotor angle and speed deviation corresponding to sudden resistive load change without the FLBPSS (operating condition OC3), (a)-rotor angle, (b)-speed deviation 128

6.16 Rotor angle and speed deviation corresponding to sudden resistive load change with the FLBPSS (operating condition OC3), (a)-rotor angle, (b)-speed deviation 128

6.17 Rotor angle and speed deviation corresponding to sudden resistive load change without the FLBPSS (operating condition OC4), (a)-rotor angle, (b)-speed deviation 129

6.18 Rotor angle and speed deviation corresponding to sudden resistive load change with the FLBPSS (operating condition OC4), (a)-rotor angle, (b)-speed deviation 129

6.19 Rotor angle and speed deviation corresponding to a three-phase fault at A (Figure 2.2) sustained for 125 milliseconds (without the FLBPSS), (a)-rotor angle, (b)-speed deviation 130

6.20 Rotor angle and speed deviation corresponding to a three-phase fault at A (Figure 2.2) sustained for 125 milliseconds (with the FLBPSS), (a)-rotor angle, (b)-speed deviation 130

7.1 Terminal voltage corresponding to a 10% step change in reference voltage at generator 1 side, (a)-terminal voltage for generator 1, (b)-terminal voltage for generator 2 139

7.2 Terminal voltage corresponding to 3/4 rated inductive load change, (a)-terminal voltage for generator 1, (b)-terminal voltage for generator 2 139

7.3 Terminal voltage corresponding to 3/4 rated capacitive load change, (a)-terminal voltage for generator 1, (b)-terminal voltage for generator 2 140

7.4 Terminal voltage corresponding to 3/4 rated resistive load change, (a)-terminal voltage for generator 1, (b)-terminal voltage for generator 2 140

7.5 Terminal voltage corresponding to a three-phase to ground fault, (a)-terminal voltage for generator 1, (b)-terminal voltage for generator 2 141

7.6 Excitation control signal corresponding to a three-phase to ground fault, (a)-control signal for generator 1, (b)-control signal for generator 2 141

7.7 System response corresponding to a 10% step change in reference voltage and mechanical torque without PSS, (a)-speed deviation for generator 1, (b)-speed deviation for generator 2 142

7.8 System response corresponding to a 10% step change in reference voltage and mechanical torque with the FLBPSS, (a)-speed deviation for generator 1, (b)-speed deviation for generator 2 142

7.9 System response corresponding to a 20% step change in reference voltage and mechanical torque without the FLBPSS, (a)-speed deviation for generator 1, (b)-speed deviation for generator 2 143

7.10 System response corresponding to a 20% step change in reference voltage and mechanical torque with the FLBPSS, (a)-speed deviation for generator 1, (b)-speed deviation for generator 2 143

7.11 Rotor angle and speed deviation for generator 1 corresponding to a 10% step increase in the reference voltage at generator 1 sustained for 7.5 seconds (without the FLBPSS), (a)-rotor angle, (b)-speed deviation 144

7.12 Rotor angle and speed deviation for generator 1 corresponding to a 10% step increase in the reference voltage at generator 1 sustained for 7.5 seconds (with the FLBPSS), (a)-rotor angle, (b)-speed deviation 144

7.13 Rotor angle and speed deviation for generator 2 corresponding to a 10% step increase in the reference voltage at generator 1 sustained for 7.5 seconds (without the FLBPSS), (a)-rotor angle, (b)-speed deviation 145

7.14 Rotor angle and speed deviation for generator 2 corresponding to a 10% step increase in the reference voltage at generator 1 sustained for 7.5 seconds (with the FLBPSS), (a)-rotor angle, (b)-speed deviation 145

7.15 Rotor angle and speed deviation for generator 1 corresponding to sudden resistive load change (without the FLBPSS), (a)-rotor angle, (b)-speed deviation 146

7.16 Rotor angle and speed deviation for generator 1 corresponding to 3/4 rated sudden resistive load change (with the FLBPSS), (a)-rotor angle, (b)-speed deviation 146

7.17 Rotor angle and speed deviation for generator 2 corresponding to 3/4 rated sudden resistive load change (without the FLBPSS), (a)-rotor angle, (b)-speed deviation 147

7.18 Rotor angle and speed deviation for generator 2 corresponding to 3/4 rated sudden resistive load change (with the FLBPSS), (a)-rotor angle, (b)-speed deviation 147

7.19 Rotor angle and speed deviation for generator 1 corresponding to 3/4 rated sudden inductive load change (without the FLBPSS), (a)-rotor angle, (b)-speed deviation 149

7.20 Rotor angle and speed deviation for generator 2 corresponding to 3/4 rated sudden inductive load change (without the FLBPSS), (a)-rotor angle, (b)-speed deviation 149

7.21 Rotor angle and speed deviation for generator 1 corresponding to 3/4 rated sudden inductive load change (with the FLBPSS), (a)-rotor angle, (b)-speed deviation 150

7.22 Rotor angle and speed deviation for generator 2 corresponding to 3/4 rated sudden inductive load change (with the FLBPSS), (a)-rotor angle, (b)-speed deviation 150

7.23 Rotor angle and speed deviation for generator 1 corresponding to 3/4 rated sudden capacitive load change (without the FLBPSS), (a)-rotor angle, (b)-speed deviation 151

7.24 Rotor angle and speed deviation for generator 2 corresponding to 3/4 rated sudden capacitive load change (without the FLBPSS), (a)-rotor angle, (b)-speed deviation 151

7.25 Rotor angle and speed deviation for generator 1 corresponding to 3/4 rated sudden capacitive load change (with the FLBPSS), (a)-rotor angle, (b)-speed deviation 152

7.26 Rotor angle and speed deviation for generator 2 corresponding to 3/4 rated sudden capacitive load change (with the FLBPSS), (a)-rotor angle, (b)-speed deviation 152

7.27 Rotor angle and speed deviation for generator 1 corresponding to 3/4 rated sudden resistive load change without the FLBPSS (Operating condition OC1), (a)-rotor angle, (b)-speed deviation 153

7.28 Rotor angle and speed deviation for generator 2 corresponding to 3/4 rated sudden resistive load change without the FLBPSS (Operating condition OC1), (a)-rotor angle, (b)-speed deviation 153

7.29 Rotor angle and speed deviation for generator 1 corresponding to 3/4 rated sudden resistive load change with the FLBPSS (Operating condition OC1), (a)-rotor angle, (b)-speed deviation 154

7.30 Rotor angle and speed deviation for generator 2 corresponding to 3/4 rated sudden resistive load change with the FLBPSS (Operating condition OC1), (a)-rotor angle, (b)-speed deviation 154

7.31 Rotor angle and speed deviation for generator 1 corresponding to a three-phase fault at B (Figure 2.4) sustained for 125 milliseconds (without the FLBPSS), (a)-rotor angle, (b)-speed deviation 155

7.32 Rotor angle and speed deviation for generator 1 corresponding to a three-phase fault at B (Figure 2.4) sustained for 125 milliseconds (with the FLBPSS), (a)-rotor angle, (b)-speed deviation 155

7.33 Rotor angle and speed deviation for generator 2 corresponding to a three-phase fault at B (Figure 2.4) sustained for 125 milliseconds (without the FLBPSS), (a)-rotor angle, (b)-speed deviation 156

7.34 Rotor angle and speed deviation for generator 2 corresponding to a three-phase fault at B (Figure 2.4) sustained for 125 milliseconds (with the FLBPSS), (a)-rotor angle, (b)-speed deviation 156

7.35 Rotor angle and speed deviation for generator 1 corresponding to the loss of the transmission line (without the FLBPSS), (a)-rotor angle, (b)-speed deviation 157

7.36 Rotor angle and speed deviation for generator 2 corresponding to the loss of the transmission line (without the FLBPSS), (a)-rotor angle, (b)-speed deviation 158

7.37 Rotor angle and speed deviation for generator 1 corresponding to the loss of the transmission line (with the FLBPSS), (a)-rotor angle, (b)-speed deviation 158

7.38 Rotor angle and speed deviation for generator 2 corresponding to the loss of the transmission line (with the FLBPSS), (a)-rotor angle, (b)-speed deviation 159

8.1 Speed deviation and rotor angle corresponding to a 10% step increase in mechanical torque followed by a 10% step increase in the reference voltage sustained for 7.5 seconds with the original 49-rule FLC . . . 168

8.2 Speed deviation and rotor angle corresponding to a 10% step increase in mechanical torque followed by a 10% step increase in the reference voltage sustained for 7.5 seconds with the 24-rule FLC 168

8.3 Speed deviation and rotor angle corresponding to a 20% step increase in mechanical torque followed by a 20% step increase in the reference voltage sustained for 7.5 seconds with the original 49-rule FLC . . . 169

8.4 Speed deviation and rotor angle corresponding to a 20% step increase in mechanical torque followed by a 20% step increase in the reference voltage sustained for 7.5 seconds with the 24-rule FLC 169

C.1 Two adjacent linear membership functions 215

C.2 Two adjacent quadratic membership functions 217

C.3 Two adjacent exponential membership functions 219

D.1 Two frames of reference for phasor quantities for a voltage V_i 224

List of Tables

2.1 Ratings of the single-machine infinite bus power system 21

2.2 Generator parameters 21

2.3 Ratings of the two-machine infinite bus power system 23

2.4 Generator parameters 23

4.1 The decision table 62

4.2 Comparison of the defuzzification methods 64

5.1 Some usual membership functions and WOR evaluation formulas . . 73

5.2 The performance index corresponding to changes in WOR (10% step change in T_m and V_{ref}) 73

5.3 The performance index corresponding to changes in WOR (20% step change in T_m and V_{ref}) 74

5.4 The performance index corresponding to changes in WOR with different defuzzification methods (20% step change in T_m) 75

5.5 The performance index corresponding to changes in WOR with different defuzzification methods (three-phase to ground fault) 75

5.6 The performance index corresponding to changes in WOR (Mamdani, Centroid, 20% step increase in mechanical torque) 76

5.7 The performance index corresponding to changes in WOR (Mamdani, Means of maximum, 20% step increase in mechanical torque) 76

5.8 The performance index corresponding to changes in WOR (Larsen, Centroid, 20% step increase in mechanical torque) 77

5.9 The performance index corresponding to changes in WOR (Larsen, Means of maximum, 20% step increase in mechanical torque) 77

5.10 The performance index corresponding to changes in WOR with different implication and defuzzification methods, three-phase to ground fault 78

5.11 Operating conditions 78

5.12 Performance index corresponding to changes in WOR under different operating conditions (Mamdani, Means of maximum or centroid, 20% step increase in mechanical torque) 78

5.13 Performance index corresponding to changes in WOR under different operating conditions (Larsen, Means of maximum or centroid, 20% step increase in mechanical torque) 79

5.14 Performance index corresponding to changes in WOR under different operating conditions (Mamdani, Centroid, three-phase to ground fault) 79

5.15 Performance index corresponding to changes in WOR under different operating conditions (Mamdani, Means of maximum, three-phase to ground fault) 79

5.16 Optimal settings of the FLBPSS for different operating conditions . . 95

5.17 Comparison of the performance index (small perturbation of a 20% step change in mechanical torque T_m) 99

5.18 Comparison of the performance index (large perturbation of a three-phase fault at A of Figure (2.2) sustained for 125 milliseconds) 99

5.19 Comparison of the performance index for parameter changes (small perturbation of a 20% step change in mechanical torque T_m) 99

5.20 Comparison of the performance index for parameter changes (large perturbation of a three-phase fault at A of Figure (2.2) sustained for 125 milliseconds) 100

5.21 Comparison of the performance index (small perturbation of a 20% step change in mechanical torque T_m) 100

5.22 Comparison of the performance index (large perturbation of a three-phase fault at A of Figure (2.2) sustained for 125 milliseconds) 100

5.23 Comparison of the performance index of the FLC and the FLBPSS (small perturbation of a 20% step increase in mechanical torque) . . . 101

5.24 Comparison of the performance index of the FLC and the FLBPSS (large perturbation of a three-phase to ground fault) 102

6.1 Operating conditions for single-machine infinite bus power system . . 119

7.1 Operating conditions for two-machine infinite bus power system . . . 148

8.1 The decision table after learning 166

8.2 The performance index corresponding to changes in WOR (20% step increase in mechanical torque followed by a 10% step increase in the reference voltage sustained for 7.5 seconds) 167

8.3 The performance index corresponding to different mechanical torque changes 167

List of Principal Symbols and Abbreviations

Unless otherwise stated, the following definitions of the notation are applied throughout this thesis.

Symbol or Abbreviation	Description	Defined in Section
A	field drive unit gain	3.2
a, b, c	phase identification	App.A
A, B, C	phase identification	6.2
A, B	linear continuous time system state matrix	App.A
AC	Alternative Current	2.2, 6.1
A/D	Analog to Digital	2.2, 6.1
abs	absolute value	5.2
arg	argument	4.2
AVQ	Adaptive Vector Quantisation	8.1
AVR	Automatic Voltage Regulator	1.1, 6.1
B	voltage sensor gain	3.2
CON	Concentration	App.B
COS	Corresponding Optimal Setting	5.3
CPSS	Conventional Power System Stabiliser	1.4
D	Damping constant	App.A, 3.3
D-D'	generator damper winding	App.A
D/A	Digital to Analog	2.2, 6.1
d-axis	direct axis	App.A, App.D
$D(k), D_r$	distance parameter	4.4
DC	Direct Current	2.2, 6.1
DIL	Dilation	App.B
EMF	Electromotive Force	App.A
$E_{FD}(t)$	generator stator EMF	App.A
$E_{FD\Delta}(t)$	linearised generator stator EMF	App.A

$e(t), e(kT)$	error signal	3.3
$E_q(t)$	generator q-axis component of stator EMF	App.A
$E_d(t)$	generator d-axis component of stator EMF	App.A
$E'_q(t), e'_q(t)$	generator q-axis transient stator EMF	App.A
$E'_d(t)$	generator d-axis transient stator EMF	App.A
E'_{q0}	steady-state value of $E'_q(t)$	App.A
$E'_{q\Delta}$	linearised generator q-axis transient stator EMF	3.2
f	a set of non-linear function	App.A
F	Fuzzy set	App.B
F-F'	generator field winding	App.A
FLC	Fuzzy Logic Controller	1.7, 4.2
FLBPSS	Fuzzy Logic Based Power System Stabiliser	1.7, 4.4
FNN	Fuzzy Neural Networks	9.2
FPL	Fuzzy Programming Language	8.2, App.E
F(t)	restore force of an inverted pendulum	8.1
F(z)	desired close loop pulse transfer function	3.3
F_α	α-cut of fuzzy set F	App.B
$F_{\bar{\alpha}}$	strong α-cut of fuzzy set F	App.B
$G(k)$	gain factor	4.4
$G_s(s)$	continuous time power system stabiliser transfer function	1.4
$G(z)$	z transform of the plant $G_p(s)$	3.3
$G_{AVR}(z)$	discrete time transfer function of the AVR	3.3
H	generator inertia constant	2.2
h	maximum height of the intersection between two adjacent MFs	App.C
$height(F)$	height of a fuzzy set F	App.B
I/O	Input Output port	6.1
INT	Intensification	App.B
$i(t)$	generator current	App.A
$i_a(t), i_b(t), i_c(t)$	generator three-phase stator current	App.A
$i_F(t)$	generator field current	App.A

$i_{F\Delta}(t)$	linearised generator field current	App.A
$i_D(t), i_Q(t)$	generator damper winding current	App.A
$i_{D\Delta}(t)$	linearised generator damper winding current	App.A
$i_d(t)$	generator d-axis stator current	App.A
$i_{d\Delta}(t)$	linearised generator d-axis stator current	App.A
$I_d(t)$	generator d-axis stator current	App.A
$i_q(t)$	generator q-axis stator current	App.A
$i_{q\Delta}(t)$	linearised generator q-axis stator current	App.A
$I_q(t)$	generator q-axis stator current	App.A
$i_{Q\Delta}(t)$	linearised generator damper winding current	App.A
$I_t(t)$	generator terminal current	App.A
$\bar{I}$	complex current vector for multi-machine system	App.D
$\hat{I}$	complex current vector use common reference frame	App.D
J	performance index	5.1
J_{min}	minimum performance index	5.3
K	generator DC gain	3.2
K_A	voltage regulator gain	1.1
KB	Knowledge Base	4.2
K_0	conventional power system stabiliser DC gain	1.4
K	number of required sample period	3.4
$K_1 \sim K_6$	coefficient of single-machine infinite bus power system	3.1, App.A
L	transportation lag	3.3
L	switching line in the phase plane	4.4
L_e	transmission line inductance	App.A
L_{jk}	generator self or mutual inductance	App.A
m, m_1, m_2	parameters of two adjacent MFs	App.C
MAX, max	maximum	4.2, App.C
MIN	minimum	App.C
MF	Membership Function	4.4
MIMO	Multi-Input Multi-Output	1.6
MISO	Multi-Input Single-Output	4.3

$\bar{M}$	matrix for linearised multi-machine system	App.D
$\bar{m}_{ij}$	general term of the matrix $\bar{M}$	App.D
$N\{\theta_i(k)\}$	membership function for the FLBPSS	4.4
NB	Negative Big	4.3
NM	Negative Medium	4.3
NN	Neural Networks	8.1
NOS	Nominal Optimal Setting	5.3
NS	Negative Small	4.3
OC1 $\sim$ OC4	Operating Conditions	6.4, 7.5
P	real power	5.2, 7.5.3
PB	Positive Big	4.3
$p_i(k)$	a point in the phase plane	4.4
$P0 \sim P4$	operating conditions	5.2
$P_e(t)$	electrical power	App.A
PF	Power Factor	7.5
PM	Positive Medium	4.3
$P_m(t)$	mechanical power	App.A
PS	Positive Small	4.3
PSS	Power System Stabiliser	1.3
pu	per unit	2.2, 2.3
$P\{\theta_i(k)\}$	membership function for the FLBPSS	4.4
q-axis	quadrature axis	App.A, App.D
R, S	fuzzy relation	App.B
r	generator winding resistance	App.A
r	number of elements	4.2
R_e	transmission line resistance	2.2
R_{10}, R_{12}, R_{20}	transmission line resistance	2.3
R_B	Boolean fuzzy implication	App.B
R_G	Goguen's fuzzy implication	App.B
R_l	Larsen's product operation of fuzzy implication	App.B
R_m	Mamdani's mini operation of fuzzy implication	App.B
R_s	standard fuzzy implication	App.B

R_{Z_a}	sequence fuzzy implication	App.B
R_{Z_m}	Zadeh's max-min rule of implication	App.B
$s_1, \cdots, s_n$	linguistic variables	4.3
S_i^j	linguistic values of the linguistic variables	4.3
sup	supremum	App.B
SECV	State Electricity Commission Victoria	3.2, 9.2
SISO	Single-Input Single-Output	1.6
SMIB	Single-Machine Infinite Bus	App.G
STFLBPSS	Self-tuned Fuzzy Logic Based PSS	1.7, 5.4
$T_d(.)$	damping torque	1.1, App.A
$T_e(t)$	electrical torque	App.A
$T_m(t)$	mechanical torque	App.A
T_m	mechanical torque	5.2
$T_{m\Delta}(t)$	linearised mechanical torque	3.2, App.A
$T_a(t)$	accelerating torque	App.A
t_r	rising time	3.4
ΔT_s	synchronising component of the electrical torque	1.1
$u(kT)$	control signal	3.2, 3.3
u	driving function	App.A
u	a generic element in a universe of discourse	App.B
U	control signal	3.4, 4.2
U, V, W	universe of discourse	App.B
U_{max}	maximum stabilising signal	4.4
U_s	stabilising signal	5.6
$v(t)$	generator voltage	App.A
$v_d(t)$	generator d-axis stator voltage	App.A
$v_{d\Delta}(t)$	linearised generator d-axis stator voltage	App.A
$V_d(t)$	generator d-axis stator voltage	App.A
$v_F(t)$	generator field voltage	App.A
$v_{F\Delta}(t)$	linearised generator field voltage	App.A
$v_q(t)$	generator q-axis stator voltage	App.A
$v_{q\Delta}(t)$	linearised generator q-axis stator voltage	App.A

$V_q(t)$	generator q-axis stator voltage	App.A
$V_{ref}, V_{ref}(t)$	reference voltage	1.4, 3.2
$V_t(t)$	generator terminal voltage	3.2, App.A
$V_{t\Delta}(t)$	linearised generator terminal voltage	3.2
VS	Very Small	4.3
V_∞	infinite bus voltage	App.A
$\bar{V}$	complex voltage vector for multi-machine system	App.D
$\hat{V}$	complex voltage vector use common reference frame	App.D
WOR	Whole Overlap Ratio	1.10, 5.2
x	state variable	App.A
x_d	generator d-axis component of synchronous reactance	2.2, 2.3
x_q	generator q-axis component of synchronous reactance	2.2, 2.3
x'_d	generator d-axis transient reactance	2.2, 2.3
x'_q	generator q-axis transient reactance	2.2, 2.3
X_e	transmission line reactance	2.3
X_{10}, X_{12}, X_{20}	transmission line reactance	2.3
$x(t), \theta(t)$	linear and angular position of an inverted pendulum	8.1
$\bar{Y}$	short circuit state admittance matrix	App.D
$\bar{Z}$	open circuit state impedance matrix	App.D
ZR	Zero	4.3
α	infinite bus voltage angle	App.A
α	threshold level which forms a parameter varying as [0,1]	4.2
α, β	parameters in the phase plane for FLBPSS	4.4
τ	voltage sensor time constant	3.2
$\tau_0 \sim \tau_4$	time constant of conventional PSS	1.4
τ'_{d0}	d-axis open circuit transient time constant	2.2, 3.2
τ_A	conventional analog AVR time constant	1.1
ω	angular velocity	1.1
ω_R	rated synchronous generator speed	3.2
ω_{syn}	synchronous speed	2.2
$\omega(t)$	generator speed	App.A

$\omega_\Delta(t)$	linearised generator speed	App.A
δ	distance parameter between two adjacent MFs	App.C
$\delta(t)$	generator rotor angle	App.A
$\delta_\Delta(t)$	linearised generator rotor angle	App.A
ΔT	sampling interval	4.3
$\Delta\omega$	speed deviation	4.3
$\Delta\dot{\omega}$	acceleration	4.3
δ_{ij}	rotor angle between machine i and j	App.D
$\delta_{ij\Delta}$	linearised value of δ_{ij}	App.D
$\lambda(t)$	flux linkage of the synchronous generator	App.A
$\lambda_d(t)$	generator d-axis stator flux linkage	App.A
$\lambda_D(t)$	generator d-axis damper winding flux linkage	App.A
$\lambda_F(t)$	generator field winding flux linkage	App.A
$\lambda_q(t)$	generator q-axis stator flux linkage	App.A
$\lambda_Q(t)$	generator q-axis damper winding flux linkage	App.A
θ	rotor position	App.A
$\theta_i(k)$	phase angle in the phase plane	4.4
θ_0	initial angle	4.4
μ	fuzzy membership function	App.B
$\mu_F(u)$	membership function of a fuzzy set F	App.B
μ_A, μ_B	membership function for two fuzzy sets A and B	App.B
$\bigcup$	union	App.B
$\bigcap$	intersection	App.B
$\bullet$	algebraic product	App.B
$\odot$	bounded product	App.B
$\dot{\cap}$	drastic product	App.B
$*$	triangular norm	App.B
$\dot{+}$	triangular co-norm	App.B
$\hat{+}$	algebraic sum	App.B
$\oplus$	bounded sum	App.B
$\uplus$	drastic sum	App.B
Δ	disjoint sum	App.B

$\vee$	max	App.B
$\wedge$	min	App.B
$\sum$	summation	5.1, App.D

Abstract

This thesis investigated the application of fuzzy controllers as real-time power system stabilisers for single-machine and two-machine infinite bus power systems.

The advantages of using **the-state-of-the-art** power system stabilisers to damp low-frequency oscillation in power systems is well known. The most widely used conventional power system stabiliser is the lead-lag compensator where the gain settings are fixed at certain values and determined for a particular operating condition. The design of the conventional power system stabiliser is based on a linear approximation of the non-linear power plant. This means that the conventional power system stabiliser can provide the optimal performance only for that particular operating point. Since the operating point of a power system drifts as a result of continuous load changes or unpredictable major disturbances such as a three-phase fault, the fixed gain conventional power system stabiliser can not adapt the stabiliser parameters in real time based on on-line measurements. Although general parameters can be decided for a conventional power system stabiliser according to a particular range of operating conditions, the design procedure is very complex. For multi-machine systems, individual machine may have different requirements of damping torque and synchronising torque, and multi-machine multi-mode power system stabilisation techniques must be sought, especially when many conventional power system stabilisers are used in the system and their coordination has to be taken into consideration. These constraints made the design of the conventional power system stabiliser even more complex.

Self-tuning and adaptive power system stabilisers have been employed to adapt the stabiliser parameters to maintain good dynamic performance over a wide range of operating conditions. However, self-tuning and adaptive power system stabilisers suffer from a major drawback of requiring model identification in real-time which is very time consuming and computational intensive. Therefore, self-tuning and adaptive power system stabilisers are difficult to realise because they require parameter identification, state observation and feedback gain computation.

This thesis is mainly concerned with new simpler alternative fuzzy control schemes for power system stabilisation. Two fuzzy control schemes are proposed and explored in the thesis. One of the fuzzy control schemes involves a **fuzzy logic controller (FLC)** being applied to a power system as a power system stabiliser. The core of the FLC is a set of linguistic control rules related by the dual concepts of fuzzy implication and the compositional rule of inference. In essence, the FLC provides an algorithm which can convert the linguistic control strategy based on expert knowledge into an automatic control strategy. The second fuzzy control scheme involves the development of a **Fuzzy Logic Based Power System Stabiliser (FLBPSS)** based on fuzzy set theory. The stabilising signal is computed according to the proposed new non-linear fuzzy membership functions depending on the speed and acceleration states of the synchronous generator. These fuzzy control schemes are very suitable for on-line control due to their lower computational burden, simplicity and robustness. The design frame work of these control schemes does not necessitate the use of a mathematical model to describe the dynamics of the control system. Comprehensive sensitivity analysis has been carried out to assess the robustness of the FLC and FLBPSS for changes in system parameters and under different operating conditions for both small and large perturbations. The input and output membership functions of the FLC were adjusted according to an evaluation index in order to achieve the optimal performance. The initial FLC design with a complete filled rule table (49 rules) have been reduced using neural network techniques to improve the dynamic performance. Optimisation of the two fuzzy control schemes is carried out through digital simulation using a performance index.

In order to carry out an investigation into the design, optimisation and implementation of the two fuzzy control schemes, it is essential to design a digital **automatic voltage regulator (AVR)**. A discrete-time analytical design method is employed. The effectiveness of the designed automatic voltage regulator is demonstrated through simulation and implementation.

The optimised fuzzy controller has also been implemented in real-time for online control of both single-machine and two-machine infinite bus power systems. The effectiveness of the fuzzy controller was experimentally confirmed by observing the effects of a step change in reference voltage, a step change in load and a three-phase to ground fault. Numbers of tests have also been conducted at various operating conditions. A very oscillatory generator rotor angle and speed deviation were observed without any stabilisation control when the system is subjected to the above disturbances. The oscillation of rotor angle and speed deviation were substantially damped out with the fuzzy controller in operation. The simulation and experimental results reveal that the optimised fuzzy controller has enhanced the damping of both the dynamic and transient stability of the single-machine and two-machine infinite bus power systems.

Statement of Originality

I hereby certify that the work embodied in this thesis is the result of original research and has not been submitted for a higher degree to any other University or Institution.

This thesis may be made available for consultation within the University Library and may be photocopied or lent to other libraries for the purposes of consultation if accepted for the award of the degree.

(Signed) ---- Juan Shi ----------------

Juan Shi

Preface

This thesis examines the optimisation and implementation of fuzzy controllers for power system stabilisation. An optimal fuzzy controller has been used on-line in real time for both single-machine and two-machine infinite bus power systems. A digital automatic voltage regulator has also been designed. A listing of all the relevant publications [Shi, Herron and Kalam, 1992; Shi, Herron and Kalam, 1993 and Shi, Herron and Kalam, 1994] is provided here:

1. J.Shi, L.H.Herron, A.Kalam," Design and Implementation of a Fuzzy Logic Based Power System Stabilizer "AMSE periodicals: ADVANCES IN MODELLING and ANALYSIS, C. AMSE Press, Vol. 42, NO.4, 1994, pp. 39-52.

2. J.Shi, L.H.Herron, A.Kalam, "Optimization of Fuzzy Controllers as Real-time Power System Stabilizers ", Accepted for publication in the special issue on "Control Applications of Fuzzy Logic" of the International Journal for Engineering Applications of Artificial Intelligence, Pergamon Press, 1994.

3. J.Shi, L.H.Herron, A.Kalam, "Comparison of Fuzzy Logic Based and Rule Based Power System Stabilizer", The first IEEE Conference on Control Applications, September 13-16, 1992, Stouffer Center Plaza Hotel, Dayton, Ohio, USA, pp. 692-697.

4. J.Shi, L.H.Herron, A.Kalam, "Application of Fuzzy Logic Based Power System Stabilizer for a Synchronous Machine", Australasia Universities Power and Control Engineering Conference, 1-2 October, 1992, Brisbane, Australia, pp. 285-290.

5. J.Shi, L.H.Herron, A.Kalam, "A Fuzzy Logic Controller Applied to Power System Stabilizer for a synchronous Machine Power System", IEEE Region 10 Conference, TENCON'92, 11th-13th November, 1992, Melbourne, Australia, pp. 346-350.

6. J.Shi, L.H.Herron, A.Kalam, "Application of Fuzzy Logic Controller for

Power System Stabilization", IEEE Region 10 Conference, TENCON'93, 18-22 October, 1993, Beijing , China, Vol.5, pp. 200-204.

7. J.Shi, L.H.Herron, A.Kalam, "Simulation Study and Application of A Fuzzy Logic Controller for Power System Stabilization", The 2nd International Conference on Modelling and Simulation, July 12-14, 1993, Melbourne, Australia, Vol.2, pp. 725-734.

8. L.Reznik, J.Shi, "Simulation Study of the Choice of A Membership Function Model For Control Applications", The 2nd International Conference on Modelling and Simulation, July 12-14, 1993, Melbourne, Australia, Vol.1, pp. 209-217.

9. J.Shi, L.H.Herron, A.Kalam, " Design and Implementation of a PC Based Automatic Voltage Regulator and Fuzzy Logic Power System Stabilizer", IEE International Conference on Advances in Power System Control, Operation and Management, 7-10 Dec, 1993, Hong Kong, pp. 293-298.

10. J.Shi, L.H.Herron, A.Kalam, " Design and Implementation of a Fuzzy Logic Controller for Power System Stabilization ", The 2nd IEEE Conference on Control Applications, Le Meridien Vancouver Hotel, Vancouver, Canada, September 13-16, 1993, Vol.1, pp. 61-67.

Acknowledgements

First of all, I would like to thank my principal supervisor, Dr. Len H. Herron, for his invaluable support and encouragement throughout this research. I am very grateful to his help in administrative as well as financial matters.

I would also like to express my gratitude to my co-supervisor, Dr. Akhtar Kalam, for his guidance and support during this research and in the writing of this thesis.

My acknowledgement and gratitude also go to Mr. Ralph Phillips for his skillful assistance in setting up the equipment in the Power Laboratory. Thanks also go to Mr. Neil Hunter who helped me set up A/D and D/A converters for my digital controller.

I have received generous assistance from other staff members in the Department. My gratitude goes to Dr. Lige Xia for initial assistance in using the *MatrixX* software package and his advice on the controller design. I would also like to thank Dr. Qin Jiang for providing me with her work and for being an excellent host in a very helpful visit to the Power Laboratory at Monash University, Clayton. I would like to thank Dr. Leon Reznik and Mr. Adrian Stoica for many helpful discussions on neural networks and fuzzy set theory.

I sincerely thank my colleagues Mr. Zejian Chen and Mr. Huang Ming Li for advice on setting up the single-machine infinite bus power system.

I appreciate the financial support from the Department of Electrical and Electronic Engineering at Victoria University of Technology. The department also provided me with financial assistance to participate in international and national conferences in which I exchanged information with other colleagues in the area. I have also been financially supported by a Special Overseas Postgraduate Fund Scholarship provided by Department of Employment, Education and Training for which I am thankful.

Finally, I wish to dedicate this thesis to my parents. They have brought me up with all the love, understanding and wisdom for which I am greatly indebted. I would also like to express my gratitude to my husband Les Nakonieczny for his encouragement and support to accomplish my education. My gratitude also extends to my brother and sister, my friend Yiqiu Li and Jian Wang for their encouragement and support during all these years.

Chapter 1

Introduction

1.1 Excitation Control and Its Role on Power System Stability

In the last few decades, considerable attention has been given to the excitation system and its role in improving power system stability. Because of the small effective time constants in the excitation control loop, it was assumed that a large control effort could be expanded through excitation control with a relatively small input of control energy. By the use of a voltage regulator in the excitation control system, the output of the exciter can be adjusted so that the generated voltage and reactive power change in a desired way. In early systems, the voltage regulator was entirely manual. In modern control systems the voltage regulator is an automatic controller that senses the generator output voltage as a feedback signal then adjusts the generator excitation level in the desired direction. This kind of voltage regulator has been known as an *Automatic Voltage Regulator* or **AVR**.

Early investigators realised that the so-called "steady-state" power limits of power networks could be increased by using the high-gain AVRs [Concordia, 1944]. A high-gain AVR was also recommended for reducing the steady state error of the system output. Although modern voltage regulators and excitation systems with fast speed of response and with a high ceiling voltage can be used to improve the transient stability (defined in Section 1.2) by increasing the synchronising torque of the machine, their effects on the damping torque are rather small. It was also recognised that the voltage regulator gain requirement was different at no-load conditions from that needed for good performance under load. For different stability (transient or dynamic) control problems, the requirements on the excitation control system may be significantly different. In transient stability studies, a very fast and high-ceiling voltage control action from the excitation control system is needed to reduce the amplitude of the first oscillatory swing and to help the generator to maintain its synchronism. Due to this reason, a fast excitation system with a high-gain AVR is beneficial to the control of the system transient stability. However, in the case where the system may operate with negative damping characteristics the high-gain excitation control system aggravates the situation by increasing the negative damping and hence instability may result in the system [DeMello, 1969], [Heffron, 1952], [Anderson, 1977]. This can be analysed in dynamic stability studies by using the small signal linearised system model given in Section A.3 of Appendix A, with constant reference signals [Heffron, 1952], [DeMello, 1969]. For a system without the AVR regulation, the damping torque component of the electrical torque at frequency ω is given by

$$\Delta T_d(\omega) = \frac{K_2 {K_3}^2 K_4 \tau'_{d0} \omega}{1 + {K_3}^2 {\tau'_{d0}}^2 \omega^2} \Delta\delta(\omega) \tag{1.1}$$

Since the parameters K_2, K_3, and K_4 are all positive, the damping torque given by equation (1.1) is positive. However, for a system with the AVR in operation, the damping torque component of the electrical torque can be expressed approximately as follows:

$$\Delta T_d(\omega) \approx \frac{K_2 K_5 K_A (\tau'_{d0} + \tau_A / K_3)\omega}{[(1/K_3 + K_6 K_A) - \tau_{d0}' \tau_A \omega^2]^2 + (\tau'_{d0} + \tau_A / K_3)^2 \omega^2} \Delta\delta(\omega) \tag{1.2}$$

where $\Delta T_d(\omega)$ has the same sign as K_5. At low frequencies, the synchronising component of the electrical torque is described approximately by

$$\Delta T_s(\omega) \approx [K_1 - \frac{K_2 K_5}{K_6}] \Delta\delta(\omega) \tag{1.3}$$

At some operating conditions such as for moderate to high system transfer impedances, and heavy loadings, the parameter K_5 can be negative [DeMello, 1969], [El-Sherbiny, 1973]. In these cases the damping torque in equation (1.2) becomes negative. Thus it can be assumed that the voltage regulator in the excitation system introduces negative damping when K_5 is negative.

In the 1950s engineers became aware of the instabilities introduced by the (then) modern voltage regulators, and stabilising feedback circuits came into common use [Crarg, 1950].

In the 1960s large interconnected systems experienced growing oscillations that disrupted parallel operation of large systems [Ellis, 1966], [Schleif, 1966], [Byerly, 1967], [Schleif, 1967], [Hanson, 1968], [Dandeno, 1968], [Shier, 1968], [DeMello, 1969], [Schleif, 1969]. The first example of inter-system low-frequency oscillations was observed during a WSCC (Western Systems Coordinating Council) in the USA [Schleif, 1966]. The interconnected system operated satisfactorily for a while, but low-frequency oscillations at about 6 cycles per minute developed. The interconnection was then tripped off, leaving the Northwest Power Pool oscillating about 3 cycles per minute and the Southwest Power Pool oscillating at about 11 cycles per minute.

A number of minor oscillations of system frequency were also observed in the South East Australian interconnected system [Bolden, 1982]. This system is characterised by having two main generator centres of La Trobe Valley in Victoria and the Snowy Mountains Hydro-electric Scheme, each connected to Melbourne (load centre) by links of length 120 and 360 km respectively.

With more and more experience accumulated from interconnected electrical power system operation, power system engineers are now convinced that the low-frequency oscillations are due to the inherently weak natural damping of large and weakly coupled systems. The situations of negative damping were further aggravated by the regulator gain [Klopfenstein, 1971]. Engineers learned that the system damping could be enhanced by artificial signals introduced through the excitation system. This scheme has been very successful in combating growing oscillation problems experienced in the power systems. As a result, the use of power system stabiliser (PSS) to dampen the oscillations in the power system was introduced.

1.2 The Definition of Power System Stability

The definition of power system stability is as follows [Anderson, 1977]:

- **Power System Stability**. If the oscillatory response of a power system during the transient period following a disturbance is damped, and the system settles in a finite time to a new steady operating condition at constant frequency, the system is said to be *stable.* If the system is not stable according to this definition, then it is considered *unstable.*

Power system stability is further classified into two categories: *dynamic stability* due to small disturbances, and *transient stability* due to large disturbances. It should be noted that this classification is not universally used. For example, in some different classifications, the dynamic stability is called *steady-state stability.*

- **Dynamic Stability**. *Dynamic stability* refers to the stability of a power system subject to small and sudden perturbations.

Typical perturbations under this category may be small, randomly occurring changes in load or small alterations in reference voltage settings. If the system is *dynamically stable*, it is expected that after a temporary small disturbance the system will return to its initial state, while for a permanent small disturbance the system will acquire a new operating point after a transient period [Anderson, 1977]. In both cases the synchronism of the system should not be lost. The size of small disturbances may be measured by the criterion that the perturbed system can be stabilised in an approximately linear region [Anderson, 1977].

- **Transient Stability**. *Transient stability* refers to the stability of power system subject to severe disturbances which are maintained for a short time and causes a significant reduction in the machine terminal voltage and the ability to transfer power.

The severe disturbances which cause transient stability problems may typically be large changes in load, three-phase faults or transmission line switching. It is usually assumed that the system under study is stable before a large disturbance happens. If the system is *transiently stable*, the system oscillations resulting from large disturbances are damped. However, transient stability of the system depends very much on the initial operating condition of the system and the nature (i.e., the type, magnitude, duration, and location, etc.) of the large disturbances that are applied to the system [Anderson, 1977], as well as on the post-fault system configuration.

For successful operation and control of power systems, the *dynamic stability* and *transient stability* of the system must be carefully considered.

1.3 The Application of Power System Stabilisers (PSSs)

The application of a power system stabiliser (PSS) is to generate a supplementary stabilising signal, which is applied to the excitation control loop of a generating unit, to introduce a positive damping torque. By using the supplementary stabilising signal, the negative damping effect of the AVR regulation can be cancelled, at the same time, the positive damping effect of the system can also be increased so that the system can operate even beyond the steady-state stability limit.

Stabilising signals are introduced in excitation systems at the summing junction where the reference voltage and the signal produced from the terminal voltage are added to obtain the error signal fed to the regulator-exciter system. The stabilising signal V_s is usually obtained from speed or a related signal such as the rotor speed, bus frequency and electrical power [DeMello, 1969], [Keay, 1971], [IEEE, 1980], [Larsen, 1981], is proceeded through a suitable network to obtain the desired phase relationship. Other input signals, such as the accelerating power [Bayne, 1977], [DeMello, 1978], [Lee, 1981] have also been used. During the last decade, the deviation on equivalent rotor speed ($\Delta\omega_{eq}$) derived from the shaft speed and integral of change in terminal electrical power has been used [Lee, 1981], [Kundur, 1989].

In the analysis and control of power system stability, two distinct types of system oscillations are usually recognised [Kundur, 1989]. One type is associated with units at a generating station swinging with respect to the rest of the power system. Such oscillations are referred to as **local plant mode oscillations**. The frequencies of these oscillations are typically in the range of 0.8 to 2.0 Hz. The second type of oscillation is associated with the swinging of many machines in one part of the system against machines in other parts. These are referred to as **inter-area mode** oscillations. The frequencies of the second type oscillations are in the range of 0.1 to 0.7 Hz. The basic function of the PSS is to add damping to both types of system oscillations.

The overall excitation control system with PSS in operation is designed so as to :

- maximise the damping of local mode as well as inter-area mode oscillations without compromising the stability of other mode;
- enhance both the steady state stability or dynamic stability, and transient stability of the power system;
- not adversely affect system performance during major system upsets which cause large frequency excursions;
- minimise the consequences of excitation system malfunction due to component failures.

1.4 Conventional Power System Stabilisers (CPSSs)

Power System Stabilisers designed using classical control theory can be called conventional power system stabilisers (CPSSs). The CPSS which is a feedback element from the shaft speed and is often given in the form [DeMello, 1969]:

$$G_s(s) = \frac{K_0 \tau_0 s}{1 + \tau_0 s} [\frac{(1 + \tau_1 s)(1 + \tau_3 s)}{(1 + \tau_2 s)(1 + \tau_4 s)}] \tag{1.4}$$

The first term in equation (1.4) is a reset term that is used to "wash out" the compensation effect after a time lag τ_0, with typical values of 4 seconds [DeMello, 1969] to 20 seconds or 30 seconds [Schleif, 1969]. The use of reset control will assure no permanent offset in the terminal voltage due to a prolonged error in frequency, such as might occur in an overload or islanding condition. The second term in $G_s(s)$ is a lead compensation pair that can be used to improve the phase lag through the system from V_{ref} to $\Delta\omega$ at the power system frequency of oscillation.

The settings of the time constants of the phase compensating lead-lag functions of the stabiliser can be determined by several techniques ([Schleif, 1968], [DeMello, 1969], [Schleif, 1969], [Warchol, 1971], [Gerheart, 1971], [Hayes, 1973], [Bollinger, 1975]) once the frequency response of the excitation control system has been known [Yu, 1971], [Vaahedi, 1986], [Arnautovic, 1987], [Chow, 1989], [Bollinger, 1975].

The design of the most widely used CPSS is based on linearised fixed-parameter models of the non-linear power system which are derived from the linearisation of the system at a given operating point. The parameters of the CPSSs are fixed at certain values which are determined under this particular operating point. Since the operating point of a power system drifts as a result of continuous load changes or unpredictable major disturbances such as a three-phase fault, the fixed parameter CPSSs can not adapt the stabiliser parameters in real time based on on-line measurements, i.e., they can not track the variations in the system operating conditions over a wide range of operating conditions. Therefore, they can not provide the best response in real time.

Although general parameters can be decided for a CPSS according to a particular range of operating condition, the design and analysis of the CPSS are very complex. For multi-machine system, it is difficult to consider the interaction of the individual generating machines [Laughton, 1966], [El-sherbiny, 1971]. Moreover, individual machines in multi-machine systems may have different requirements of damping torque and synchronising torque, and multi-machine multi-mode power system stabilisation techniques must be sought, especially when many CPSSs are used in the system and their coordination has to be taken into consideration. This made the selection of the CPSS parameters and the CPSS design for multi-machine power system even more complex [Fleming, 1981], [Crusca, 1991].

Another problem with the CPSS is that because there are uncertainties in the electric power system, there always exist unmodelled dynamics in the power system. As a result, the CPSS does not always perform effectively in the real electrical power system.

It is well understood that the optimal settings of the above mentioned CPSSs at one optimal condition are no longer the optimal one under the other. Therefore, in order to get optimal response using CPSS, resetting and tuning of the CPSS parameters are necessary for different operating conditions.

In the past decade, much effort has been directed towards the development of microcomputer-based digital controllers, such as adaptive or self-tuning PSSs, to generate desired supplementary stabilising signals in order to improve the overall power system stability over a wide range of operating conditions.

1.5 Adaptive Power System Stabilisers

The self-tuning regulator in control system is obtained by combining control design and recursive parameter estimation method. One of the ways automating modelling and design is the following:

1. Determine a model structure;

2. Estimate the parameters of the model recursively using the methods such as least squares, maximum likelihood, extended and generalised least squares, instrumental variables, extended Kalman filtering and stochastic approximation;

3. Use the estimates to calculate the control law by a suitable design method, e.g. phase and amplitude margins, pole-placement, minimum variance control and Linear Quadratic Gaussian (LQG) control.

The regulator obtained in such a way is called a self-tuning regulator because it has facilities for tuning its own parameters.

The self-tuning regulator is motivated by the desire to obtain automatic tuning of a control loop. An adaptive regulator can be achieved by modifying a self-tuning regulator to control a plant with varying parameters. The parameter estimation algorithm has to be changed so that it can track varying plant parameters. There are many schemes for adaptive control that are closely related to the self-tuning control. Three of these schemes are *Gain Scheduling, Model-Reference Adaptive Systems (MRAS)*, and an adaptive regulator obtained from *Stochastic-Control Theory.*

In the late 1970's and 1980's, much effort had been devoted to the application of self-tuning and adaptive control theory to the stabilisation of power systems to counteract the problem of variations in the system parameters and operating conditions. Pierre [Pierre, 1987] and Chalam [Chalam, 1987] have summarised the approaches and developments of adaptive power system control. The adaptive controllers have been used as either power system stabilisers [Ghosh, 1984], [Ghosh, 1985], [Sen Gupta, 1985], [Cheng, 1986a], [Hsu, 1987], [Wu, 1988], [Gu, 1989], [Seifi, 1990], [Mao, 1990a], [Ghandakly, 1990], [Wu, 1991], [Pahalawaththa, 1991], [Norum, 1993] or excitation controllers [Ledwich, 1979], [Sheirah, 1979], [Xia, 1983], [Kanniah, 1984b], [Kanniah, 1984c], [Romero, 1986], [Wu, 1986], [Ibrahim, 1989a], [Ibrahim, 1989b], [Lim, 1989], [Mao, 1990b] for single-machine power systems. Moreover, the power systems under study have been extended to multi-machine power systems [Cheng, 1986b], [Chandra, 1987], [Chandra, 1988], [Cheng, 1988], [Fan, 1990], [Wu, 1990], [Lim, 1990], [Bollinger, 1990], [Ostojic, 1990], [Norum, 1993].

The adaptive and self-tuning PSS have offered better dynamic performance than the fixed gain CPSS because it has the ability to automatically track the variations in power system parameters and operating conditions. However, for the realisation of such adaptive and self-tuning PSS, on-line identification of system parameters, observation of system states and computation of feedback gains in a short sampling period are needed which are so time consuming and computational intensive that it becomes infeasible to implement it in a real time control environment. As an alternative to a self-tuning PSS, variable structure PSSs have been proposed in the literature [Hsu, 1983], [Chan, 1983], [Hsu, 1986].

Lately, simpler alternative control schemes for stabilisation of power systems were proposed, they are the rule-based PSS [Hiyama, 1989] and fuzzy logic controllers [Hsu, 1990], [Hiyama, 1991]. These schemes are very suitable for on-line control due to their lower computational burden and simplicity. A comparison study between a fuzzy controller and a rule-based PSS [Hassan, 1991] shows that fuzzy controller is more suitable due to its robustness.

1.6 Fuzzy Logic and Fuzzy Control

Over the past years, the design of control systems has been based on classical or modern control theory (such as Nyquist, Bode, state-space, optimal control, root locus, H_∞, μ-analysis, etc.). Both approaches require a mathematical model based upon assumptions of linearity and stationarity to describe the plant to be controlled. Few of these design methods represent uncertainty and incompleteness in process knowledge or complexity in the resultant design. Classical control theory still provides good solution to linear single-input, single-output (SISO) systems. Modern control theory is also useful in solving multiple-inputs, multiple-outputs (MIMO) problems using state-space methods. However, the mathematical model represents a formulation of prior information into an analytic structure. In the real world, systems have some unknown parameters or highly complex and non-linear characteristics. Attempts to overcome this difficulty have resulted in research in adaptive control but the structure of such systems is very complex and non-linear, and its stability requirements often limit its successful application. Recent work on H_∞ and μ-analysis in robust control design deals with multi-variable linear systems with additive disturbances and parametric uncertainty, but still requires a notional low order model of the process, measures of the process and disturbance variations, and frequently leads to controller designs of very high order. Whilst many of these new techniques are mathematically advanced, their adoption by industry has been slow, this apparent reluctance is due to the amount and quality of information that has to be gathered to ensure adequate controller performance, and the constraints associated with the applicability of the method.

However there are many processes that are too complex, highly non-linear, uncertain (in parameters and disturbances), incomplete (aspects of the process or systems are unknown) or non-stationary, and have subtle and interactive exchanges with the operating environment. Yet such processes are successfully controlled by skilled human operators, using only experiential knowledge [Efstathiou, 1988]. The human operator also has the attribute of providing highly non-linear controls, with time varying parameters; additionally elements of learning and self-organisation are natural aspects of human control. Classical expert systems based upon a domain-independent inference engine which manipulates the heuristic based domain-dependent knowledge base; have been investigated widely in control systems design [Astrom, 1986], [Harris, 1985], [Trankle, 1985], [Mamdani, 1986]. Expert systems are usually *rule based* systems which have the attribute of being very fast to execute, with simple pattern matching of the antecedent being sufficient to activate a response under forward chaining inference. However under classical rule based systems a (situation/action) pair is required for every possible combination. The deliberate overlapping or interference of fuzzy sets avoids this problem by allowing rule generation within the quantisation range of the variable under control, which provides a tool that efficiently copes with adequately precise linguistic representations of the system, and produces a control protocol that satisfies some performance criterion that may be mathematical or linguistically prescribed.

Fuzzy sets are a generalisation of conventional set theory that were introduced by Zadeh in 1965 as a mathematical way to represent vagueness in every day life

[Zadeh, 1965]. Nowadays, fuzzy sets are equipped with their own mathematical foundations, rooting from set-theoretical basis and many-valued logic. Their achievements have already enriched the classic two-valued calculus with a deep and novel perspective. In more than two decades since its inception by Zadeh, the theory of fuzzy sets has matured into a wide-ranging collection of concepts, models, and techniques for dealing with complex phenomena which do not lend themselves to analysis by classical methods based on probability theory and bivalent logic.

Applications of fuzzy set theory have been already found in many different areas. One could probably classify those applications as follows [Zimmermann, 1990]:

- Applications to mathematics, that is, generalisations of traditional mathematical such as topology, graphy theory, algebra, logic, etc.;
- Applications to algorithms such as clustering methods, control algorithms, mathematical programming, etc.;
- Application to standard models such as "the transportation model," "inventory control models," "maintenance models", etc.;
- And finally applications to real-world problems of different kinds.

Fuzzy set theory is a generalisation of classical set theory that allows more realistic mathematical representation of linguistic values that contain a degree of fuzziness. Detailed overviews of fuzzy set theory are presented in Zadeh [Zadeh, 1973], Lee [Lee, 1990a and 1990b] and Gupta et al [Gupta, 1977].

The first application of fuzzy set theory to the control of systems was by Mamdani and Assilian [Mamdani, 1975], who reported on the control of a laboratory model steam engine. This was followed by Kickert and Van Nauta Lemke [Kickert, 1976], who derived a PI type FLC for a warm water plant; the FLC had a fast response, with same accuracy as the PI controller. For the same laboratory plant Mamdani developed a self-organising FLC that synthetised the control rule base by observing the process response; later this approach was extended by Procyk and Mamdani [Procyk, 1979] and by Harris et al for autonomous guided vehicles

[Harris, 1989a]. Since the mid 1980s fuzzy control has become more popular among control engineers working in industry, and more and more systems are implemented [Sugeno, 1985b]. Application of fuzzy control includes automatic train operation [Yasunobu, 1985], [Yasunobu, 1986], water quality control [Yagishita, 1985], [Itoh, 1987], elevator control [Fujitec, 1988], automobile transmission control [Kasai, 1988], fuzzy logic controller hardware systems [Yamakawa, 1986a], [Yamakawa, 1987a], [Yamakawa, 1987c] fuzzy memory devices [Yamakawa, 1986b], [Yamakawa, 1988] and fuzzy computers [Yamakawa, 1987b]. These applications have demonstrated the use of fuzzy control in the context of ill defined processes that can be controlled by a skilled human operator without the knowledge of the underlying dynamic operation. The advantage of using fuzzy set theory to construct controller lies in its ability to merge the experience, heuristic and intuition of expert operators in the control design. Fuzzy logic, the logic in which fuzzy control is based, provides an effective means of capturing the approximate, inexact nature of the real world. The core of a fuzzy logic controller (FLC) is a set of linguistic control rules related by the dual concepts of fuzzy implication and the compositional rule of inference. In essence, a FLC provides an algorithm which can convert the linguistic control strategy based on expert knowledge into an automatic control strategy. Fast fuzzy controllers have been designed and fabricated using different technologies [Lim, 1990], [Lee, 1990a], [Yamakawa, 1987c], [Manzoul, 1992]. Fuzzy control literature has reported superior performance to those obtained by conventional control algorithms.

1.7 The Application of Fuzzy Controllers as PSSs

The first application of a traditional fuzzy logic controller (FLC) as a PSS was reported in 1990 [Hsu, 1990]. The FLC has been applied to a multi-machine power system. The performance of the FLC has been compared with the CPSS through digital simulation and found to be better. However, comprehensive analysis and fine tuning of the FLC has not been investigated and the FLC has not been implemented in real time. The system exhibited minor oscillation under steady state since the rule base and the membership function shapes have not been fine tuned.

Hiyama et al proposed a PSS based on fuzzy set theory in 1991 [Hiyama, 1991] and it has been named a *fuzzy logic based power system stabiliser (FLBPSS)*. For the FLBPSS, operating conditions of the synchronous machine are expressed by the quantities of speed deviation and acceleration in the phase plane. The generator speed is measured at every sampling instant. Only one set of previous data is required to evaluate the generator acceleration. Therefore, the heavy calculation burden is avoided. The design framework of a fuzzy controller does not necessitate the use of a mathematical model to describe the dynamics of the control system and experience has shown that it yields results which are better than those obtained by conventional schemes. The fuzzy control schemes can be constructed using a simple microcomputer or a PC associated with A/D and D/A converters. Comparison studies between a self-tuning stabiliser and a fuzzy logic stabiliser has been done by Lim and Hiyama [Lim, 1993]. In the studies, different tests were simulated, with the non-linear power systems operating over a wide power range. Simulation results show that both stabilisers are suitable for, and effective in, enhancing the damping of the mechanical mode oscillations in a single-machine infinite bus power system and two-machine power systems without an infinite bus, of which one exhibits multi-mode oscillations. Recently, Hassan et al have proposed a self-tuned FLBPSS to improve the system dynamic performance [Hassan, 1992], [Hassan, 1993a], [Hassan, 1993b].

1.8 Motivation for the Thesis

This thesis involves the optimisation and implementation of fuzzy controllers for power system stabilisation. The objective is to incorporate the advantage of fuzzy controllers with the digital AVR to enhance the damping for both dynamic and transient responses and to improve the stability of power systems.

In the literature, no research has been carried out to optimise the above mentioned fuzzy logic controller (FLC) and fuzzy logic based power system stabiliser (FLBPSS). No real time implementation had been done at the time of initiating this project. Moreover, performance of the fuzzy controllers must be improved, comparison study of the two fuzzy control schemes must be carried out and most importantly, the optimal fuzzy controller must be tested in real time.

In order to improve the performance of the FLC, a different design method has been utilised. Continuous membership functions have been used and adjusted to obtain the best performance. An index named *Whole Overlap Ratio (WOR)* has been defined to assist in the fine tuning of the fuzzy membership function shape in order to improve the performance of the FLC. The initial FLC was designed with a complete filled rule table (49 rules). Neural network techniques were used for learning the corresponding control surface and for extracting a reduced set of rules describing the system.

Also to improve the performance of the FLBPSS, new non-linear membership functions that differ from the ones used in the past ([Hiyama, 1991], [Hassan, 1992]) have been proposed. Comprehensive analysis has been examined to optimise the settings of the FLBPSS. Sensitivity analysis has been carried out to assess the robustness of the proposed FLBPSS for changes in system parameters and under different operating conditions for both small and large perturbations.

Hassan et al [Hassan, 1992] suggested a self-tuned FLBPSS (STFLBPSS) whose performance has been shown to be better than that of the FLBPSS proposed by Hiyama et al [Hiyama, 1991]. However, they have not considered any comprehensive analysis to test the robustness of the FLBPSS. In this work, it is intended to compare the performance of the proposed FLBPSS with that of the STFLBPSS of Hassan et al.

Comparison studies of the two kinds of fuzzy control schemes (FLC and FLBPSS) have also been explored. The most effective one has been chosen for real time implementation. The implementation has been carried out on a single-machine infinite bus and a two-machine infinite bus power system respectively.

The availability of inexpensive microprocessors and digital controllers has prompted a great deal of attention towards digital excitation control [Runtz, 1973], [Kanniah, 1984a], [Kanniah, 1984b], [Kanniah, 1984c], [Ghandakly, 1987a], [Ghandakly, 1987b]. These microprocessor control systems have a great deal of flexibility and have the ability to implement sophisticated control algorithms efficiently and economically. In order to get the knowledge of how to apply a fuzzy controller to power system stabiliser, it is necessary to complete the following tasks:

- Design of digital voltage regulator. To avoid complexities as the design of self-tuned regulators, an effective and straightforward digital AVR design has been carried out which can be easily implemented;
- Develop a fuzzy logic controller (FLC) and a fuzzy logic based power system stabiliser (FLBPSS);
- Optimise the above fuzzy logic control schemes;
- Comparison study of the proposed fuzzy controllers with self-tuned FLBPSS (STFLBPSS);
- Implementation of an optimal fuzzy controller in a single-machine infinite bus power system;
- Implementation of an optimal fuzzy controller in a multi-machine power system.

So far, the fuzzy PSS is still the only one put into real operation in an experimental power system in Australia. During this research time, similar work has been carried out in Canada [Hassan, 1993a], [Hassan, 1993b] and Japan [Matsuki, 1991].

1.9 Contributions of the Thesis

The original contributions of this thesis are summarised as follows:

1. Two types of fuzzy controllers have been proposed and analysed;
2. Discrete-time analytical design of an Automatic Voltage Regulator has been employed;

3. Insight into the influence of different membership function shapes to the performance of the fuzzy controller has been examined;

4. Comprehensive sensitivity analysis of the two fuzzy control schemes have been investigated to assess the robustness of the proposed FLC and FLBPSS;

5. Neural Network techniques have been used to simplify the original fuzzy controller by learning the FLC control surface;

6. The effectiveness of the FLBPSS was experimentally corroborated by observing the effects of a step change in the load on the system, a three-phase fault and a step change in reference voltage. The implementation has been carried out on both a single-machine infinite bus and a multi-machine power system.

1.10 Organisation of the Thesis

This thesis consists of nine chapters. The rest of the eight chapters are organised as follows:

In Chapter 2, the single-machine and multi-machine power systems used for this research are described.

In Chapter 3, the design of the automatic voltage regulator (AVR) has been carried out in the z-domain. The voltage regulator is the intelligence of the power system and controls the output of the exciter so that the generated voltage and reactive power change in a desired way. Mathematical modelling of the single-machine infinite bus experimental system is detailed in Chapter 3 for the analysis and design of the AVR. Chapter 3 also provides the theoretical design and simulation result of the digital AVR. The z-domain analytical design method has been employed.

Fuzzy Logic Controller (FLC) structure has been described in the beginning of the Chapter 4. Two fuzzy control schemes for power system stabilisation have been proposed in this chapter. One uses traditional FLC as a power system stabiliser and the other is a fuzzy logic based power system stabiliser (FLBPSS). For the FLC 49 rules have been used and 7 rules have been utilised for the FLBPSS. Two new non-linear membership functions have been proposed for the FLBPSS in order to improve its performance.

After the fuzzy controller had been designed in Chapter 4, the remainder of the work was to adjust the fuzzy controller parameters to obtain the optimal performance. In Chapter 5, an index–Whole Overlap Ratio (WOR)– has been defined to assist in the fine tuning of the FLC membership function shape so that the optimal performance of the FLC can be achieved. The optimal setting of the proposed FLBPSS has also been studied in detail in this chapter. Comprehensive sensitivity analysis has been carried out to assess the robustness of the proposed FLC and FLBPSS for changes in system parameters and operating conditions under both small and large perturbations. The performance of the proposed FLBPSS has also been compared with that of the self-tuned FLBPSS of Hassan et al. The comparison study has been evaluated by using both a discrete-type quadratic performance index and the dynamic response. The performance indices and the dynamic responses of the optimised FLC and FLBPSS has also been compared. The most effective one has been chosen for real time implementation.

The implementation study of the proposed fuzzy PSS applied to a single-machine infinite bus system is demonstrated in Chapter 6. The development of the hardware and software is described in detail in this chapter. The performance of the optimised fuzzy PSS is evaluated when the power system is subjected to both small and large perturbations under wide range of operating conditions for the single-machine infinite bus power system.

To evaluate the effectiveness of the proposed fuzzy controller for multi-machine systems, simulation and implementation studies are carried out on a two-machine infinite bus system. Chapter 7 presents both the simulation and implementation results. Due to the equipment limitation, the multi-machine system study have only been carried out on a two-machine infinite bus power system.

In Chapter 8, Neural Networks (NN) have been used for learning the corresponding control surface and for extracting a reduced set of rules describing the system. The performance of the fuzzy controller with 24 rules is compared with the original 49 rules fuzzy controller in this chapter.

Finally, Chapter 9 presents the general conclusions and suggestions for further work. The advantages of using the proposed fuzzy control scheme are given in this final chapter.

Appendix A derives the mathematical model of the single-machine infinite bus power system. Appendix B introduces basic concepts of fuzzy set theory. Appendix C presents the derivation of the proposed membership function evaluation parameter Whole Overlap Ratio (WOR) for different membership functions. Appendix D includes the modelling of the multi-machine power systems. Appendix E demonstrates the input FPL (Fuzzy Programming Language) file and the generated rule base by using neural network techniques followed by the bibliography.

Chapter 2

Experimental Systems Used in the Power Laboratory

2.1 Introduction

Research into using fuzzy controllers for power system stabilisation in the Department of Electrical and Electronic Engineering at Victoria University of Technology started in 1991. The proposed fuzzy controllers have been optimised and implemented on a single-machine infinite bus and a two-machine infinite bus power system respectively. These two power systems are demonstrated in the following sections.

2.2 Single-machine Infinite Bus Power System

The circuit configuration of the single-machine infinite bus system built is as shown in Figure (2.1). The synchronous generator is a salient pole type with a damping winding on the rotor shaft and driven by a DC motor.

The AC generator is driven by a DC motor controlled to simulate a steam turbine. A local load has been connected to the generator terminal bus. The mechanical power output from the DC motor to drive the AC generator is set constant during the operation. Thus it is assumed that the generator has a constant mechanical power input during testing. The generator delivers the electrical output via the transmission lines to the infinite bus and the load bank depending on the operating condition. If these two powers are equal (neglecting the relatively insignificant machine losses), the generator will run at its constant synchronous speed, ω_{syn}.

If, on the contrary, a difference exists between these two powers, this difference will be used to change the kinetic energy, resulting in the swing of the rotor speed. This happens when the generator is subject to a disturbance.

The digital controller, implemented by an IBM-PC compatible system and associated with A/D and D/A interfaces, acts as the AVR and PSS on the laboratory generator system. Figure (2.2) shows an experimental single-machine infinite bus system.

The ratings of the single-machine infinite bus power system is shown in Table (2.1). The generator parameter values have been experimentally determined according to the IEEE test procedure on a 5kVA, 240V synchronous machine and shown in Table (2.2).

DC machine (Scott)	5kW, 240V, 21A,1500rpm
Generator (Scott)	5kVA, 400/415V,4 Pole,50Hz

Table 2.1: Ratings of the single-machine infinite bus power system

The equivalent transmission line resistance and inductance are:
$R_e = 0.02pu$, $X_e = 0.4pu$

Generator	kVA	$x_d(pu)$	$x'_d(pu)$	$x_q(pu)$	$\tau'_{d0}(s)$	H(s)
Generator (Scott)	5	1.027	0.479	0.489	0.345	1

Table 2.2: Generator parameters

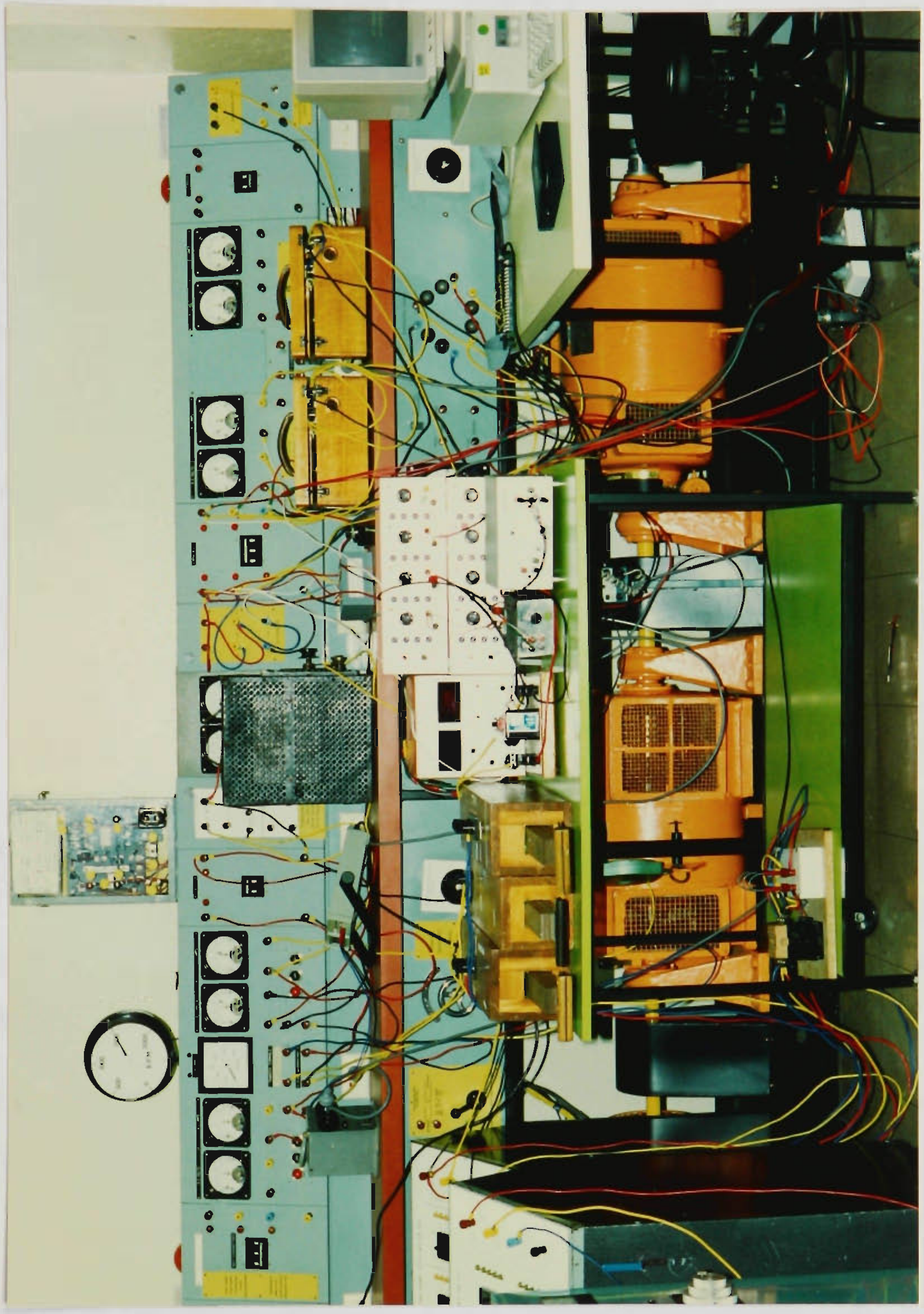

Figure 2.1: The overall view of the single-machine infinite bus experimental power system

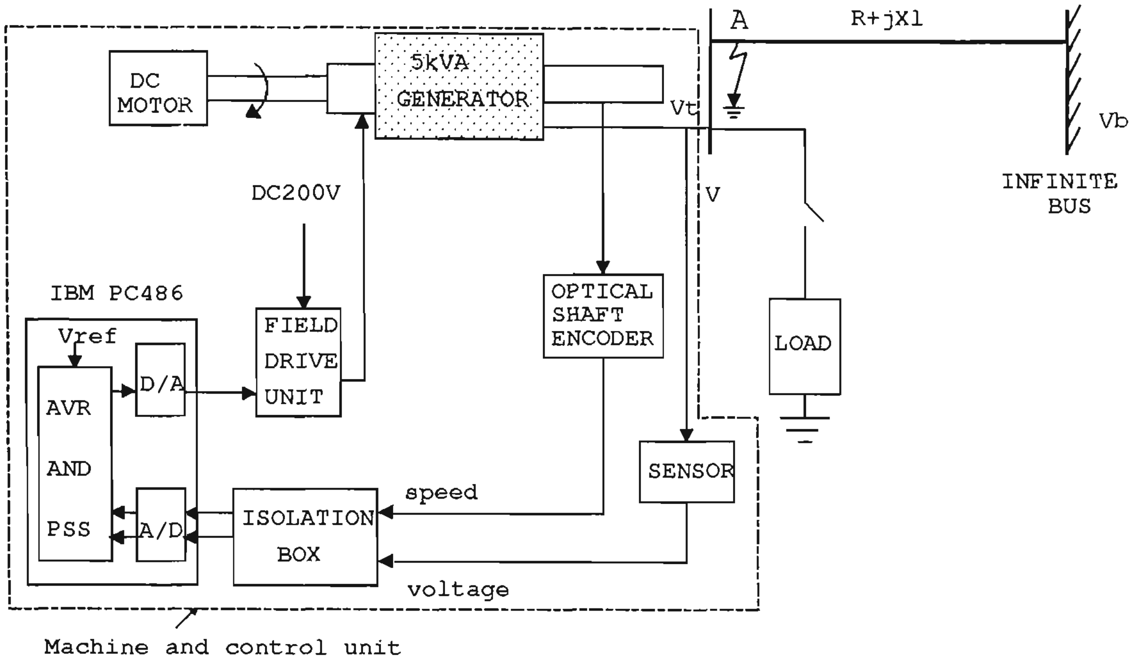

Figure 2.2: Experimental circuit configuration of single-machine infinite bus power system

2.3 Two-machine Infinite Bus Power System

The configuration of the two-machine infinite bus experimental power system is shown in Figure (2.3). The block diagram of the system is shown in Figure (2.4). The system consists of two units and an infinite bus with the transmission lines and associated loads.

Ratings related to the two-machine infinite bus power systems are given in Table (2.3). The generator parameters are shown in Table (2.4).

DC Machine (Macfarlane)	5kW, 200V, 22.8A, 1500rpm
Generator (Macfarlane)	5kVA, 400/415V, 4 Pole, 50Hz
DC machine (Scott)	5kW, 240V, 21A, 1500rpm
Generator (Scott)	5kVA, 400/415V,4 Pole, 50Hz

Table 2.3: Ratings of the two-machine infinite bus power system

Generator No.	kVA	$x_d(pu)$	$x'_d(pu)$	$x_q(pu)$	$\tau'_{d0}(s)$	H(s)
Generator 1 (Scott)	5	1.027	0.479	0.489	0.345	1
Generator 2 (Macfarlane)	5	0.777	0.1003	0.546	0.643	0.524

Table 2.4: Generator parameters

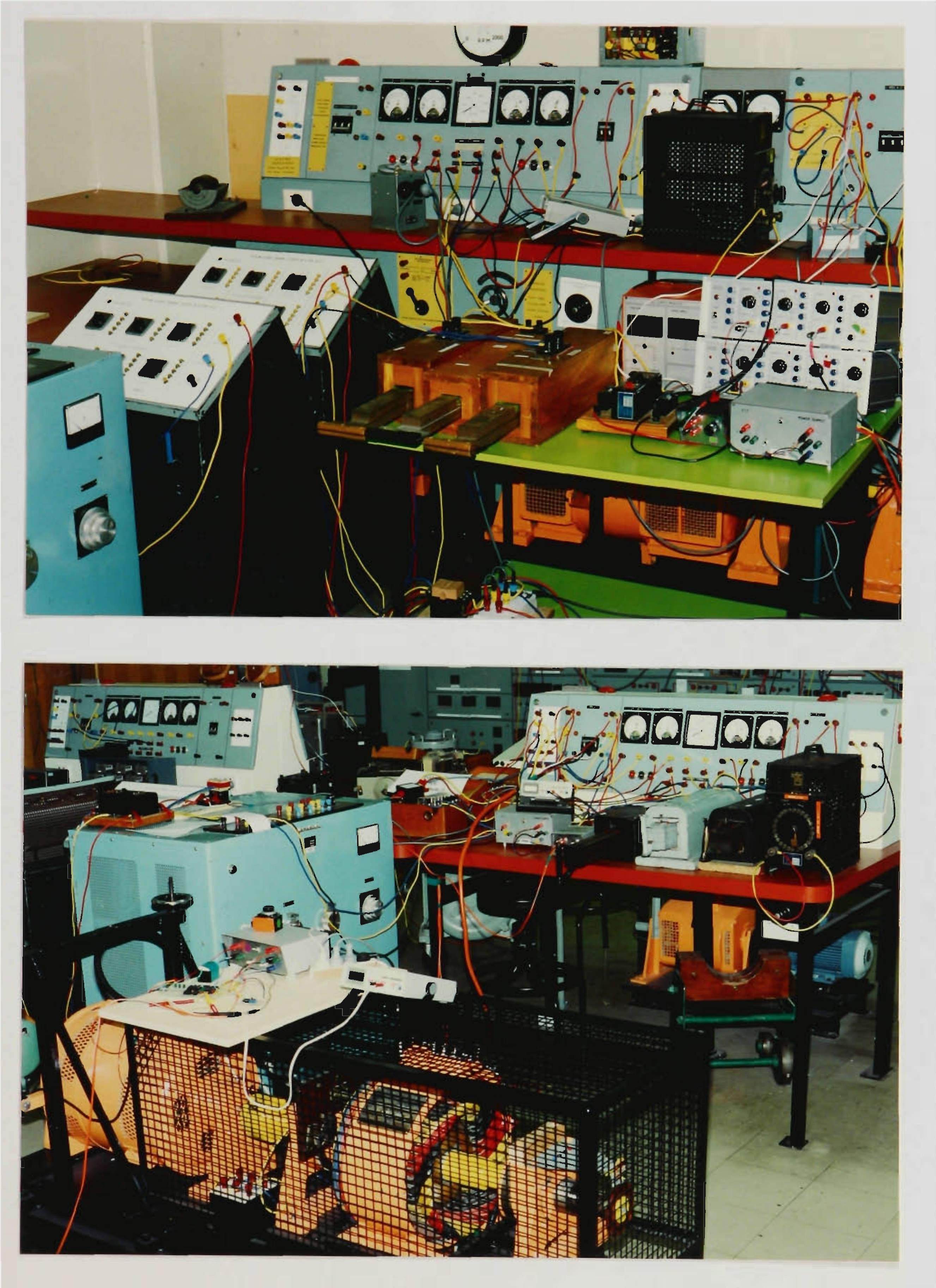

Figure 2.3: The overall view of the two-machine infinite bus experimental power system

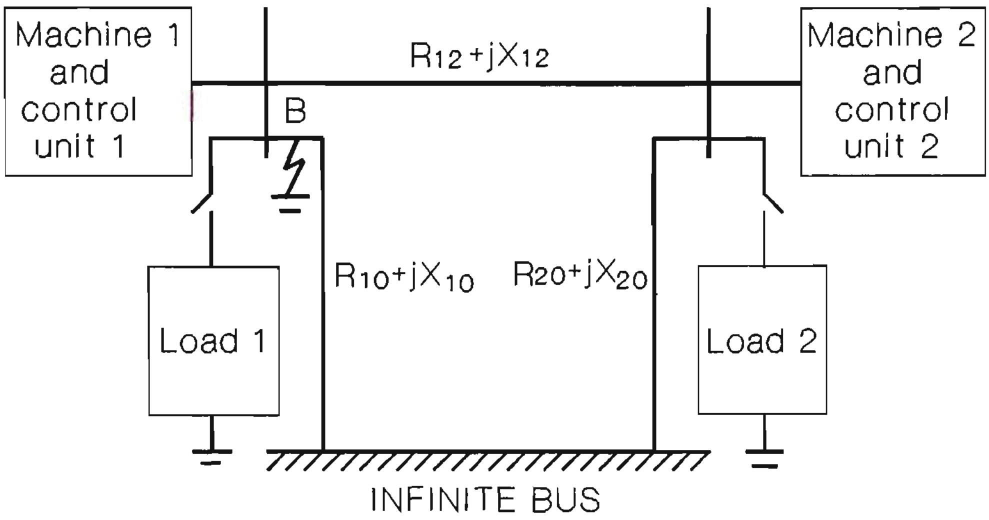

Figure 2.4: Two-machine infinite bus power system

The equivalent transmission line resistance and inductance are:

$R_{10} = 0.02pu$

$X_{10} = 0.5pu$

$R_{12} = 0.02pu$

$X_{12} = 0.6pu$

$R_{20} = 0.02pu$

$X_{20} = 0.4pu$

Chapter 3

Excitation Control System Design

3.1 Introduction

The role and effect of excitation control systems in improving power system stability has been given considerable attention in the last few decades. A synchronous generator or alternator is equipped with an automatic voltage regulator (AVR), which is responsible for keeping the generator output voltage constant under normal operating conditions at various load levels. With the advancement in the design of fast acting AVRs as well as the increasing complexity of large interconnected power systems, oscillations may continue for an extended period of time and even instability may occur following system disturbances. The control algorithms to overcome these problems are generally implemented using analog components.

Currently, the availability of powerful PC's has led to their increasing use in all aspects of power control engineering. In future years, they are expected to play an even greater role in power system control schemes because of their ability in combining various tasks, on-line updating of data and providing a logical or quick decision. Thus, the application of PC-based control in power system is being increasingly used for monitoring, data acquisition and on-line control. In addition to performing the primary control functions traditionally offered by analog controls, PC-based controls have a far greater deal of flexibility and ability to implement sophisticated control algorithms.

Most of the recent investigations of digital AVRs have been focusing on sophisticated control algorithms such as those of self-tuning and adaptive regulators. Some improvements of system performance have been reported using self-tuning regulators over that of traditional AVRs. However, in view of their large computational requirements and complexity of their software, the degree of improvement obtained needs to be examined carefully for optimum solutions.

To avoid these complexities, this project presents an effective and straightforward AVR design which can be easily implemented by computer facilities with high accuracy. The design has been carried out in the z-domain using analytical design method.

The organisation of this chapter is as follows:

The mathematical modelling of the experimental system is described in Section 3.2. In Section 3.3, discrete-time analytical design method is introduced. The design of the digital AVR using discrete time analytical design method is presented in Section 3.4. In section 3.5, the designed AVR is tested on the experimental single-machine infinite bus power system. Finally, the concluding remarks are summarised.

3.2 Mathematical Modelling of the Experimental System

Mathematical model of a synchronous machine connected to a very large power system through transmission lines is given in Appendix A for use in the design of the AVR.

The synchronous machine equations, for small perturbations about a quiescent operating condition, are summarised by the following equations (in the s domain)

[Anderson, 1977]:

$$E'_{q\Delta} = \frac{K_3}{1 + K_3\tau'_{d0}s}(E_{FD\Delta} - K_4\delta_\Delta) \tag{3.1}$$

$$T_{e\Delta} = K_1\delta_\Delta + K_2E'_{q\Delta} \tag{3.2}$$

$$V_{t\Delta} = K_5\delta_\Delta + K_6E'_{q\Delta} \tag{3.3}$$

$$2H\dot{\omega} = T_{m\Delta} - T_{e\Delta} - T_{d\Delta} \tag{3.4}$$

$$T_{d\Delta} = D\omega_\Delta \tag{3.5}$$

$$\dot{\delta}_\Delta = \omega_\Delta \tag{3.6}$$

The definitions of $K_1 - K_6$ can be found in Section A.3 of Appendix A. The resulting block diagram is shown in Figure (3.1) (with script Δ omitted for convenience).

By designating the state variables as E'_q, ω, and δ and the input signals as E_{FD} and T_m, the system equations is in the desired state-space form

$$\begin{bmatrix} \dot{E}'_{q\Delta} \\ \dot{\omega}_\Delta \\ \dot{\delta}_\Delta \end{bmatrix} = \begin{bmatrix} \frac{-1}{K_3\tau'_{d0}} & 0 & \frac{-K_4}{\tau'_{d0}} \\ \frac{-K_2}{2H} & \frac{-D}{2H} & \frac{-K_1}{2H} \\ 0 & 1 & 0 \end{bmatrix} \begin{bmatrix} E'_{q\Delta} \\ \omega_\Delta \\ \delta_\Delta \end{bmatrix} + \begin{bmatrix} \frac{1}{\tau'_{d0}} & 0 \\ 0 & \frac{1}{2H} \\ 0 & 0 \end{bmatrix} \begin{bmatrix} E_{FD\Delta} \\ T_{m\Delta} \end{bmatrix} \tag{3.7}$$

The configuration of the single-machine infinite bus experimental power system was shown previously in Figure (2.1). The synchronous generator is a salient pole type with a damper winding on the rotor shaft and driven by a DC motor.

The generator is equipped with an AVR and an IBM PC-486 associated with

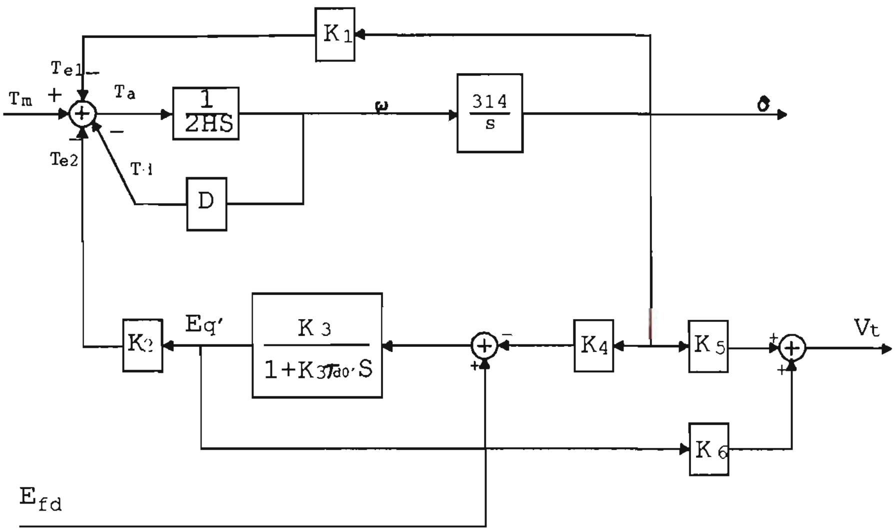

Figure 3.1: Block diagram of the simplified linear model.

A/D and D/A converters acts as the real time controller. The synchronous generator is connected to an infinite bus (SECV grid) through a modelled short transmission line. There is a resistive load bank connected to the generator bus terminal as a local load. A system transient can be generated by a step change in the resistive, inductive or capacitive load bank, a three-phase to ground fault.

The dynamic behaviour of the generator is described by a simplified linear model.

In a practical system, the system parameters have been measured and calculated according to the IEEE test procedure for a 5kVA, 240V synchronous machine at the Power System Laboratory of Victoria University of Technology. These parameters under a nominal operating condition (real power $P = 1pu$, power factor $PF = 0.85$ lag) are shown as follows:

- $K_1 = 0.9785$
- $K_2 = 0.8461$
- $K_3 = 0.6162$
- $K_4 = 0.3616$

- $K_5 = -0.1439$
- $K_6 = 0.42567$
- $M = 2H = 2 * 1$
- $\tau'_{d0} = 0.345$
- $D = 4$

Here, with the exception of K_3, all other parameters change with load change. At some operating conditions such as for moderate to high system transfer impedances and heavy loadings, K_5 becomes negative. K_1 is decreased by increasing system and machine reactance (X_e).

Consideration of the single voltage-regulator loop results in the block diagram of Figure (3.2):

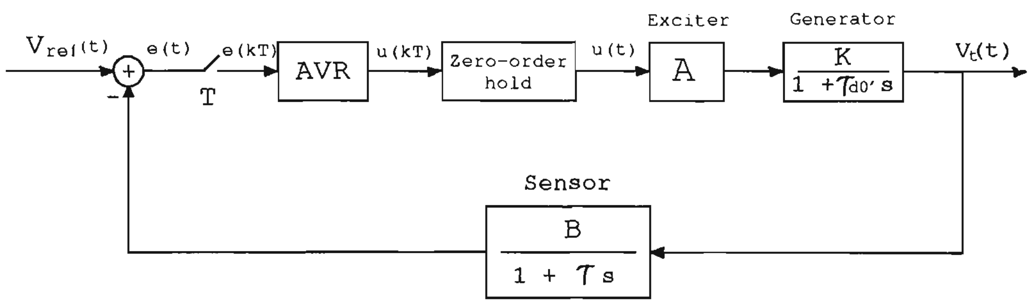

Figure 3.2: The voltage regulator loop

A simplified first order approximation voltage loop of the machine is given by:

$$G_v(s) = \frac{K}{1 + \tau'_{d0}s} \tag{3.8}$$

Where K is the DC gain and τ'_{d0} is the open circuit d-axis time constant of the generator respectively. The transfer function between the terminal voltage and the field voltage can be represented as:

$$G_v(s) = \frac{0.2622}{1 + 0.2126s} \tag{3.9}$$

The exciter is modelled using a field drive unit and the time constant of the unit is found to be very small compared to the significant time constant of the system under study and is therefore neglected. The transfer function of the field drive unit is:

$$G_{FDU} = A \tag{3.10}$$

where A is the gain of the field drive unit and is found to be 25 in this case.

The three-phase line voltages are transformed to a proportional DC signal which is measured by the A/D converter. The sensor circuit, which rectifies, filters and reduces the terminal voltage to 5V for comparison, whose transfer function is found experimentally and is given by:

$$G_s(s) = \frac{B}{1 + \tau s} \tag{3.11}$$

Again, the time constant τ of the sensor circuit is found to be $0.015s$ which is neglected as it is very small compared to the machine time constant. The sensor DC gain B is found to be $5V/240V = 0.0208$, If using reference voltage V_{ref} as 1pu, the sensor gain is $0.0208/5 = 0.0042$.

3.3 Discrete-time Analytical Design Method

For the digital voltage regulator design, an analytical design method that will force the error sequence, when subjected to a specific type of time-domain input, to become zero after a finite number of sampling periods and, in fact, to become zero and stay zero after the minimum possible number of sampling periods, has been employed.

The error signal $e(t)$, which is the difference between the input $V_{ref}(t)$ and output $V_t(t)$, is sampled every time interval T. The input to the digital controller is the error signal $e(kT)$. The output of the digital controller is the control signal $u(kT)$. The control signal $u(kT)$ is fed to the zero-order hold, and the output of the hold, $u(t)$, which is a piecewise continuous-time signal, is fed to the plant (Figure 3.2). It is desired to design a digital controller $G_{AVR}(z)$ such that the closed-loop control system will exhibit the minimum possible settling time with zero steady-state error in response to a step, a ramp, or an acceleration input. It is required that the output not exhibit inter-sampling ripple after the steady state is reached. The system must satisfy any other specifications, if required.

Let us define the z transform of the plant $G_p(s)$ which is preceded by the zero-order hold as $G(z)$, or

$$G(z) = \mathcal{Z}[\frac{1 - e^{-Ts}}{s} G_p(s)] \tag{3.12}$$

Then, the open-loop pulse transfer function becomes $G_{AVR}(z)G(z)$. Next, define the desired closed-loop pulse transfer function as $F(z)$:

$$\frac{V_t(z)}{V_{ref}(z)} = \frac{G_{AVR}(z)G(z)}{1 + G_{AVR}(z)BG(z)} = F(z) \tag{3.13}$$

Since it is required that the system exhibit a finite settling time with zero steady-state error, the system must exhibit a finite impulse response. Hence, the desired closed-loop pulse transfer function must be of the following form:

$$F(z) = \frac{a_0 z^N + a_1 z^{N-1} + \cdots + a_N}{z^N} \tag{3.14}$$

or

$$F(z) = a_0 + a_1 z^{-1} + \cdots + a_N z^{-N} \tag{3.15}$$

where $N \geq n$ and n is the order of the system. To find the pulse transfer function $G_{AVR}(z)$ that will satisfy equation (3.13), it can be obtained

$$G_{AVR}(z) = \frac{F(z)}{G(z) - BG(z)F(z)} \tag{3.16}$$

The designed system must be physically realisable. The conditions for physical realisability place certain constraints on the closed-loop pulse transfer function $F(z)$ and the digital controller pulse transfer function $G_{AVR}(z)$. The conditions for physical realisability may be stated as follows [Ogata, 1987]:

1. The order of the numerator of $G_{AVR}(z)$ must be equal to or lower than the order of the denominator. (otherwise, the controller requires future input data to produce the current input.)
2. If the plant $G_p(s)$ involves a transportation lag e^{-Ls}, then the designed closed-loop system must involve at least the same magnitude of the transportation lag. (Otherwise, the closed-loop system would have to respond before an input was given, which is impossible for a physically realisable system.)
3. If $G(z)$ is expanded into a series in z^{-1}, the lowest-power term of the series expansion of $F(z)$ in z^{-1} must be at least as large as that of $G(z)$. For example, if an expansion of $G(z)$ into a series in z^{-1} begins with the z^{-1} term, then the first term of $F(z)$ given by equation (3.15) must be zero, or a_0 must equal to 0; that is, the expansion has to be of the form

$$F(z) = a_1 z^{-1} + a_2 z^{-2} + \cdots + a_N z^{-N} \tag{3.17}$$

where $N \geq n$ and n is the order of the system. This means that the plant cannot respond instantaneously when a control signal of finite magnitude is applied: the response has a delay of at least one sampling period if the series expansion of $G(z)$ begins with a term in z^{-1}.

In addition to the physical realisability conditions, attention must be paid to the stability aspects of the system. Specifically, to avoid cancelling an unstable pole of the plant by a zero of the digital controller. If such a cancellation is attempted, any error in the pole-zero cancellation will diverge as time elapses and the system will become unstable. Similarly, the digital controller pulse transfer function should not involve unstable poles to cancel plant zeros which lie outside the unit circle.

Since $e(kT) = V_{ref}(kT) - V_t(kT)$, referring to equation (3.13), it can be derived that

$$E(z) = V_{ref}(z) - V_t(z) = V_{ref}(z)[1 - F(z)] \tag{3.18}$$

Note that for a unit step input $V_{ref}(t) = 1(t)$, $V_{ref}(z) = 1/(1 - z^{-1})$, thus

$$E(z) = \frac{1 - F(z)}{1 - z^{-1}} \tag{3.19}$$

3.4 Digital Automatic Voltage Regulator (AVR) Design

For a system transfer function $G_p(s)$, the z-domain transfer function $G(z)$ of the plant which is preceded by the zero-order hold $G_h(s)$, can be obtained as follows:

$$G(z) = \mathcal{Z}[G_h(s)G_p(s)] = \mathcal{Z}[\frac{1 - e^{-Ts}}{s} \cdot A \cdot \frac{0.6162 \times 0.4256}{1 + 0.2126s}] = \mathcal{Z}[\frac{1 - e^{-Ts}}{s} \cdot \frac{1.2337}{s + 4.704}] * A$$
$$G(z) = A * (1 - z^{-1}) \cdot \mathcal{Z}[\frac{0.2623}{s} - \frac{0.2623}{s + 4.704}]$$
$$G(z) = A * (1 - z^{-1})[\frac{0.2623z}{z - 1} - \frac{0.2623z}{z - e^{-4.704T}}] \tag{3.20}$$

Sampling frequency selection:

Since the design of AVR is in discrete time, the choice of sampling frequency is important. The rule of thumb for choosing the sampling frequency is to have the system 'activity' with three decades of the Nyquist frequency. If the sampling rate is increased beyond this, the activity effectively gets pushed to the left (on a Bode diagram). This should not cause any problems, however, a digital system operates with fixed point precision, hence if the sampling rate is too high, the system can experience numerical problems during computations.

On dealing with the low frequency which is of the order of a fraction of 1 Hz to a few Hz for large scale power system and to satisfy the transient criteria, the sampling time has been chosen as 25 milliseconds which gives the step response of the open loop system rise time $t_r = 0.3$ *seconds*. From equation (3.12) and equation (3.20), it can be obtained that:

$$G(z) = A * \frac{0.029z^{-1}}{1 - 0.889z^{-1}} \tag{3.21}$$

From the given system transfer function the output sequence of the system can be expected to satisfy the transient criteria. It is required that the system exhibit a finite settling time with zero steady-state error.

It is required to derive the exponential curve of the system response to an unit step input.

$$\begin{aligned} V_t(t) &= U \times A \times \mathcal{L}^{-1}[\frac{1}{s} \times \frac{1.2337}{s + 4.704}] \\ &= U \times A \times \mathcal{L}^{-1}[\frac{0.2623}{s} - \frac{0.2623}{s + 4.704}] \\ &= U \times A \times 0.2623(1 - e^{-4.704t}) = 240V \end{aligned} \tag{3.22}$$

U is the control signal which will be applied to the generator field. The terminal voltage V_t is equal to $240V$ (or 1 pu) when t is equal to 0.3 seconds.

$$U = \frac{240}{A * 0.2623(1 - e^{-4.704t})} \simeq 48.4V \tag{3.23}$$

If the desired settling time is 0.3 *seconds*, the required number of the sampling period:

$$K = \frac{settling\ time}{sampling\ time} = \frac{0.3}{0.025} = 12 \tag{3.24}$$

The output sequences are designed as follows:

$$V_t(kT) = 48.4 \times A \times 0.2623(1 - e^{-4.704kT}) \tag{3.25}$$

$V_t(0) = V_t(0) = 0V$

$V_t(T) = V_t(0.025) = 35.2V$

$V_t(2T) = V_t(0.05) = 66.528V$

$V_t(3T) = V_t(0.075) = 94.344V$

$V_t(4T) = V_t(0.1) = 119.088V$

$V_t(5T) = V_t(0.125) = 141.096V$

$V_t(6T) = V_t(0.15) = 160.656V$

$V_t(7T) = V_t(0.175) = 178.056V$

$V_t(8T) = V_t(0.2) = 193.512V$

$V_t(9T) = V_t(0.225) = 207.264V$

$V_t(10T) = V_t(0.25) = 219.48V$

$V_t(11T) = V_t(0.275) = 230.328V$

$V_t(12T) = V_t(0.3) = 240V$

The z-transform of the output sequences is:

$$\begin{aligned} V_t(z) &= 35.2z^{-1} + 66.528z^{-2} + 94.344z^{-3} + 119.088z^{-4} + 141.096z^{-5} + 160.656z^{-6} \\ &+ 178.056z^{-7} + 193.512z^{-8} + 207.264z^{-9} + 219.48z^{-10} + 230.328z^{-11} + 240z^{-12} \end{aligned} \tag{3.26}$$

For an unit step input $V_{ref}(z) = 1/(1 - z^{-1})$, then the closed-loop transfer function between $V_t(z)$ and $V_{ref}(z)$ is:

$$\begin{aligned} F(z) &= \frac{V_t(z)}{V_{ref}(z)} = \frac{V_t(z)}{1 - z^{-1}} = \\ &35.2z^{-1} + 31.328z^{-2} + 27.816z^{-3} + 24.744z^{-4} + 22.008z^{-5} + 19.56z^{-6} \\ &+ 17.4z^{-7} + 15.456z^{-8} + 13.752z^{-9} + 12.216z^{-10} + 10.848z^{-11} + 9.672z^{-12} \end{aligned} \tag{3.27}$$

$$BF(z) = 0.1467z^{-1} + 0.1304z^{-2} + 0.1160z^{-3} + 0.1031z^{-4} + 0.0917z^{-5} + 0.0815z^{-6} + 0.0725z^{-7} + 0.0644z^{-8} + 0.0573z^{-9} + 0.0509z^{-10} + 0.0453z^{-11} + 0.0402z^{-12} \quad (3.28)$$

Using equation (3.16), equation (3.21) and equation (3.27), the AVR transfer function can be easily derived as

$$G_{AVR}(z) = \frac{F(z)}{G(z) - BG(z)F(z)} = A\frac{5.0586 - 1.2345z^{-12}}{1 - BF(z)} \quad (3.29)$$

The terminal voltage response corresponding to a unit step input in the voltage regulator loop is shown in Figure (3.3).

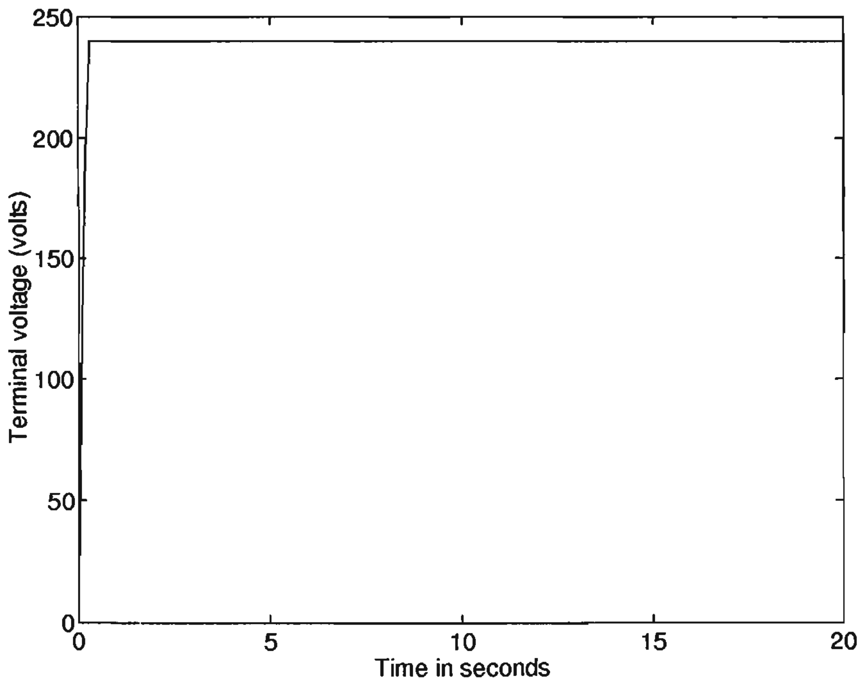

Figure 3.3: Unit step response of the voltage regulator loop

3.5 Experimental Test Results

Figures (3.4) to (3.14) are the implementation results. Figures (3.4) (a) to (3.9) (a) show the terminal voltage response subject to 1/2 and 3/4 rated sudden inductive, capacitive or resistive load changes without the AVR respectively; Figures (3.4) (b) to (3.9) (b) show the terminal voltage corresponding to 1/2 and 3/4 rated inductive, capacitive and resistive load changes with the designed AVR respectively. Figures (3.10)-(3.12) present the control signals corresponding to the above sudden load changes. Figure (3.13) demonstrates the terminal voltage and control signal corresponding to a 10% step increase in the reference voltage sustained for 7.5 seconds. Figure (3.14) shows the terminal voltage and control signal in response to a three-phase to ground fault at A (Figure 2.2) sustained for 125 milliseconds. It can be seen that the system equipped with the designed AVR kept the output constant under both small (a 10% step change in the reference voltage) and large (sudden load change and three-phase fault) disturbance conditions. Extensive tests were conducted at various operating conditions and similar results were obtained. The performance of the digital AVR is then theoretically analysed and experimentally verified in this chapter.

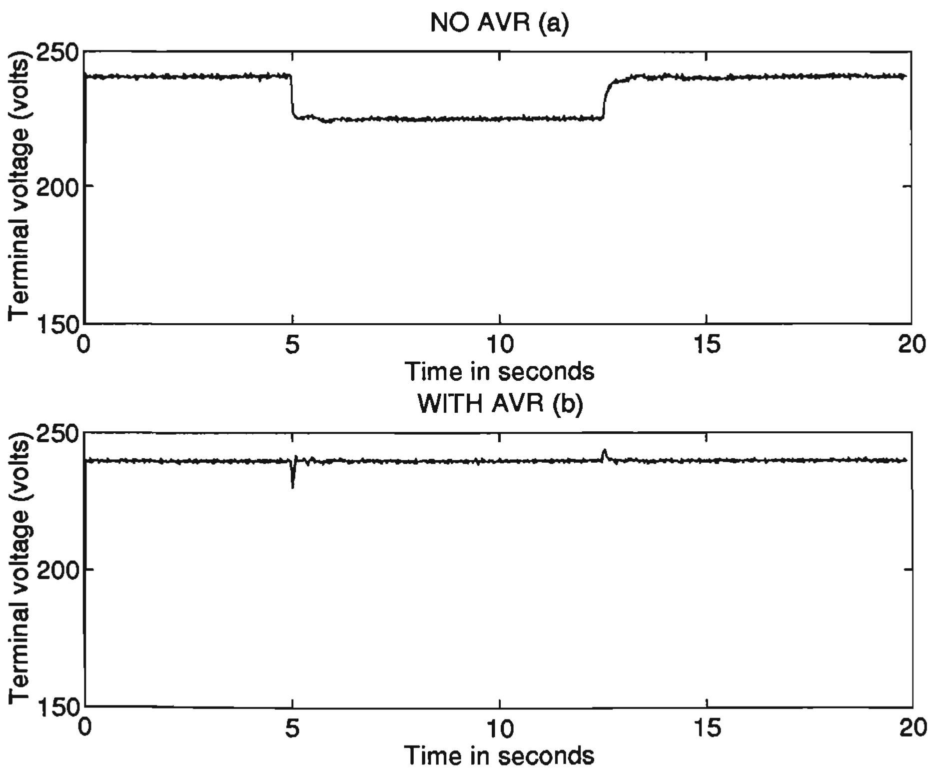

Figure 3.4: Terminal voltage corresponding to 1/2 sudden inductive load change without and with the AVR, (a)-without AVR, (b)-with the designed AVR

3.6 Concluding Remarks

In this chapter, the design and experimental test of an AVR is discussed. The simplified linear mathematical model of single-machine infinite bus power system is described in Section 3.2. The design of the AVR is based on this model. The discrete time analytical design method is introduced in Section 3.3. Followed by the theoretical analysis of the AVR in Section 3.4, the designed AVR has been experimentally verified in real time. The designed AVR has been tested on a single-machine infinite bus power system as shown previously in Figure (2.1) under the following disturbance conditions:

- 1/2 rated and 3/4 rated inductive step load change;
- 1/2 rated and 3/4 rated capacitive step load change;
- 1/2 rated and 3/4 rated resistive step load changes;
- a 10% step change in reference voltage;
- a three-phase to ground fault;
- at various operating conditions with the above disturbances.

The designed AVR performs satisfactorily as the AVR kept the generator output voltage constant under normal operating conditions at various load levels. The dynamic performance satisfy IEEE standard of excitation control system dynamic performance indices [IEEE, 1978]. This is confirmed by both the simulation and real time implementation.

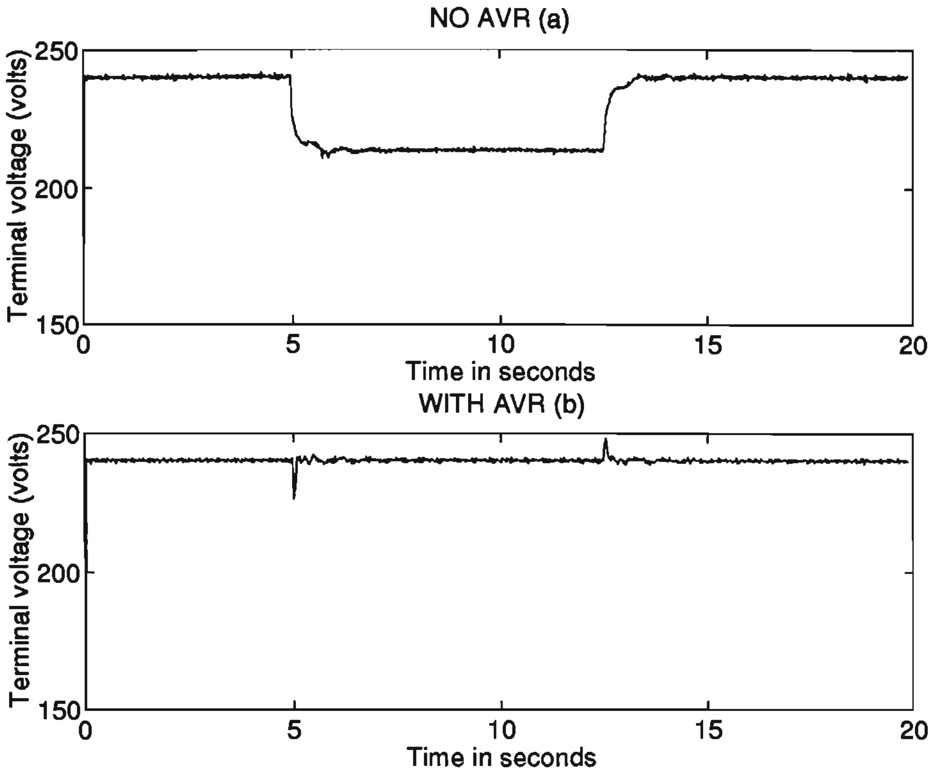

Figure 3.5: Terminal voltage corresponding to 3/4 sudden inductive load change without and with the AVR, (a)-without AVR, (b)-with the designed AVR

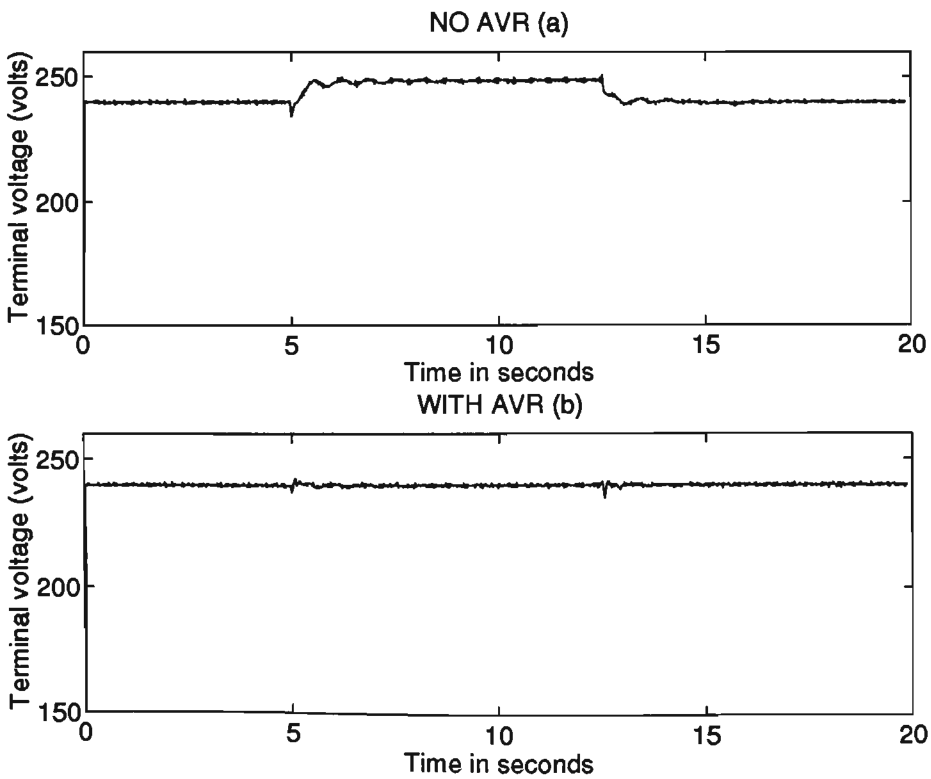

Figure 3.6: Terminal voltage corresponding to 1/2 sudden capacitive load change without and with the AVR, (a)-without AVR, (b)-with the designed AVR

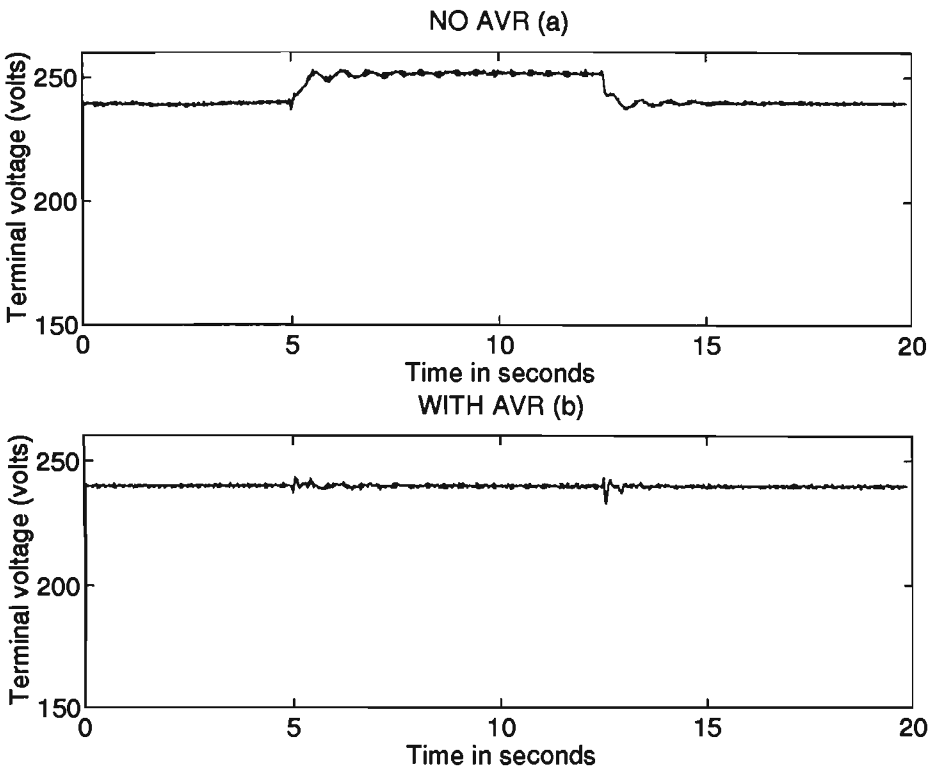

Figure 3.7: Terminal voltage corresponding to 3/4 sudden capacitive load change without and with the AVR, (a)-without AVR, (b)-with the designed AVR

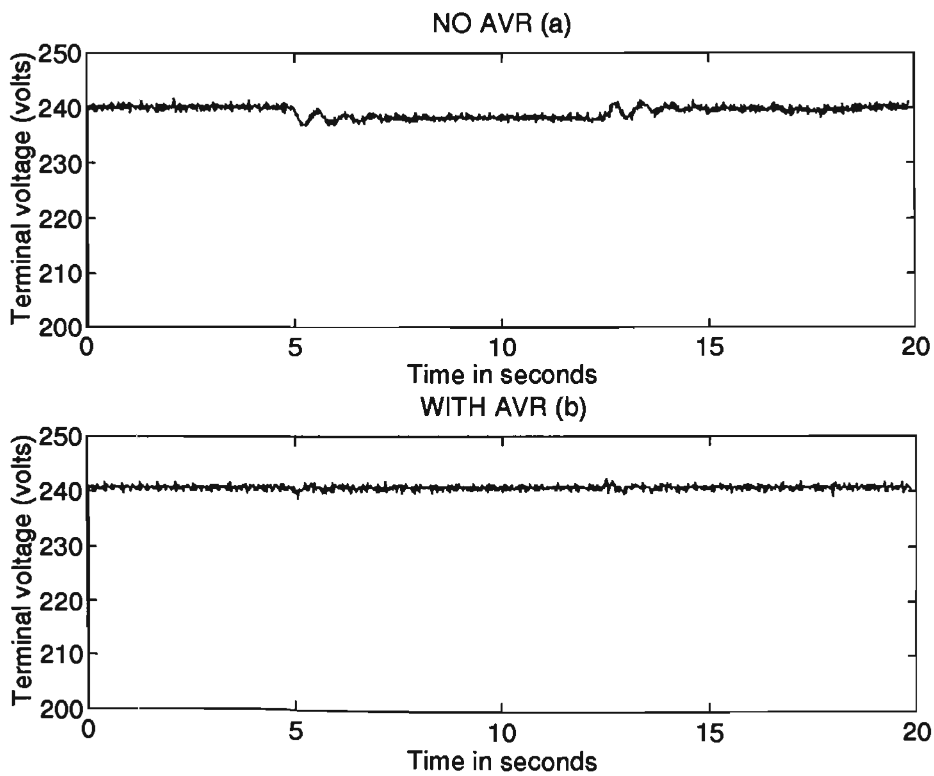

Figure 3.8: Terminal voltage corresponding to 1/2 sudden resistive load change without and with the AVR, (a)-without AVR, (b)-with the designed AVR

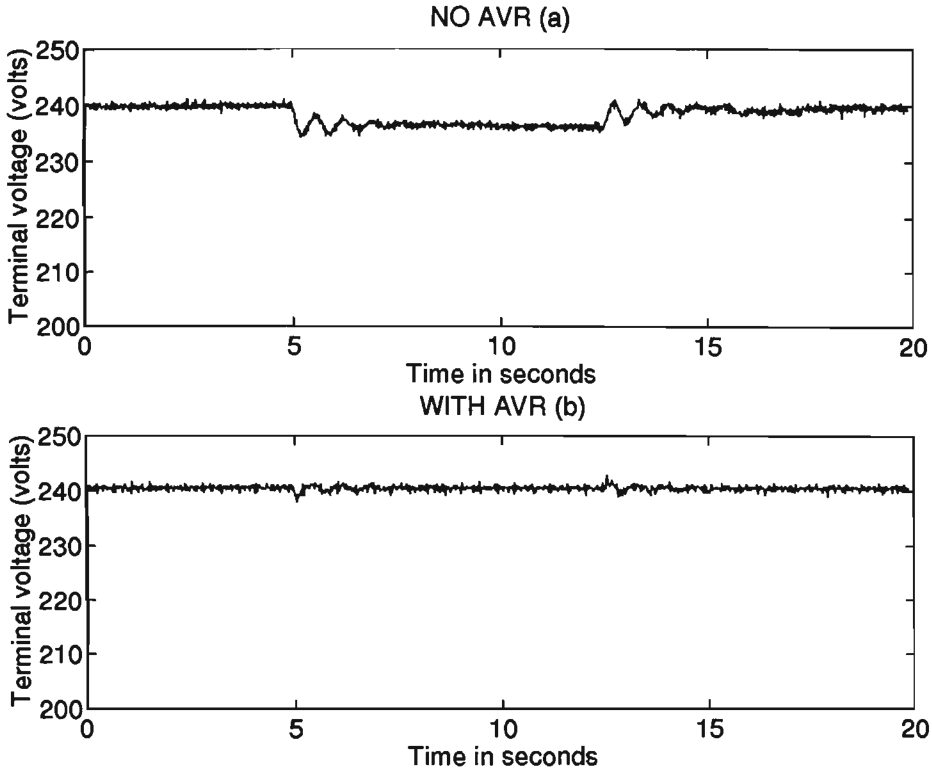

Figure 3.9: Terminal voltage corresponding to 3/4 sudden resistive load change without and with the AVR, (a)-without AVR, (b)-with the designed AVR

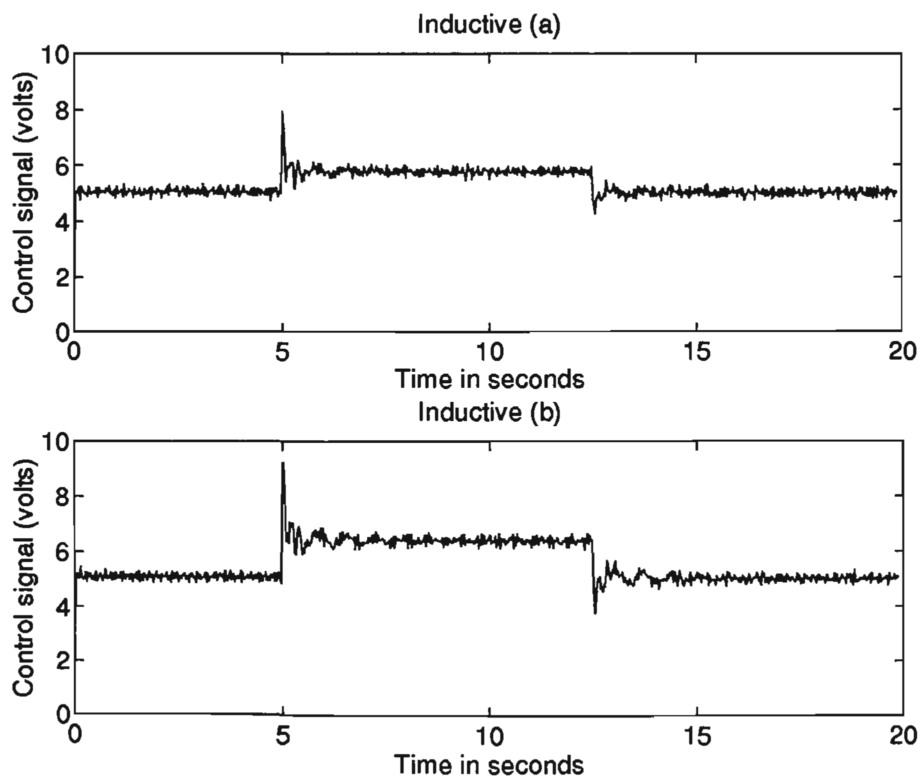

Figure 3.10: Control signals corresponding to 1/2 and 3/4 sudden inductive load changes with the AVR, (a)-1/2 rated inductive load change, (b)-3/4 rated inductive load change

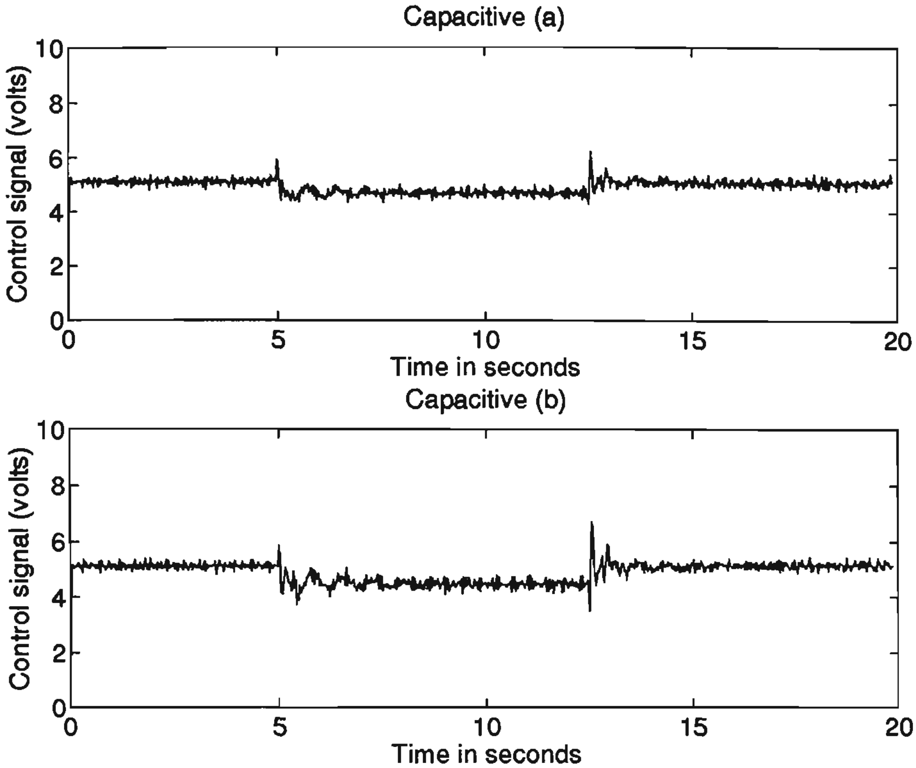

Figure 3.11: Control signals corresponding to 1/2 and 3/4 sudden capacitive load changes with the AVR, (a)-1/2 rated capacitive load change, (b)-3/4 rated capacitive load change

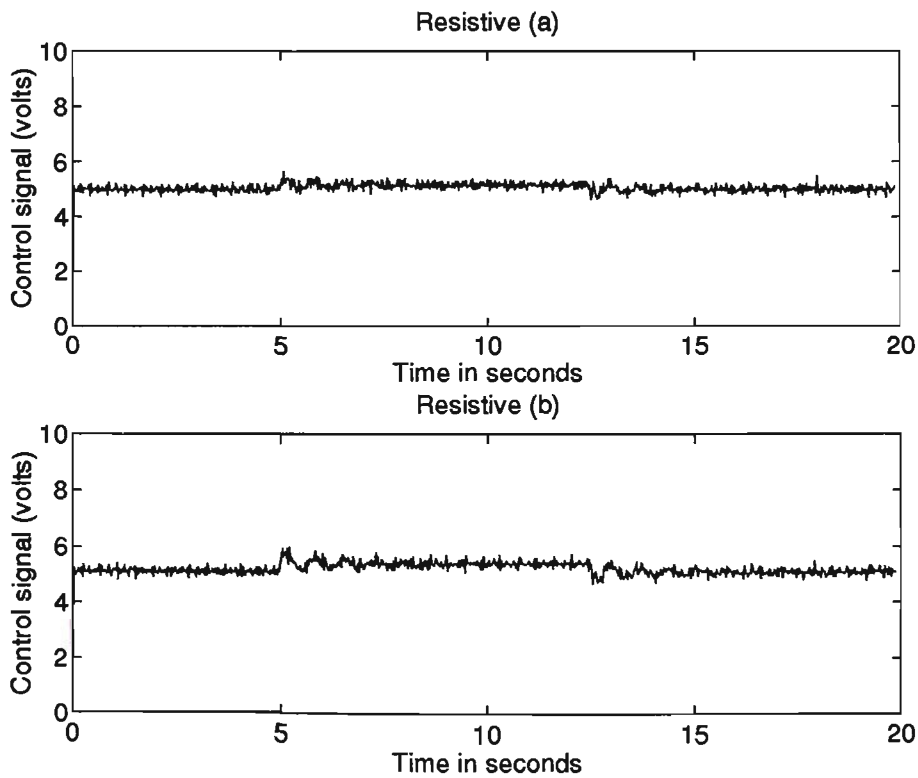

Figure 3.12: Control signals corresponding to 1/2 and 3/4 sudden resistive load changes with the AVR, (a)-1/2 rated resistive load change, (b)-3/4 rated resistive load change

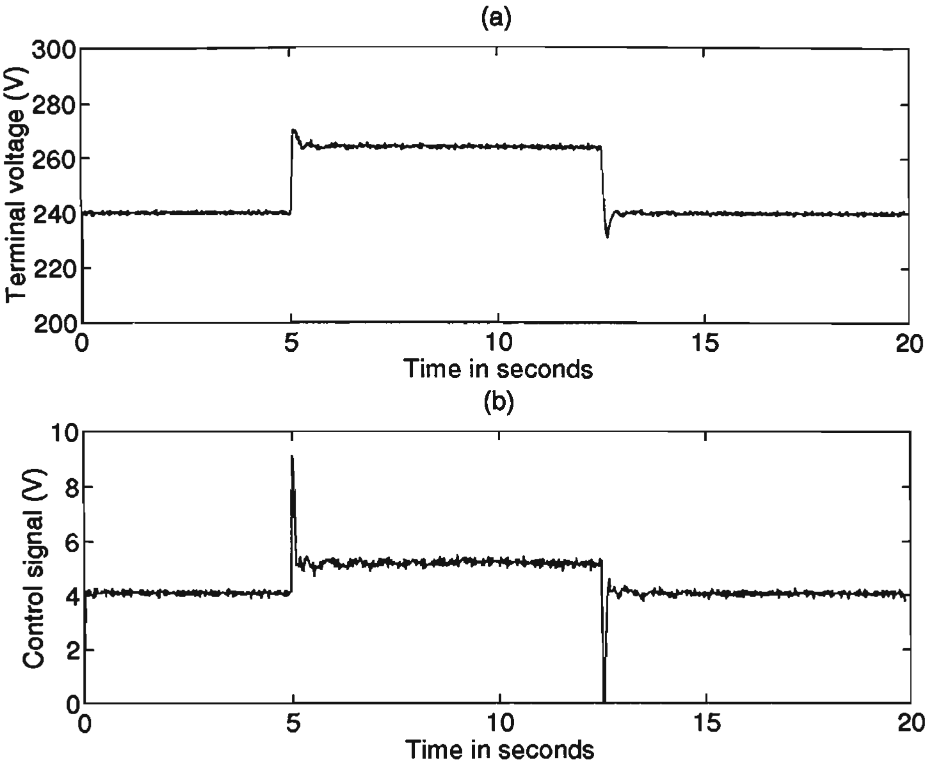

Figure 3.13: Terminal voltage and control signal corresponding to a 10% step increase in the reference voltage sustained for 7.5 seconds, (a)-terminal voltage, (b)-control signal

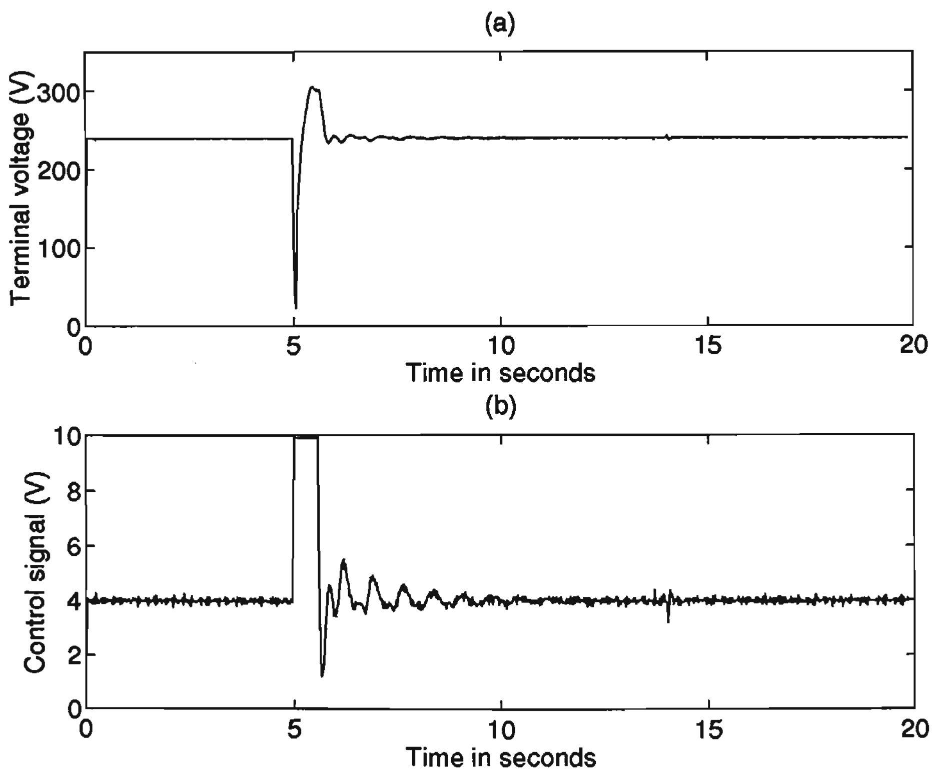

Figure 3.14: Terminal voltage and control signal corresponding to a three-phase to ground fault at A (Figure 2.2) sustained for 125 milliseconds, (a)-terminal voltage, (b)-control signal

Chapter 4

Proposed Design of Two Fuzzy Control Schemes

4.1 Introduction

In this chapter, proposed design of the fuzzy logic controller (FLC) and fuzzy logic based power system stabiliser (FLBPSS) are carried out. In Section 4.2, the structure of the FLC is demonstrated and explained. Two fuzzy control schemes, i.e., the FLC and the FLBPSS are designed as PSSs in Section 4.3 and 4.4 respectively. The basic concepts of fuzzy set theory, such as fuzzy sets and terminology, fuzzy set theoretical operations, fuzzy inference and composition are included in Appendix B.

4.2 Introduction to Fuzzy Logic Controller (FLC)

4.2.1 Structure of the FLC

The essential part of the FLC is a set of linguistic control rules related by the dual concepts of fuzzy implication and the compositional rule of inference. The FLC provides an algorithm which can convert the linguistic control strategy based on expert knowledge into an automatic control strategy. Figure (4.1) shows the basic configuration of a FLC, which comprises four principle components: fuzzification interface, knowledge base (KB), decision-making logic, and defuzzification interface [Lee, 1990a], [Lee, 1990b].

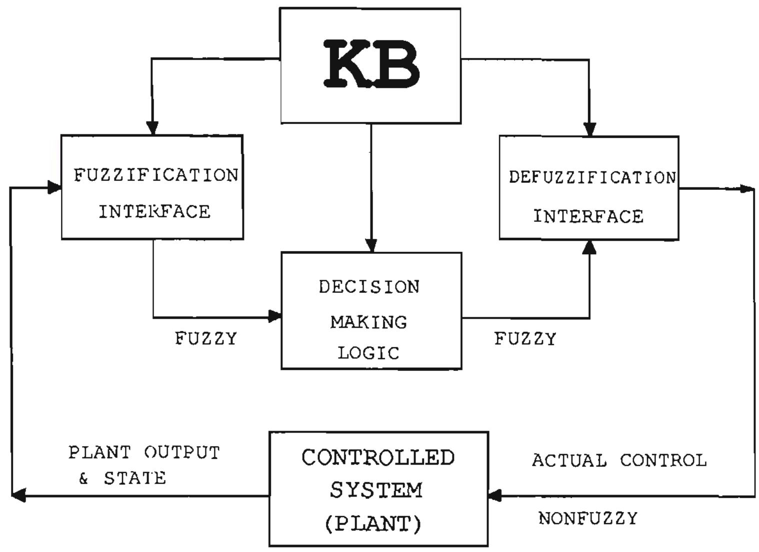

Figure 4.1: Schematic diagram of a FLC

Fuzzification Interface: The function of the fuzzification interface involves:

- measures the values of input variables;
- performs a scale mapping that transfers the range of values of input variables into a corresponding *normalised* universes of discourse (normalised domain). It also maps the normalised value of the control output variable onto its physical domain (output denormalisation). When a non-normalised domain is used then there is no need for this function;
- performs the function of fuzzification that converts input (crisp) data into suitable linguistic values which may be viewed as labels of fuzzy sets, in order to make it compatible with the fuzzy set representation of the process state variable in the rule-antecedent.

Knowledge Base: The knowledge base comprises a knowledge of the application domain and the attendant control goals. This knowledge is classified as the *data base* and *linguistic control rule base*. The basic function of the *data base* is to provide the necessary information for the proper functioning of the fuzzification interface, the rule base, and the defuzzification interface. This information includes:

- Fuzzy sets (membership functions) representing the meaning of the linguistic values of the process (plant) state and control output variables.
- Physical domains and their normalised counterparts together with the normalisation/denormalisation (scaling) factors.

If the continuous domains of the process (plant) state and control output variables have been discretised then the data base also contains information concerning the quantisation (discretisation) look-up tables defining the discretisation policy. For the case of continuous, normalised domains the design parameters of the data base include:

- Choice of membership functions;
- Choice of scaling factors.

The *rule base* characterises the control goals and control policy of the domain experts by means of a set of linguistic control rules. The design parameters involved in the construction of the rule base include:

- Choice of process state and control output variables;
- Choice of the contents of the rule-antecedent and the rule-consequent;
- Choice of the term-sets (ranges of linguistic values) for the process state and control output variables;
- Derivation of the set of rules.

Decision Making Logic: The decision making logic is the core of a FLC. It has the capability of simulating human decision making based on fuzzy concepts and of inferring fuzzy control actions employing fuzzy implication and the rules of inference in fuzzy logic. In the context the design parameters for the decision making logic are as follows:

- Choice of representing the meaning of a single production rule;
- Choice of representing the meaning of the set of rules;
- Choice of inference engine.

Defuzzification Interface: The defuzzification interface performs the following functions:

- a scale mapping, which converts the range of values of output variables into corresponding universe of discourse. This is also called *demormalisation.* This function is not needed if non-normalised domains are used.
- defuzzification yields a non-fuzzy control action from an inferred fuzzy control action.

The design parameter of the defuzzification interface is:

- Choice of defuzzification operators.

4.2.2 Data Base

The concepts associated with a data base are used to characterise the fuzzy control rules and the data manipulation in the FLC. Some of the aspects relating to the data base will be discussed here.

- **Discretisation/Normalisation of Universe of Discourse**

  A universe of discourse can be discrete or continuous depending on the nature of the application. Sometimes it is necessary to change a continuous universe into a discrete one. This can be achieved by discretisation. Furthermore, a continuous universe may be mapped to another universe of different range by normalisation [Lee, 1990a].

1. *Discretisation of Universe of Discourse*:

   Discretisation of a Universe is often referred to quantisation. Quantisation divides an universe into a number of segments called quantisation level. Each level is labelled as a generic element. A fuzzy set can be defined by assigning grade of membership values to each generic element of the new discrete universe. A table for quick reference is formed to define the output of the controller for every possible combination of the inputs. The number of quantisation level determines the fineness of a control. In other words, the controller will be more sensitive to the observed data if the number of quantisation level increases. In most cases, fuzzy logic operations are performed on computers. Therefore, the number of quantised level should be large enough to provide an adequate approximation of the original continuous universe and yet be small enough to save memory.

   Discretisation can be viewed as a scale mapping of the measured data to the discrete universe. The scaled mapping can be linear or non-linear or a combination of both. It is common that coarse resolution is used for large errors and small resolution is used for small errors. In practice, due to discretisation, the performance of a FLC is less sensitive to small deviations in the values of the state variables.

2. *Normalisation of a Universe of Discourse*:

   The normalisation of a universe of discourse requires a discretisation of the universe of discourse into finite number of segments, with each segment mapped into a suitable segment of the normalised universe. A fuzzy set is then defined by assigning an explicit function to its membership function.

   The number of segments of the required number of fuzzy sets is a trade-off between the accuracy and the complexity of the model. The size of the relation matrix or number of fuzzy rules increases rapidly with increasing number of fuzzy sets. Since fuzzy modelling is an attempt at developing a mathematical representation of a linguistic description of a control process, this becomes meaningless if number of fuzzy sets becomes too large. It is also difficult to put sensible labels on more than

7 fuzzy sets for a variable. The trade-off against the accuracy of the model is that number of fuzzy sets increases with an increase in accuracy. However, more information is required to be able to specify a sensible model.

The two design parameters involved in the construction of the data base are:

- Choice of membership functions;
- Choice of scaling factors.

- **Membership Function of a Fuzzy Set**

  Fuzzy sets are defined in two ways, numerical or functional, depending whether the universe of discourse is continuous or discrete.

  1. *Numerical*

     Fuzzy sets defined by numerical method have grade of membership function as a vector of numbers whose dimension depends on the degree of discretisation.

  2. *Functional*

     A functional definition expresses the membership function of a fuzzy set in a functional form, typically a bell-shaped function, triangular-shaped function, trapezoid-shaped function, etc. Such functions are used in a FLC because they lead themselves to manipulation through the use of fuzzy arithmetic. The functional definition can readily be adapted to a change of the normalisation of a universe.

  Either a numerical or functional definition can be used to assign the grades of membership to the fuzzy sets. There are few guidelines exist for defining the shape of fuzzy sets. The only necessary criterion to enable the fuzzy logic to work effectively is that a set of fuzzy sets should cover the operating range of the variable. Given that the set satisfy this, the choice of the actual shape described by the membership functions is entirely subjective. It may be noted that the linguistic label of the fuzzy set implies a particular shape for the set.

- **Choice of Scaling Factors**

  The use of normalised domains (universe of discourse) requires a scale transformation which maps the physical values of the process state variables into a normalised domain. This is called the input normalisation. Furthermore, output denormalisation maps the normalised value of the control output variables into their respective physical domains.

4.2.3 Rule Base

The most important element of a FLC is the set of linguistic statements based on expert knowledge. The expert knowledge is usually described in the form of **if-then** rules. They can be easily implemented using fuzzy conditional statements in fuzzy logic. The collection of fuzzy conditional rules forms the rule base of a FLC.

- **Choice of Process State Variables and Control Variables of Fuzzy Control Rules**

  Identifying and choosing suitable process state variables and control variables is essential to the characterisation of the operation of a fuzzy system. The assignment of linguistic variables and their membership function also have an influence on the structure of a FLC. The process of this selection depends heavily on the experience and the control engineering knowledge. The common linguistic variables used are the state, state error, state error derivative, state deviation and its derivative, etc.

- **Source of Fuzzy Control Rules**

  There are basically four methods of deriving a fuzzy control rule base [Takagi, 1983], [Sugeno, 1985], [Lee, 1990a], [Lee, 1990b]; these approaches are not mutually exclusive and in practice a combination of these methods are likely to be utilised.

  1. Expert's experience and knowledge

Fuzzy control rules specify the necessary action to be taken if certain conditions are satisfied. Since information and problems are described in linguistic rather than numerical in daily life, it should be obvious that fuzzy control rules provide a framework for the characterisation of human behaviour and decision analysis. There are two heuristic approaches which can be used to formulate fuzzy control rules. The most common one is the verbalisation of human expertise. Another approach involves forming a prototype of fuzzy control rules by gathering information from a number of experienced experts or operators. Whilst the approach is problem domain specific, non-generic and highly subjective, it has been applied with considerable success [Sugeno, 1985], [Larsen, 1980].

2. Modelling the operator's control actions

   In many industrial man-machine applications, the transfer function of the system cannot be found using classical control theory due to the complicated structure and insufficient precision of the system. However, very often those human operators are able to monitor such systems without actually understanding the actual model of the system. Therefore, it is possible to extract fuzzy control rules by expressing the operator's control rules using linguistic variables. In practice, rules can be deduced from the observation of human controllers actions in terms of input-output operating data [Sugeno, 1985], [Harris, 1989b].

3. Modelling a process

   A linguistic description of a dynamic characteristics of a controlled process can be viewed as a fuzzy model of the process. Fuzzy control rules can then be developed based on this fuzzy model to obtain desirable performance. This approach is more complicated than others but it is more reliable and yields better results. This approach has been successfully applied to car driving by Sugeno and Nishida [Sugeno, 1985].

4. Self organisation

   Many of the FLCs built so far can only imitate human decision making. It is possible to design a FLC which has the ability to create fuzzy control rules and to modify them based on experience. Procyk and Mamdani [Procyk, 1979] described the first self organisation controller (SOC) which consists of two rule bases. One of them is the general rule base of a FLC. The other is constructed so that it has the human-like learning ability to create and to modify the general rules based on the desired overall performance of the system. An example of a fuzzy rule based which has a learning capability is Sugeno's fuzzy car [Sugeno, 1984], [Sugeno, 1985] which can be trained to park by itself.

4.2.4 Defuzzification Strategies

Defuzzification is required because many practical control actions are crisp in nature. Defuzzification is a mapping from a space of fuzzy control actions defined over a output universe of discourse into space of non fuzzy (crisp) control actions. There is still no systematic approach to defuzzification but there are a few ways of tackling this problem which are reviewed as follows:

- **Max-procedure**

  The first and simplest method relies on choosing the control value for which the membership function attains a maximum, namely:

$$\max_{u \in U} U(u) = U(u_0) \tag{4.1}$$

  A difficulty arises when more than one element of U possesses this maximal value and thus u_0 is not uniquely determined. For instance, one can take randomly one of the elements with the highest grade of membership, or treat their average value as the representative one (means of maximum approach), thus:

$$u_0 = \sum_{i=1}^{r} \frac{u^i}{r} \tag{4.2}$$

where

$$u^i \in \{u \in U \mid \max_{u \in U} U(u) = U(u^i)\}$$

and this set consists of "r" elements.

- **Centre-of-gravity (centroid) procedure**

  The centre of gravity of the fuzzy control U is:

$$u_0 = \frac{\int_u uU(u)du}{\int_U U(u)du} \tag{4.3}$$

  (it is assumed that both the integrals exist). Here, u_0 is determined bearing in mind a surface of the fuzzy set U. In comparison to the max-procedure, it can be observed that $u_0 = g(x)$ has no switching points, but a smooth transition between the control values for different x is visible.

- **Indexed max or centre-of-gravity method**

  Both **Max** and **Centroid** methods have been modified so that u_0 is computed according to

$$u_0 = arg \max_{u \in U(\alpha)} U(u) \tag{4.4}$$

$$u_0 = \frac{\int_{u(\alpha)} uU(u)du}{\int_{U(\alpha)} U(u)du} \tag{4.5}$$

  with

$$U(\alpha) = \{u \in U \mid U(u) \geq \alpha\}$$

  .

  Where α forms a parameter varying as $[0, 1]$. The idea is that the threshold level α allows us to eliminate in the computation of u_0 those elements of the membership function that have non-significant grades of membership function (lower than α), which may cause biased results. This threshold has to be determined with respect to disturbances in the input data and the properties of the process controlled.

4.2.5 Design Parameters of the FLC

In summary. consideration are needed for several principal factors in designing a FLC. The principal factors are listed below:

- fuzzification strategies and the interpretation of a fuzzification operator;
- data base:
    1. discretisation/normalisation of universes of discourse,
    2. fuzzy partition of the input and output spaces,
    3. choice of membership function of a primary fuzzy set;
- rule base:
    1. choice of process state (input) variables and control (output) variables of fuzzy control rules,
    2. source and derivation of control rules,
    3. types of fuzzy control rules (Appendix B);
- decision making logic:
    1. definition of a fuzzy implication (see definition in Appendix B),
    2. definitions of a compositional operator (see definition in Appendix B),
    3. inference mechanism (see definition in Appendix B);
- defuzzification strategies and the interpretation of a defuzzification operator.

4.3 Design of a FLC as a PSS

The design of the FLC as a PSS can be separated into the following four steps:

- **Step 1).** Identify inputs and outputs

Define input and control variables, that is, determine which states of the process should be observed and which control actions are to be taken. When applying a FLC as a PSS, generator speed deviation $\Delta\omega$ and acceleration $\Delta\dot{\omega}$ have been chosen as the input signals of the FLC. The generator speed deviation $\Delta\omega$ can be readily obtained. The acceleration $\Delta\dot{\omega}$ can be obtained from the speed measured at two successive sampling instants using the following equation:

$$\Delta\dot{\omega}(k) = (\Delta\omega(k) - \Delta\omega(k-1))/\Delta T \tag{4.6}$$

where ΔT is the sampling interval. The control variable is the output from the FLC. The control signal from the FLC is fed to the summing junction of the excitation control loop.

- **Step 2).** Define input and output membership functions

This is fuzzification step which includes three sub-steps. Fuzzification strategies and interpretation of a fuzzification operator (fuzzifier), i.e. to transform crisp data into fuzzy sets.

- **Step 2.1).** Specify universe of discourse

Experts define universe of discourse in different ways. Some specify it within a very broad context as the range of all real numbers from minus infinity to positive infinity in units of the input/output variable under consideration. Others limit the universe of discourse to the range of interest to the application at hand.

To specify a universe of discourse for inputs $\Delta\omega$ and $\Delta\dot{\omega}$, the range should be carefully considered. If a specified range is too small, regularly occurring data will be "off scale", which may impact overall system performance. This can be shown in Figure (4.2).

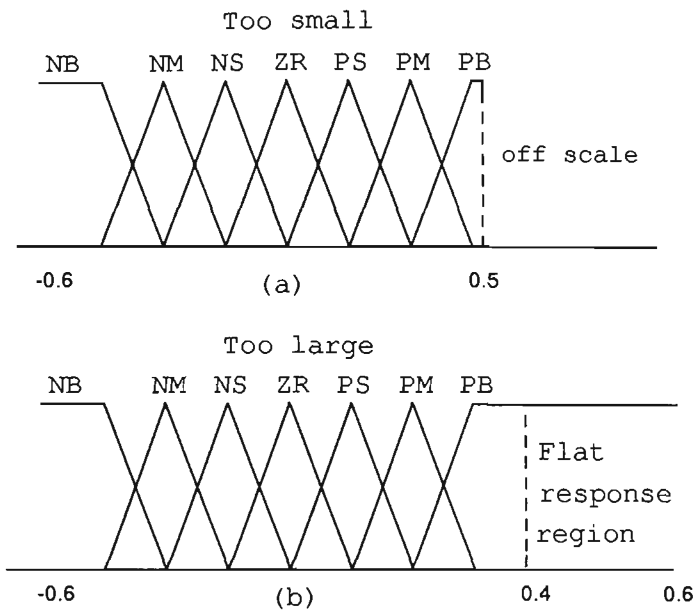

Figure 4.2: Inappropriate universe of discourse

If the top end of the acceleration range (Figure 4.2 (a)) is set at 0.5 instead of 0.6 and the acceleration in the region regularly exceeds that value, the system response will depend on the hardware implementation rather than a well-designed and simulated fuzzy logic model.

Conversely, if the universe of discourse for an input is too large, which is shown in Figure (4.2) (b), the temptation will often be to have large "flat response" membership functions on the right or left to capture the extreme input values. The input will always be fuzzified to the same value for all the acceleration signal higher than 0.4.

When designing a FLC as a PSS, the universe of discourse for speed deviation has been specified to be between -0.05pu and 0.05pu. Correspondingly, the universe of discourse for acceleration has been specified to be between -0.6 and 0.6. The lower and upper limit are both specified considering the effects of both small and large perturbations on the power system.

The range of the universe of discourse for the stabilising signal output must also be carefully considered. Problems will occur if the output universe of discourse is too large. In this case, one or both extremities will be far away from the boundary of "maximum meaningfulness" as shown in Figure (4.3). As with inputs, the

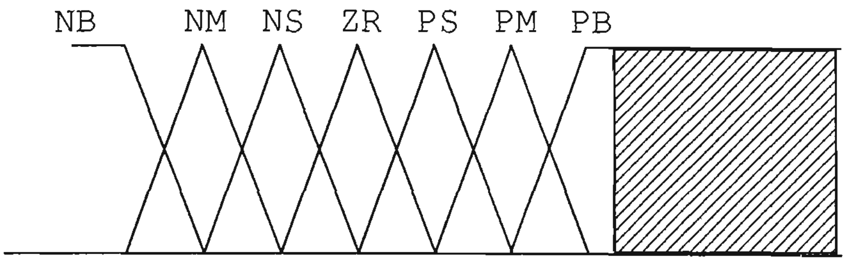

Figure 4.3: Inappropriate output universe of discourse

temptation will be to have large, "flat response" membership functions at each extremity. This problem manifests itself in defuzzification. Such disproportionately large membership functions will overpower the others by lending their entire mass to the defuzzification process. A similar effect can occur when singletons are disproportionately positioned to the extreme left or right. With disproportionately large membership functions, the result of defuzzification will be strongly biased by the mass of the large membership functions. This can be shown in Figure (4.4) in which centroid defuzzification method has been used.

The universe of discourse for the stabilising output signal has been specified evenly to be between -0.8 and 0.8.

- **Step 2.2).** Scale/Normalise universe of discourse

It is usually desirable and often necessary to scale or normalise the universe of discourse of an input or output variable. For example, the speed sensor is used to measure the speed signal from the synchronous machine shaft. The output voltage range from the sensor is between -12V and +12V, representing the corresponding shaft speed or rotor angle. However, the hardware component such as the A/D converter may only be able to accept input voltage between 0 and 5V with an 8bit

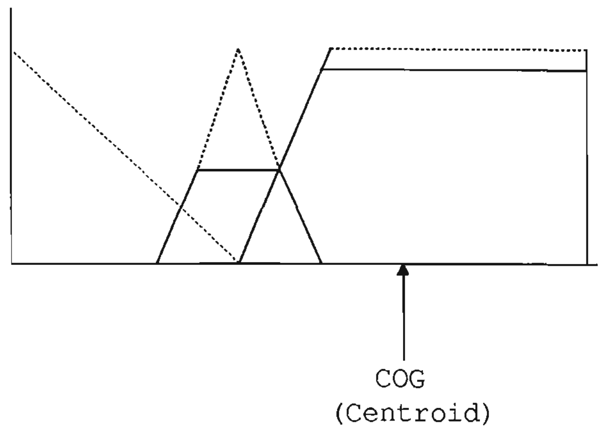

Figure 4.4: Disproportionately large output membership function

resolution. Scaling is thus necessary to map the measured voltage into a different range.

- **Step 2.3).** Determine number and distribution of membership functions:

There are several issues to consider when determining the number of membership functions and their overlap characteristics. The number of membership functions is quite often odd-generally, anywhere from 3 to 9. If too few membership functions have been chosen for a given application, the response may be too lethargic and may fail to provide the output control in time to recover from a small input changes. This may cause the system to oscillate around the desired value. Too many membership functions might rapidly fire different rules for small changes in input values, resulting in large output changes which could cause system instability.

For this FLC design, 7 membership functions have been chosen for both inputs and output.

The most common shapes for membership functions are monotonic, triangular and trapezoidal. Occasionally, bell-shaped MF's are used. These are used to accommodate low-cost implementation hardware. The added smoothness provided by this shape is often not discernible in control applications.

Figure (4.5) shows the proposed functional membership function for the FLC input and output respectively.

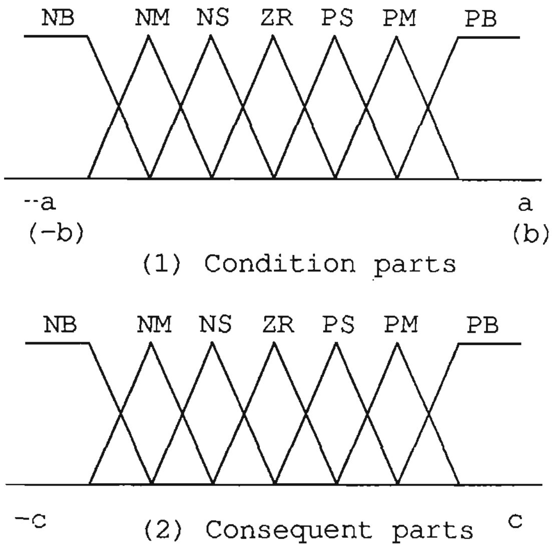

Figure 4.5: Membership functions for both condition parts and consequent parts

Either a numerical definition or functional definition may be used to assign the grades of membership function to the primary fuzzy sets. The choice of grades of membership function is used on the subjective criteria of the decision. In particular, if the measurable data is disturbed by noise, the membership functions should be sufficiently wide to reduce the sensitivity to noise. This states the issue of the fuzziness or, more accurately, the efficiency of a membership function, which affects the robustness of a FLC.

- **Step 3).** Development of the control knowledge base.

The relationship between system inputs and system outputs is important in control engineering. Fuzzy relations describe the relationship between fuzzy input variables and fuzzy output variables of a control system. The fuzzy relations are defined in forms of fuzzy conditional statement. These conditional statements form the decision rule base with a set of control decision rules. Fuzzy control rules can take one of the two basic forms:

1. State based fuzzy control rules

   For a system with linguistic state variables $(s_1, s_2, \cdots, s_n)$ and control u, defined on universes of discourse $(S_1, S_2, \cdots, S_n)$, and U respectively; fuzzy control rules that take the system state (e.g. error, change of error) at time k and evaluates the control action at time k as a function of the system states are of the form:

   $R_i : IF\ s_1\ is\ S_1{}^i, AND\ s_2\ is\ S_2{}^i, \cdots, AND\ s_n\ is\ S_n{}^i$

   $THEN\ u\ is\ f_i(s_1, s_2, \cdots, s_n)$

   for $i = 1, 2, \cdots, n$; where $(S_i{}^j)$ are the linguistic values of the linguistic variables $(s_1, \cdots, s_n)$, and f_i is in general a non-linear function of the multi-input single-output (MISO) system state variables-frequency f_i is linear and in most practical applications $f_i = U_i$ a constant linguistic control qualifier. The connective between the n rules, R_i is **ALSO** (includes union connectives **OR** and **ELSE**). The majority of FLC are based upon a state evaluation rule base.

2. Object evaluation fuzzy control rules

   Object evaluation fuzzy control or predictive fuzzy control, predicts current and future control actions and evaluates control objectives. The control rules are formulated from observing a skilled human operator or from his experience data base, rules are of the general form:

   $R_i : IF\ (u\ is\ U_i \rightarrow (s_1\ is\ S_1{}^i\ AND\ s_2\ is\ S_2{}^i\ AND\ \cdots s_n\ is\ S_n{}^i))$

   $THEN\ u\ is\ U_i$

   for $i = 1, 2, \cdots, n$; that is a control command is inferred from an evaluation of a fuzzy control in achieving the desired system states $\{s_j\}$. The states $\{s_j\}_i$ are considered as cost criteria for assessing the fuzzy rule R_i, taking linguistic values such as 'good', 'poor' or 'bad'. The most suitable control is chosen from prediction $\{s_j\}_i$ corresponding to every control command U_i.

FLC are effective in formulating control actions for systems that are complex, uncertain and have multiple conflicting performance criteria. Whilst the state based fuzzy control rule base does not directly emulate control actions of human operators, its simple structure and strong mathematical basis makes it highly attractive for practical implementation. Hence, when applying a FLC as a power system stabiliser to the excitation control loop, the state based fuzzy control rule base has been utilised. The fuzzy control objective is to enhance the damping characteristics of the power system including its external system through the application of a supplementary stabilising signal to the excitation control loop. Since there are seven linguistic variables describing each of the two inputs, there are a total of 49 decision rules through all possible combination. It is convenient to present these decision rules using a decision table as shown in Table (4.1) [Hsu, 1990].

$\Delta\omega$	$\Delta\dot{\omega}$						
	NB	NM	NS	ZR	PS	PM	PB
PB	**ZR**	**PS**	**PM**	**PB**	**PB**	**PB**	**PB**
PM	**NS**	**ZR**	**PS**	**PM**	**PM**	**PB**	**PB**
PS	**NM**	**NS**	**ZR**	**PS**	**PS**	**PM**	**PM**
ZR	**NM**	**NM**	**NS**	**ZR**	**PS**	**PM**	**PM**
NS	**NB**	**NM**	**NS**	**NS**	**ZR**	**PS**	**PM**
NM	**NB**	**NB**	**NM**	**NM**	**NS**	**ZR**	**PS**
NB	**NB**	**NB**	**NB**	**NB**	**NM**	**NS**	**ZR**

Table 4.1: The decision table

The abbreviation used for linguistic variables above means:

PB: Positive Big

PM: Positive Medium

PS: Positive Small

ZR: Zero

NS: Negative Small

NM: Negative Medium

NB: Negative Big

The idea of a decision table is to provide a summary of reference for given inputs. From the decision table, the control algorithm for the action to be taken using shaft speed and acceleration can be summarised as follows:

- If the speed deviation and the acceleration are **Zero** (in the sense of the linguistic labels), the control applied is **Zero** (also in the sense of the respective linguistic label of control).

- If speed deviation is **Positive Big** and the same as the acceleration, a **Positive Big** control has to be used to reach the state in which the change of speed and the acceleration are reduced to zero. (decelerating control is achieved by applying a positive stabilising signal to the excitation loop, as the electrical output can be increased by the positive stabilising signal).
- If the speed deviation is **Negative Big** and the same holds for the acceleration, the control is set to generate a **Negative** value (i.e., **Negative Big**). (Accelerating control of the study unit can be achieved by applying a negative stabilising signal to the excitation loop, as the electrical output of the study unit can be decreased by the negative stabilising signal).
- ⋮

The control actions in the decision table is symmetric about the main diagonal but in opposite sign. Furthermore, if the number of linguistic variable is increased, the fineness of the control actions is also increased. However, the use of large size of linguistic variable leads to an increase in the number of rules.

- **Step 4)** Determine the stabiliser output by using defuzzification.

The output of the fuzzy controller is a fuzzy set of control. As a power plant usually requires a non-fuzzy value of control, a "defuzzification stage " is needed. The membership function for the control signal was shown previously in Figure (4.5). Different defuzzification methods (described in Section 4.2.4) often give rise to various characteristics of a fuzzy control system. Table (4.2) provides characteristics of a few typical defuzzification methods in terms of memory requirement, speed and output quality [Motorola, 1992].

Note: In Table (4.2), Memory requirement [1]=low and [5]=high, Computational speed [1]=slow and [5]=fast.

Defuzzification method	Characteristics of the crisp output
COG (centroid) (with singleton output membership functions)	Memory requirement[1], Speed [5], Some output fluctuations
COG (centroid) (with non-singleton output membership functions)	Memory requirement [5], Speed [1], Smooth output
Maximum	Memory requirement [2], Speed [1], Optimistic output
Means of Maximum	Memory requirement [4], Speed [3], Optimistic output

Table 4.2: Comparison of the defuzzification methods

The *means of maximum* and *centroid* defuzzification methods have been used in the design of the FLC as a PSS.

4.4 Design of the Proposed Fuzzy Logic Based PSS (FLBPSS)

The proposed Fuzzy Logic Based Power System Stabiliser (FLBPSS) for a synchronous generator connected to an infinite bus utilises new non-linear membership functions to determine the resultant stabilising signal. For the FLBPSS design, the synchronous generator condition can be expressed with the quantities of speed deviation and acceleration in the phase plane. The phase plane is divided into two sectors as shown in Figure (4.6) [Hiyama, 1991].

The required control strategy becomes as follows for the sample point A_1, A_2, A_3 in the sector A.

1. Slight decelerating control should be applied to the study unit at sample point A_1 in sector A to prevent excessive shift of the speed deviation to the positive side because the generator speed is approaching the desired speed from the negative side with relatively high acceleration. Therefore, the stabilising signal should be **Positive Small** at this state.
2. Strong decelerating control should be applied to the study unit at sample point A_2 in sector A because both the generator speed and the accelera-

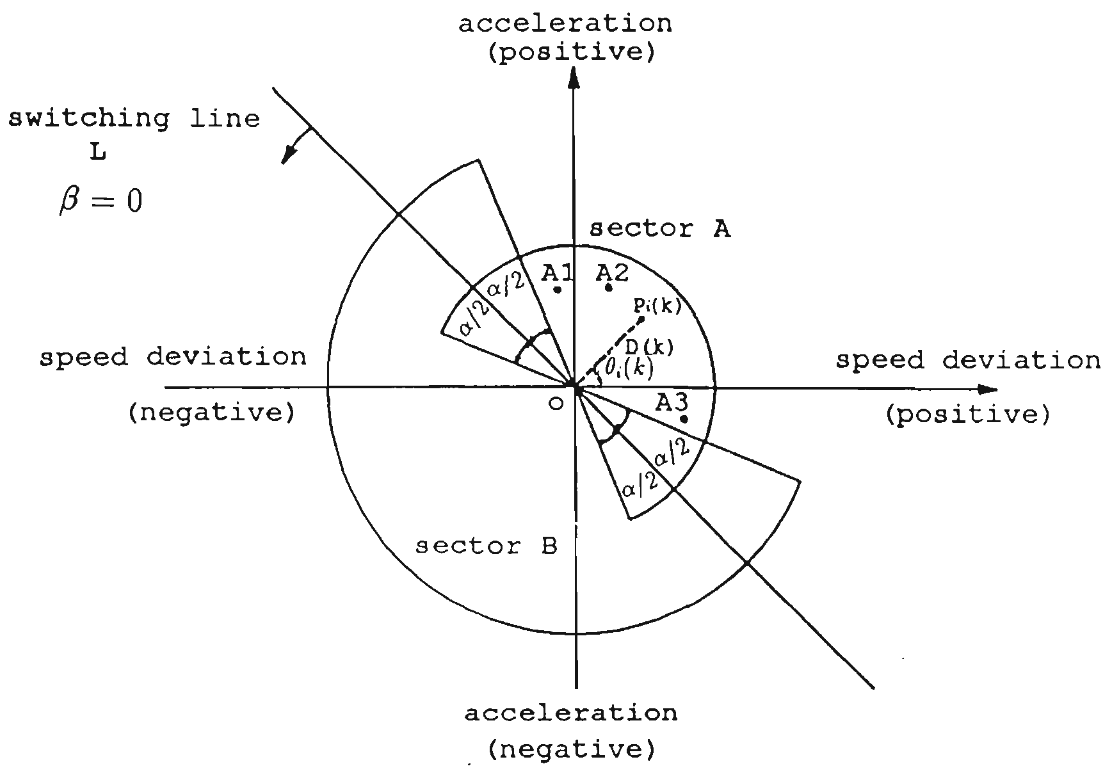

Figure 4.6: Two sectors in the phase plane

tion are relatively large at the positive side. The stabilising signal should be **Positive Big** at this state.

3. Slight decelerating control should be applied to the study unit at point A_3 in sector A to shift the generator speed to the desired one because the study unit is already in the region of slightly higher deceleration, but the generator speed is still large at the positive side. The stabilising signal should be **Positive Small** at this state.

4. In sector B, the situation is completely opposite to those in sector A. Therefore, the control strategy should be reversed. Namely, acceleration control should be applied to the study unit. The stabilising signal should be negative in sector B.

The stabilising signal $U_s(t)$ is given by:

$$U_s(t) = U_s(k), \tag{4.7}$$

for $k\Delta T \leq t < (k+1)\Delta T$ in a discrete form, where k indicates the time $k\Delta T$, and ΔT represents the sample interval. The generator condition at the time $t = k\Delta T$ is given by the point $p(k)$ in the phase plane (Figure 4.6) of speed deviation and acceleration.

$$p(k) = [\Delta\omega(k), \{\Delta\omega(k) - \Delta\omega(k-1)\}/\Delta T] \tag{4.8}$$

The origin in the phase plane is the desired equilibrium point. All the control effort should be directed to moving the current condition $p(k)$ towards the origin as quickly as possible. Angle β represents the position of the switching line L which separates the two sectors A and B. $\beta = 0$ degree corresponds to the switching line placed at $\theta_i(k) = 135$ degrees. β becomes negative if the switching line L is turned clockwise from $\theta_i(k) = 135$ around the equilibrium point O and β becomes positive if the switching line L is turned anti-clockwise. Angle α represents the overlap between sectors A and B and α has been divided equally by the switching line L.

Two new fuzzy non-linear membership functions, $N\{\theta_i(k)\}$ and $P\{\theta_i(k)\}$, are defined for the proposed FLBPSS as shown in Figure (4.7) to represent both the sectors A and B respectively. Figures 4.7 (a) and (b) demonstrate the membership functions corresponding to $\alpha = 90$, $\beta = 0$ degrees and $\alpha = 30$, $\beta = -40$ degrees respectively.

The term $\theta_i(k)$ indicates the phase angle of the point $p_i(k)$ as shown in Figure (4.6). By using these membership functions, the stabilising signal is computed as follows:

$$U_s(k) = \frac{G(k)[N\{\theta_i(k)\}U_{max} - P\{\theta_i(k)\}U_{max}]}{N\{\theta_i(k)\} + P\{\theta_i(k)\}} \tag{4.9}$$

$$U_s(k) = G(k)[2N\{\theta_i(k)\} - 1]U_{max} \tag{4.10}$$

where

$$P\{\theta_i(k)\} = 1 - N\{\theta_i(k)\} \tag{4.11}$$

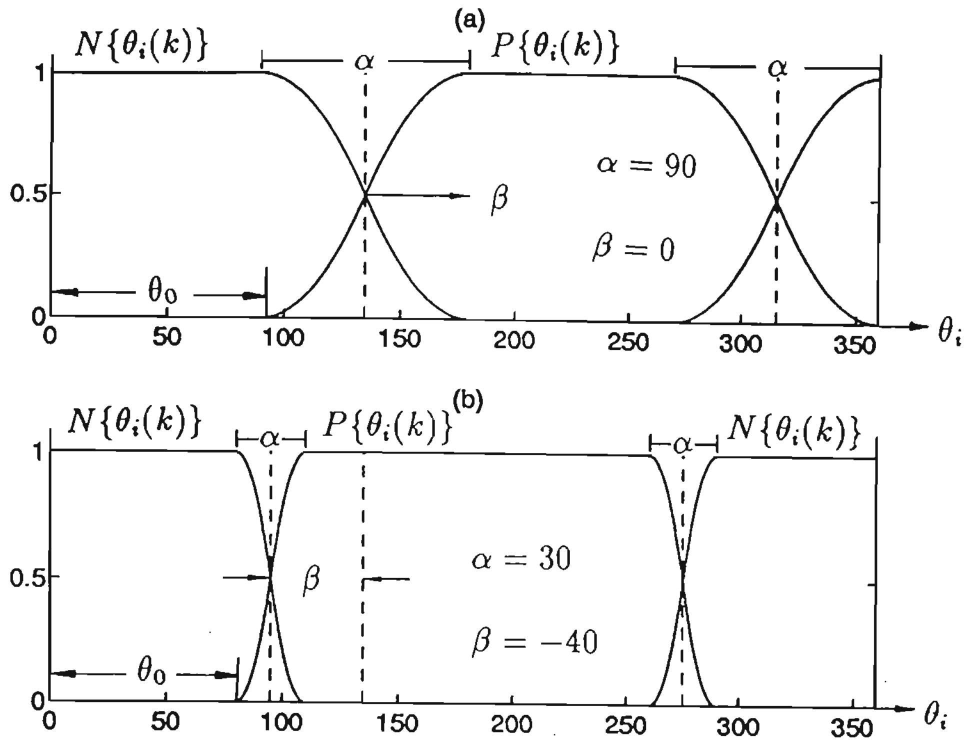

Figure 4.7: The proposed non-linear membership functions

$$G(k) = \begin{cases} D(k)/D_r & \text{for } D(k) < D_r \\ 1.0 & \text{for } D(k) \geq D_r \end{cases} \tag{4.12}$$

$$D(k) = \mid p(k) \mid . \tag{4.13}$$

The term $G(k)$ indicates the gain factor at the time $t = k\Delta T$, and $G(k)$ is given by a non-linear function as shown in Figure (4.8).

The function $P\{\theta_i(k)\}$ as shown in Figure (4.7) can be expressed as follows:

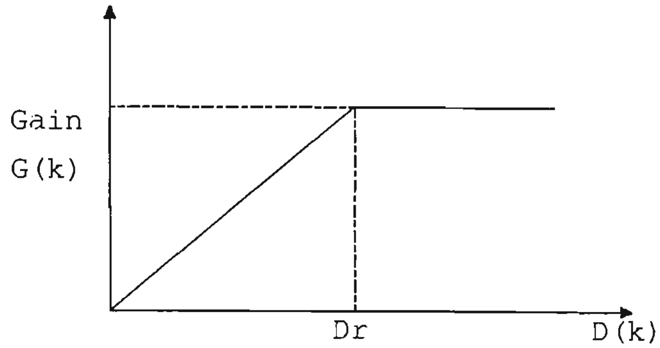

Figure 4.8: Gain factor related to distance $D(k)$

$$P\{\theta_i(k)\} = \begin{cases} 0 & \text{for } 0 \leq \theta_i < \theta_0, \\ 2[\frac{\theta_i - \theta_0}{\alpha}]^2 & \text{for } \theta_0 \leq \theta_i < \theta_0 + \alpha/2, \\ 1 - 2[\frac{\theta_i - (\theta_0 + \alpha)}{\alpha}]^2 & \text{for } \theta_0 + \alpha/2 \leq \theta_i < \theta_0 + \alpha, \\ 1 & \text{for } \theta_0 + \alpha \leq \theta_i < \theta_0 + 180 \ , \\ 1 - 2[\frac{\theta_i - (\theta_0 + 180)}{\alpha}]^2 & \text{for } \theta_0 + 180 \leq \theta_i < \theta_0 + 180 + \alpha/2, \\ 2[\frac{\theta_i - (\theta_0 + 180 + \alpha)}{\alpha}]^2 & \text{for } \theta_0 + 180 + \alpha/2 \leq \theta_i < \theta_0 + 180 + \alpha, \\ 0 & \text{for } \theta_0 + 180 + \alpha \leq \theta_i < 360 \ . \end{cases} \quad (4.14)$$

where all the angles in the above equation are in degrees. The crossover points are $\theta_0 + \alpha/2$ and $\theta_0 + 180 + \alpha/2$.

The parameters to be optimised for the optimal setting of the proposed FLBPSS are the location of the switching line L (i.e., angle β) between the positive and the negative stabilising signals, the size of the cross-sections between the sectors A and B (i.e., angle α) and the distance parameter D_r (Figure 4.6) [Hiyama, 1991]. The maximum value of the stabilising signal U_{max} depends on the generating unit studied.

A performance index J is specified to investigate the time optimality of the study unit. According to the values of the performance index, the optimal setting of the FLBPSS can be determined. Namely, the parameters D_r, α and β can be adjusted to their optimal values by minimising the performance index J.

4.5 Concluding Remarks

The basic structure of a FLC has been described and the design of a FLC as a PSS has been developed. The generator speed $\Delta\omega$ and acceleration $\Delta\dot{\omega}$ have been chosen as the input signals of the FLC. The triangular membership function shape has been chosen for both the input and output signal and the universe of discourse has been specified. A 49 rules decision table has been developed based on the theoretical knowledge. Different defuzzification methods have been introduced and the performance have been compared in terms of memory requirement, speed, etc. However, further tuning and modification of the input and output membership functions and the decision table are necessary in order to provide better performance.

The design of the FLBPSS has been presented and two new non-linear membership functions have been proposed which differ from the ones used in the past. The FLBPSS calculates the resultant stabilising output according to the fuzzy membership functions depending on the speed $\Delta\omega$ and acceleration $\Delta\dot{\omega}$ states of the synchronous generator.

The fine tuning of the proposed FLC membership functions and the optimisation of the parameter values of the proposed FLBPSS will be discussed in detail in the next chapter.

Chapter 5

Optimisation of the Fuzzy Control Strategy

5.1 Introduction

In order to achieve the best performance for the proposed FLC and the FLBPSS, the membership functions, rules or defuzzification method and the parameter settings have to be tuned, adjusted or compared according to a performance index. Two aspects of evaluating the PSS performance are maximum transient deviation and settling time. The performance index is defined as follows:

$$J = \sum_{k=1}^{M} [t_k \Delta\omega(k)]^2 \tag{5.1}$$

The speed deviation $\Delta\omega(k)$ is weighted by the discrete time $t_k = k\Delta T$. M in equation (5.1) stands for the total data number.

Comprehensive sensitivity analysis has been carried out to assess the robustness of the proposed fuzzy controllers for changes in system parameters and under different operating conditions for both small and large perturbations. The comparison study between the proposed FLBPSS and the Self-tuned FLBPSS (STFLBPSS) [Hassan, 1992] has also been investigated. Finally, the proposed two fuzzy control schemes have been evaluated by comparing the performance indices and the dynamic responses.

5.2 Optimisation of the FLC by Observation of Model Behaviour

5.2.1 Optimisation of the FLC using Whole Overlap Ratio (WOR)

Based on observations, the membership functions, rules or defuzzification method have to be tuned for the proposed FLC.

By adjusting the shapes of the membership functions, i.e., by altering the shapes of the fuzzy sets defining the meaning of linguistic values, the performance of the FLC can be improved. The rule of adjusting the membership function is: the greater the control required (i.e. the more sensitive the stabilising signal to input $\Delta\omega$ and $\Delta\dot{\omega}$ changes), the greater the membership function density in that input region. Figure (5.1) shows the membership function for both inputs and output after tuning.

The above membership function adjustment is based on trial and error. In order to improve the efficiency, the choice of a parameter to evaluate the width selection of the membership function is needed. The absolute value of the width is not proper for this goal as it does not compare the width of the separate membership function with the number of classes and the universe of discourse. Marsh [Motorola, 1992] has proposed two indices which meet this demand: the overlap ratio and the overlap robustness. These indices evaluate the width of the membership functions through the overlap of two adjacent functions. The idea is very fruitful because it allows comparison of the scope of the separate membership function with the universe of discourse and the number of classes.

Marsh [Motorola, 1992] considered only linear membership functions and these

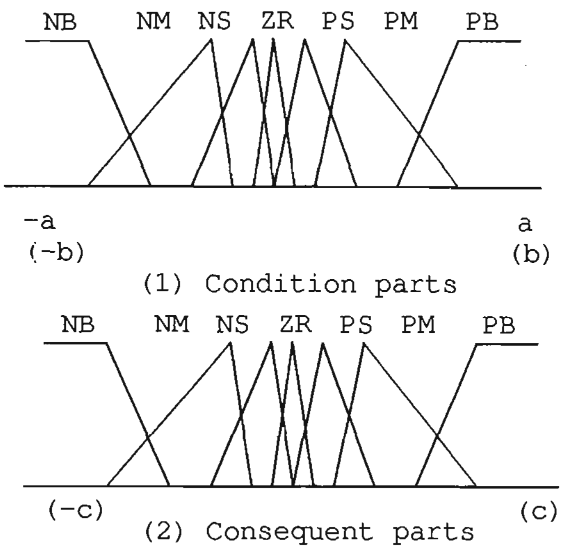

Figure 5.1: Membership functions after tuning

indices work very well in this case. Their disadvantage is that although they can be easily calculated for membership functions with the limited discourse area, they cannot be calculated for functions with the infinite discourse area, for example the exponential (Gaussian) membership function. Moreover, the first index does not depend on the membership function shape at all and the second one depends on the shape in the overlap area only.

For these reasons, the index of the Whole Overlap Ratio (WOR) has been proposed which compares the width of the individual membership function with the universe of discourse and the number of classes [Reznik and Shi, 1993]:

$$WOR = \frac{\int_{-\infty}^{\infty} MIN(\mu_1(x), \mu_2(x))dx}{\int_{-\infty}^{\infty} MAX(\mu_1(x), \mu_2(x))dx} \tag{5.2}$$

where $\mu_1(x)$ and $\mu_2(x)$ are two adjacent membership functions. The evaluation formulas for this index and some usual membership functions are given in Table (5.1).

$F(x) = \frac{1}{\sqrt{2\pi}} \int_{-\infty}^{x} exp(\frac{-u^2}{2})du$ used for deriving the formulas in Table (5.1) is the cumulative distribution function of a standardised normal random variable. Values of x corresponding to values of $F(x)$ can be found in *normal distribution normal*

Membership function	Formula	Whole Overlap Ratio
Linear	$\mu(x) = 1 - abs(\frac{x-m}{\delta})$	$\frac{1}{\frac{2}{(1-\frac{m_2-m_1}{2\delta})^2}-1}$
Exponential (Gaussian)	$\mu(x) = exp[-(\frac{x-m}{\delta})^2]$	$\frac{1}{F(\sqrt{2}\cdot\frac{m_2-m_1}{2\delta})} - 1$
Quadratic	$\mu(x) = max[0, 1 - (\frac{x-m}{\delta})^2]$	$\frac{\frac{2}{3}-\frac{m_2-m_1}{2\delta}+\frac{1}{3}(\frac{m_2-m_1}{2\delta})^3}{\frac{2}{3}+\frac{m_2-m_1}{2\delta}-\frac{1}{3}(\frac{m_2-m_1}{2\delta})^3}$

Table 5.1: Some usual membership functions and WOR evaluation formulas

probability function table [Tuma, 1979].

The detail derivation of the above formulas can be found in Appendix C.

It can be seen that the index of the WOR can be easily calculated in the cases of membership functions with the unlimited discourse area as well as in the cases of simple functions with the limited area. Also it gives us the complete information about the width of membership function comparing it with the number of classes and the area of discourse.

Table (5.2) shows the performance index corresponding to changes of both input and output membership functions WOR in response to a 10% step increase in mechanical torque T_m followed by a 10% step increase in reference voltage V_{ref} and a 10% step decrease in V_{ref}. It can be seen that the FLC gives best performance when the WOR is approximately from 12% to 15%.

Table (5.3) shows the performance index corresponding to changes of both input and output membership functions WOR in response to a 20% step increase in mechanical torque T_m followed by a 20% step increase in reference voltage V_{ref} and a 20% step decrease in V_{ref}. It can be seen that the FLC gives best performance when the WOR is approximately from 12% to 15%.

WOR %	30.95	26.78	24.27	21.95	18.79	15.98	15.12	14.7
J %	*1.36*	*0.96*	*0.73*	*0.70*	*0.66*	*0.58*	*0.54*	*0.51*
WOR %	14.45	14.29	13.48	12.72	11.98	11.27	10.58	9.93
J %	*0.49*	*0.48*	*0.49*	*0.50*	*0.51*	*0.53*	*0.54*	*0.56*
WOR %	9.3	8.7	8.1	7.6	5.1	3.2		
J %	*0.58*	*0.60*	*0.62*	*0.65*	*0.97*	*14.35*		

Table 5.2: The performance index corresponding to changes in WOR (10% step change in T_m and V_{ref})

WOR %	30.95	26.78	24.27	21.95	18.79	15.98	15.12	14.7
J %	*4.31*	*3.51*	*2.82*	*2.79*	*2.74*	*2.63*	*2.58*	*2.54*
WOR %	14.45	14.29	13.48	12.72	11.98	11.27	10.58	9.93
J %	*2.52*	*2.50*	*2.53*	*2.56*	*2.59*	*2.63*	*2.67*	*2.71*
WOR %	9.3	8.7	8.1	7.6	5.1	3.2		
J %	*2.76*	*2.82*	*2.88*	*2.94*	*3.50*	*12.83*		

Table 5.3: The performance index corresponding to changes in WOR (20% step change in T_m and V_{ref})

The *means of maximum* defuzzification method has been used to obtain the performance indices in Table (5.2) and (5.3).

Based on the definitions in Appendix B, many fuzzy implication functions may be generated by utilising the triangular norms and co-norms. For example, by using the definition of the fuzzy conjunction, Mamdani's [Mamdani, 1975] mini-fuzzy implication, R_m, is obtained if the intersection operator is used. Larsen's product fuzzy implication, R_l, is obtained if the algebraic product is used. A method for computing the generalised modus ponens and the generalised modus tollens laws of inference is described in [Baldwin, 1980]. Furthermore, fuzzy implication are also produced by employing bounded product and the drastic product, etc. However, when a FLC has been employed as a PSS in this project, only Mamdani's and Larsen's fuzzy implication methods were adopted.

Different defuzzification methods (Chapter 4 Section 4.2) have also been evaluated using the above performance index under various WOR values with a 20% step increase in mechanical torque T_m .

Table (5.4) shows the performance index corresponding to changes of both input and output membership functions WOR in response to a 20% step increase in mechanical torque T_m. When the *centroid* defuzzification method was used, it can be seen that the FLC gives optimal performance when the WOR is approximately from 12.72% to 14.29%. The same results were obtained with *means of maximum* defuzzification method which are also shown in this table where *Means* stands for *Means of maximum.*

Table (5.5) shows the performance index corresponding to changes of both

WOR %	30.95	24.27	18.79	14.29	13.48	12.72	10.58	7.6
J % (Centroid)	*1.05*	*0.78*	*0.75*	*0.69*	*0.69*	*0.69*	*0.71*	*0.74*
J % (Means)	*1.05*	*0.78*	*0.75*	*0.69*	*0.69*	*0.69*	*0.71*	*0.74*

Table 5.4: The performance index corresponding to changes in WOR with different defuzzification methods (20% step change in T_m)

WOR %	30.95	26.78	24.27	21.95	18.79	14.29	10.58	7.6
J % (Centroid)	*40.24*	*40.00*	*39.48*	*39.51*	*39.58*	*39.78*	*39.77*	*39.81*
J % (Means)	*40.24*	*39.89*	*39.39*	*39.40*	*39.43*	*39.48*	*39.51*	*39.61*

Table 5.5: The performance index corresponding to changes in WOR with different defuzzification methods (three-phase to ground fault)

input and output membership functions WOR in response to a three-phase fault at point A (Figure 2.2) sustained for 125 milliseconds.

From Tables (5.4) and (5.5) it can be seen that the two defuzzification methods gave the same result under small perturbation (20% step change in T_m) and the *means of maximum* defuzzification method performed better in the case of a large perturbation (three-phase to ground fault) condition. Considering the system performance under both small and large perturbations, the best WOR has been chosen as **14.29%** and the defuzzification method chosen is **Means of maximum.**

The implication method utilised to obtain the performance indices in Table (5.2)-(5.5) is *Mamdani* method.

5.2.2 Sensitivity to Nominal Parameter Variations and Robustness to Operating Condition Variations

The nominal operating point of the system is considered with real power $P = 1pu$ and *power factor* of 0.85 (lagging). The sensitivity test was performed by changing the nominal system parameters by $\pm 20\%$ and under different operating conditions and perturbations (small and large). Studies have also been carried out for changes in system parameters like inertia constant H, the d-axis open circuit transient time constant τ'_{do}, and transmission line reactance X_e.

The performance indices according to $J = \sum_{k=1}^{M} [t_k \Delta\omega(k)]^2$ are obtained for

WOR %	30.95	24.27	18.79	**14.29**	10.58	7.6	5.1	3.2
J%($H = 1.2s$)	*1.11*	*0.70*	*0.68*	**0.62**	*0.65*	*0.71*	*0.85*	*24.60*
J%($H = 1s$)	*1.05*	*0.78*	*0.75*	**0.69**	*0.71*	*0.74*	*0.85*	*4.70*
J%($H = 0.8s$)	*1.01*	*0.84*	*0.82*	**0.77**	*0.78*	*0.80*	*0.86*	*2.18*
J%($\tau'_{d0} = 0.414s$)	*1.26*	*0.93*	*0.90*	**0.81**	*0.84*	*0.89*	*1.02*	*3.83*
J%($\tau'_{d0} = 0.345s$)	*1.05*	*0.78*	*0.75*	**0.69**	*0.71*	*0.74*	*0.85*	*4.70*
J%($\tau'_{d0} = 0.276s$)	*0.87*	*0.65*	*0.63*	**0.58**	*0.60*	*0.62*	*0.70*	*6.96*
J%($X_e = 0.48pu$)	*1.17*	*0.87*	*0.84*	**0.77**	*0.79*	*0.83*	*0.93*	*47.62*
J%($X_e = 0.4pu$)	*1.05*	*0.78*	*0.75*	**0.69**	*0.71*	*0.74*	*0.85*	*4.70*
J%($X_e = 0.32pu$)	*1.02*	*0.76*	*0.73*	**0.67**	*0.69*	*0.73*	*0.83*	*2.45*

Table 5.6: The performance index corresponding to changes in WOR (Mamdani, Centroid, 20% step increase in mechanical torque)

WOR %	30.95	24.27	18.79	**14.29**	10.58	7.6	5.1	3.2
J%($H = 1.2s$)	*1.11*	*0.70*	*0.68*	**0.62**	*0.65*	*0.71*	*0.85*	*24.60*
J%($H = 1s$)	*1.05*	*0.78*	*0.75*	**0.69**	*0.71*	*0.74*	*0.85*	*4.70*
J%($H = 0.8s$)	*1.01*	*0.84*	*0.82*	**0.77**	*0.78*	*0.80*	*0.86*	*2.18*
J%($\tau'_{d0} = 0.414s$)	*1.26*	*0.93*	*0.90*	**0.81**	*0.84*	*0.89*	*1.02*	*3.83*
J%($\tau'_{d0} = 0.345s$)	*1.05*	*0.78*	*0.75*	**0.69**	*0.71*	*0.74*	*0.85*	*4.70*
J%($\tau'_{d0} = 0.276s$)	*0.87*	*0.65*	*0.63*	**0.58**	*0.60*	*0.62*	*0.70*	*6.96*
J%($X_e = 0.48pu$)	*1.17*	*0.87*	*0.84*	**0.77**	*0.79*	*0.83*	*0.93*	*47.62*
J%($X_e = 0.4pu$)	*1.05*	*0.78*	*0.75*	**0.69**	*0.71*	*0.74*	*0.85*	*4.70*
J%($X_e = 0.32pu$)	*1.02*	*0.76*	*0.73*	**0.67**	*0.69*	*0.73*	*0.83*	*2.45*

Table 5.7: The performance index corresponding to changes in WOR (Mamdani, Means of maximum, 20% step increase in mechanical torque)

system parameter changes under different values of WOR and different implication and defuzzification methods.

Table (5.6) shows the performance index corresponding to changes of both input and output membership functions WOR in response to a 20% step increase in mechanical torque T_m with system parameter variations using the *Mamdani* implication method and the *Centroid* defuzzification method. It is seen that the WOR value chosen is insensitive to system parameter changes.

Table (5.7) shows the performance index corresponding to WOR values in response to a 20% step increase in mechanical torque with ±20% system parameter variations using the *Mamdani* implication method and the *Means of maximum* defuzzification method.

Table (5.8) shows the performance index corresponding to WOR values in

WOR %	30.95	24.27	18.79	**14.29**	10.58	7.6	5.1	3.2
J%$(H = 1.2s)$	*1.00*	*0.71*	*0.70*	**0.67**	*0.72*	*0.81*	*1.07*	*24.60*
J%$(H = 1s)$	*0.98*	*0.78*	*0.76*	**0.72**	*0.76*	*0.82*	*1.00*	*4.70*
J% $H = 0.8s)$	*0.96*	*0.84*	*0.82*	**0.79**	*0.81*	*0.85*	*0.96*	*2.18*
J%$(\tau'_{d0} = 0.414s)$	*1.17*	*0.93*	*0.91*	**0.86**	*0.91*	*0.99*	*1.20*	*3.83*
J%$(\tau'_{d0} = 0.345s\ )$	*0.98*	*0.78*	*0.76*	**0.72**	*0.76*	*0.82*	*1.00*	*4.70*
J%$(\tau'_{d0} = 0.276s\ )$	*0.81*	*0.65*	*0.63*	**0.61**	*0.63*	*0.68*	*0.80*	*6.96*
J%$(X_e = 0.48pu)$	*1.08*	*0.87*	*0.85*	**0.81**	*0.84*	*0.91*	*1.09*	*47.62*
J%$(X_e = 0.4pu)$	*0.98*	*0.78*	*0.76*	**0.72**	*0.76*	*0.82*	*1.00*	*4.70*
J%$(X_e = 0.32pu\ )$	*0.96*	*0.76*	*0.74*	**0.71**	*0.74*	*0.81*	*0.98*	*2.45*

Table 5.8: The performance index corresponding to changes in WOR (Larsen, Centroid, 20% step increase in mechanical torque)

WOR %	30.95	24.27	18.79	**14.29**	10.58	7.6	5.1	3.2
J%$(H = 1.2s)$	*1.00*	*0.71*	*0.70*	**0.67**	*0.72*	*0.81*	*1.07*	*24.60*
J%$(H = 1s)$	*0.98*	*0.78*	*0.76*	**0.72**	*0.76*	*0.82*	*1.00*	*4.70*
J%$(H = 0.8s)$	*0.96*	*0.84*	*0.82*	**0.79**	*0.81*	*0.85*	*0.96*	*2.18*
J%$(\tau'_{d0} = 0.414s)$	*1.17*	*0.93*	*0.91*	**0.86**	*0.91*	*0.99*	*1.20*	*3.83*
J%$(\tau'_{d0} = 0.345s\ )$	*0.98*	*0.78*	*0.76*	**0.72**	*0.76*	*0.82*	*1.00*	*4.70*
J%$(\tau'_{d0} = 0.276s\ )$	*0.81*	*0.65*	*0.63*	**0.61**	*0.63*	*0.68*	*0.80*	*6.96*
J%$(X_e = 0.48pu)$	*1.08*	*0.87*	*0.85*	**0.81**	*0.84*	*0.91*	*1.09*	*47.62*
J%$(X_e = 0.4pu)$	*0.98*	*0.78*	*0.76*	**0.72**	*0.76*	*0.82*	*1.00*	*4.70*
J%$(X_e = 0.32pu\ )$	*0.96*	*0.76*	*0.74*	**0.71**	*0.74*	*0.81*	*0.98*	*2.45*

Table 5.9: The performance index corresponding to changes in WOR (Larsen. Means of maximum, 20% step increase in mechanical torque)

response to a 20% step increase in mechanical torque with ±20% system parameter variations using the *Larsen* implication method and the *Centroid* defuzzification method.

Table (5.9) shows the performance index corresponding to WOR values in response to a 20% step increase in mechanical torque with ±20% system parameter variations using the *Larsen* implication method and the *Means of max* defuzzification method.

Table (5.10) shows the performance index corresponding to a three-phase to ground fault at A (Figure 2.2) sustained for 125 milliseconds with different WOR values when different implication and defuzzification methods have been used. Here M, L and Means in Table (5.10) stands for *Mamdani, Larsen* and *Means of maximum* respectively.

WOR %	30.95	24.27	18.79	**14.29**	10.58	7.6	5.1	3.2
J%(M,Centroid)	*40.24*	*40.00*	*39.48*	**39.51**	*39.58*	*39.78*	*39.77*	*39.81*
J%(M, Means)	*40.24*	*39.89*	*39.39*	**39.40**	*39.43*	*39.48*	*39.51*	*39.61*
J%(L, Centroid)	*39.34*	*39.17*	*39.08*	**39.09**	*39.13*	*39.40*	*39.49*	*39.68*
J%(L, Means)	*38.84*	*38.80*	*38.81*	**38.82**	*38.87*	*39.15*	*39.30*	*39.56*

Table 5.10: The performance index corresponding to changes in WOR with different implication and defuzzification methods, three-phase to ground fault

Operating condition	P0	P1	P2	P3	P4
Real power	1 pu	0.5 pu	0.8 pu	1.2 pu	1.5 pu
Power factor	0.85 (lag)	0.95 (lag)	0.95 (lag)	0.95 (lag)	0.95 (lag)

Table 5.11: Operating conditions

Similar studies as above have also been conducted under different operating conditions. Those operating conditions are shown in Table (5.11), where P0 is the nominal operating condition used before.

Table (5.12) shows the performance index corresponding to changes of both input and output membership functions WOR in response to a 20% step increase in mechanical torque T_m under different operating conditions with the *Mamdani* implication method. It can be seen that the WOR value chosen works well under various operating conditions.

Table (5.13) shows the performance index corresponding to changes of both input and output membership functions WOR in response to a 20% step increase in mechanical torque T_m under different operating conditions with the *Larsen* implication method. It shows that the WOR value chosen also works well under different operating conditions in this case.

WOR %	30.95	24.27	18.79	**14.29**	10.58	7.6	5.1	3.2
J % ($P0$)	*1.05*	*0.78*	*0.75*	**0.69**	*0.71*	*0.74*	*0.85*	*4.70*
J % ($P1$)	*1.33*	*1.07*	*1.04*	**0.97**	*1.00*	*1.04*	*1.14*	*1.81*
J % ($P2$)	*0.97*	*0.73*	*0.70*	**0.64**	*0.66*	*0.70*	*0.80*	*1.72*
J % ($P3$)	*0.96*	*0.67*	*0.64*	**0.58**	*0.60*	*0.64*	*0.75*	*37.53*
J % ($P4$)	*5.01*	*2.02*	*1.92*	**1.70**	*1.75*	*1.86*	*2.33*	*96.50*

Table 5.12: Performance index corresponding to changes in WOR under different operating conditions (Mamdani, Means of maximum or centroid, 20% step increase in mechanical torque)

WOR %	30.95	24.27	18.79	**14.29**	10.58	7.6	5.1	3.2
J % ($P0$)	*0.98*	*0.78*	*0.76*	**0.72**	*0.76*	*0.82*	*1.00*	*4.70*
J % ($P1$)	*1.26*	*1.08*	*1.06*	**1.02**	*1.05*	*1.12*	*1.25*	*1.81*
J % ($P2$)	*0.91*	*0.73*	*0.71*	**0.68**	*0.71*	*0.78*	*0.92*	*1.72*
J % ($P3$)	*0.88*	*0.67*	*0.65*	**0.62**	*0.63*	*0.73*	*0.91*	*37.53*
J % ($P4$)	*3.37*	*2.01*	*1.92*	**1.79**	*1.89*	*2.18*	*15.84*	*96.50*

Table 5.13: Performance index corresponding to changes in WOR under different operating conditions (Larsen, Means of maximum or centroid, 20% step increase in mechanical torque)

WOR %	30.95	24.27	18.79	**14.29**	10.58	7.6	5.1	3.2
J % ($P0$)	*40.24*	*40.00*	*39.48*	**39.58**	*39.78*	*39.77*	*39.81*	*39.97*
J % ($P1$)	*13.62*	*13.52*	*13.53*	**13.58**	*13.52*	*13.43*	*13.27*	*13.30*
J % ($P2$)	*28.49*	*27.30*	*27.18*	**27.23**	*27.24*	*27.27*	*27.41*	*28.52*
J % ($P3$)	*52.19*	*49.81*	*49.53*	**48.62**	*48.62*	*48.64*	*48.69*	*79.24*
J % ($P4$)	*77.23*	*71.50*	*71.88*	**73.12**	*73.39*	*73.95*	*74.97*	*166.36*

Table 5.14: Performance index corresponding to changes in WOR under different operating conditions (Mamdani, Centroid, three-phase to ground fault)

Table (5.14) shows the performance index corresponding to changes of both input and output membership functions WOR in response to a three-phase fault under different operating conditions with the *Mamdani* implication method and *Centroid* defuzzification method. It can be seen that the WOR value chosen also works well under different operating conditions.

Table (5.15) shows the performance index corresponding to changes of both input and output membership functions WOR in response to a three-phase fault under different operating conditions with *Mamdani* implication method and *means of maximum* defuzzification method. It can be observed that the WOR value chosen also works well under different operating conditions.

WOR %	30.95	24.27	18.79	**14.29**	10.58	7.6	5.1	3.2
J % ($P0$)	*40.24*	*39.89*	*39.39*	**39.43**	*39.48*	*39.51*	*39.61*	*39.82*
J % ($P1$)	*13.63*	*13.53*	*13.54*	**13.58**	*13.53*	*13.44*	*13.29*	*13.32*
J % ($P2$)	*28.38*	*27.09*	*27.05*	**27.23**	*27.23*	*27.26*	*27.43*	*28.53*
J % ($P3$)	*51.32*	*49.33*	*49.15*	**48.46**	*48.55*	*48.66*	*48.33*	*79.83*
J % ($P4$)	*77.23*	*71.70*	*71.95*	**73.17**	*73.48*	*74.03*	*74.79*	*166.36*

Table 5.15: Performance index corresponding to changes in WOR under different operating conditions (Mamdani, Means of maximum, three-phase to ground fault)

5.3 Optimal Setting of the FLBPSS Parameters and Sensitivity Analysis

5.3.1 Optimal Setting of the FLBPSS Parameters

There are several parameters to be adjusted to their optimal values for the FLBPSS. The location of the switching line L (i.e., angle β) between the positive and the negative stabilising signals, the size of the cross-sections between the sectors A and B (i.e., angle α) and the distance parameter D_r (Figure 4.6). The maximum value of the stabilising signal U_{max} depends on the generating unit to be studied.

The parameters α, β and D_r can be adjusted to their optimal values by minimising a performance index J as defined in equation (5.1).

The performance index J has been studied for different values of α, β and D_r under nominal operating condition for both small and large perturbations. Figures (5.2)-(5.5) show the performance index J as a function of α for different values of D_r and a fixed value of β corresponds to a small perturbation of a 20% step increase in mechanical torque T_m. Figures (5.2)-(5.5) illustrate the performance index with $\beta = -35, \beta = -38, \beta = -40$ and $\beta = -42$ degrees respectively. Figures (5.6)-(5.9) show the performance index J as a function of α for different values of D_r and a fixed value of β corresponds to a large perturbation of a three-phase to ground fault at A (Figure 2.2) sustained for 125 milliseconds under nominal operating condition. Figures (5.6)-(5.9) illustrate the performance index with $\beta = -35, \beta = -38, \beta = -40$ and $\beta = -42$ degrees respectively.

Similar studies as above were carried out for $\pm 20\%$ changes in certain system parameters like inertia constant H and open circuit time constant τ'_{d0} under both small and large perturbations. As an example, for $H = 1.2s$ (+20% variation in H), Figures (5.10)-(5.13) show the performance index J as a function of α for different values of D_r corresponds to a small perturbation of 20% step change in mechanical torque T_m with $\beta = -35, \beta = -38, \beta = -40$ and $\beta = -42$ degrees respectively. For $H = 0.8s$ (-20% variation in H), Figures (5.14)-(5.17) show the performance index

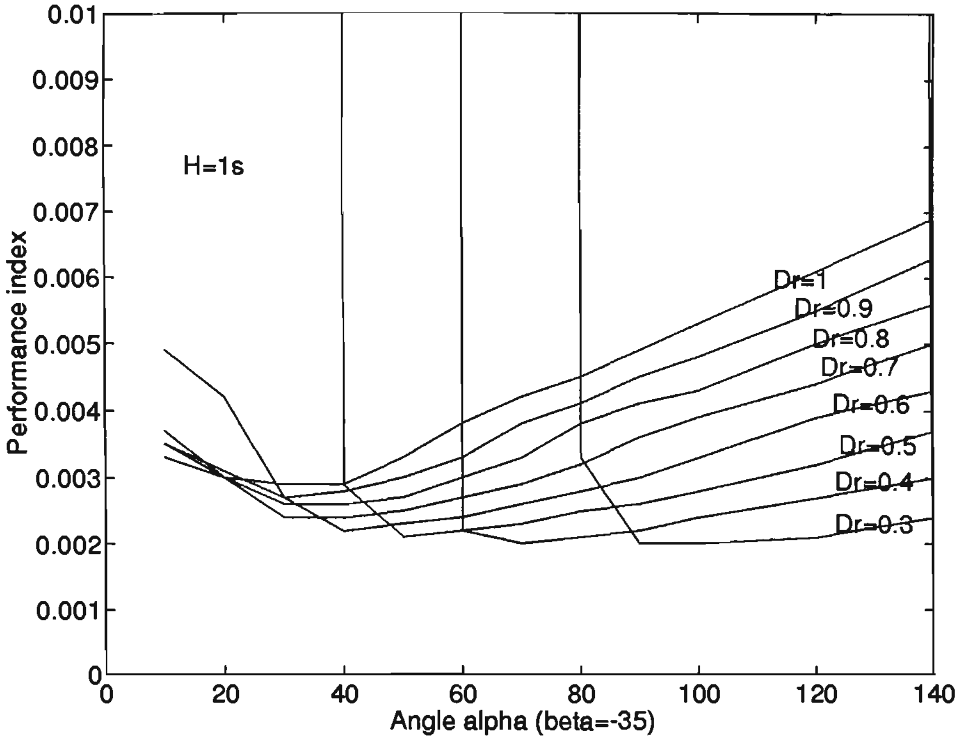

Figure 5.2: Performance index corresponding to α changes $J = f(\alpha)$ with different D_r values under the nominal operating condition for a 20% step change in mechanical torque ($\beta = -35$)

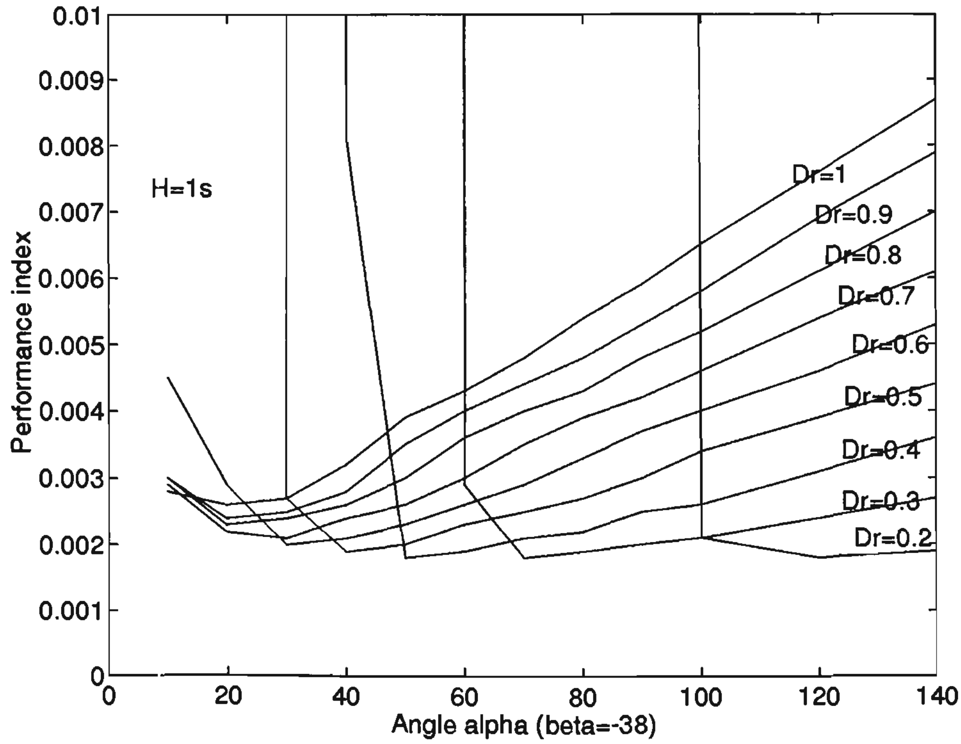

Figure 5.3: Performance index corresponding to α changes $J = f(\alpha)$ with different D_r values under the nominal operating condition for a 20% step change in mechanical torque ($\beta = -38$)

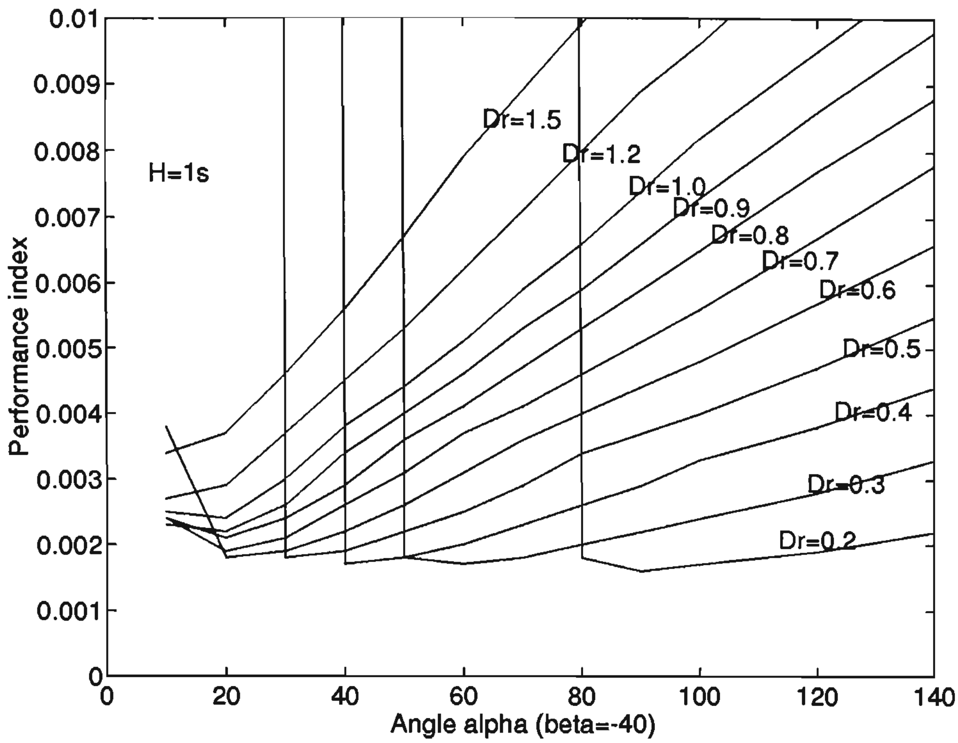

Figure 5.4: Performance index corresponding to α changes $J = f(\alpha)$ with different D_r values under the nominal operating condition for a 20% step change in mechanical torque ($\beta = -40$)

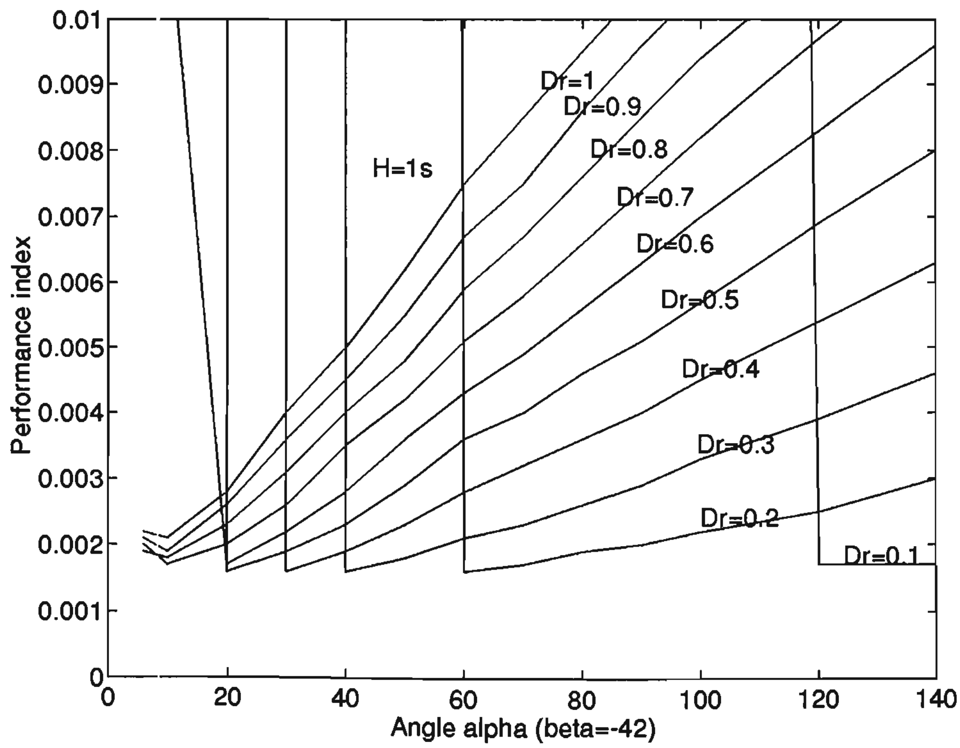

Figure 5.5: Performance index corresponding to α changes $J = f(\alpha)$ with different D_r values under the nominal operating condition for a 20% step change in mechanical torque ($\beta = -42$)

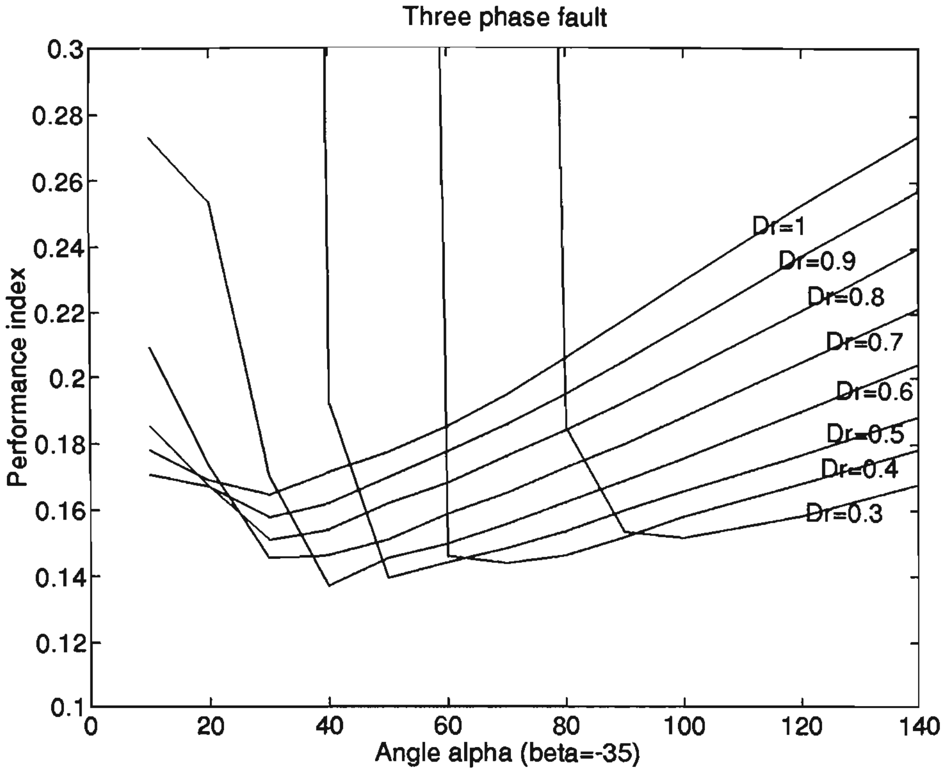

Figure 5.6: Performance index corresponding to α changes $J = f(\alpha)$ with different D_r values under the nominal operating condition in response to a three-phase to ground fault ($\beta = -35$)

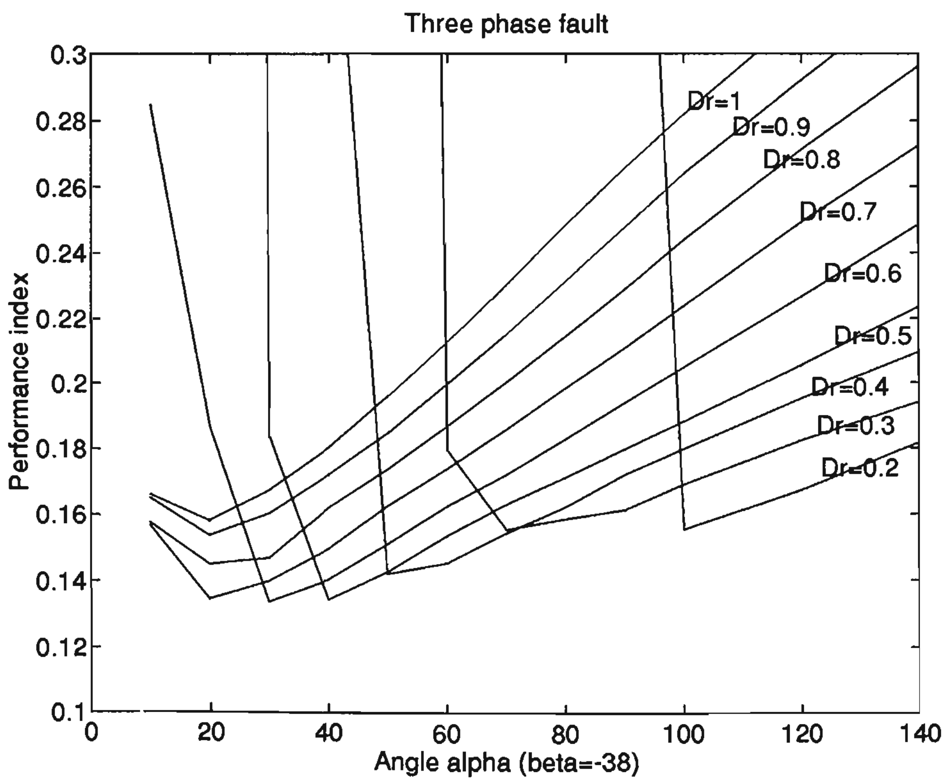

Figure 5.7: Performance index corresponding to α changes $J = f(\alpha)$ with different D_r values under the nominal operating condition in response to a three-phase to ground fault ($\beta = -38$)

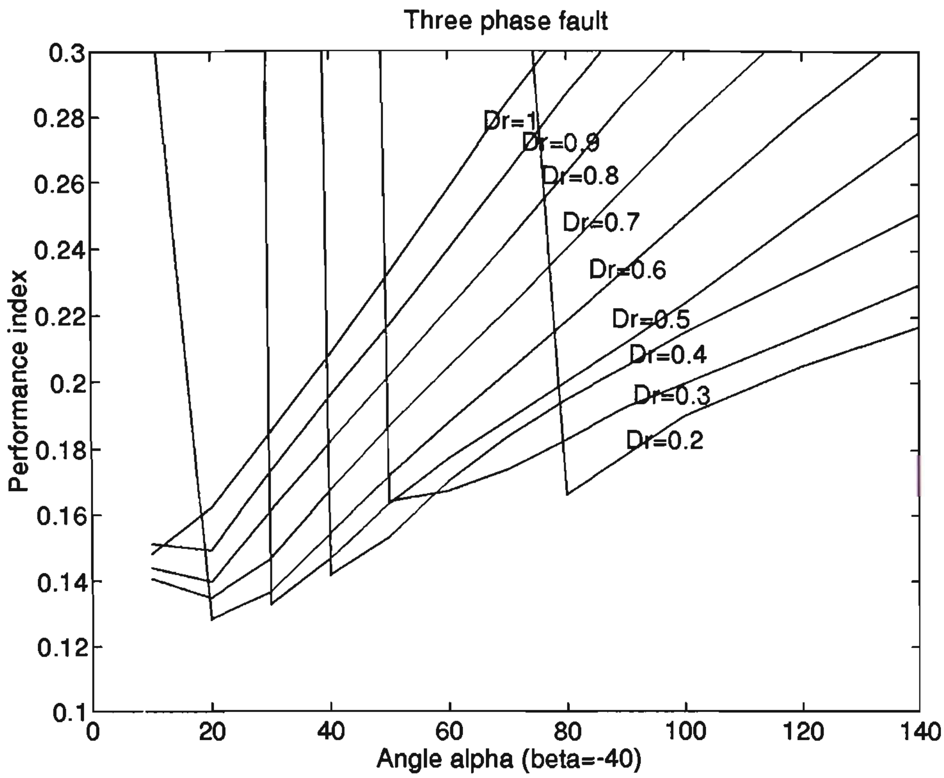

Figure 5.8: Performance index corresponding to α changes $J = f(\alpha)$ with different D_r values under the nominal operating condition in response to a three-phase to ground fault ($\beta = -40$)

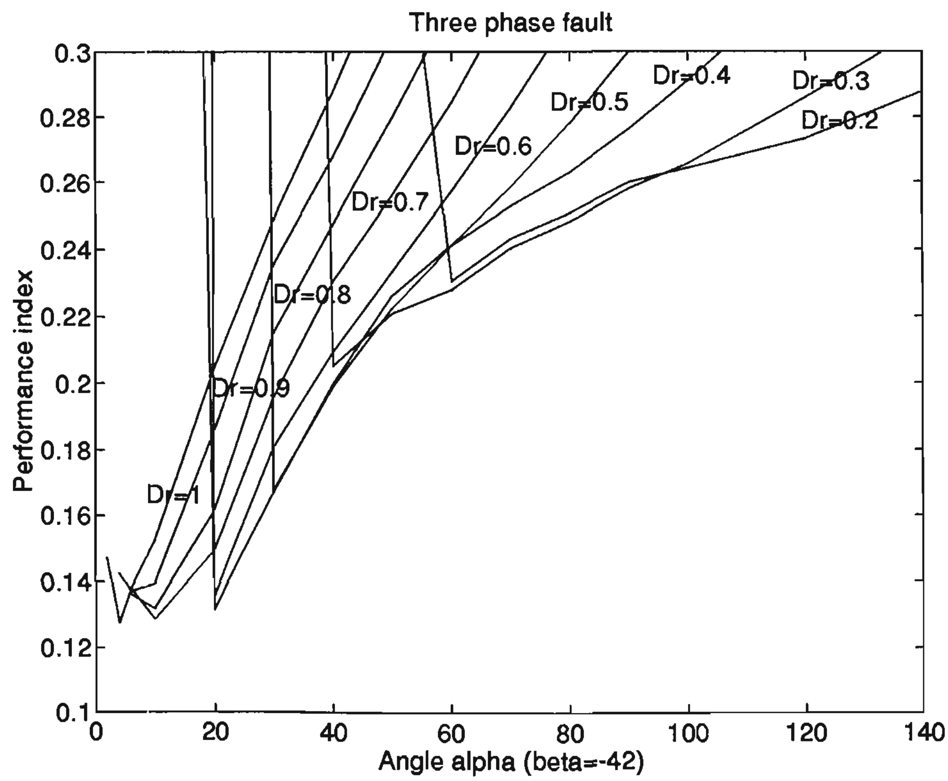

Figure 5.9: Performance index corresponding to α changes $J = f(\alpha)$ with different D_r values under the nominal operating condition in response to a three-phase to ground fault ($\beta = -42$)

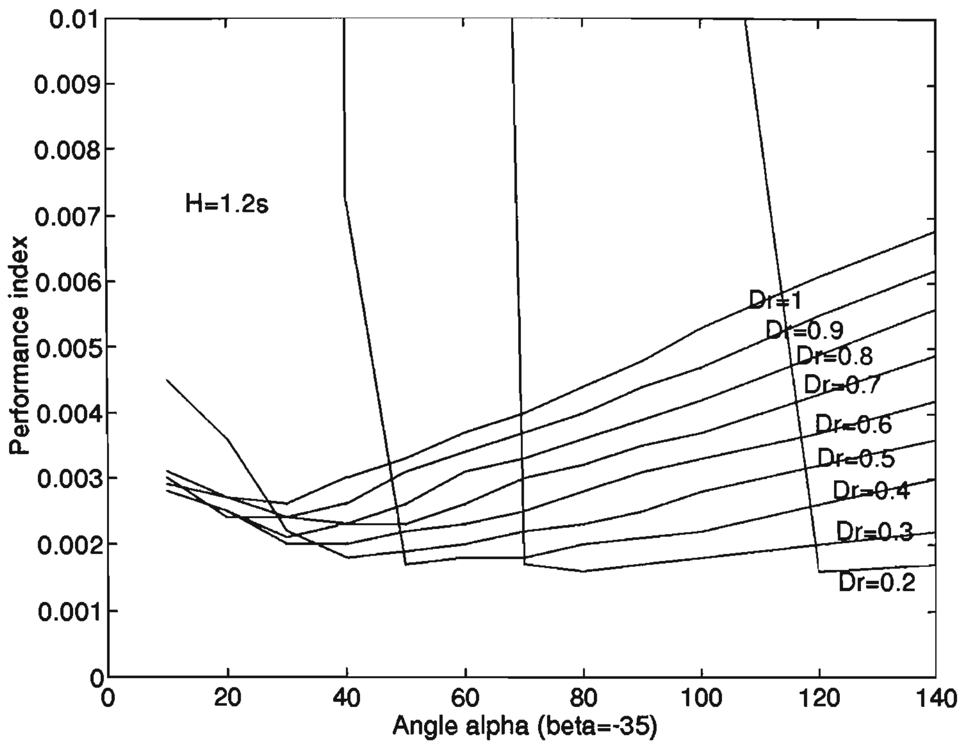

Figure 5.10: Performance index corresponding to α changes $J = f(\alpha)$ with different D_r values and +20% variation in inertia constant H for a 20% step change in mechanical torque ($H = 1.2s, \beta = -35$)

J as a function of α for different values of D_r corresponds to a small perturbation of a 20% step change in mechanical torque T_m with $\beta = -35, \beta = -38, \beta = -40$ and $\beta = -42$ degrees respectively.

The minimum value of the performance index J can be found easily from the above figures and plots of such figures for a large range of β are shown in Figures (5.18) and (5.19) respectively. Figure (5.18) shows all the minima versus β for a nominal operating point and a ±20% change in inertia constant H under a small perturbation of 20% step change in mechanical torque T_m. Figure (5.19) shows the case for the nominal operating condition under a large perturbation of a three-phase fault.

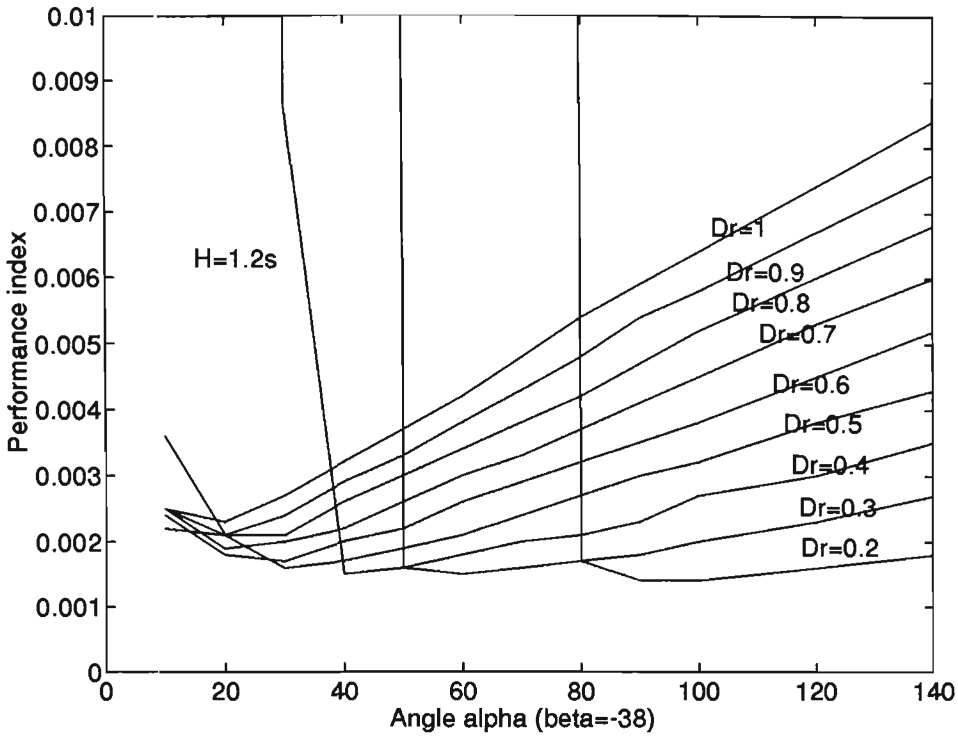

Figure 5.11: Performance index corresponding to α changes $J = f(\alpha)$ with different D_r values and +20% variation in inertia constant H for a 20% step change in mechanical torque $(H = 1.2s, \beta = -38)$

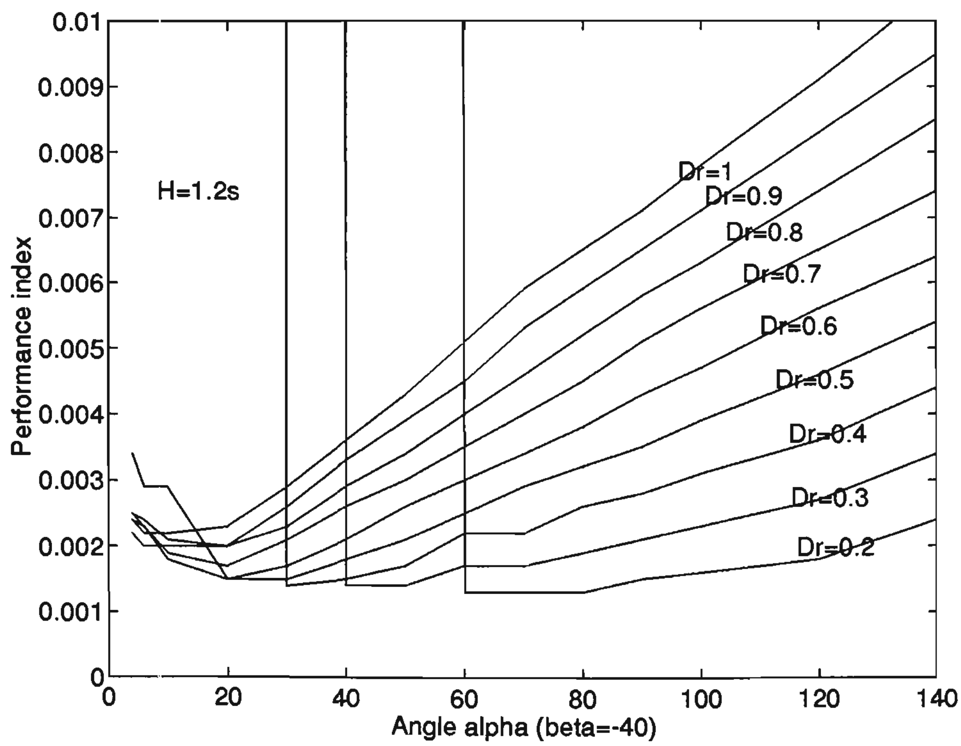

Figure 5.12: Performance index corresponding to α changes $J = f(\alpha)$ with different D_r values and +20% variation in inertia constant H for a 20% step change in mechanical torque $(H = 1.2s, \beta = -40)$

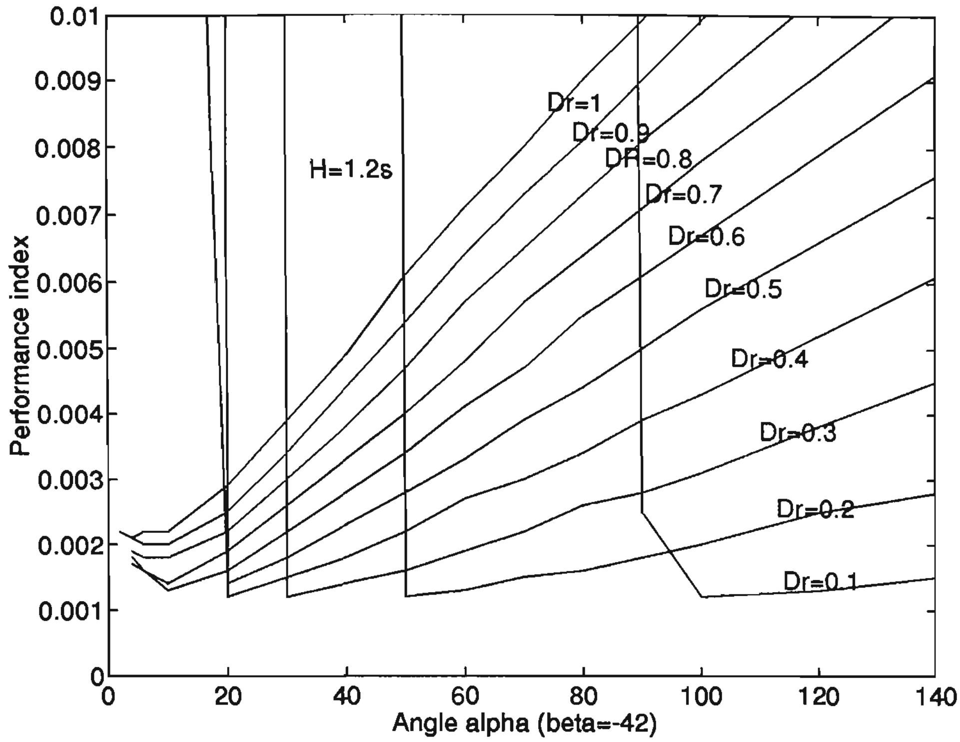

Figure 5.13: Performance index corresponding to α changes $J = f(\alpha)$ with different D_r values and +20% variation in inertia constant H for a 20% step change in mechanical torque ($H = 1.2s, \beta = -42$)

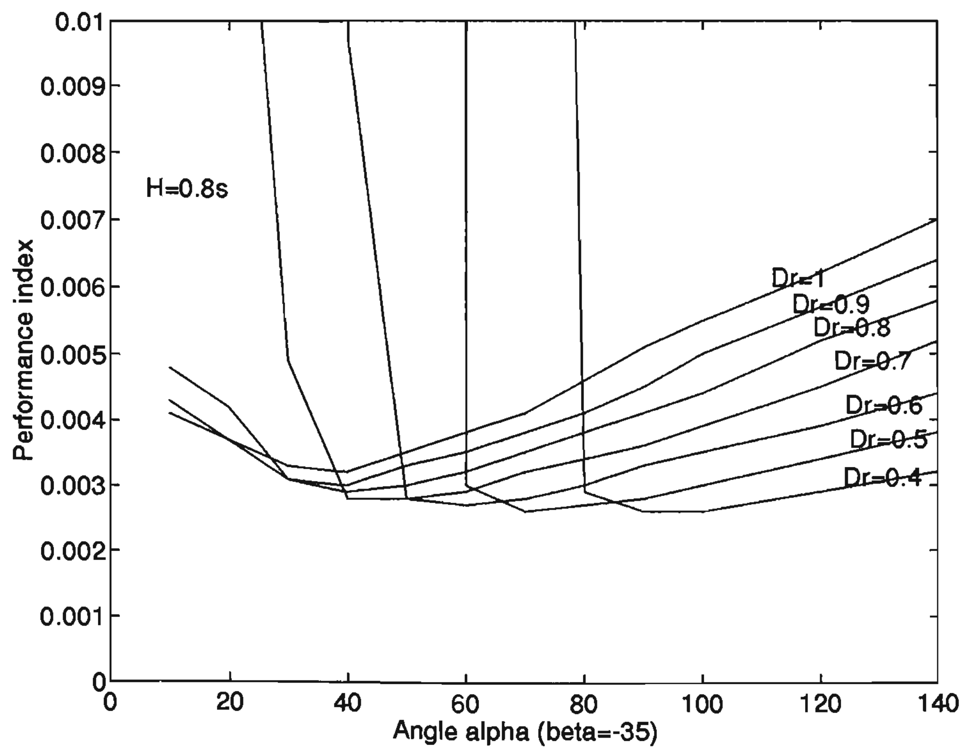

Figure 5.14: Performance index corresponding to α changes $J = f(\alpha)$ with different D_r values and -20% variation in inertia constant H for a 20% step change in mechanical torque ($H = 0.8s, \beta = -35$)

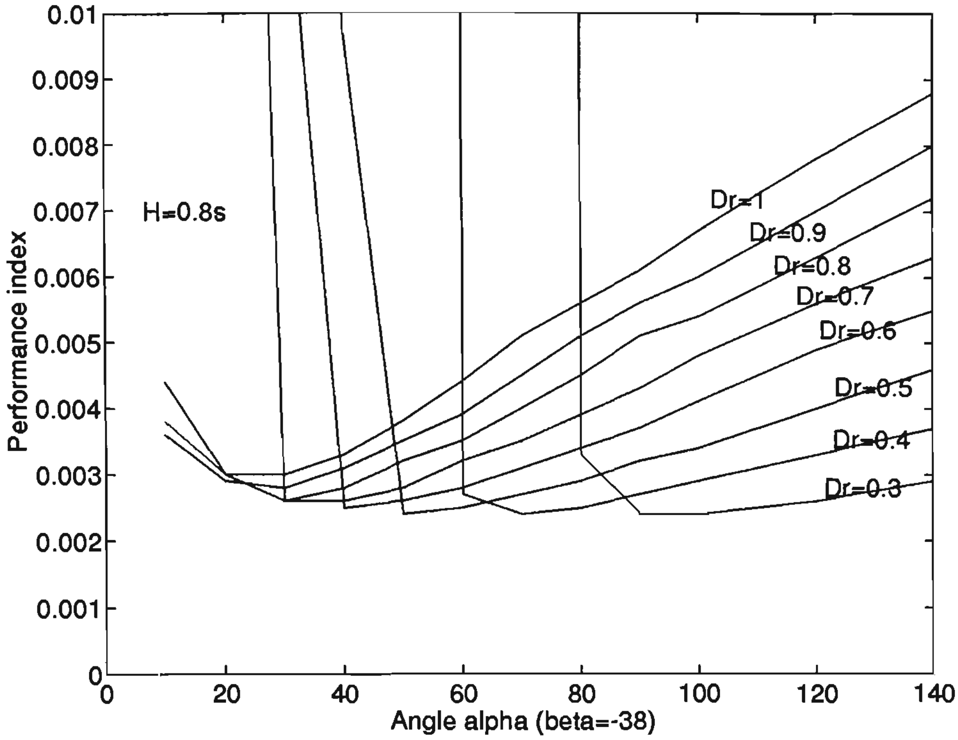

Figure 5.15: Performance index corresponding to α changes $J = f(\alpha)$ with different D_r values and -20% variation in inertia constant H for a 20% step change in mechanical torque ($H = 0.8s, \beta = -38$)

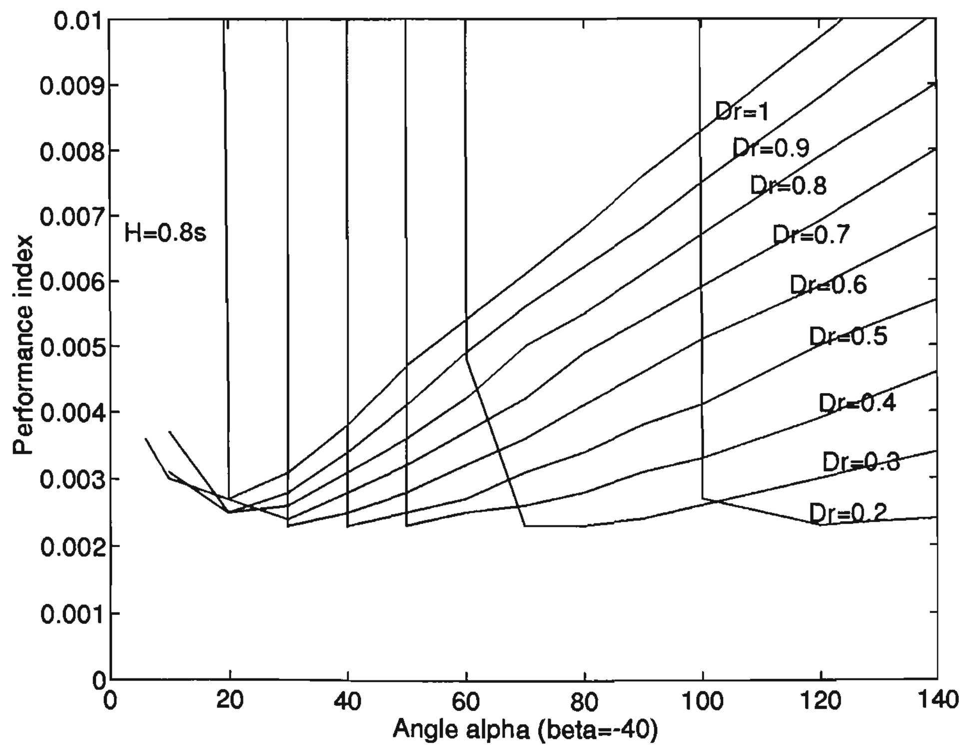

Figure 5.16: Performance index corresponding to α changes $J = f(\alpha)$ with different D_r values and -20% variation in inertia constant H for a 20% step change in mechanical torque ($H = 0.8s, \beta = -40$)

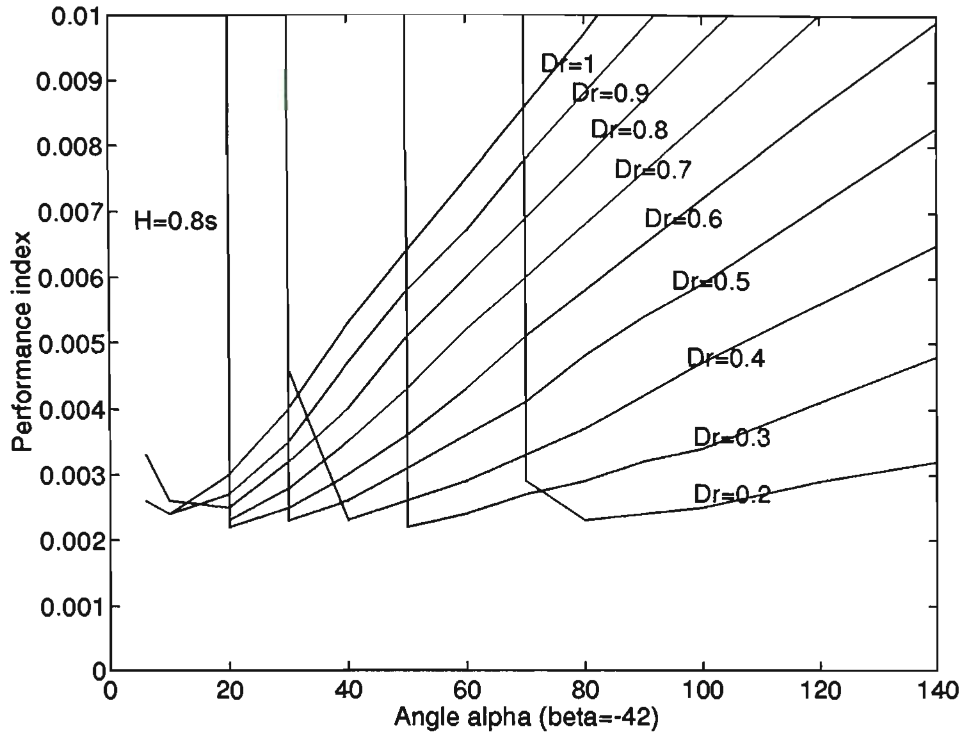

Figure 5.17: Performance index corresponding to α changes $J = f(\alpha)$ with different D_r values and -20% variation in inertia constant H for a 20% step change in mechanical torque ($H = 0.8s, \beta = -42$)

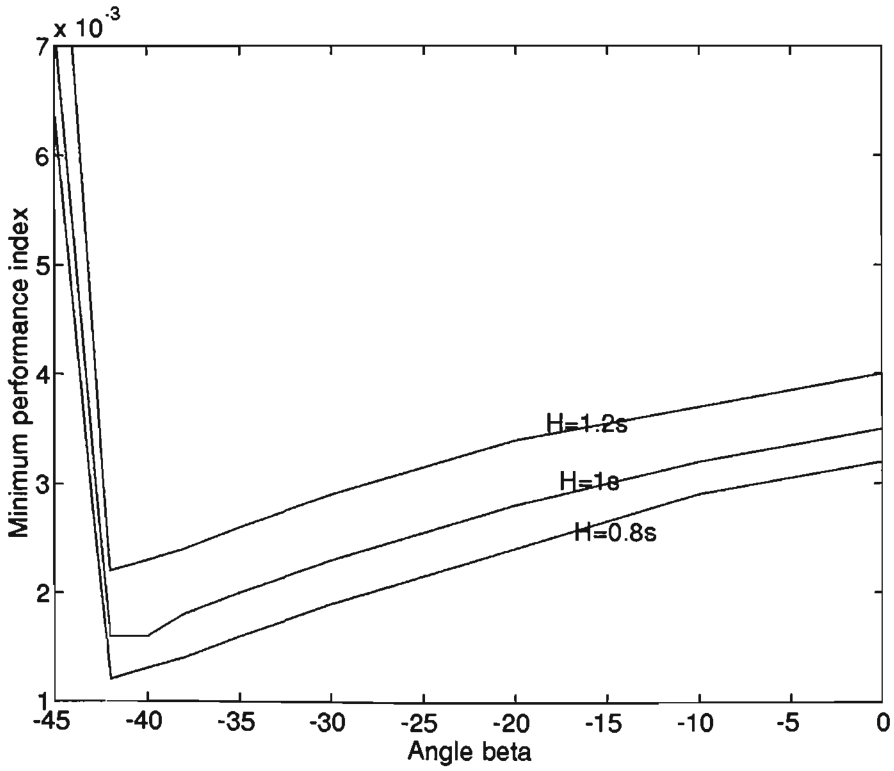

Figure 5.18: Minimum performance index corresponding to changes in β values $J_{min} = f(\beta)$ (20 % step increase in mechanical torque)

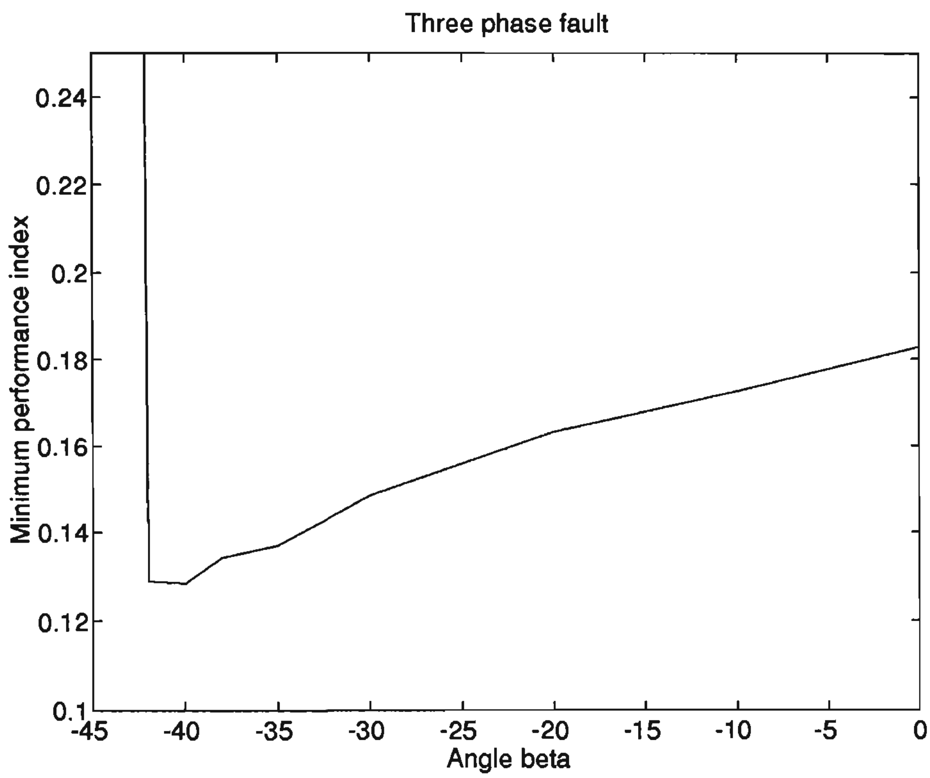

Figure 5.19: Minimum performance index corresponding to changes in β values $J_{min} = f(\beta)$ (three-phase to ground fault)

From the above figures it can be seen that the optimal performance can be achieved with $\beta = -42$ degrees. However, it is seen that when β decreases marginally from -42 degrees the performance index becomes very high resulting in system instability. In order to provide a larger stability margin β is set to -40 degrees.

On further examining Figures (5.4) and (5.8) for the chosen $\beta = -40$, it is seen that for a given value of D_r, starting from a higher value of α, as α decreases, the performance index J decreases, then starts increasing and abruptly becomes very high indicating instability.

All the minima for a different D_r in Figures (5.4) and (5.8) do not differ much from each other and studies also reveal that there is not much difference in the dynamic responses for such values. As an example, there is hardly any difference in the dynamic responses for two J_{min} (Figure 5.4) corresponding to $D_r = 0.2$ and 0.3. This is corroborated by a plot of the responses shown in Figure (5.20).

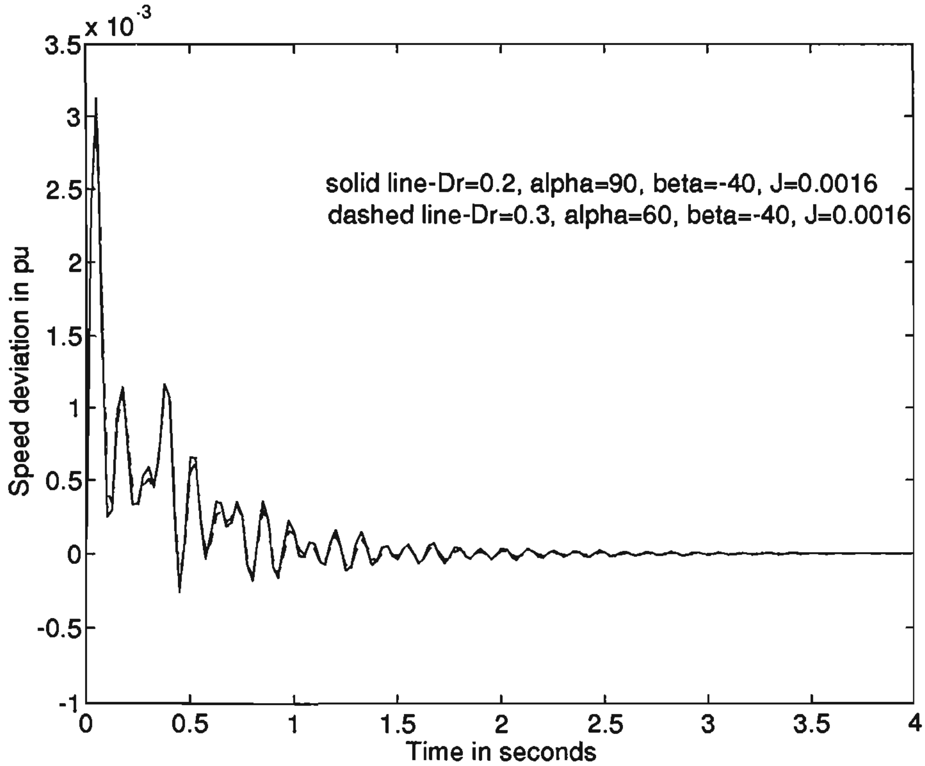

Figure 5.20: System response corresponding to a 20% step change in T_m under two optimal settings

Figure (5.8) shows the overall minimum J is achieved for the settings: $D_r = 0.6, \beta = -40$ and $\alpha = 20$. Since a value of α little less than 20 can provide instability because of high value of J, it is safer to choose for the three-phase fault situation a value of α somewhat greater than 20.

Considering Figures (5.4) and (5.8) for both small and large perturbations comprehensively, the optimal parameter settings can be chosen as $D_r = 0.6, \beta = -40$ and $\alpha = 30$.

The optimal setting of α, β and D_r obtained by applying large perturbations such as a three-phase fault works well for a small perturbations of 20% step change in T_m , and vice versa. This is verified in Figure (5.21). Figure (5.21) shows (a) the system dynamic response under a 20% step change in mechanical torque T_m and (b) the response under a three-phase to ground fault sustained for 125 milliseconds.

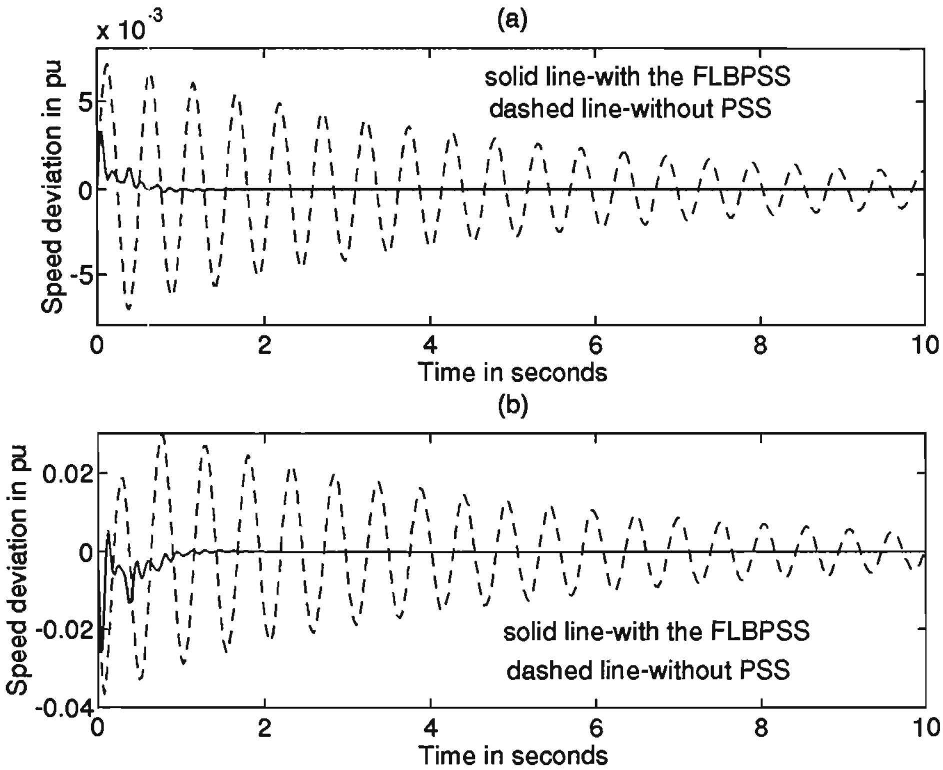

Figure 5.21: System response corresponding to a 20% step change in T_m and a three-phase to ground fault, (a)-20% step increase in mechanical torque, (b)-three-phase to ground fault

5.3.2 Robustness to Operating Condition Variations and Sensitivity to Nominal Parameter Variations

The nominal operating point of the system is considered with real power $P = 1pu$ and *power factor* of 0.85 (lagging) for which the optimal settings of the FLBPSS have already been determined as $D_r = 0.6, \beta = -40$ and $\alpha = 30$. It is intended to investigate whether this optimal setting needs to be changed with changes in system operating conditions and parameters.

The performance of the proposed FLBPSS is studied under different operating conditions given in Table (5.11). Similar procedure has been adopted as described in the last section to obtain the optimal settings of α, β and D_r for these operating conditions. As an example, Figures (5.22)-(5.25) show the performance index J as a function of α for different value of D_r and a fixed value of β corresponds to small and large perturbations under operating conditions P1 and P4 respectively.

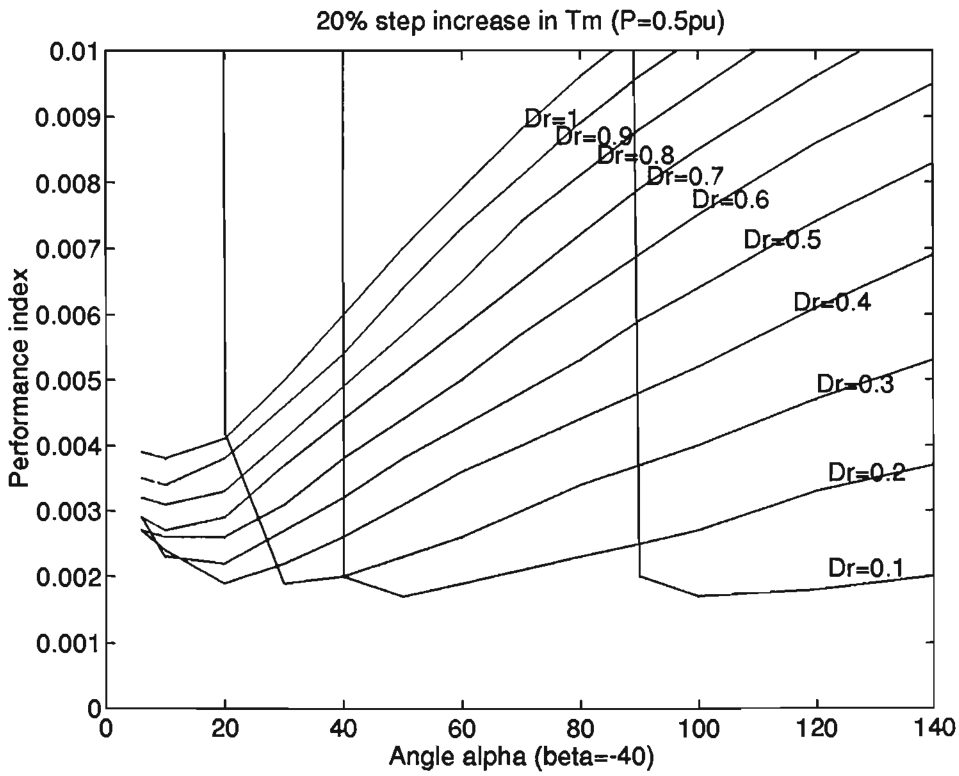

Figure 5.22: Performance index corresponding to changes in α $J = f(\alpha)$ with different D_r values in response to a 20% step increase in T_m under operating condition P1 ($\beta = -40$)

The optimal settings of α, β and D_r for these operating conditions are given

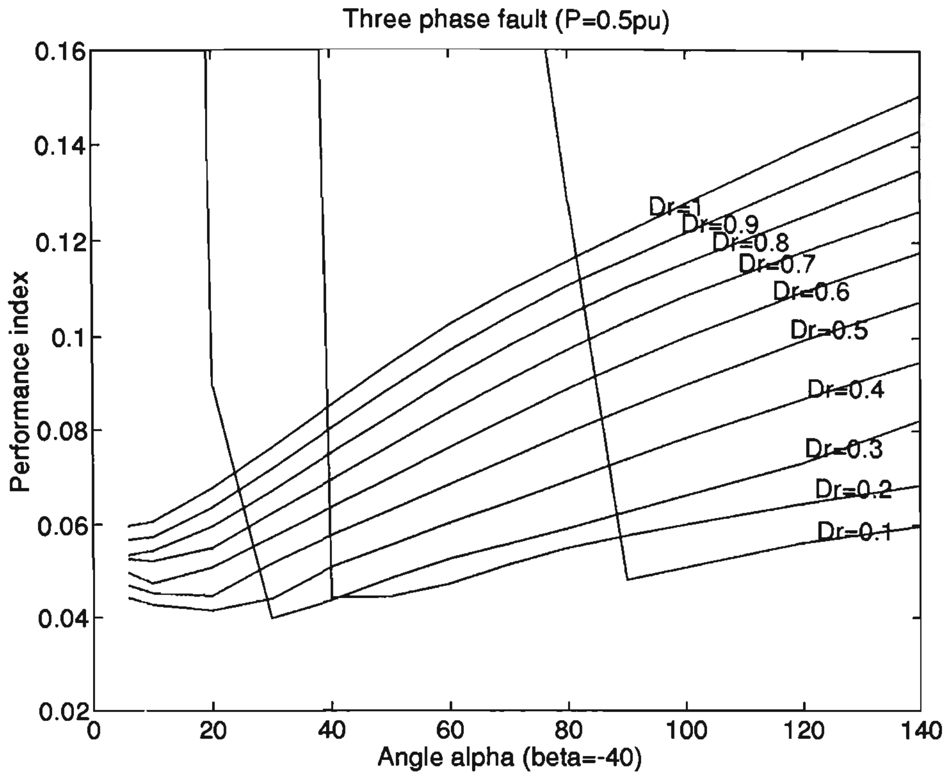

Figure 5.23: Performance index corresponding to changes in α $J = f(\alpha)$ with different D_r values in response to a three-phase fault under operating condition P1 ($\beta = -40$)

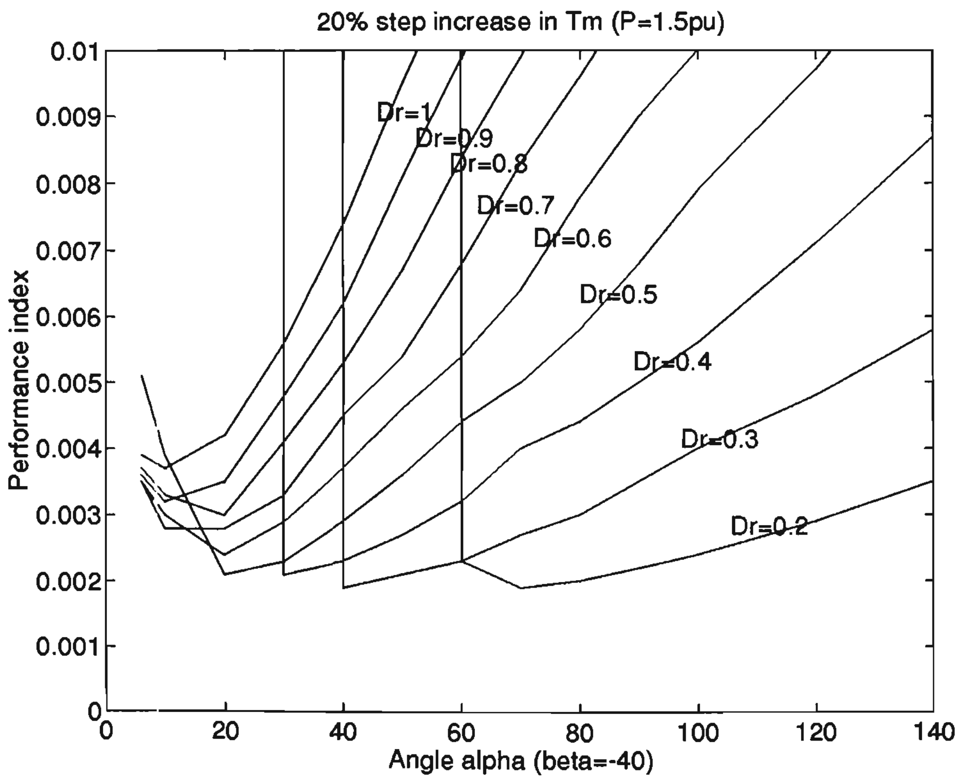

Figure 5.24: Performance index corresponding to changes in α $J = f(\alpha)$ with different D_r values in response to a 20% step increase in T_m under operating condition P4 ($\beta = -40$)

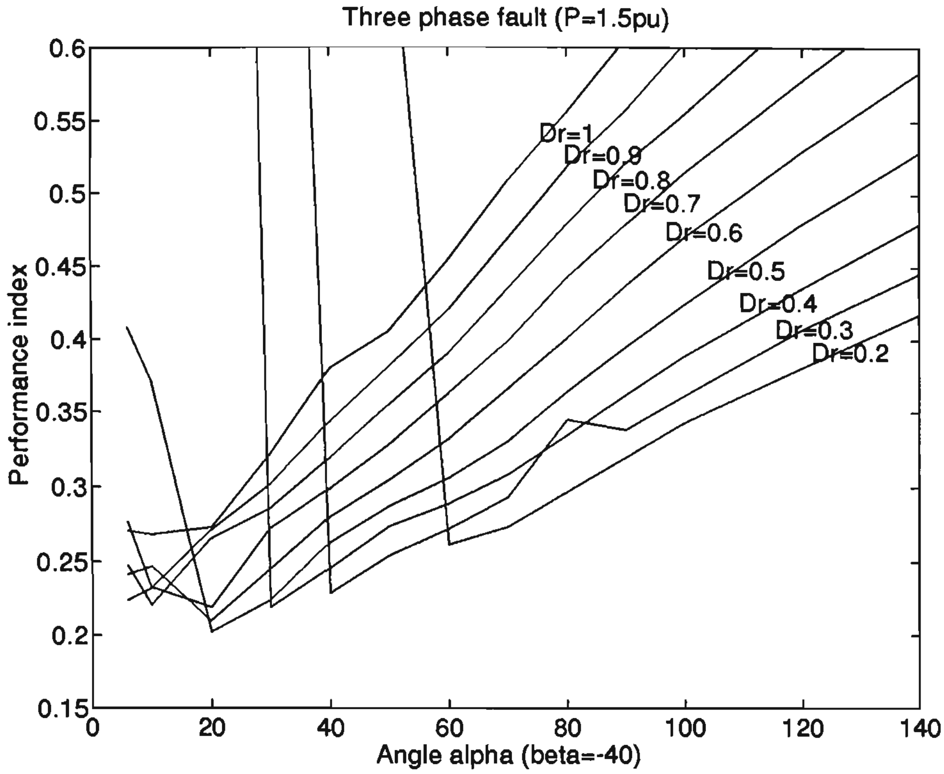

Figure 5.25: Performance index corresponding to changes in α $J = f(\alpha)$ with different D_r values in response to a three-phase fault under operating condition P4 ($\beta = -40$)

OC	P0	P1	P2	P3	P4
Optimal α	**30**	**20**	**30**	**30**	**20**
Optimal β	**-40**	**-40**	**-40**	**-40**	**-40**
Optimal D_r	**0.6**	**0.4**	**0.5**	**0.6**	**0.6**

Table 5.16: Optimal settings of the FLBPSS for different operating conditions

in Table (5.16).

Studies reveal that the optimal values of α, β and D_r obtained at the nominal operating condition works well for wide variation in the operating conditions under both small or large perturbations. As an example, Figures 5.26(a) and 5.26(b) give system responses for an operating condition P4 with its optimal setting of $\alpha = 20$, $\beta = -40$ and $D_r = 0.6$ (solid line) and the nominal optimal setting of $\alpha = 30$, $\beta = -40$ and $D_r = 0.6$ (dashed line) for a small perturbation of 20% step change in mechanical torque and a large perturbation of three-phase fault at A (Figure 2.2) sustained for 125 milliseconds respectively.

Similar studies as aforementioned were carried out for ±20% changes in certain system parameters like inertia constant H and open circuit time constant τ'_{d0} under both small and large perturbations. Examination of the dynamic responses reveal that the nominal optimal setting of α, β and D_r need not be changed following such changes in system parameters. As an example for $H = 1.2s$, Figure 27(a) provides the dynamic responses under 20% change in mechanical torque and Figure 27(b) provides the responses for a three-phase fault corresponding to both nominal operating setting and the corresponding optimal setting.

Figure (5.28) shows the system response corresponding to a three-phase fault at A (Figure 2.2) sustained for 125 milliseconds under different operating conditions using nominal optimal setting. Figure (5.28) (a) are the results under operating condition P0, P1, P2 and P4 with the proposed FLBPSS. The system response under operating condition P3 with and without the FLBPSS are shown in Figure (5.28) (b).

Figure (5.29) (a) and (b) shows the system response with ±20% change in inertia constant H and d-axis open circuit transient time constant τ'_{d0} respectively for a 20% step increase in T_m using the nominal optimal setting.

5.4 Comparison of the Proposed FLBPSS and Hassan's Self-tuned FLBPSS

5.4.1 Review of Hassan's Self-tuned FLBPSS (STFLBPSS)

Hassan et al [Hassan, 1992], [Hassan, 1993a], [Hassan, 1993b] have suggested a self-tuned FLBPSS (STFLBPSS) whose performance has been shown to be better than that of the FLBPSS proposed by Hiyama et al [Hiyama, 1991]. In this work, it is intended to compare the performance of the proposed FLBPSS with that of the STFLBPSS of Hassan et al.

The significant differences in the design concept of the STFLBPSS and the proposed FLBPSS are the following:

1. The proposed FLBPSS uses different membership functions (Figure 4.7) than those used by Hassan et al (Figure 5.30) [Hassan, 1992];

   The membership functions shown in Figure (5.30) are defined below:

$$S(x;a,b,c) = \begin{cases} 0.0 & \text{for } x \le a \\ 2[(x-a)/(c-a)]^2 & \text{for } a < x \le b \\ 1 - 2[(x-c)/(c-a)]^2 & \text{for } b < x < c \\ 1 & \text{for } x \ge c \end{cases} \tag{5.3}$$

$$\Pi(x;B,C) = \begin{cases} S(x;C-B, C-B/2, C) & \text{for } x \le C \\ 1 - S(x;C, C+B/2, C+B) & \text{for } x > C \end{cases} \tag{5.4}$$

   The membership functions $P\{\theta_i(k)\}$ and $N\{\theta_i(k)\}$ are expressed in terms of the above membership functions:

$$P\{\theta_i(k)\} = \Pi(\theta, 2\pi - \theta_0, \theta_m) \tag{5.5}$$

$$N\{\theta_i(k)\} = \begin{cases} 1 - S(x;\theta_0, \theta_{m1}, \theta_m) & \text{for } x \le \theta_m \\ S(x;\theta_m, \theta_{m2}, 2\pi) & \text{for } x > \theta_m \end{cases} \tag{5.6}$$

   where $\theta_m = (2\pi + \theta_0)/2, \theta_{m1} = (\theta_0 + \theta_m)/2$, and $\theta_{m2} = (2\pi + \theta_m)/2$.

2. The proposed FLBPSS uses acceleration $\Delta\dot{\omega}$ as one of the input signal to the PSS whereas Hassan et al use $\Delta\dot{\omega}$ multiplied by a scaling factor F_a:

3. In the proposed FLBPSS, D_r is optimised in a complete different manner than being self-tuned according to a strategy discussed by Hassan et al; The value of D_r will be self tuned according to the amount of disturbance. A starting value D_{r0} will be assigned to D_r at the initialisation of the FLBPSS. The parameter $D(k)$ in the phase plane as shown in Figure (4.6) will be calculated at each sampling time and compared to D_r. If the value of $D(k)$ will be less than D_r, the value of D_r will be the same

as mentioned previously, otherwise, the value of D_r will be chosen as:

$$D_r = 1.01(max(D(k))) \tag{5.7}$$

4. The proposed FLBPSS optimises the parameters α and β (discussed in Section 5.3) whereas Hassan et al considered optimisation of θ and F_a for the STFLBPSS [Hassan, 1992].

5.4.2 Optimal Setting of the STFLBPSS Parameters

The optimal settings of the STFLBPSS parameters are also evaluated by using the performance index as defined in equation (5.1). There are three parameters which need to be adjusted to their optimal values namely angle θ, initial distance parameter D_{r0} and scaling factor F_a. Studies reveal that at any operating point, the optimal values of θ, D_{r0} obtained by applying small perturbations of a 20% step change in T_m differs from the ones for large perturbations such as a three-phase fault, and vice versa. Considering the system performance under different operating conditions with different perturbation (small or large) and system parameter variations, a compromise values of θ and D_{r0} were chosen as 105 degrees and 0.7 respectively (the optimisation procedure is not shown here). For the chosen θ and D_{r0}, the performance index was also evaluated with different values of F_a. The optimal value of F_a is found to be 0.8.

5.4.3 Comparison of the Performance Index

In order to compare the performance of the proposed FLBPSS and Hassan's STFLBPSS, the following procedure is adopted:

For the system studied, we determine the optimal setting of α, β and D_r parameters according to the strategy discussed in Section 5.3 for the nominal operating condition, and keep this setting the same for all other operating conditions as justified by the sensitivity analysis performed in Section 5.3.2. However, in STFLBPSS

Operating Condition	P0	P1	P2	P3	P4
J % (Proposed FLBPSS)	**0.19**	**0.31**	**0.17**	**0.16**	**0.29**
J % (STFLBPSS)	**0.31**	**0.40**	**0.25**	**0.25**	**0.69**

Table 5.17: Comparison of the performance index (small perturbation of a 20% step change in mechanical torque T_m)

Operating Condition	P0	P1	P2	P3	P4
J% (FLBPSS)	**13.67**	**5.73**	**9.43**	**15.00**	**24.50**
J% (STFLBPSS)	**17.46**	**5.74**	**10.10**	**17.22**	**33.84**

Table 5.18: Comparison of the performance index (large perturbation of a three-phase fault at A of Figure (2.2) sustained for 125 milliseconds)

the optimal θ, F_a and D_{r0} for different operating conditions are self-tuned according to the procedure of Hassan et al [Hassan, 1992]. The performance index according to $J = \sum_{k=1}^{M} [t_k \Delta\omega(k)]^2$ is obtained for different operating conditions for both FLBPSS and STFLBPSS under small and large perturbations (Tables 5.17 and 5.18). From the performance index, it is evident that the proposed FLBPSS performs better than the STFLBPSS.

Similar studies as aforementioned have also been carried out for changes in system parameters like inertia constant H, open circuit field time constant τ'_{d0} and transmission line reactance X_e. Investigations reveal that the proposed FLBPSS performs better than the STFLBPSS which is evident from Tables (5.19)-(5.22) by comparing the J values.

5.4.4 Comparison of the Dynamic Response

A few typical responses for different operating conditions P1-P4 are provided in this section.

Figures (5.31) (a) and (b) show the system responses corresponding to a 20%

Parameters	$H = 1.2s$	$H = 1s$	$H = 0.8s$
J% (FLBPSS)	**0.17**	**0.19**	**0.23**
J% (STFLBPSS)	**0.30**	**0.31**	**0.35**

Table 5.19: Comparison of the performance index for parameter changes (small perturbation of a 20% step change in mechanical torque T_m)

Parameters	$H = 1.2s$	$H = 1s$	$H = 0.8s$
J% (FLBPSS)	**12.51**	**13.67**	**17.21**
J% (STFLBPSS)	**16.56**	**17.46**	**20.57**

Table 5.20: Comparison of the performance index for parameter changes (large perturbation of a three-phase fault at A of Figure (2.2) sustained for 125 milliseconds)

Parameters	$\tau'_{d0} = 0.414s$	$\tau'_{d0} = 0.276s$	$X_e = 0.48pu$	$X_e = 0.32pu$
J% (FLBPSS)	**0.20**	**0.18**	**0.21**	**0.18**
J% (STFLBPSS)	**0.31**	**0.32**	**0.39**	**0.27**

Table 5.21: Comparison of the performance index (small perturbation of a 20% step change in mechanical torque T_m)

step change in T_m and a three-phase to ground fault under nominal operating condition with the proposed FLBPSS and the STFLBPSS respectively.

Figures (5.32) (a-d) show the system response corresponding to a 20% step increase in T_m under different operating conditions P1-P4 respectively. Figures (5.33) (a-d) show the system response corresponding to a three-phase to ground fault at A (Figure 2.2) sustained for 125 milliseconds under different operating conditions P1-P4 respectively.

Figure (5.34) shows the system response corresponding to a 20% step change in T_m with ±20% variations in inertia constant H. Figure (5.34) (a) shows the response with the proposed FLBPSS and STFLBPSS respectively when H has been increased by 20% and Figure (5.34) (c) is the result when H has been decreased by 20%. Figure (5.34) (b) is the response with no variation in H.

Figure (5.35) shows the system response corresponding to a 20% step change in T_m with a ±20% variation in d-axis open circuit time constant τ'_{d0}. Figure (5.35) (a) shows the response with the proposed FLBPSS and STFLBPSS when τ'_{d0} has been increased by 20% and Figure (5.35) (c) is the result when τ'_{d0} has been decreased by 20%. Figure (5.35) (b) is the response with no variation in τ'_{d0}.

Parameters	$\tau'_{d0} = 0.414s$	$\tau'_{d0} = 0.276s$	$X_e = 0.48pu$	$X_e = 0.32pu$
J% (FLBPSS)	**15.75**	**12.37**	**12.69**	**16.56**
J% (STFLBPSS)	**16.56**	**17.96**	**18.31**	**19.48**

Table 5.22: Comparison of the performance index (large perturbation of a three-phase fault at A of Figure (2.2) sustained for 125 milliseconds)

Figure (5.36) shows the system response corresponding to a 20% step change in T_m with $\pm 20\%$ variations in the transmission line reactance X_e. Figure (5.36) (a) shows the response with the proposed FLBPSS and STFLBPSS respectively when X_e has been increased by 20% and Figure (5.36) (c) is the result when X_e has been decreased by 20%. Figure (5.36) (b) is the response with no variation in X_e.

It is clearly seen from the above figures that the maximum transient deviation for both the FLBPSS and STFLBPSS are more or less the same, whereas the settling time for the proposed FLBPSS is much faster than that for the STFLBPSS.

5.5 Comparison Study of the Two Fuzzy Control Schemes

5.5.1 Comparison of the Performance Index

The performance indices according to $J = \sum_{k=1}^{M} [t_k \Delta\omega(k)]^2$ are obtained for different operating conditions for both the proposed FLBPSS and FLC under both small and large perturbations.

Table (5.23) shows the performance index for the two fuzzy control schemes for different operating conditions under a 20% step increase in mechanical torque T_m.

Fuzzy controller	P0	P1	P2	P3	P4
J% (FLC)	**0.42**	**0.64**	**0.39**	**0.35**	**0.89**
J% (FLBPSS)	**0.19**	**0.31**	**0.17**	**0.16**	**0.29**

Table 5.23: Comparison of the performance index of the FLC and the FLBPSS (small perturbation of a 20% step increase in mechanical torque)

Table (5.24) shows the performance index for the two fuzzy control schemes for different operating conditions under a three-phase fault.

From these tables it can be seen that the FLBPSS provides better performance than the FLC since the performance index for the FLBPSS is much smaller than

Fuzzy controller	P0	P1	P2	P3	P4
J% (FLC)	**39.48**	**13.58**	**27.23**	**48.46**	**73.17**
J% (FLBPSS)	**13.67**	**5.73**	**9.43**	**15.00**	**24.50**

Table 5.24: Comparison of the performance index of the FLC and the FLBPSS (large perturbation of a three-phase to ground fault)

the performance index for the FLC. As an example, the performance index for the FLC under operating condition P0 is 2.2 times and 2.8 times larger than that of the FLBPSS for small and larger perturbations respectively.

5.5.2 Comparison of the Dynamic Response

Comparison of the dynamic responses for the FLBPSS and the FLC for different operating conditions P1-P4 under both small and large perturbations have been studied in this section. A few typical responses for operating condition P0 are provided in Figures (5.37)-(5.39). Figures (5.38)-(5.39) show the system dynamic performance under a 20% step change in mechanical torque T_m followed by a 20% step increase in reference voltage V_{ref} sustained for 7.5 seconds with the proposed FLBPSS and the FLC respectively. To demonstrate the effectiveness of the FLBPSS and the FLC, Figure (5.37) shows the speed deviation and rotor angle responses without the PSS in operation. It is clearly seen that the FLBPSS provides much better dynamic responses than the FLC since the maximum transient deviation and settling time are both smaller with the FLBPSS in operation.

5.6 Concluding Remarks

In this chapter, the optimisation of the FLC and the FLBPSS have been investigated and a performance index has been defined for this purpose.

The WOR has been proposed to evaluate the membership function shape for the FLC. It has been found that the FLC gives best performance when the WOR is approximately from 12% to 15%. Different implication methods, such as *Mamdani* and *Larsen* methods, and different defuzzification methods, such as *Means of max* and *Centroid* methods, have also been evaluated by using the performance index. Sensitivity test of the FLC has been demonstrated by varying the system parameters for $\pm 20\%$ and for various operating conditions under both small and large perturbations.

The optimal setting of the proposed FLBPSS parameters has also been evaluated by using the performance index. Two new non-linear membership functions have been proposed. The optimal settings of the FLBPSS parameters α, β and D_r have been obtained either by applying small or large perturbations. The optimal setting chosen at the nominal operating condition is quite robust and need not be reset for a wide variation of operating conditions and parameters under both small and large perturbations. The optimal values of α, β and D_r at one optimal point is sub-optimal at the other point with hardly any difference in the quality of the dynamic response.

STFLBPSS has also been introduced in order to compare with the FLBPSS. The optimal settings of θ, F_a and D_{r0} values have also been explored. It has been found that at any operating point, the optimal values of the above mentioned parameters obtained by applying small perturbations differ from that for large perturbations and vice versa. Considering the system performance under different operating conditions with different perturbations and the system parameter variations, a compromise values of θ, F_a and D_{r0} have been chosen.

Comparison study between the proposed FLBPSS and the STFLBPSS has been demonstrated through both the performance index and the dynamic response. Extensive study has been performed when the system is subject to small or large disturbances, variations in the system parameters and under wide variation of the operating conditions. The performance of the proposed FLBPSS is found to be superior to that of the STFLBPSS.

Comparison study between the proposed FLBPSS and the FLC has also been investigated through both the performance index and the dynamic response. Extensive study has been performed when the system is subject to small or large disturbances, variations in the system parameters and under wide variation of the operating conditions. The performance index of the FLC is more than twice larger than that of the FLBPSS. From the dynamic response, it can be seen that the maximum transient deviation is smaller and the settling time is shorter when the system is equipped with the FLBPSS. Therefore, the FLBPSS has been chosen as the practical PSS for real time implementation.

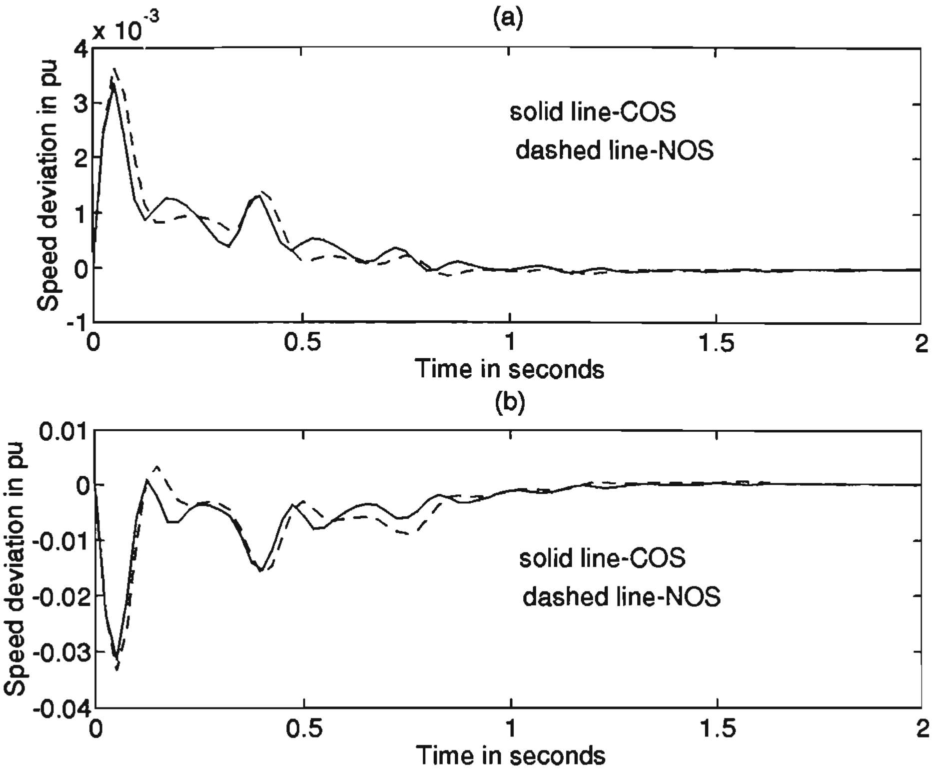

Figure 5.26: System responses at operating condition P4 with the corresponding optimal settings (COS) and the nominal optimal settings (NOS), (a)-20% step increase in mechanical torque, (b)-three-phase to ground fault

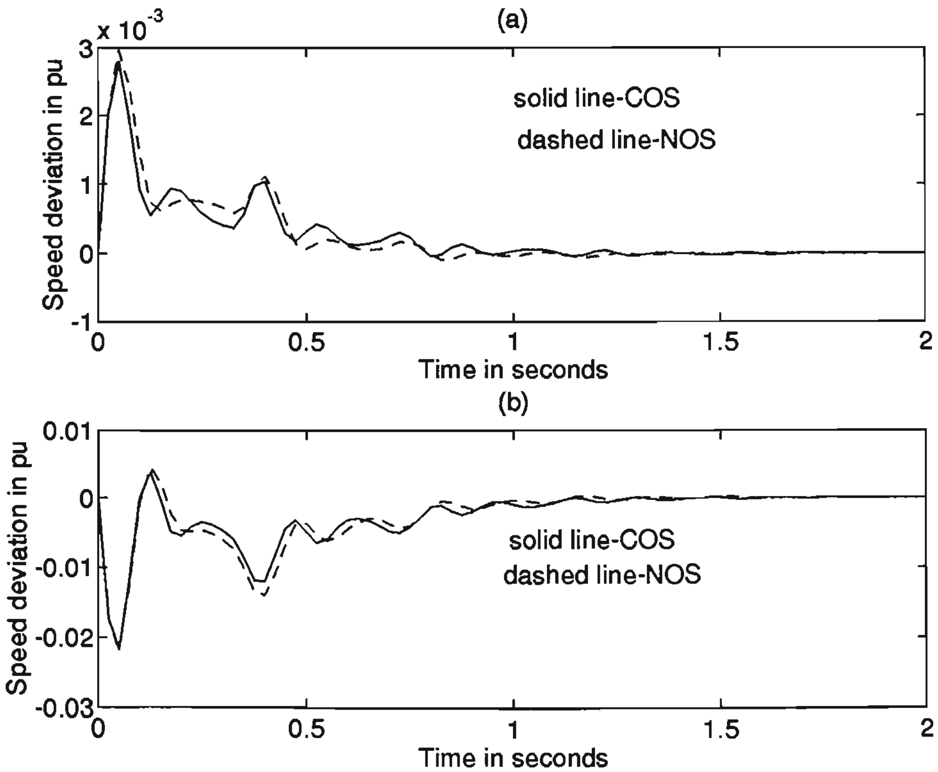

Figure 5.27: System responses at P0 with inertia constant parameter variation $H = 1.2s$ with the corresponding optimal settings (COS) and the nominal optimal settings (NOS), (a)-20% step increase in mechanical torque, (b)-three-phase to ground fault

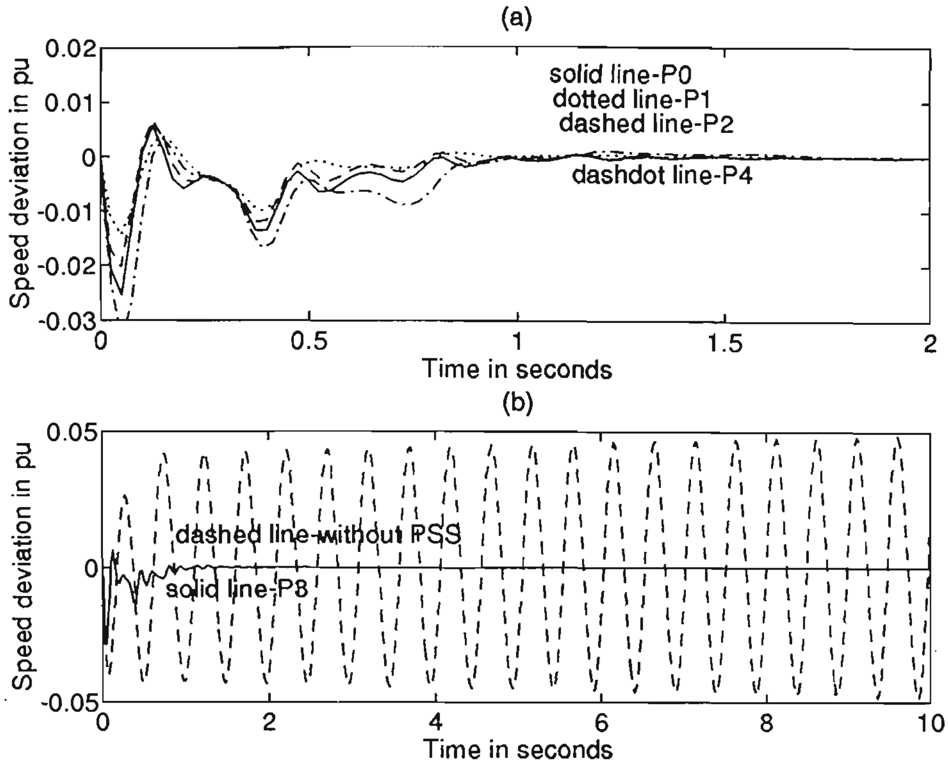

Figure 5.28: System response corresponding to three-phase to ground fault under different operating conditions with the nominal optimal settings (NOS), (a)-operating conditions P0, P1, P2 and P4, (b)-operating condition P3

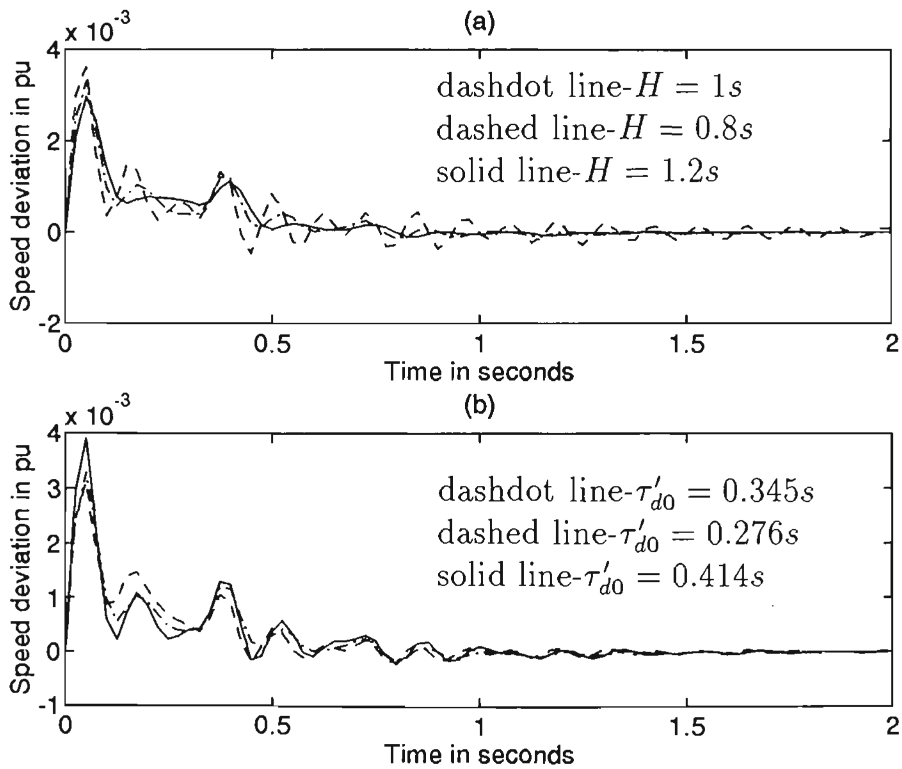

Figure 5.29: System response corresponding to a 20% step increase in mechanical torque with the nominal optimal settings (NOS) for different system parameter changes, (a)-$\pm 20\%$ variation in H, (b)-$\pm 20\%$ variation in τ'_{d0}

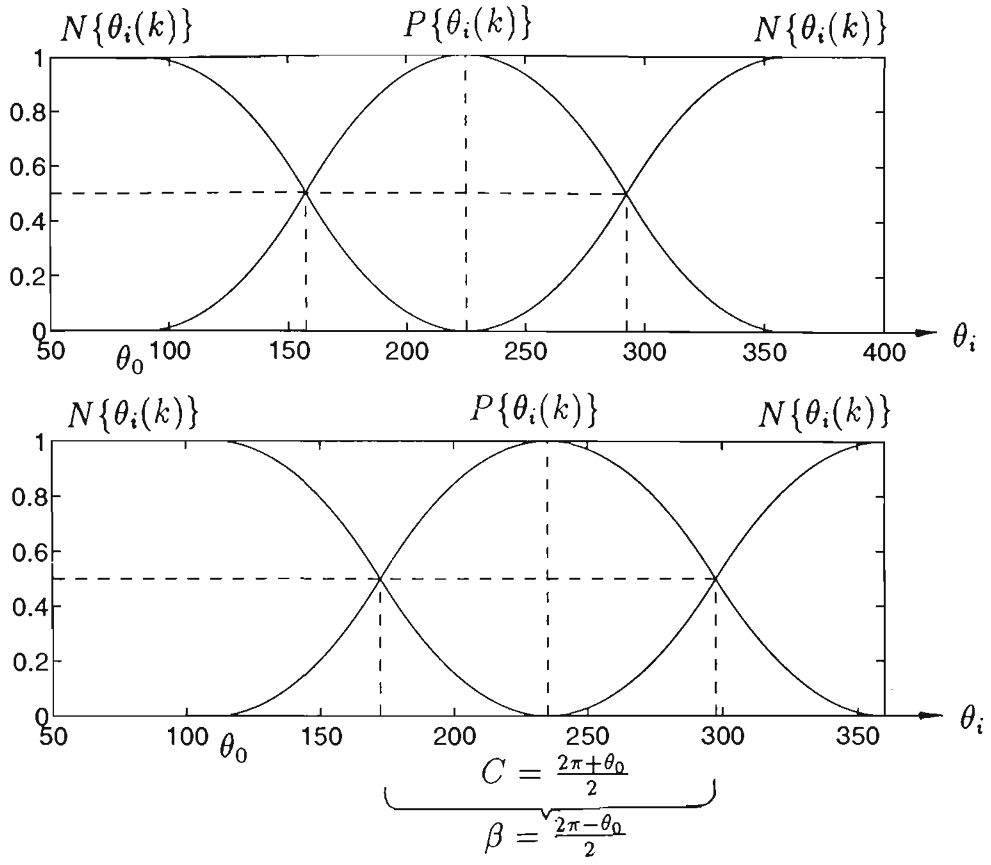

Figure 5.30: Membership functions used for the STFLBPSS

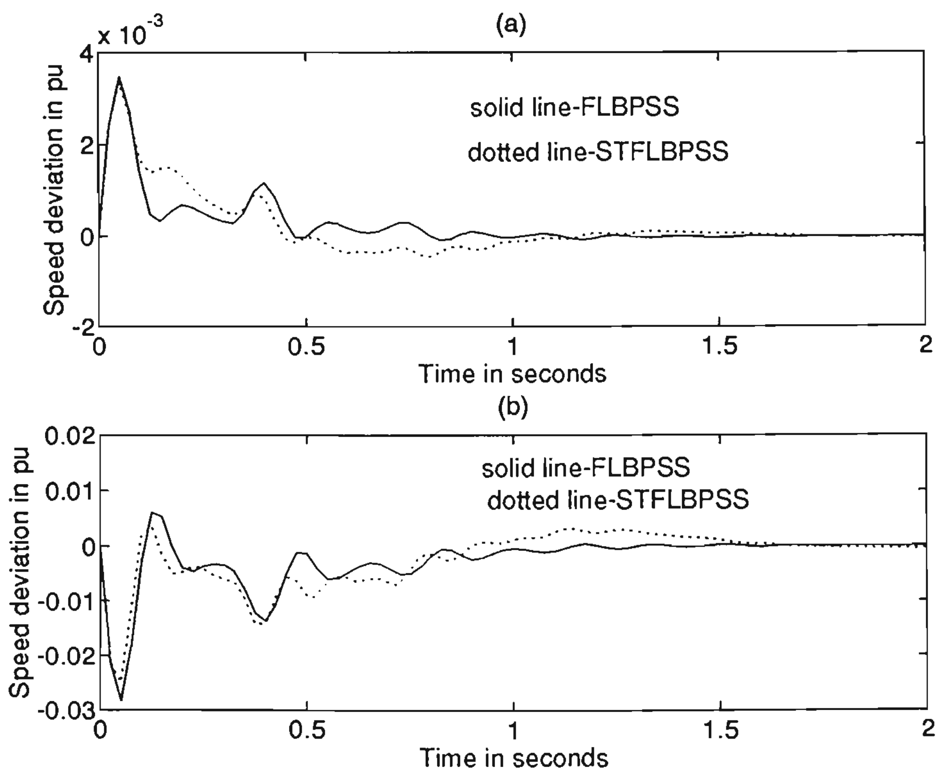

Figure 5.31: System response corresponding to a 20% step change in mechanical torque and a three-phase fault under the nominal operating condition, (a)-20% step increase in mechanical torque, (b)-three-phase fault

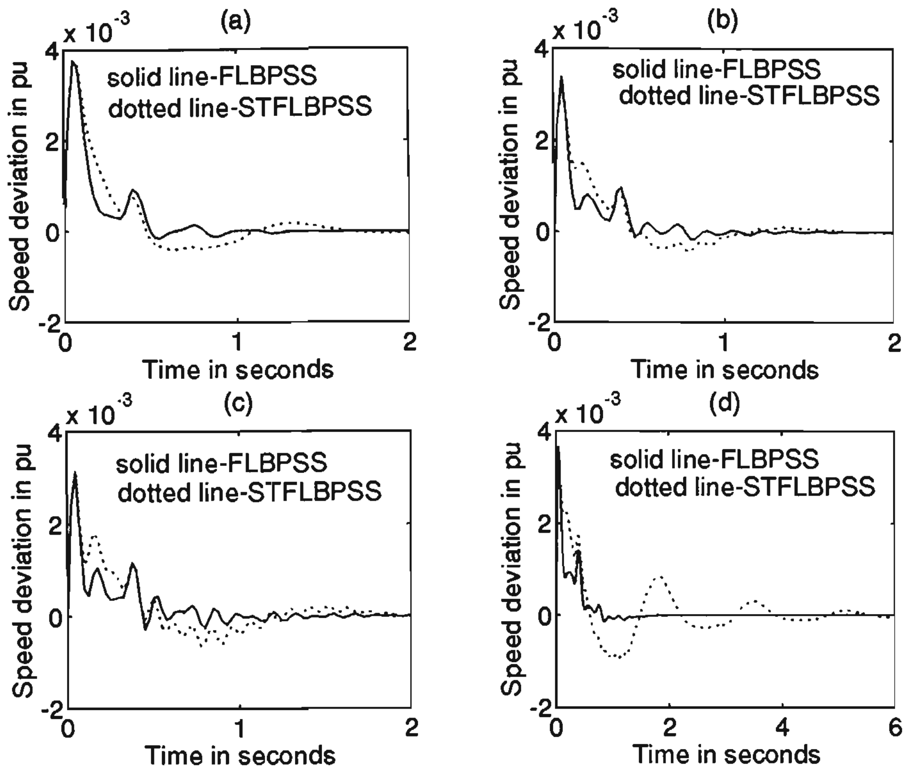

Figure 5.32: System response corresponding to a 20% step change in mechanical torque under different operating conditions, (a)-(d) provide the speed deviation responses under operating conditions P1-P4 respectively

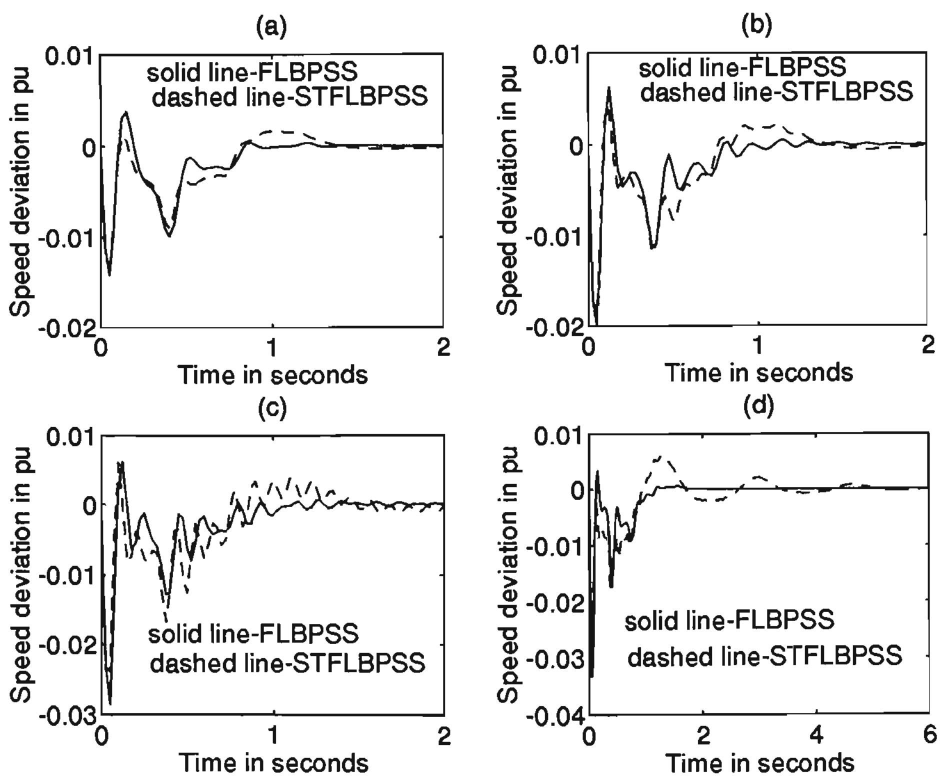

Figure 5.33: System response corresponding to a three-phase to ground fault under different operating conditions, (a)-(d) provide the speed deviation responses under operating conditions P1-P4 respectively

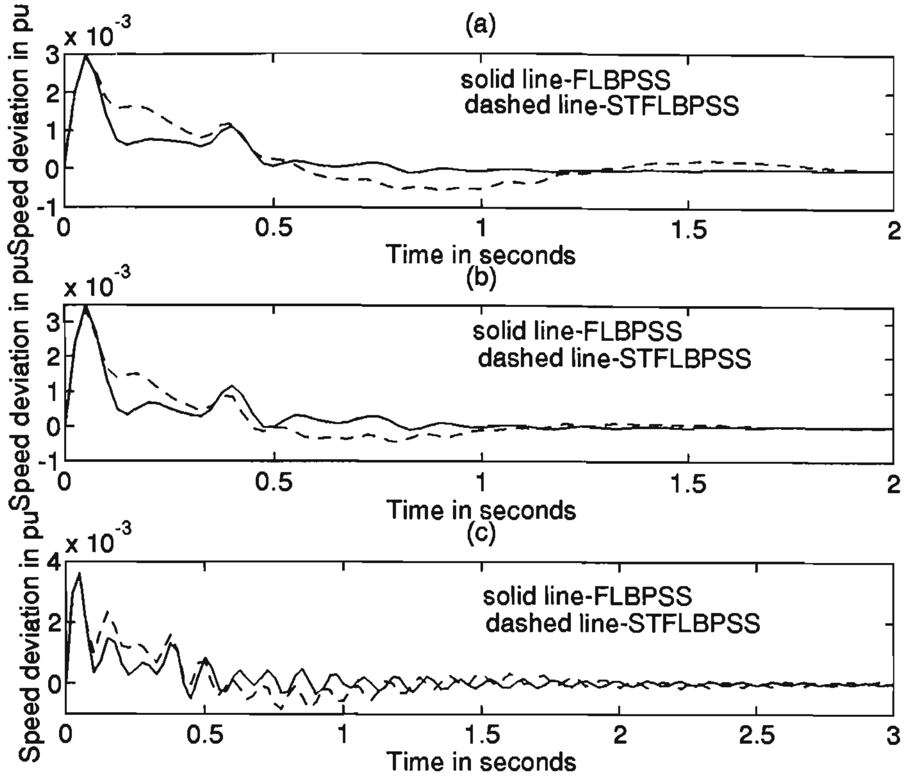

Figure 5.34: System response corresponding to a 20% step change in mechanical torque with ±20% variation in inertia constant H, (a)-$H = 1.2s$, (b)-$H = 1s$, (c)-$H = 0.8s$

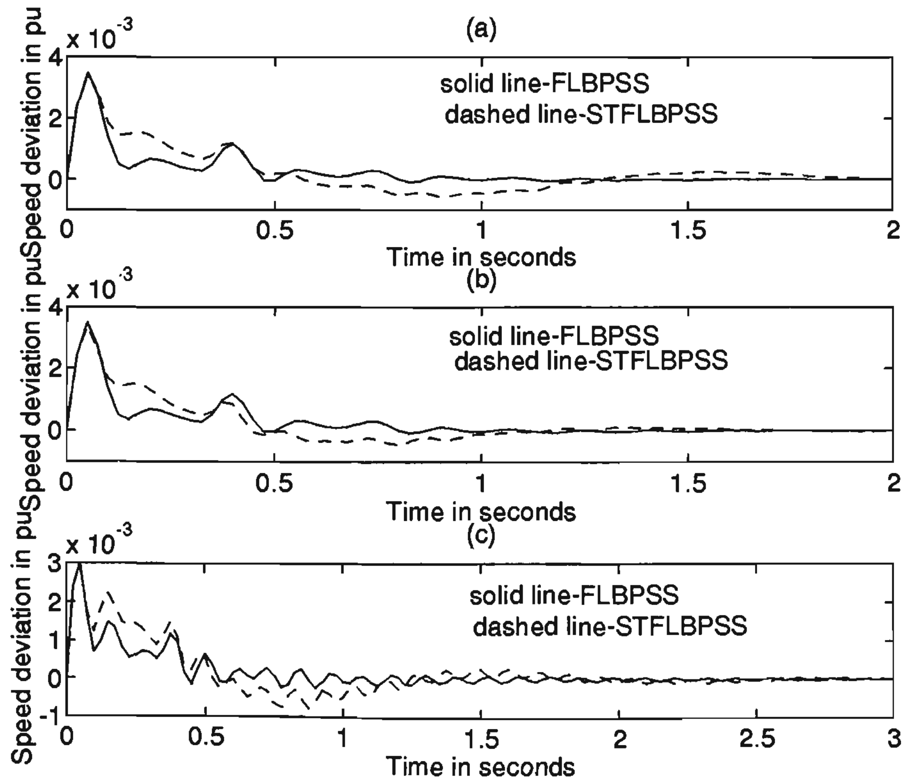

Figure 5.35: System response corresponding to a 20% step change in mechanical torque with ±20% variation in τ'_{d0}, (a)-$\tau'_{d0} = 0.414s$, (b)-$\tau'_{d0} = 0.345s$, (c)-$\tau'_{d0} = 0.276s$

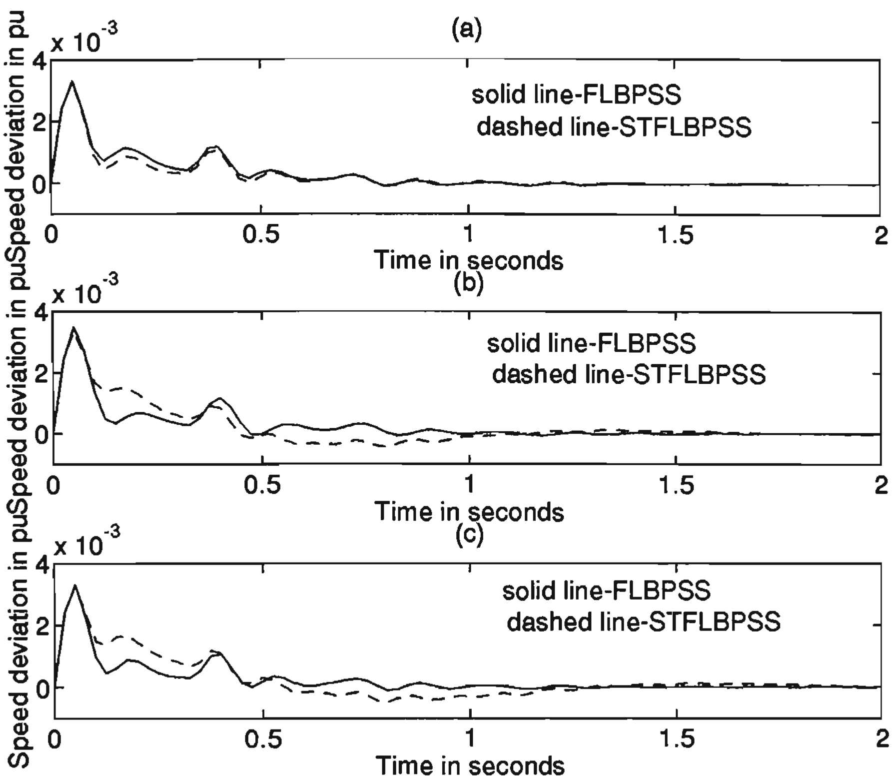

Figure 5.36: System response corresponding to a 20% step change in mechanical torque with $\pm 20\%$ variation in X_e, (a)-$X_e = 0.48pu$, (b)-$X_e = 0.4pu$, (c)-$X_e = 0.32pu$

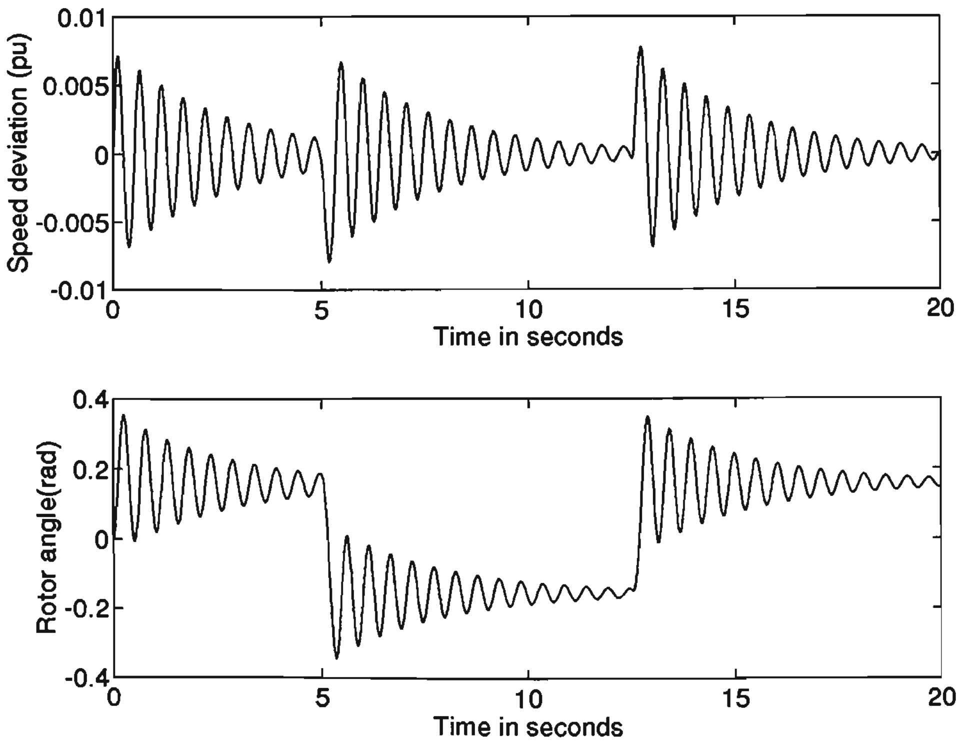

Figure 5.37: System response corresponding to a 20% step change in mechanical torque and reference voltage change (without PSS)

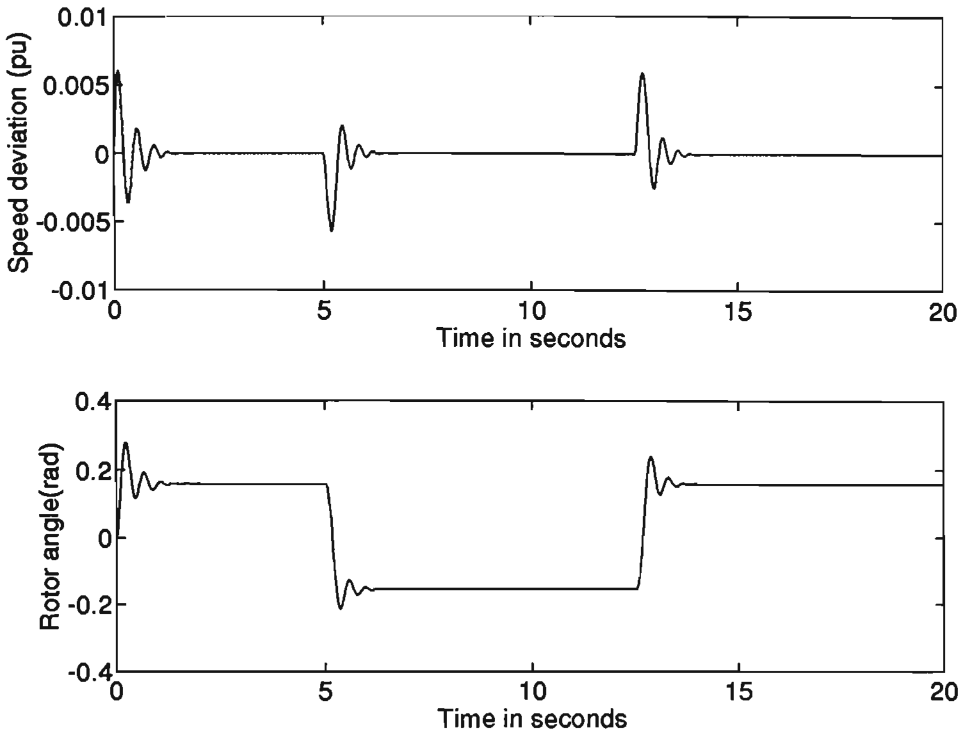

Figure 5.38: System response corresponding to a 20% step change in mechanical torque and reference voltage change (with the FLC)

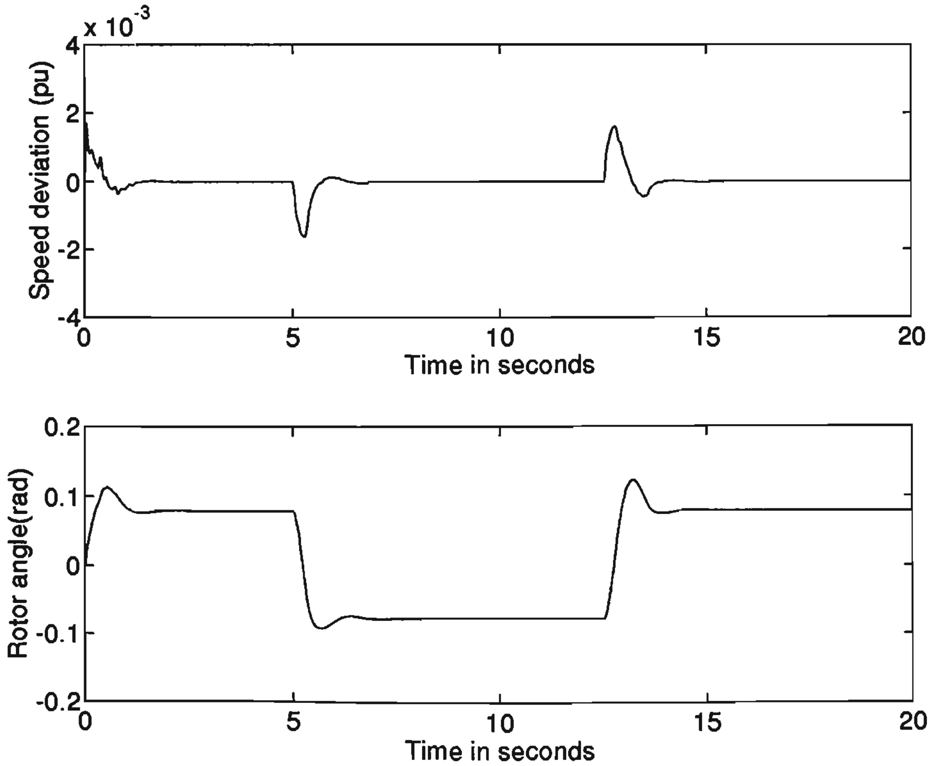

Figure 5.39: System response corresponding to a 20% step change in mechanical torque and reference voltage change (with the FLBPSS)

Chapter 6

Implementation Study

6.1 Introduction

In order to verify the design for the optimised FLBPSS as well as the simulation results, the digital AVR and the FLBPSS were implemented and tested on the single-machine infinite bus system in the power laboratory. The configuration of the single-machine infinite bus power system was shown previously in Figures (2.1) and (2.2). The synchronous generator is a salient pole type with a damping winding on the rotor shaft and driven by a DC motor. The generator was synchronised and connected to the infinite bus.

The implementation of the optimised FLBPSS is tested on the single-machine infinite bus power system. The hardware development is described in Section 6.2. The sensor circuit which has been used to transform the three-phase line voltages of 400V into a reduced magnitude proportional DC signal is presented in Section 6.2.1. In Section 6.2.2 and 6.2.3, the A/D and D/A converter and the field drive unit are described. An optical shaft encoder which has been used for rotor position measurement is described in detail in Section 6.2.4. The software development is presented in Section 6.3 which includes a description of the **main** program, the driver routines, the interrupt set up and the handling routine, the AVR routine and the FLBPSS as well as other features. The flow chart of the software is illustrated in Section 6.3.7.

The implementation test results are presented in Section 6.4. In order to test the robustness of the optimised FLBPSS, three kinds of disturbances were applied to the system, a 10% step change in the reference voltage as a small perturbation, a sudden load change and a three-phase to ground fault as large perturbations. The real time evaluation has also been tested under a wide range of operating conditions which is also shown in Section 6.4.

6.2 Hardware Development

6.2.1 Sensor

The three-phase line voltages of 400V are transformed into DC by a six-pulse three-phase rectifier circuit. The rectified voltage is reduced to 5V using a potential divider and then filtered to get a smooth DC voltage, which is the input to an A/D converter. The transducer output, a voltage between 0V and 5V, which represents a phase to phase voltage input between 0V and 400V, is fed directly into the multiplexer of the A/D converter. Figure (6.1) shows the rectifier, the potential divider and the filter circuit.

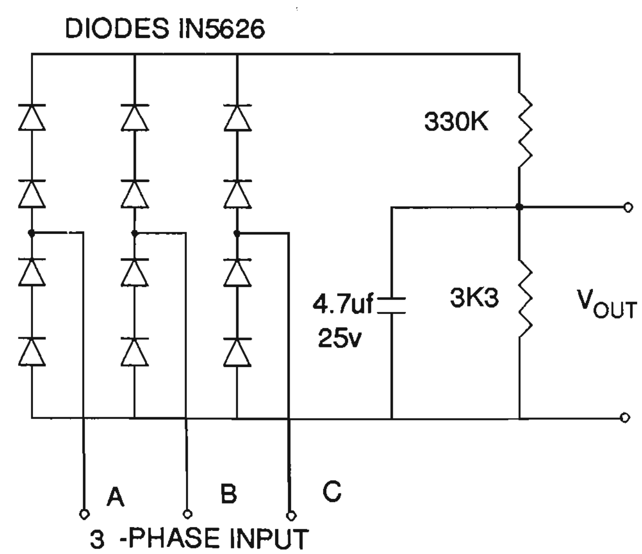

Figure 6.1: Sensor circuit of rectifier, potential divider and filter circuit

6.2.2 A/D and D/A Adapter

The IBM data acquisition adapter card is used for all A/D and D/A functions. A DT2801 card has been used as the means to perform A/D and D/A conversions. The data acquisition adapter which provides eight analog input channels multiplexed into an Analog to Digital converter and two analog output channels, all with 12 bit resolution.

6.2.3 Field Drive Unit

The field drive unit is used to model the exciter circuit. The control signal from the computer was sent out at each sample time through the D/A converter and amplified by the field drive unit to obtain the generator field voltage.

6.2.4 Rotor Position Measurement by Using an Optical Shaft Encoder

The machine is fitted with an incremental type position encoder which generates 720 pulses per revolution for a 4 pole machine. It implies 360 pulses per 360 electrical degrees, or 1 electrical degrees per pulse. By counting the number of pulses the amount of incremental movement can be accurately measured. The pulses were sent to an 8 bit hardware counter to keep track of the rotor position. A reference pulse is provided by the encoder to enable a reference position to be obtained. This occurs once per revolution in the rotary encoder. Direction can be detected enabling up/down counting to take place with regard to the reference counting.

The digital signal is then passed through a hardware D/A converter to produce a voltage signal which is proportional to the rotor position angle. The calibration test revealed that 1V is equivalent to 5 mechanical degrees or 10 electrical degrees. The computer reads the rotor position through the A/D converter and enables calculation of the speed deviation and acceleration at each sampling period.

6.3 Software Development

The functions of the PC and A/D, D/A converters are to read the terminal voltage and rotor angle, calculate the speed deviation and acceleration signal, compute the stabilising signal and excitation control signal. The excitation control signal has hence been amplified by the field drive unit to control the field voltage. The software used to achieve these objectives was arranged as a background **Main** program which provided the user interface, an interrupt routine which handled interrupts from the internal timer.

Turbo Pascal version 5.0 has been used as the programming language to implement the AVR and the FLBPSS. The DT2801 card was used as the means to perform the A/D and D/A conversions. Other necessary units such as the DT2801 drivers, graphics drivers etc. were incorporated in the program. Assembly language was used for the DT2801 A/D and D/A converter in order to achieve optimum conversion speed.

6.3.1 The Main Program

In the **main** program, the initialisation part of the program initialised the timer for a designed sampling rate of $25 milliseconds$ and also initialised the A/D and D/A ports. Once initialisation was completed, A/D conversions were performed on the data obtained. The initialisation procedure was included as a subroutine in the background **main** program.

The analog inputs, i.e., the terminal voltage, the rotor position, the real power and reactive power, etc. were obtained via the A/D converter. The results were stored in memory locations ready for use by the appropriate interrupt routine as required.

6.3.2 The Driver Routines

A separate unit called **DT2801** contained all the necessary driver routines for the **DT2801** card. Procedures **AD-READ** and **DA-WRITE** were used to perform the following functions:

1. Stop and reset the A/D converter;
2. Read the terminal voltage and rotor angle and convert them into digital signal;
3. Convert the calculated control signal into analog form and send it out to the field drive unit.

6.3.3 The Interrupt Set up and Handling Routines

The system timer and interrupt routines were used for the purpose of interrupting the software at each sampling instant. The interrupt was initialised at the beginning of the program and was restored at the end of the program.

6.3.4 The FLBPSS Routine

Procedure **FLBPSS** was used in order to calculate the stabilising signal. This procedure was used to perform the following functions:

1. Set up optimal parameters for α, β and D_r;
2. Calculate the speed deviation from the measured rotor angle;
3. Filter the speed deviation using a 4th-order digital filter with a 12 Hz cut-off frequency, and then calculate the acceleration;
4. Calculate the stabilising signal.

6.3.5 The AVR Routine

The **CONTROLLER** procedure was used in order to calculate the control signal. Since the D/A card can output a maximum of ± 10V, precaution was taken so that control signal never exceeded this limit. This was realised by using if-then statement to test and adjust the control signal before it was sent out to the D/A converter.

6.3.6 Screen Graphics

A separate unit called **SCRNPLT5** was used for drawing the trend plots for data logging. An **OUTPUT-MENU** procedure was also used to display the menus distinctively.

6.3.7 Other Features

A parallel I/O port was used to send the control signal out to switch the relay on and off in order to perform sudden load changes and three-phase to ground fault. The software was written user friendly. The user has the option of selecting reference voltage and testing time.

6.3.8 The Block Diagram of the Software

The software block diagrams are shown in Figures (6.2) and (6.3).

6.4 Implementation Tests

In order to test the robustness of the optimised FLBPSS, the following types of disturbances were applied:

- a 10% step increase in the reference voltage sustained for 7.5 seconds;

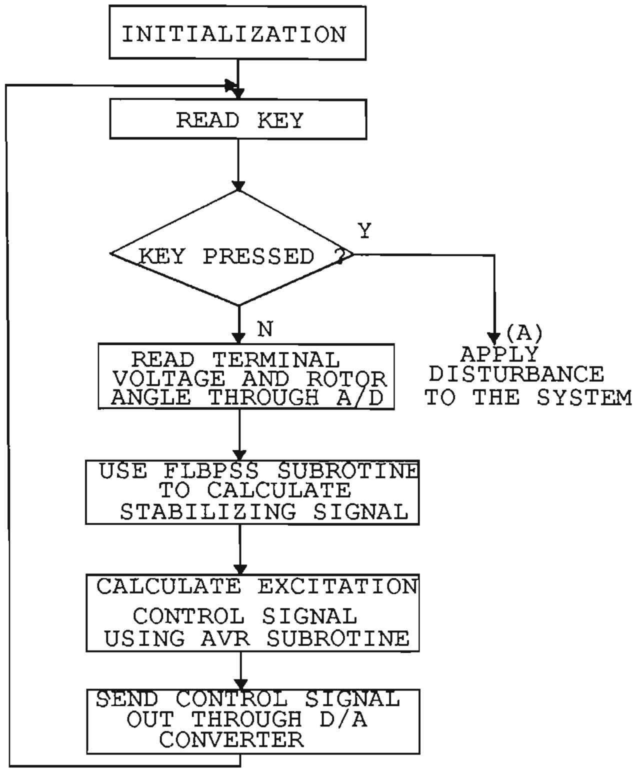

Figure 6.2: Software diagram (Part I)

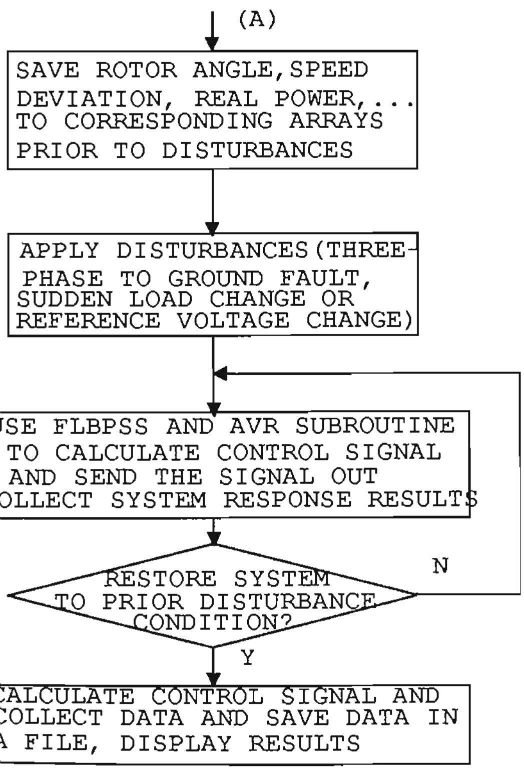

Figure 6.3: Software diagram (Part II)

- 3/4 rated load increase sustained for 7.5 seconds;
- three-phase to ground fault at A (Figure 2.2) sustained for 125 milliseconds.

6.4.1 Step Change in the Reference Voltage

The speed deviation and rotor angle corresponding to a 10% step increase in the reference voltage sustained for 7.5 seconds are shown in Figures (6.4)-(6.6). Figures (6.4) and (6.5) provide the result under nominal operating condition (*real power* $P = 1pu$, *power factor = 0.866 lag*) without and with the FLBPSS respectively. Figure (6.6) shows the control signal applied to the generator field without and with the FLBPSS respectively. It can be seen that the rotor angle and speed deviation oscillations are damped out very quickly (within 2 cycles) when the system is equipped with the FLBPSS, whereas the rotor angle and speed deviation oscillated and damped out in 8 cycles without the FLBPSS.

Similar results as above were obtained (not shown here) under various operating conditions as listed in Table (6.1).

6.4.2 Sudden Load Change

The performance of the FLBPSS has been evaluated under various operating conditions as shown in Table (6.1).

Operating condition	OC1	OC2	OC3	OC4
Real power	0.52 pu	0.9 pu	1.4 pu	0.86 pu
Power factor	0.95 (lag)	0.866 (lag)	0.42 (lag)	0.99 (lead)

Table 6.1: Operating conditions for single-machine infinite bus power system

Figures (6.7)-(6.8) show the rotor angle and speed deviation corresponding to 3/4 rated *resistive* load change without and with the FLBPSS under operating condition P1. The oscillation of the rotor angle and speed deviation have been damped out within 2 cycles with the FLBPSS in operation and the maximum transient deviation has also been reduced. Without the FLBPSS, the corresponding

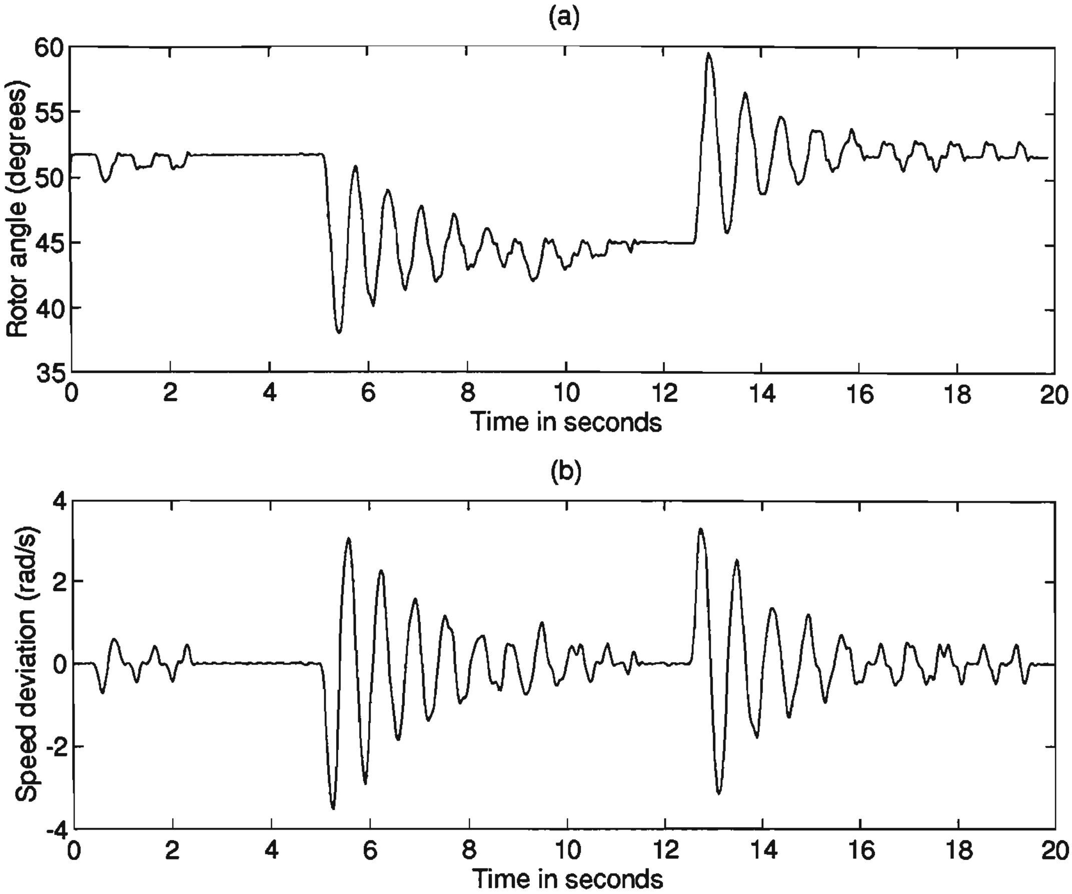

Figure 6.4: Rotor angle and speed deviation corresponding to a 10% step increase in the reference voltage sustained for 7.5 seconds (without the FLBPSS), (a)-rotor angle, (b)-speed deviation

outputs oscillated and damped out in 8 cycles. A number of tests were conducted for inductive and capacitive load changes and similar results were obtained. Figures (6.9)-(6.10) show the rotor angle and speed deviation corresponding to 3/4 rated *inductive* load change without and with the FLBPSS at operating condition P1. Figures (6.11)-(6.12) show the rotor angle and speed deviation corresponding to 3/4 rated *capacitive* load change without and with the FLBPSS under operating condition P1. The system oscillations resulted from the *inductive, capacitive and resistive* load changes have been damped out very quickly (within 1.5 to 2 cycles) and the maximum transient deviation has been reduced substantially in the presence of the FLBPSS. From the above results, it can be concluded that the FLBPSS performance is robust with different types and values of step load changes.

Figures (6.13)-(6.18) show the rotor angle and speed deviation in response to 3/4 rated resistive load change without and with the FLBPSS under operating condition P2, P3 and P4 respectively. Under the above operating conditions, the

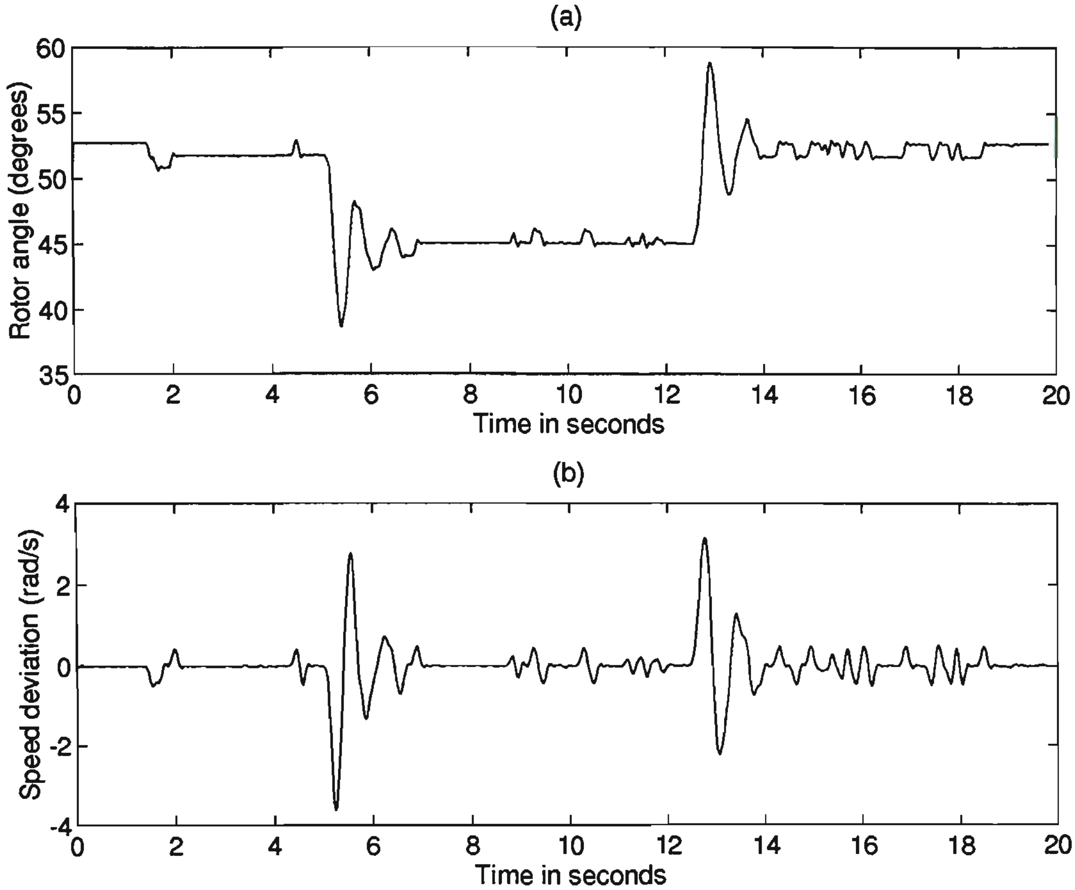

Figure 6.5: Rotor angle and speed deviation corresponding to a 10% step increase in the reference voltage sustained for 7.5 seconds (with the FLBPSS), (a)-rotor angle, (b)-speed deviation

maximum transient deviation has been reduced and the settling time is 4 times smaller when the FLBPSS was used. From these results, it can be seen that the FLBPSS works satisfactorily over a variety of operating conditions.

6.4.3 Three-phase to Ground Fault

A three-phase to ground fault was applied at the generator side of the transmission line (see Figure 2.2) and removed after 125 milliseconds. Figures (6.19) and (6.20) demonstrate the rotor angle and speed deviation in response to the three-phase to ground fault under the nominal operating condition (*real power* $P = 1pu$, *power factor = 0.866 lag*) without and with the FLBPSS respectively. It can be observed that the speed deviation and rotor angle are damped out in 3 cycles by using the FLBPSS, whereas the oscillations are damped out in 9 cycles without the FLBPSS in operation. It takes a longer settling time in the three-phase to ground fault

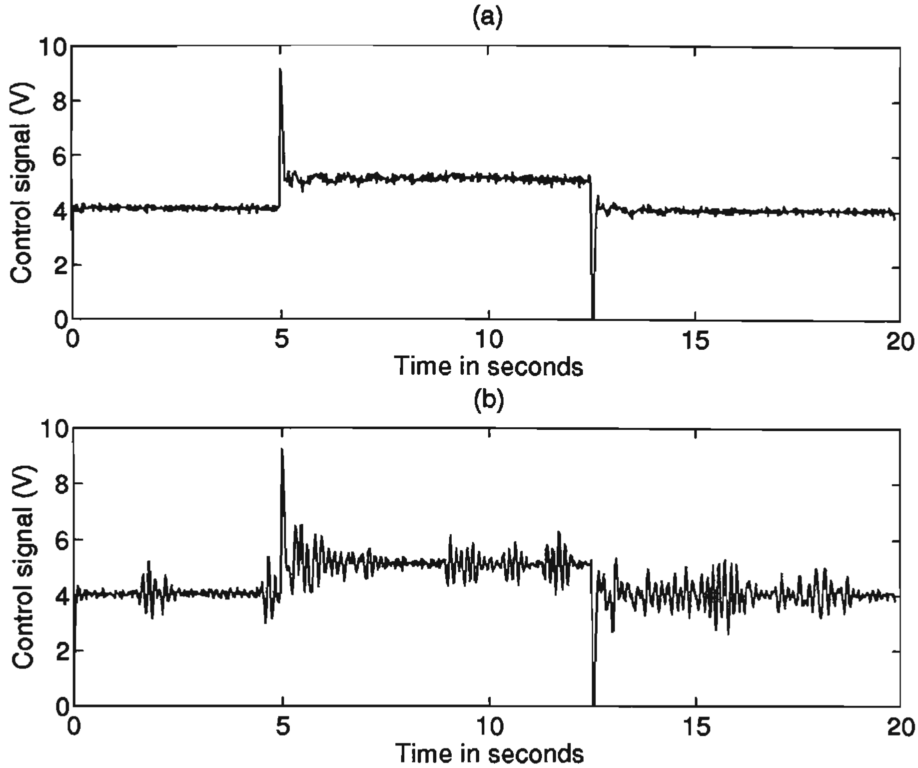

Figure 6.6: Control signal corresponding to a 10% step increase in the reference voltage sustained for 7.5 seconds, (a)-without the FLBPSS and (b)-with the FLBPSS

condition since the excitation control signal reached the hardware limit.

Similar results as above for a three-phase to ground fault were also obtained (not shown here) under various operating conditions P1-P4.

In the experimental results for the system studied, although the overall trend of the experimental results followed closely the simulation results, yet discrepancies were observed. The experimental value of D_r was found to be 2 whereas it was 0.6 by simulation (which is more than 3 times). This difference are not only due to the uncertainty in the system parameters measured, but also very low D_r requires almost bang-bang control due to the saturation in the controller. The increased value of D_r indicates that the effect of saturation is reduced and accordingly, better performance was achieved in the experiment.

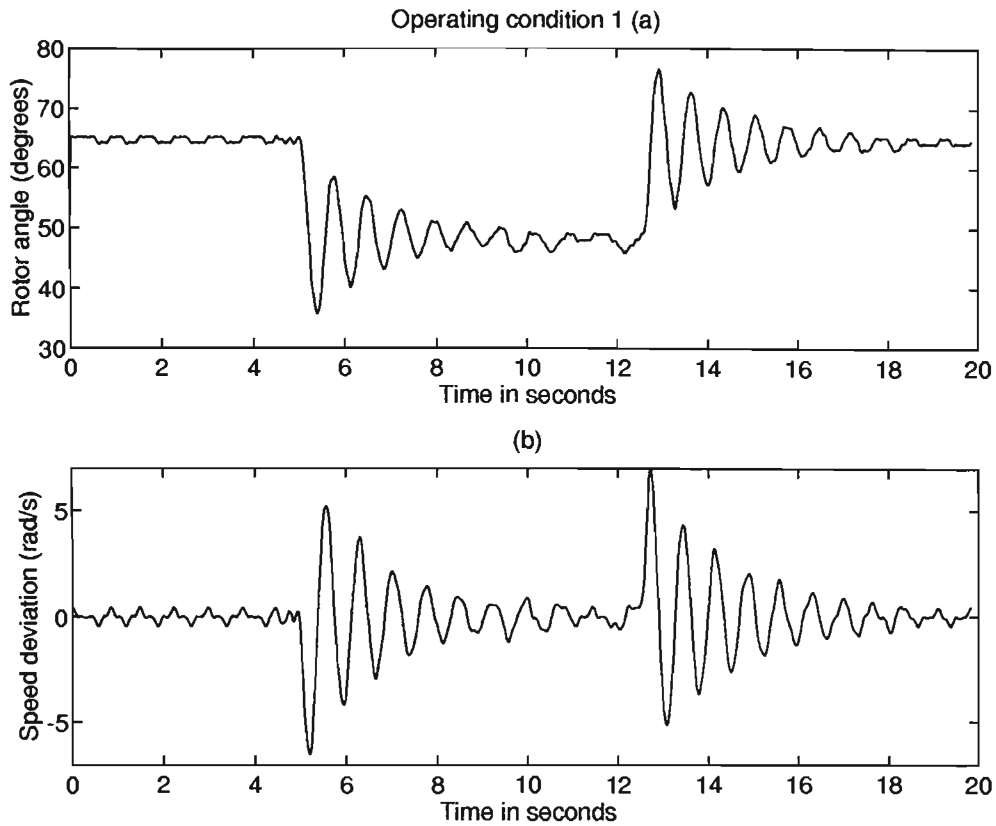

Figure 6.7: Rotor angle and speed deviation corresponding to sudden resistive load change without the FLBPSS (operating condition OC1), (a)-rotor angle, (b)-speed deviation

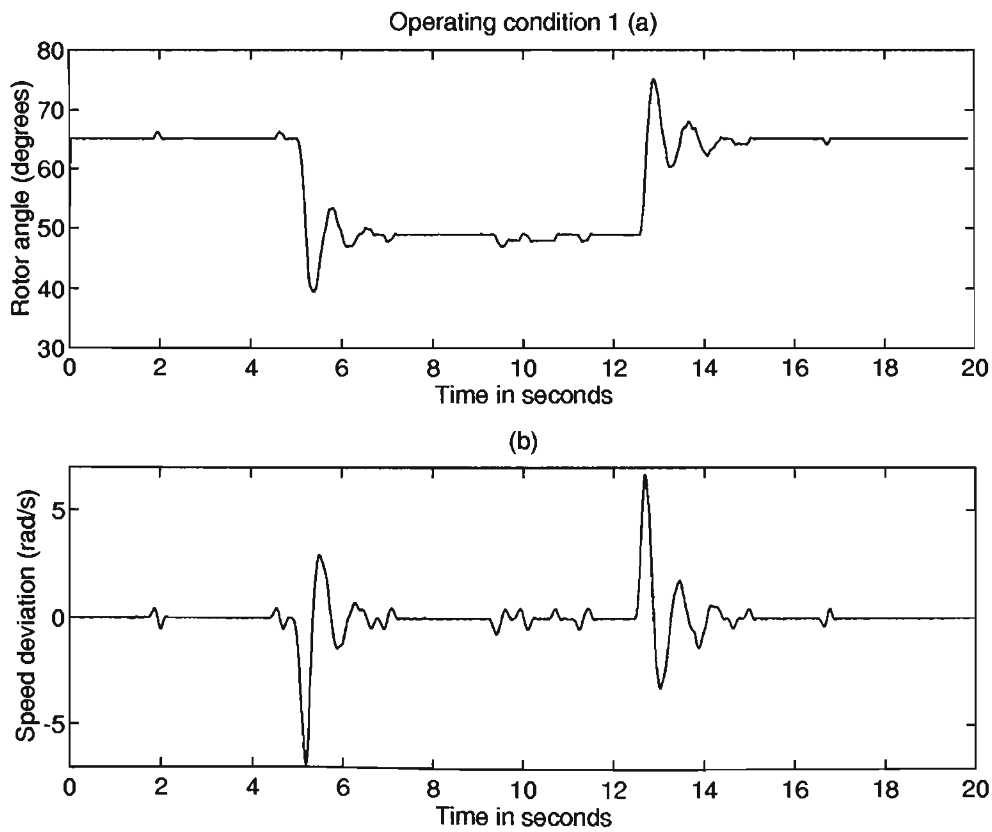

Figure 6.8: Rotor angle and speed deviation corresponding to sudden resistive load change with the FLBPSS (operating condition OC1), (a)-rotor angle, (b)-speed deviation

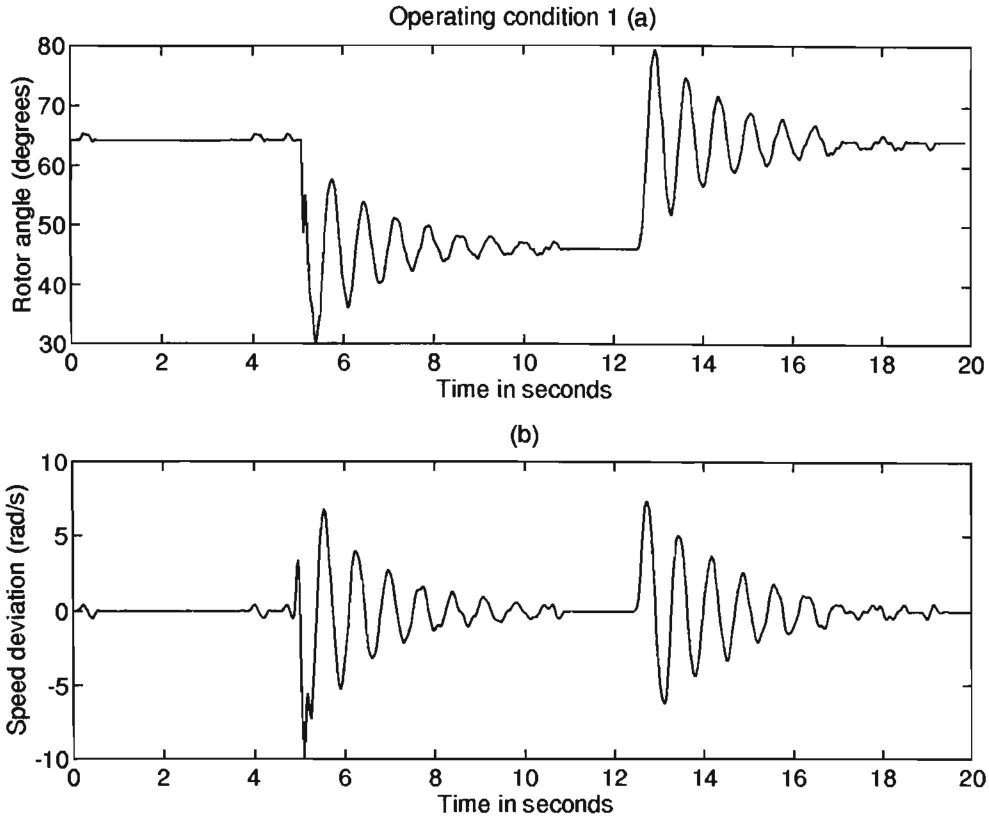

Figure 6.9: Rotor angle and speed deviation corresponding to sudden inductive load change without the FLBPSS (operating condition OC1), (a)-rotor angle, (b)-speed deviation

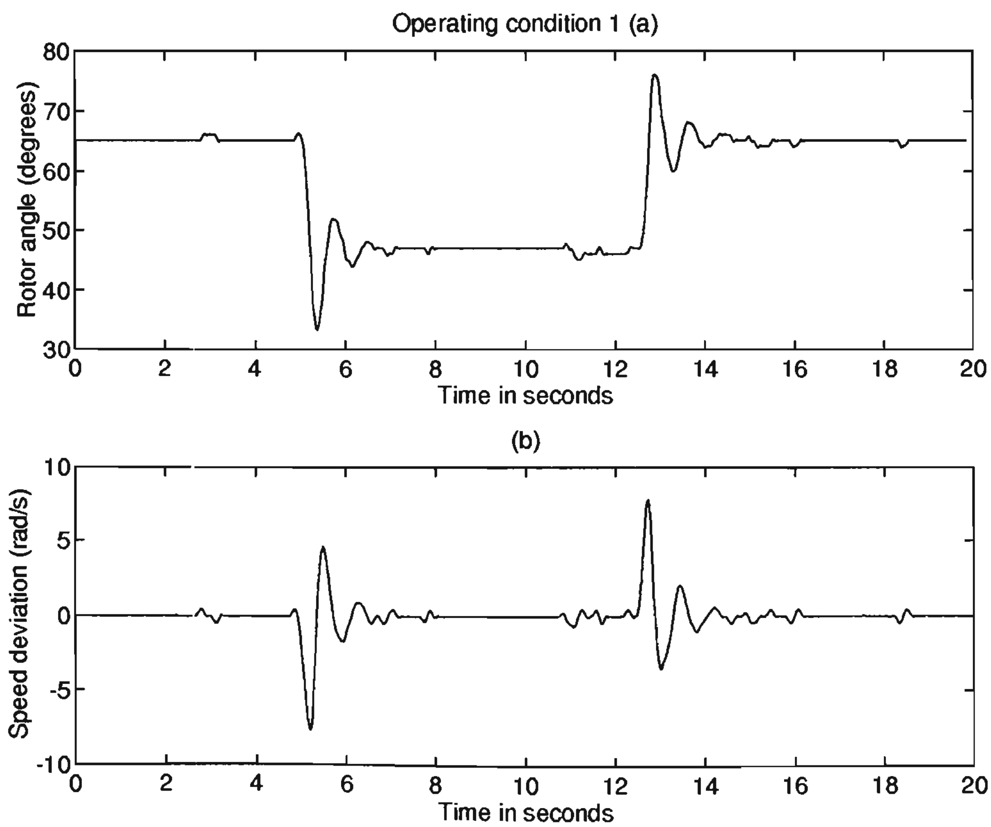

Figure 6.10: Rotor angle and speed deviation corresponding to sudden inductive load change with the FLBPSS (operating condition OC1), (a)-rotor angle, (b)-speed deviation

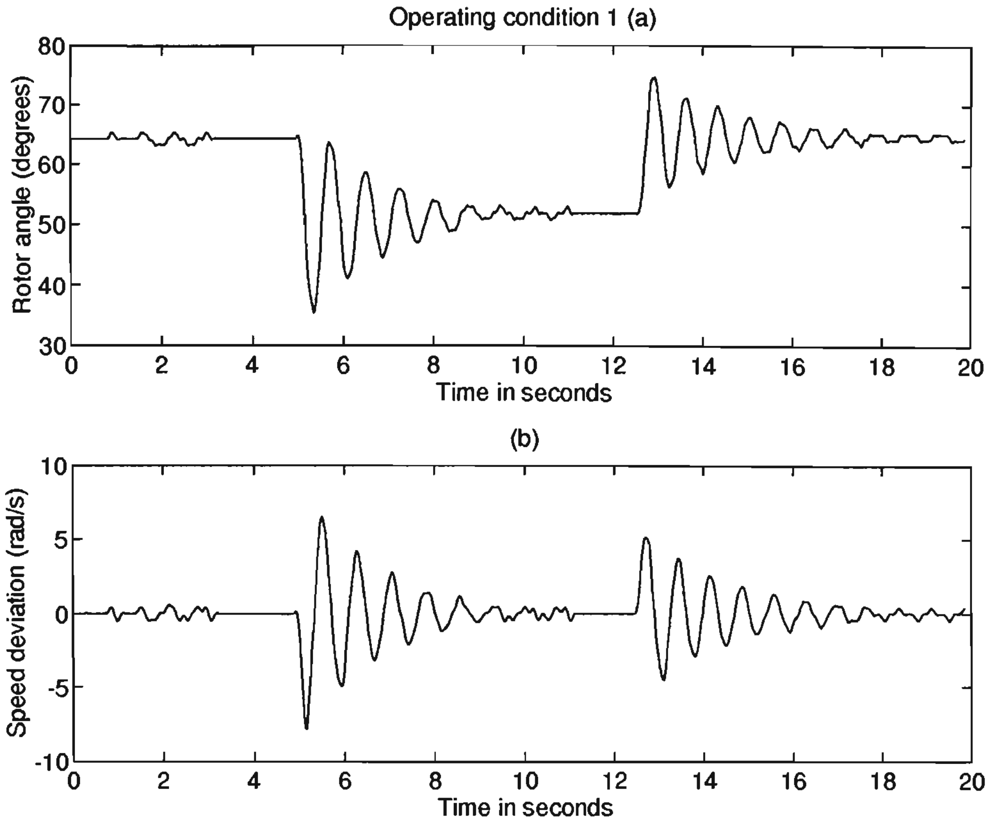

Figure 6.11: Rotor angle and speed deviation corresponding to sudden capacitive load change without the FLBPSS (operating condition OC1), (a)-rotor angle, (b)-speed deviation

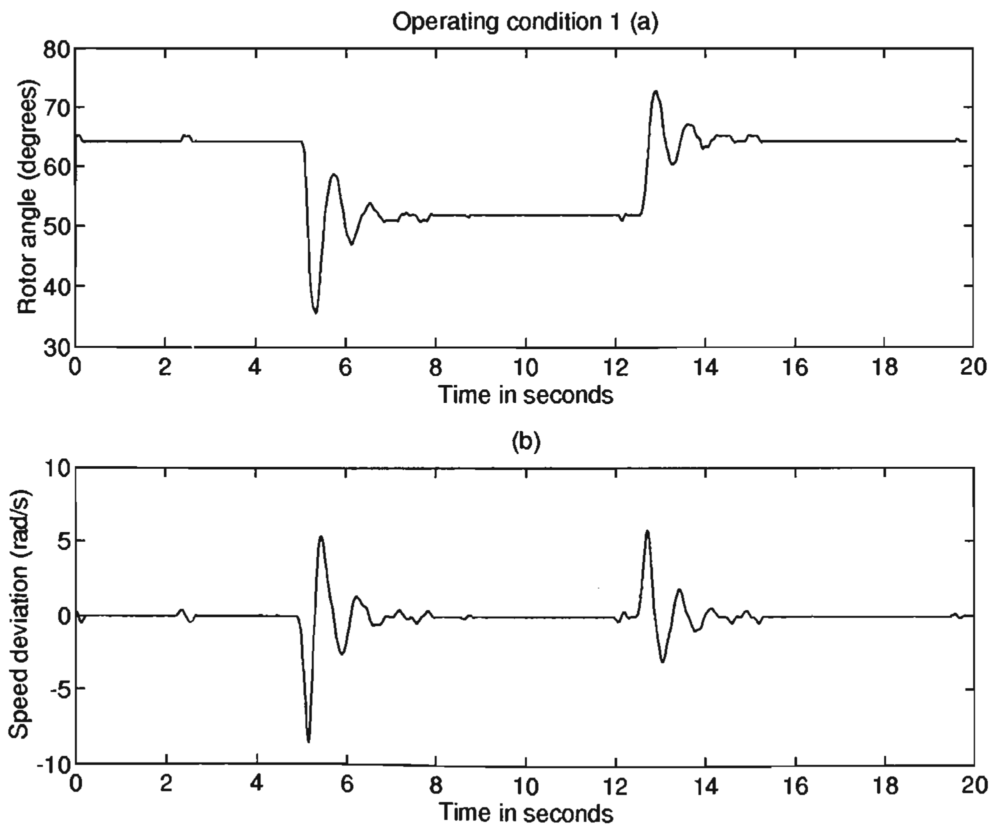

Figure 6.12: Rotor angle and speed deviation corresponding to sudden capacitive load change with the FLBPSS (operating condition OC1), (a)-rotor angle, (b)-speed deviation

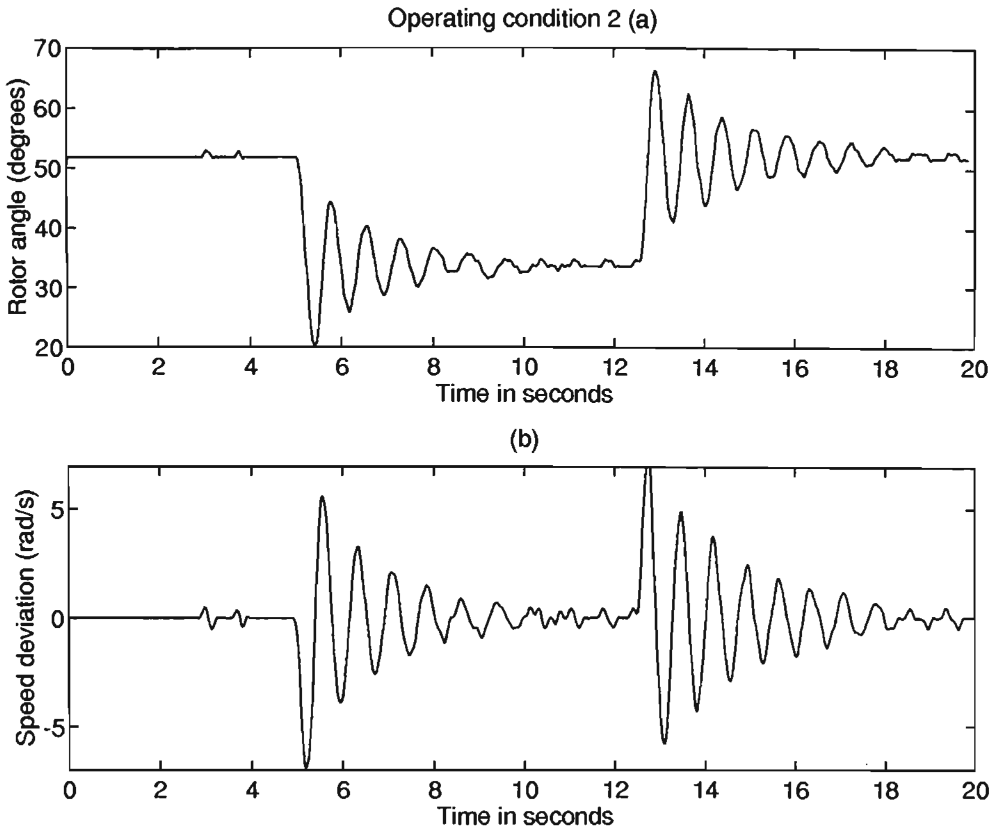

Figure 6.13: Rotor angle and speed deviation corresponding to sudden resistive load change without the FLBPSS (operating condition OC2), (a)-rotor angle, (b)-speed deviation

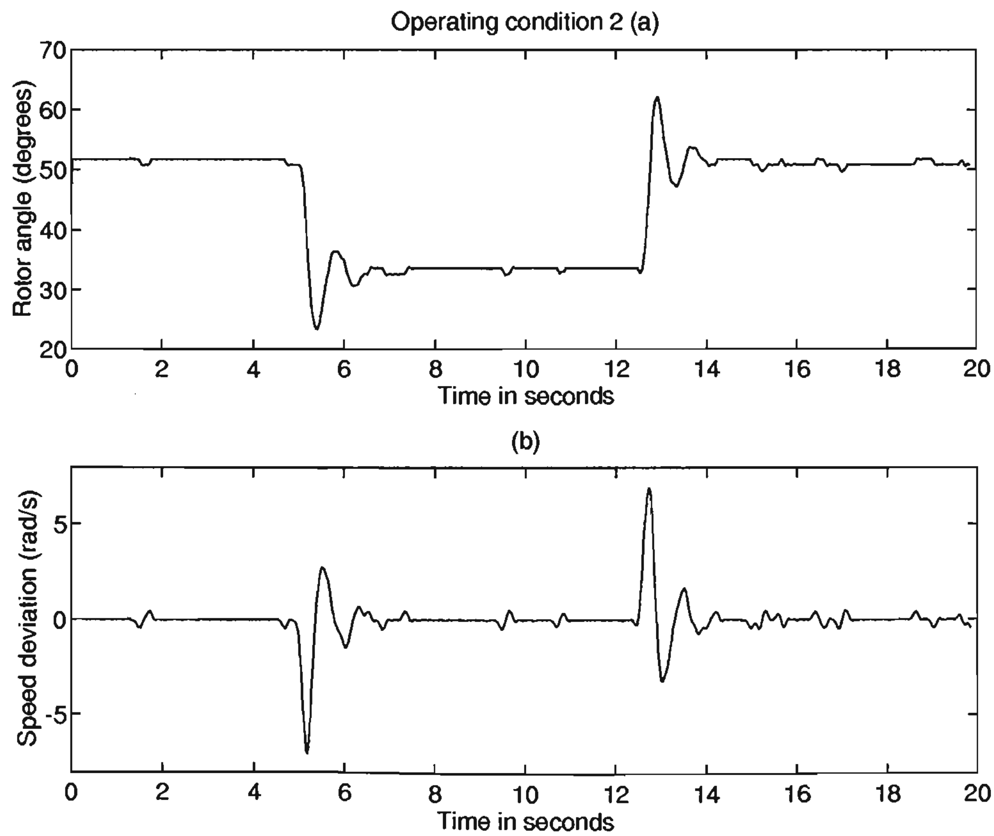

Figure 6.14: Rotor angle and speed deviation corresponding to sudden resistive load change with the FLBPSS (operating condition OC2), (a)-rotor angle, (b)-speed deviation

6.5 Concluding Remarks

The implementation of the optimised FLBPSS was tested on a single-machine infinite bus power system. The hardware and software development were described in detail in this chapter. The implementation test was carried out under different perturbations such as a 10% step change in the reference voltage as a small perturbation, a 3/4 rated sudden *resistive, inductive and capacitive* load changes and a three-phase to ground fault as large perturbations. The real time evaluation has also been tested under a wide range of operating conditions. The implementation results reveals that the optimised FLBPSS works well when the system is subject to either small or large perturbations. The performance of the optimised FLBPSS is robust with different types of step load changes (inductive, capacitive and resistive load). The optimised FLBPSS also works satisfactorily under a wide range of operating conditions without tuning or resetting of any parameters of the FLBPSS.

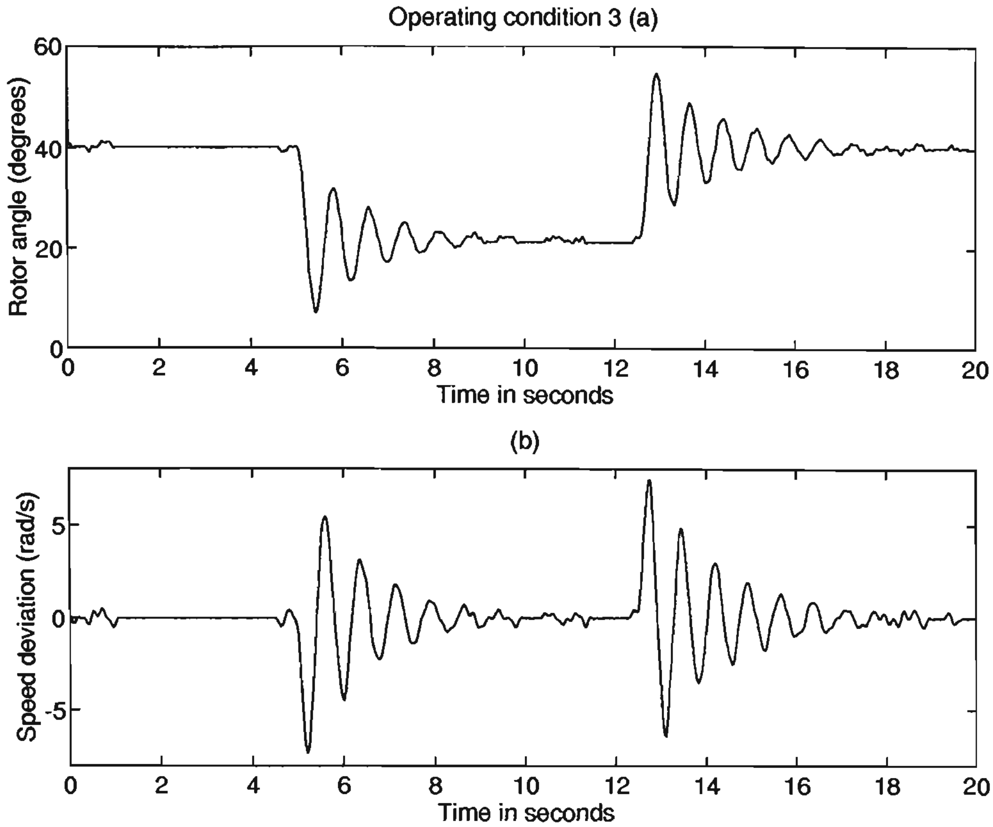

Figure 6.15: Rotor angle and speed deviation corresponding to sudden resistive load change without the FLBPSS (operating condition OC3), (a)-rotor angle, (b)-speed deviation

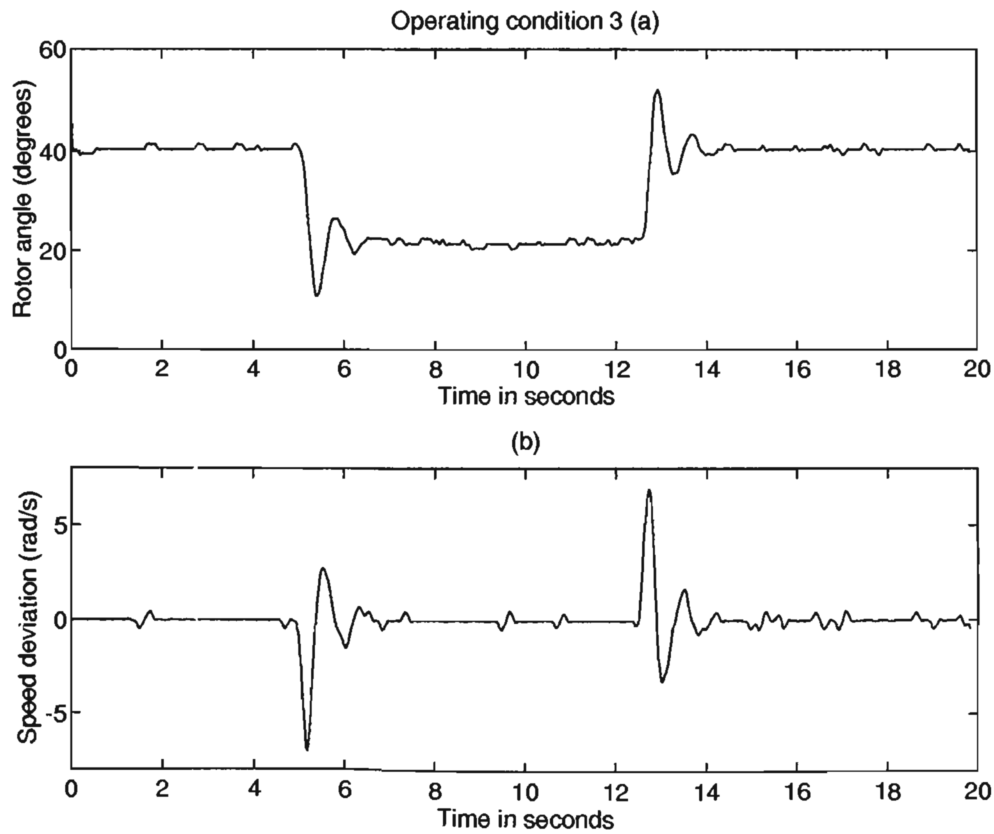

Figure 6.16: Rotor angle and speed deviation corresponding to sudden resistive load change with the FLBPSS (operating condition OC3), (a)-rotor angle, (b)-speed deviation

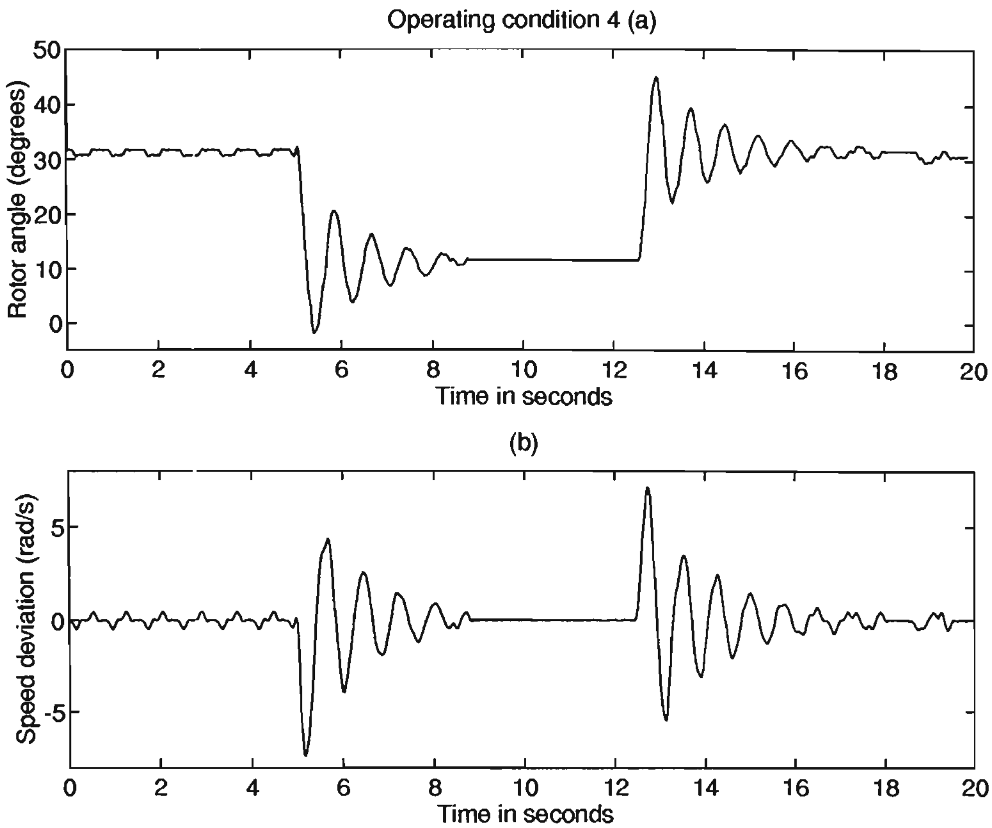

Figure 6.17: Rotor angle and speed deviation corresponding to sudden resistive load change without the FLBPSS (operating condition OC4), (a)-rotor angle, (b)-speed deviation

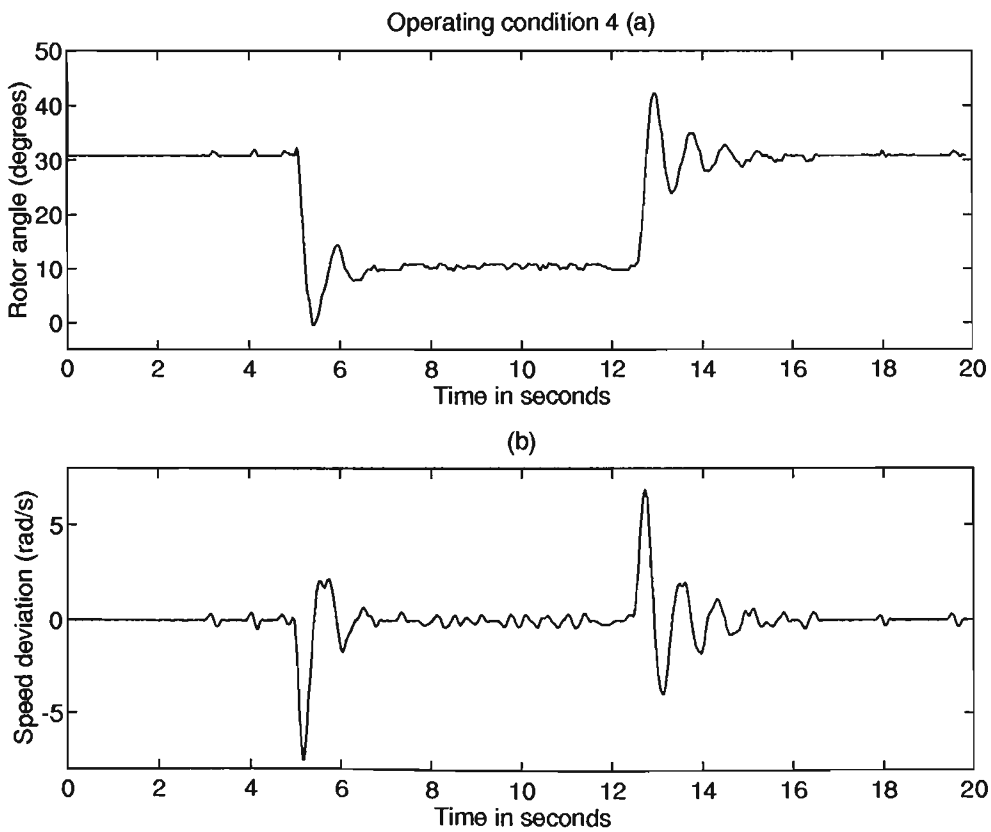

Figure 6.18: Rotor angle and speed deviation corresponding to sudden resistive load change with the FLBPSS (operating condition OC4), (a)-rotor angle, (b)-speed deviation

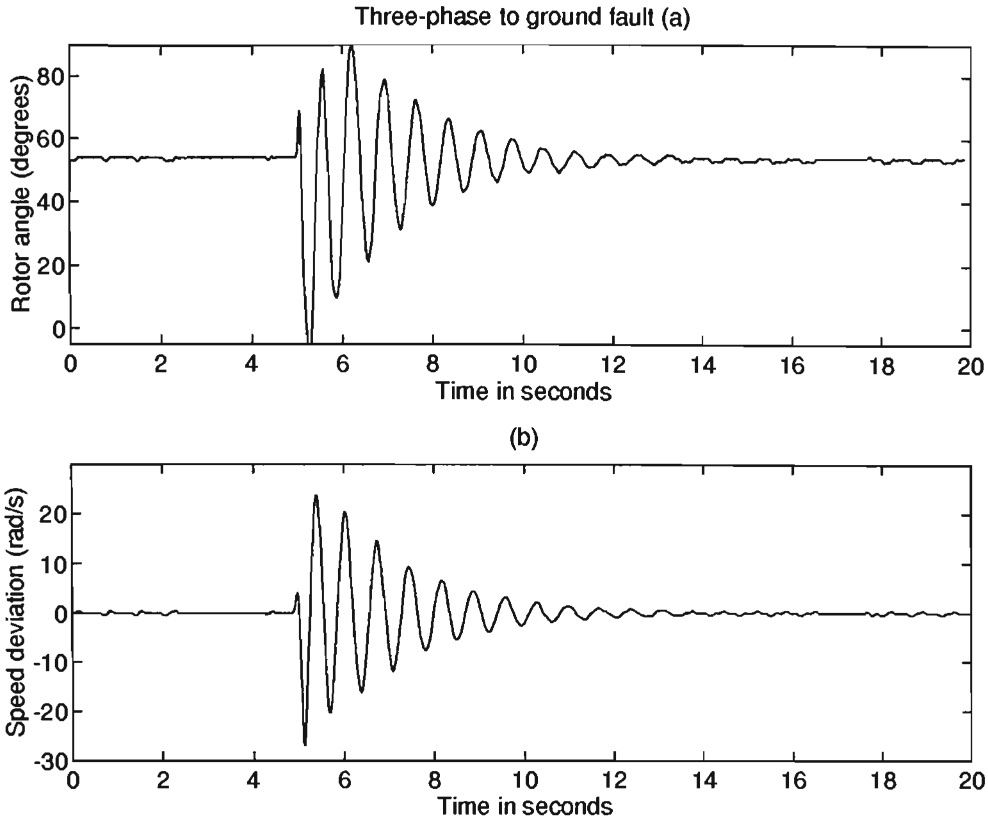

Figure 6.19: Rotor angle and speed deviation corresponding to a three-phase fault at A (Figure 2.2) sustained for 125 milliseconds (without the FLBPSS), (a)-rotor angle, (b)-speed deviation

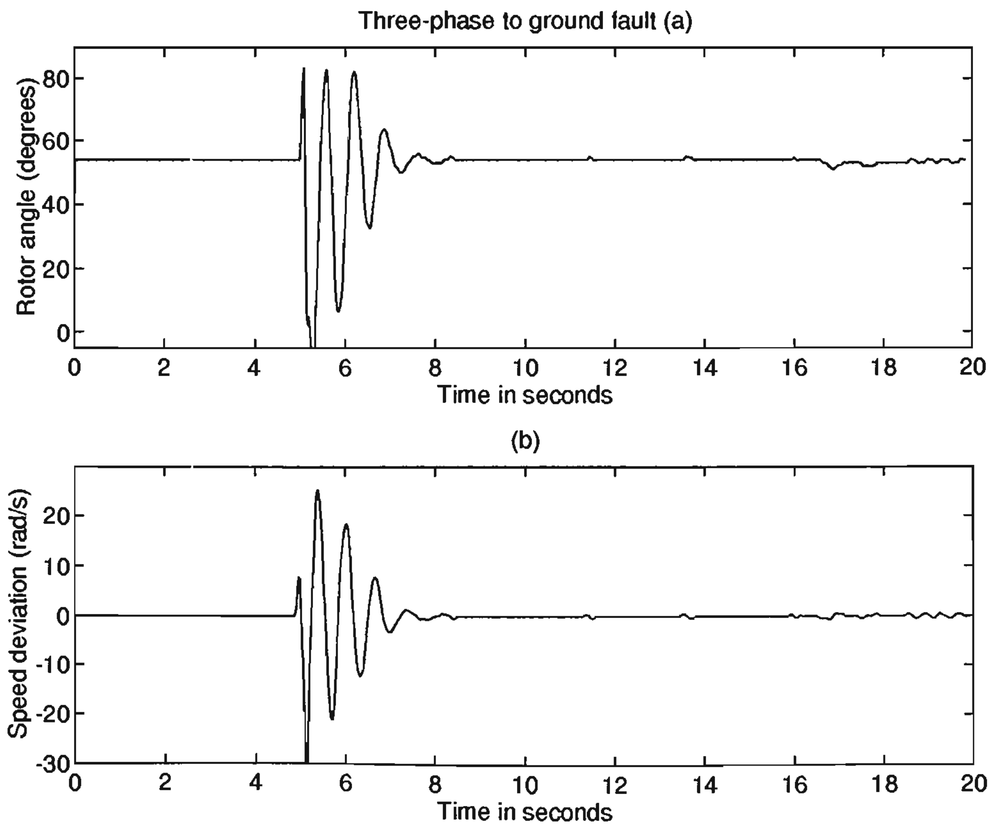

Figure 6.20: Rotor angle and speed deviation corresponding to a three-phase fault at A (Figure 2.2) sustained for 125 milliseconds (with the FLBPSS), (a)-rotor angle, (b)-speed deviation

Chapter 7

Application of the FLBPSS to Multi-machine Systems

7.1 Introduction

The interconnection of electric power systems is almost universal throughout the world. Basically, the electric power systems interconnect to each other because the interconnected systems is more reliable, it is a better system to operate and it may be operated at less cost than if left as separate parts. The merits of integrated power systems are summarised as follows [Wood, 1984]:

1. The maximum demand of an integrated system is much less than the sum of the individual non-coincident maximum demand of the sub-system comprising the system. The individual maximum demand occurs at different point of time because of diversity of the type of load, the lighting up time and the special characteristics of the systems.
2. The reserve on the system wide basis is reduced, and this means less economic operation.
3. During emergency, power can flow from surplus area to deficit areas. This makes the interconnections more reliable, since the loss of a generating unit in one of them can be made up from spinning reserve among units

throughout the interconnection. Thus, if a unit is lost in a control area, governing action from units in all connected areas will increase generation outputs to make up the deficit until standby units can be brought on-line. If a power system were to run isolated and lose a large unit, the chance of the other units in that isolated system being able to make up the deficit are greatly reduced.

4. It is possible to use large unit sizes which have better thermal efficiency so that the operating cost can be reduced.
5. The peak consumer demands can be economically distributed between the constituent sub-systems.
6. New generation size can be selected on a system wide basis rather than on local basis resulting in saving capital cost.
7. Maintenance is economical on a system wide basis which means the capital cost can be reduced.
8. For any given local demand, the cost of generation can be minimised and economic local dispatch can function most effectively.

However, it is observed that one of the most important stability problems arising from large scale electric power system interconnections is the low-frequency oscillations of interconnected systems. The frequency is of the order of a fraction of 1 Hz to a few Hz. The oscillations may be sustained for minutes and grow to cause system separation if no adequate damping at the system oscillating frequency is available.

In this project, the FLBPSS was used to damp the oscillations for a two-machine infinite bus power system.

This chapter is organised as follows:

In Section 7.2, the AVRs are designed for the two generators. The transfer function of the AVR for generator 1 is the same as in Chapter 3. The AVR for generator 2 is designed in Section 7.2.2. The practical evaluation of the AVRs are presented in Section 7.2.3. Three kinds of disturbances are applied to the system in order to test the performance of the designed AVRs. The design and optimisation of the FLBPSS is reviewed in Section 7.3. In section 7.4, simulation studies of the designed AVRs and the FLBPSS are demonstrated. The implementation results on the two-machine infinite bus power system are presented in Section 7.5 followed by the concluding remarks. A mathematical model of a three-machine power system can be found in Appendix D.

7.2 AVR Design

7.2.1 Design of the AVR for Generator 1

The design of the AVR for generator 1 in the two-machine infinite bus system was the same as in the single-machine infinite bus power system which was described previously in Chapter 3. The AVR transfer function for generator 1 can be rewritten as:

$$G_{AVR1}(z) = A\frac{5.0586 - 1.2345z^{-12}}{1 - BF(z)} \tag{7.1}$$

$$\begin{aligned} BF(z) &= 0.1467z^{-1} + 0.1304z^{-2} + 0.1160z^{-3} + 0.1031z^{-4} + 0.0917z^{-5} + 0.0815z^{-6} \\ &+ 0.0725z^{-7} + 0.0644z^{-8} + 0.0573z^{-9} + 0.0509z^{-10} + 0.0453z^{-11} + 0.0402z^{-12} \end{aligned} \tag{7.2}$$

The sensor DC gain B was found to be $5/240 = 0.0208$ and A is the gain of the field drive unit and was found to be 25 in this case.

7.2.2 Design of the AVR for Generator 2

Again the dynamic behaviour of the generator is described by a simplified linear model. The resulting block diagram was shown previously in Figure (3.1). The system parameters have been measured according to the IEEE test procedure for a 5kVA, 240V synchronous machine at the Power System Laboratory. The K parameters under one nominal operating condition (*real power* $P = 1pu$, *power factor PF=0.85 lag*) are shown as follows:

- $K_1 = 1.1158$
- $K_2 = 1.1825$
- $K_3 = 0.4347$
- $K_4 = 0.3453$
- $K_5 = 0.1161$
- $K_6 = 0.8204$
- $M = 2H = 2 * 0.524s$
- $\tau_{d0}^{'} = 0.56s$
- $D = 2$

Considering the single voltage-regulator loop in the block diagram of Figure (3.2), a simplified first order approximation voltage loop of the machine is given by

$$G_{v2}(s) = \frac{0.637}{1 + 0.28s} \tag{7.3}$$

Using discrete time analytical design methods described in Section 3.3 of Chapter 3, the transfer function for AVR2 can be expressed as in the following equation:

$$G_{AVR2}(z) = A\frac{N(z)}{1 - BF(z)} \tag{7.4}$$

where the sample time used is also 25 milliseconds and the gain A for the field drive unit is 25.

$$\begin{aligned} N(z) = 6.69 + 0.038z^{-1} - 0.038z^{-2} + 0z^{-3} + 0z^{-4} - 0.006z^{-5} + 0.045z^{-6} \\ + 0.025z^{-7} + 0.025z^{-8} - 0.045z^{-9} + 0z^{-10} + 0.064z^{-11} - 3.95z^{-12} \end{aligned} \tag{7.5}$$

$$BF(z) = 0.105z^{-1} + 0.101z^{-2} + 0.096z^{-3} + 0.092z^{-4} + 0.088z^{-5} + 0.084z^{-6}$$
$$+ 0.081z^{-7} + 0.077z^{-8} + 0.074z^{-9} + 0.07z^{-10} + 0.067z^{-11} + 0.065z^{-12} \quad (7.6)$$

7.2.3 Practical Evaluation of the Designed AVRs

The performance of the designed AVRs was tested experimentally in the power laboratory. The following disturbances were applied to the system in order to test the performance of the AVRs.

- a 10% step increase in the reference voltage at generator 1 side sustained for 7.5 seconds;
- 3/4 rated load increase at generator 1 side sustained for 7.5 seconds;
- a three-phase to ground fault at B (Figure 2.4) sustained for 125 milliseconds.

Test of AVRs on a step change in generator reference voltage

A small perturbation of a 10% step increase in the reference voltage sustained for 7.5 seconds has been applied at generator 1 side in order to test the performance of the designed AVRs on a two-machine infinite bus power system. Figure (7.1) shows the voltage response for both generators in response to the disturbance. From this figure it can be seen that the voltage is tracking the reference voltage value with no steady state error. The overshoot and settling time all satisfy the IEEE standards on excitation control [IEEE, 1978].

Test of AVRs in response to rated load change

Figures (7.2)-(7.4) show the terminal voltage response corresponding to a 3/4 rated sudden inductive, capacitive and resistive load change with the designed AVRs; It can be seen that the system equipped with the designed AVRs kept the terminal voltage output constant under various loading conditions. The performance of the digital AVRs is then theoretically analysed and experimentally verified.

Test of AVRs in response to a three-phase to ground fault

Figures (7.5)-(7.6) show the terminal voltages and control signals in response to a three-phase to ground fault at B (Figure 2.4) sustained for 125 milliseconds. It can be seen that the excitation control signals reached the ceiling (i.e., the hardware limit $\pm 10V$) very quickly when the system was subject to such a large disturbance. The terminal voltage of generator 1 reduced towards zero during the fault and has been brought back to its original value as soon as the fault was cleared. The fault occurred at generator 1 terminal, however, the terminal voltage at generator 2 has also been affected due to the interconnection.

7.3 The Design and Optimisation of the FLBPSS

The design of the proposed FLBPSS was presented previously in Chapter 4. The optimisation strategy is the same as presented in Chapter 5. For the optimisation and implementation study, only generator 1 was equipped with the proposed FLBPSS. The optimal values of α, β and D_r were found to be 30,-40 and 0.6 respectively.

7.4 Simulation Results for the FLBPSS

Figures (7.7)-(7.8) show the speed deviation of generators 1 and 2 corresponding to a 10% step increase in the reference voltage followed by a 10% step increase in the mechanical torque. Figures (7.9)-(7.10) show the speed deviation of generators 1 and 2 corresponding to a 20% step increase in reference voltage followed by a 20% step increase in the mechanical torque. Figures (7.7) and (7.9) demonstrate the results without the FLBPSS. Figures(7.8) and (7.10) show the results with the FLBPSS. Figures (7.7)-(7.10) (a) show the system response for generator 1 and Figures (7.7)-(7.10) (b) for generator 2. From those figures, it can be seen that the FLBPSS is very effective in damping the system oscillations.

7.5 Implementation and Test Results for the FLBPSS

The disturbances applied to the experimental two-machine infinite bus power system were:

- a 10% step increase in the reference voltage at generator 1 side sustained for 7.5 seconds;
- 3/4 rated load increase at generator 1 side sustained for 7.5 seconds;
- a three-phase to ground fault at B (Figure 2.4) sustained for 125 milliseconds;
- the transmission line loss between generators 1 and 2.

Generators 1 and 2 were both equipped with the designed digital AVRs. During all the tests, only generator 1 was equipped with the optimised FLBPSS.

7.5.1 Step Change in the Reference Voltage at Generator 1 Side

Figures (7.11)-(7.14) show the rotor angle and speed deviation in response to a 10% step increase in the reference voltage sustained for 7.5 seconds at generator 1 side under the nominal operating condition (real power $P_1 = 1pu, P_2 = 1pu$, power factor $PF_1 = 0.95$ (lag), $PF_2 = 0.85$ (lag)). Figures (7.11) and (7.12) show the results without and with the FLBPSS respectively for generator 1. Figures (7.13) and (7.14) demonstrate the results without and with the FLBPSS respectively for generator 2. It can be seen that the oscillation has been damped out very quickly (within 2 cycles) for both machines although only one machine was equipped with the optimised FLBPSS.

7.5.2 Rated Load Change

Figures (7.15)-(7.26) show the rotor angle and speed deviation corresponding to a 3/4 rated load change under the nominal operating condition (real power $P_1 =$

$1pu, P_2 = 1pu$, power factor $PF_1 = 0.95$ (lag), $PF_2 = 0.85$ (lag)). Figures (7.15) and (7.16) show the results corresponding to 3/4 rated sudden resistive load change for generator 1 without and with the FLBPSS respectively. Figures (7.17) and (7.18) show the results for generator 2 in response to 3/4 sudden resistive load change without and with the FLBPSS respectively. Studies were also carried out for different load changes such as inductive and capacitive load changes. Figures (7.19)-(7.22) show the results corresponding to sudden inductive load change and Figures (7.23)-7.26) show the results corresponding to sudden capacitive load change. Figures (7.19) and (7.20) show the rotor angle and speed deviation corresponding to 3/4 sudden inductive load change without the FLBPSS for generators 1 and 2 respectively. Figures (7.21) and (7.22) show the rotor angle and speed deviation corresponding to 3/4 sudden inductive load change with the FLBPSS for generators 1 and 2 respectively. Figures (7.23) and (7.24) show the rotor angle and speed deviation corresponding to 3/4 sudden capacitive load change without the FLBPSS for generators 1 and 2 respectively. Figures (7.25) and (7.26) show the rotor angle and speed deviation corresponding to 3/4 sudden capacitive load change with the FLBPSS for generators 1 and 2 respectively. It can be seen from the above figures that the optimised FLBPSS damped the system oscillations out very effectively.

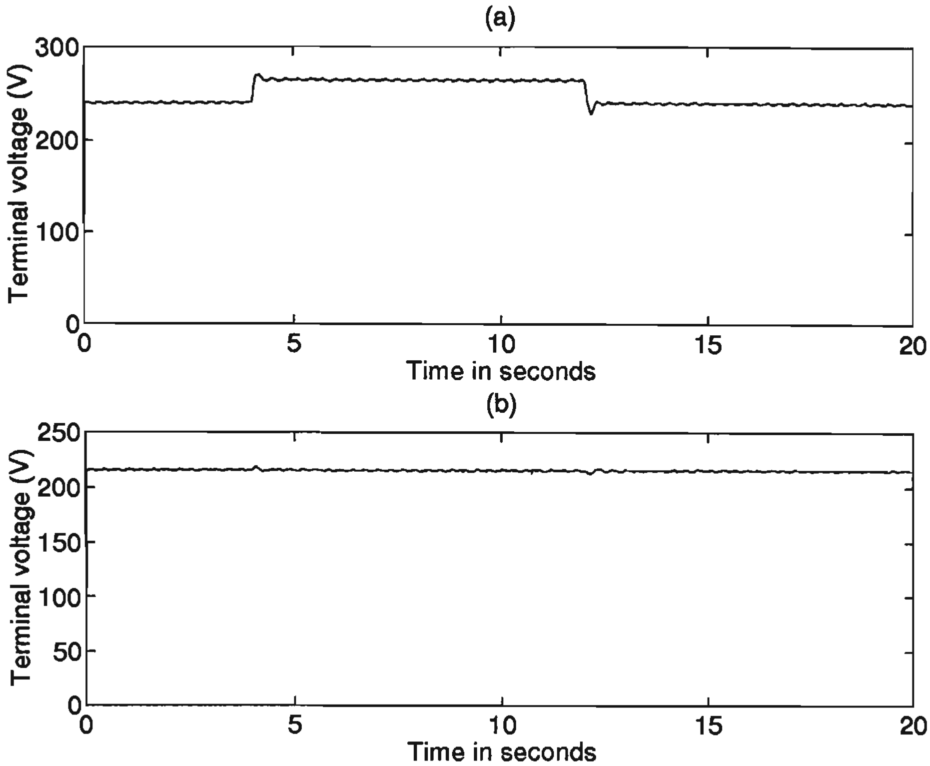

Figure 7.1: Terminal voltage corresponding to a 10% step change in reference voltage at generator 1 side, (a)-terminal voltage for generator 1, (b)-terminal voltage for generator 2

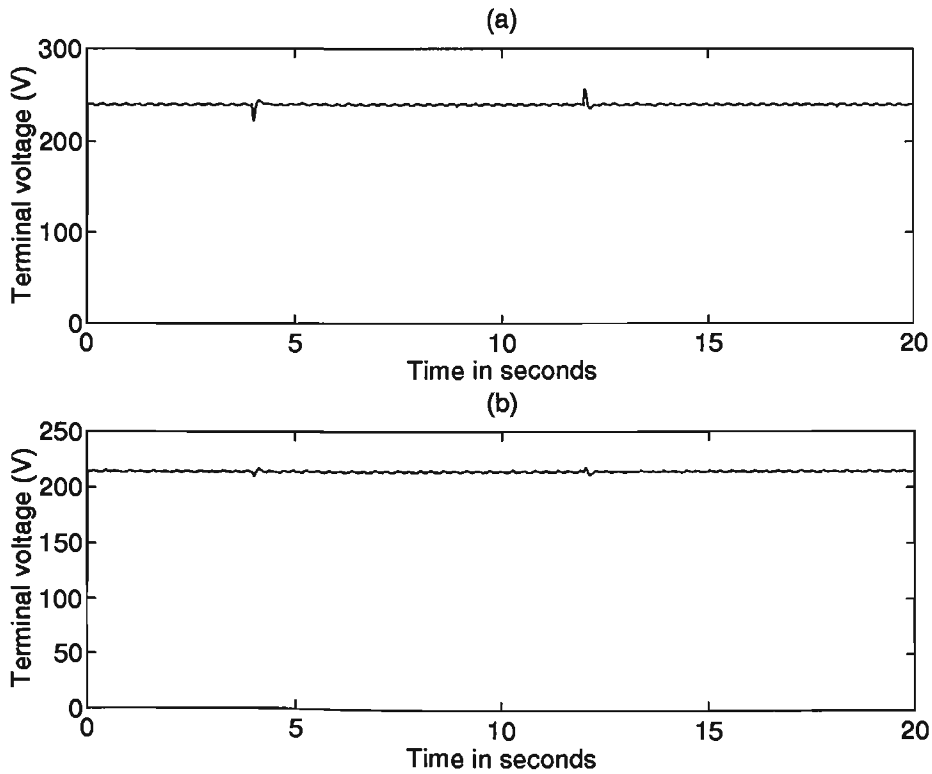

Figure 7.2: Terminal voltage corresponding to 3/4 rated inductive load change, (a)-terminal voltage for generator 1, (b)-terminal voltage for generator 2

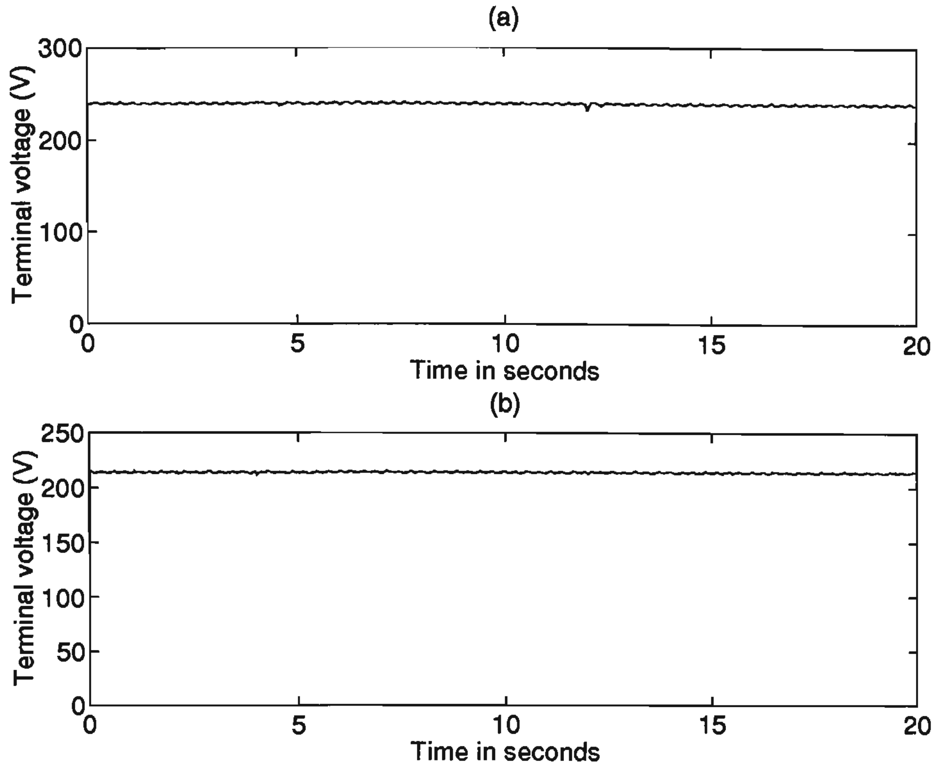

Figure 7.3: Terminal voltage corresponding to 3/4 rated capacitive load change, (a)-terminal voltage for generator 1, (b)-terminal voltage for generator 2

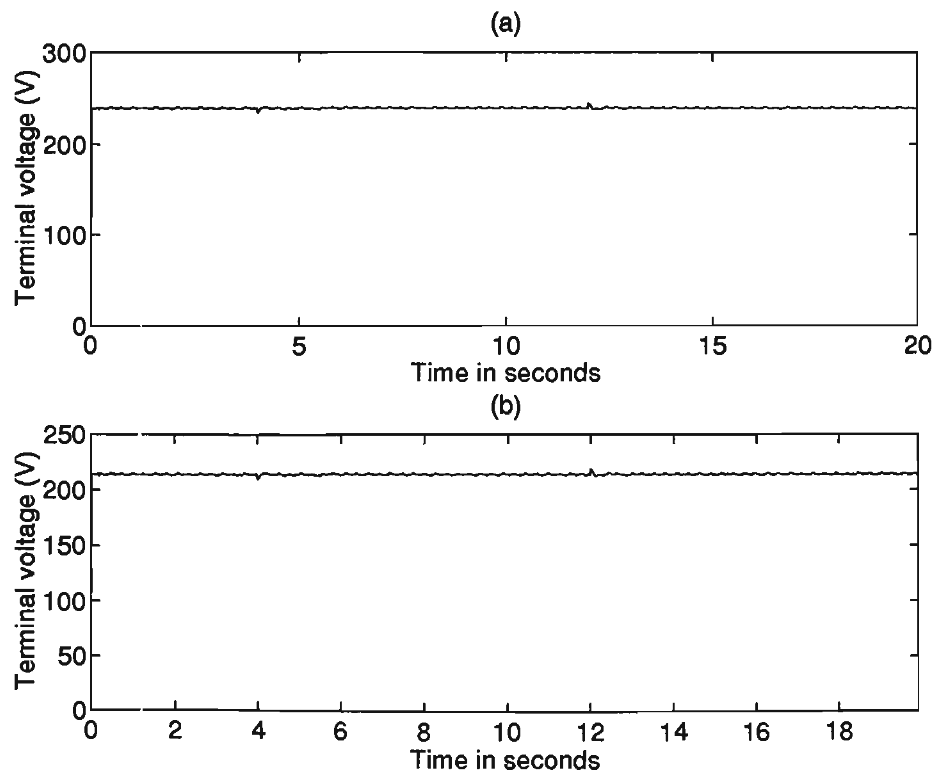

Figure 7.4: Terminal voltage corresponding to 3/4 rated resistive load change, (a)-terminal voltage for generator 1, (b)-terminal voltage for generator 2

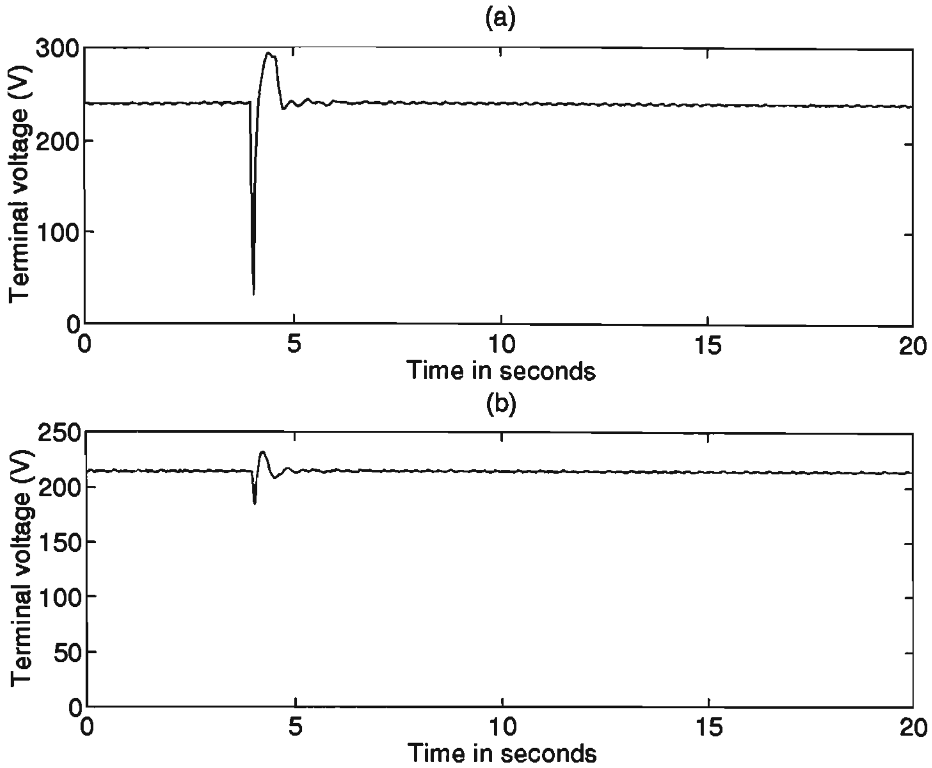

Figure 7.5: Terminal voltage corresponding to a three-phase to ground fault, (a)-terminal voltage for generator 1, (b)-terminal voltage for generator 2

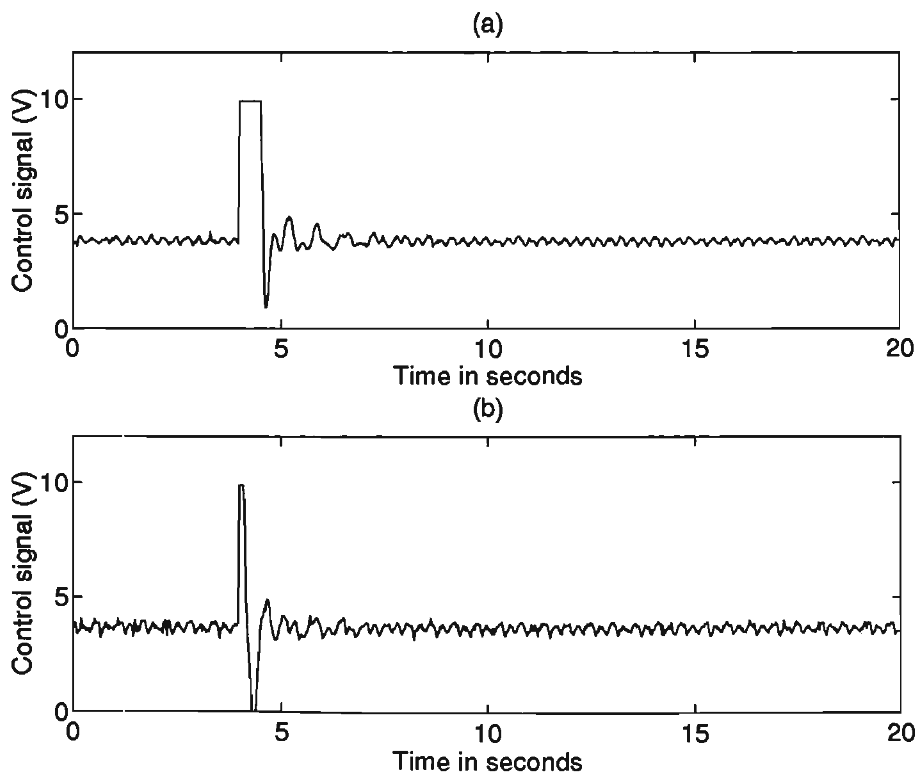

Figure 7.6: Excitation control signal corresponding to a three-phase to ground fault, (a)-control signal for generator 1, (b)-control signal for generator 2

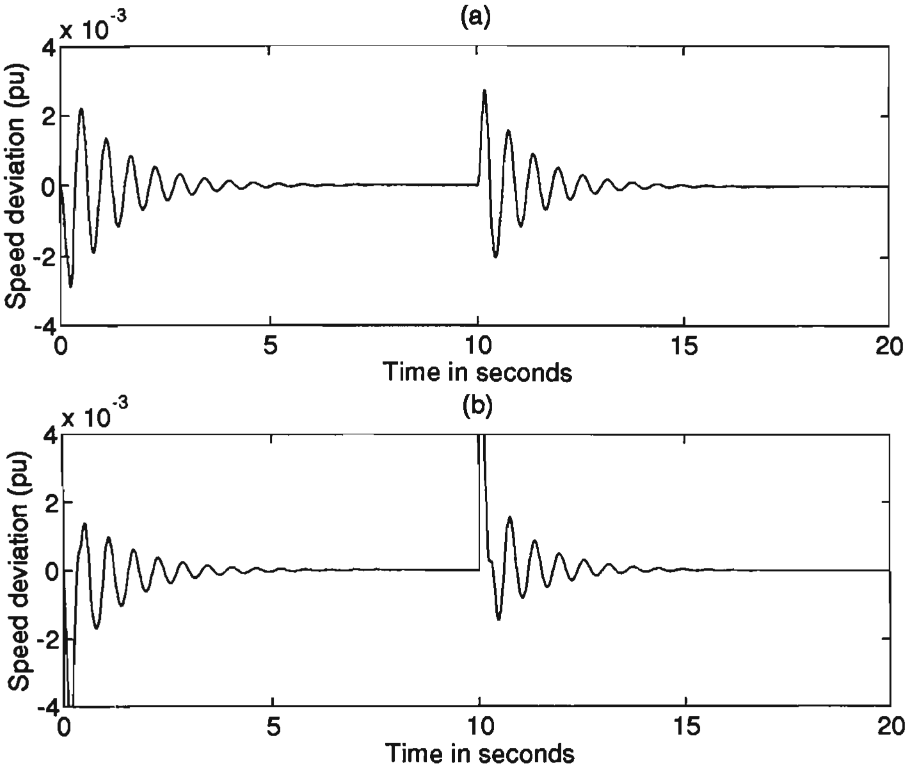

Figure 7.7: System response corresponding to a 10% step change in reference voltage and mechanical torque without PSS, (a)-speed deviation for generator 1, (b)-speed deviation for generator 2

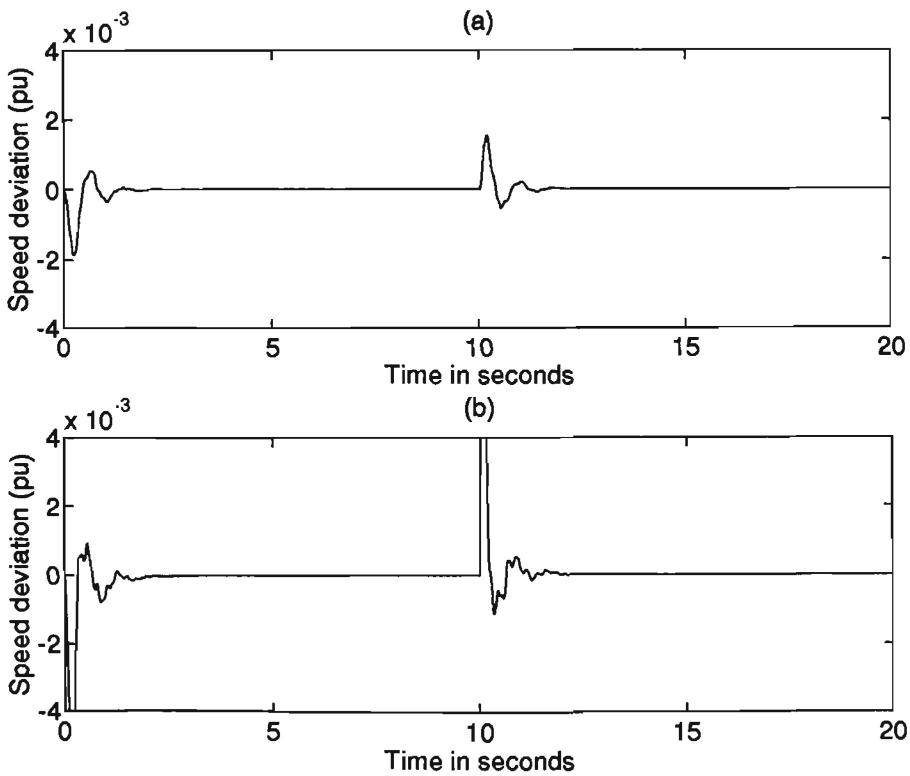

Figure 7.8: System response corresponding to a 10% step change in reference voltage and mechanical torque with the FLBPSS, (a)-speed deviation for generator 1, (b)-speed deviation for generator 2

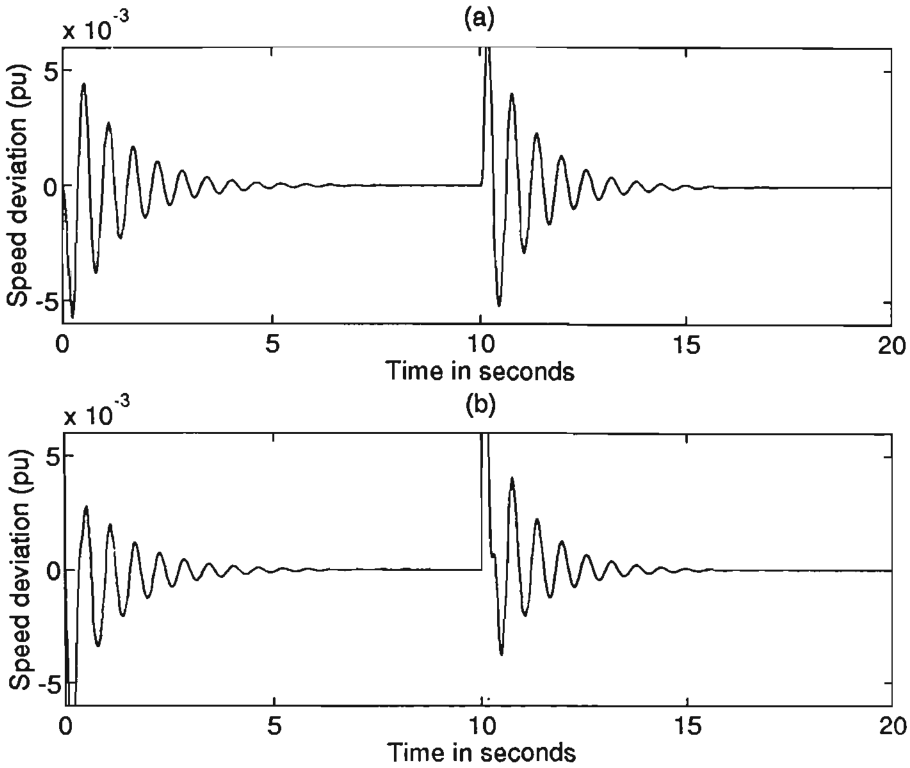

Figure 7.9: System response corresponding to a 20% step change in reference voltage and mechanical torque without the FLBPSS, (a)-speed deviation for generator 1, (b)-speed deviation for generator 2

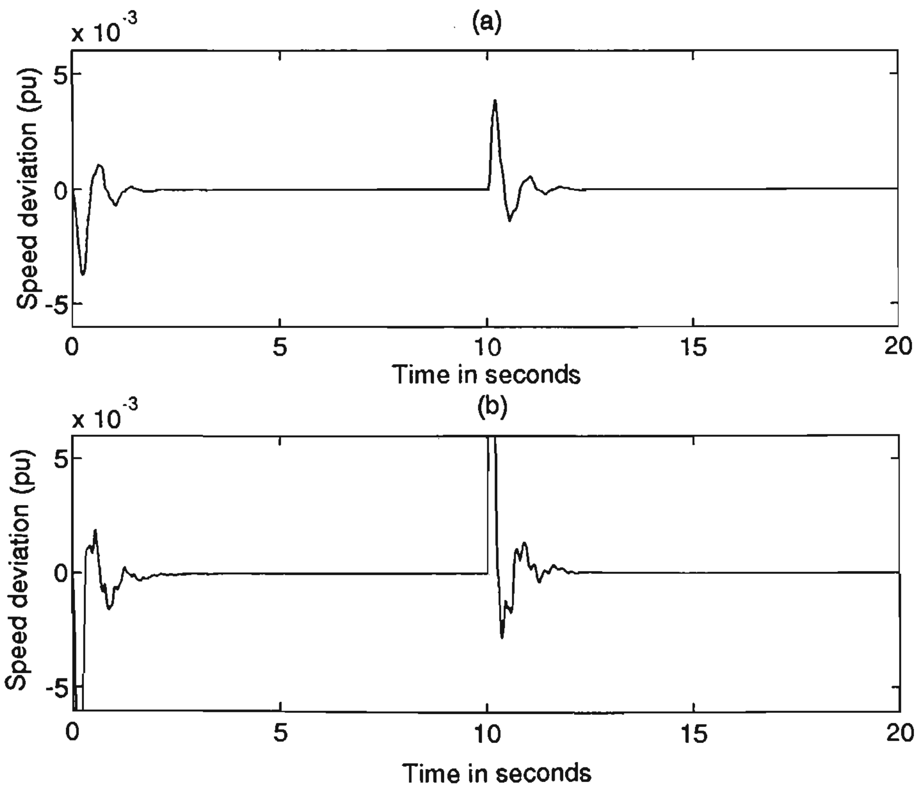

Figure 7.10: System response corresponding to a 20% step change in reference voltage and mechanical torque with the FLBPSS, (a)-speed deviation for generator 1, (b)-speed deviation for generator 2

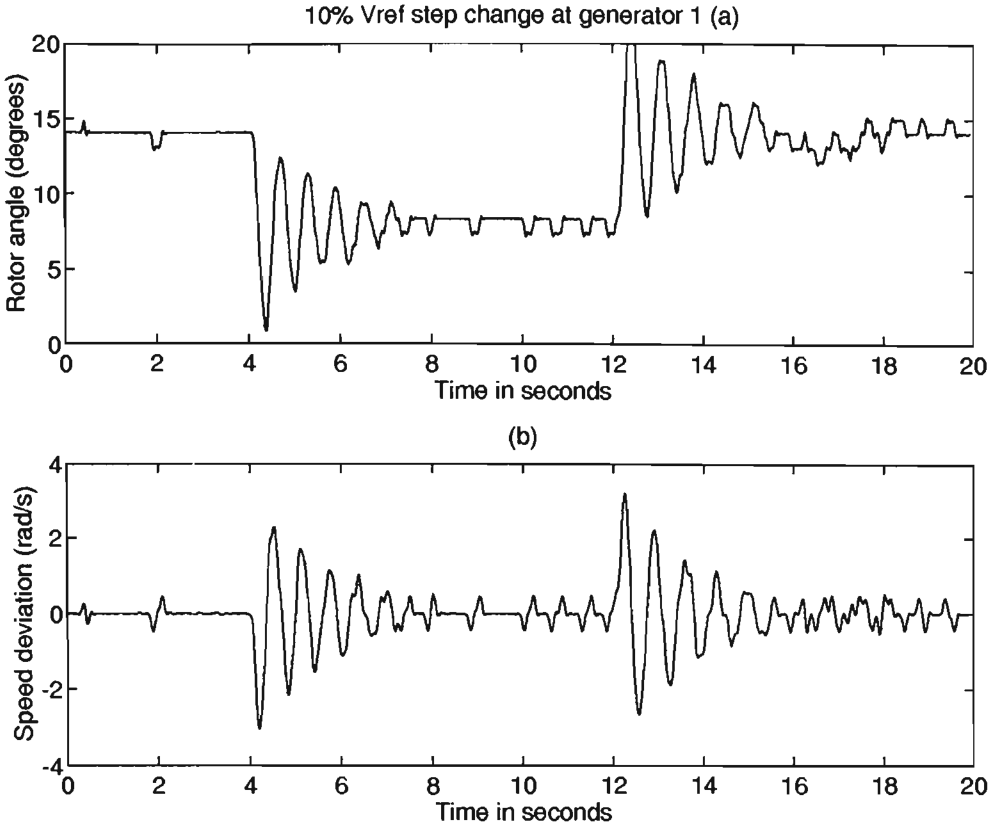

Figure 7.11: Rotor angle and speed deviation for generator 1 corresponding to a 10% step increase in the reference voltage at generator 1 sustained for 7.5 seconds (without the FLBPSS), (a)-rotor angle, (b)-speed deviation

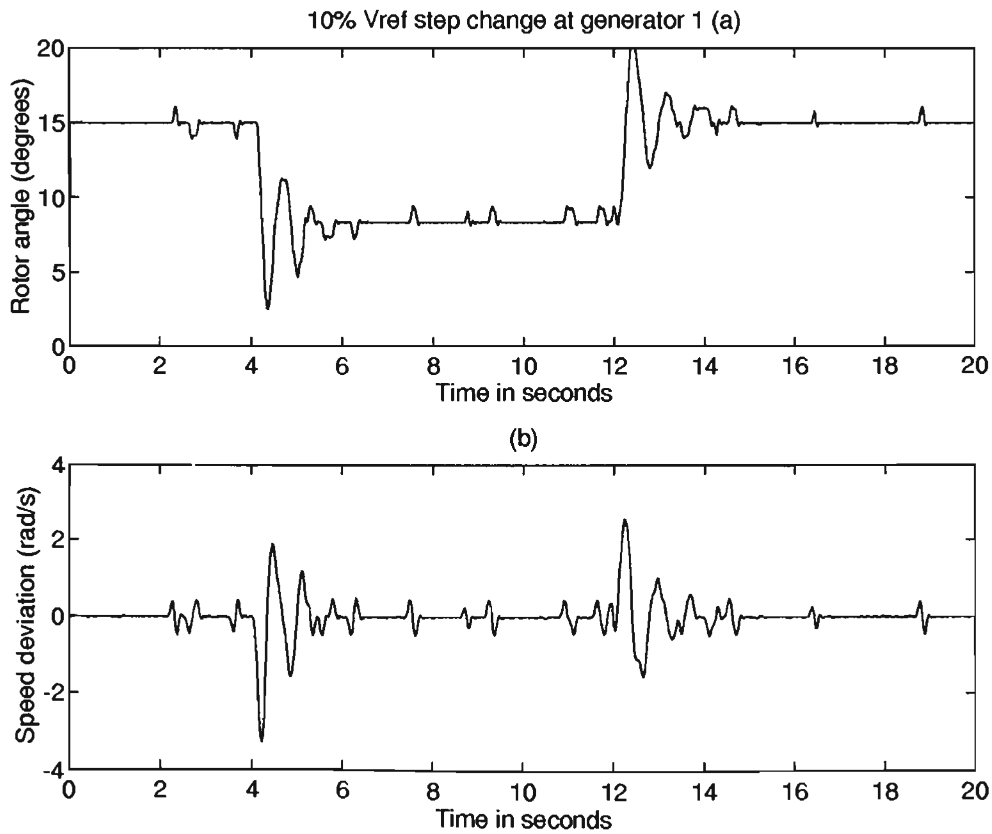

Figure 7.12: Rotor angle and speed deviation for generator 1 corresponding to a 10% step increase in the reference voltage at generator 1 sustained for 7.5 seconds (with the FLBPSS), (a)-rotor angle, (b)-speed deviation

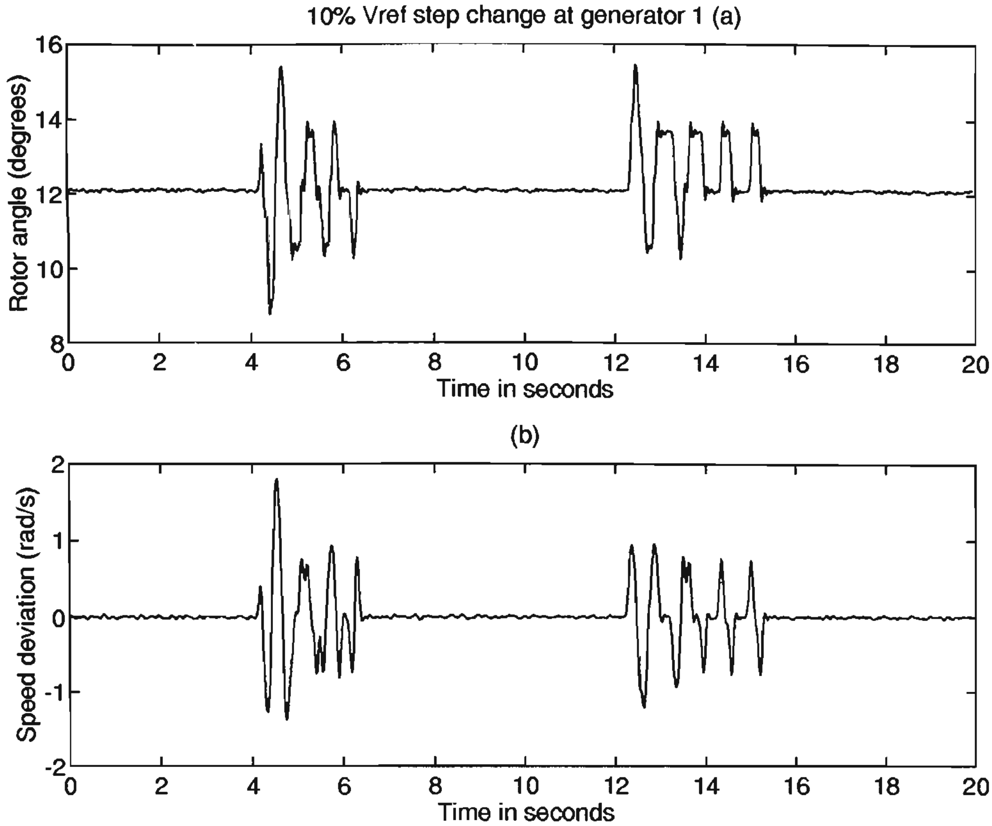

Figure 7.13: Rotor angle and speed deviation for generator 2 corresponding to a 10% step increase in the reference voltage at generator 1 sustained for 7.5 seconds (without the FLBPSS), (a)-rotor angle, (b)-speed deviation

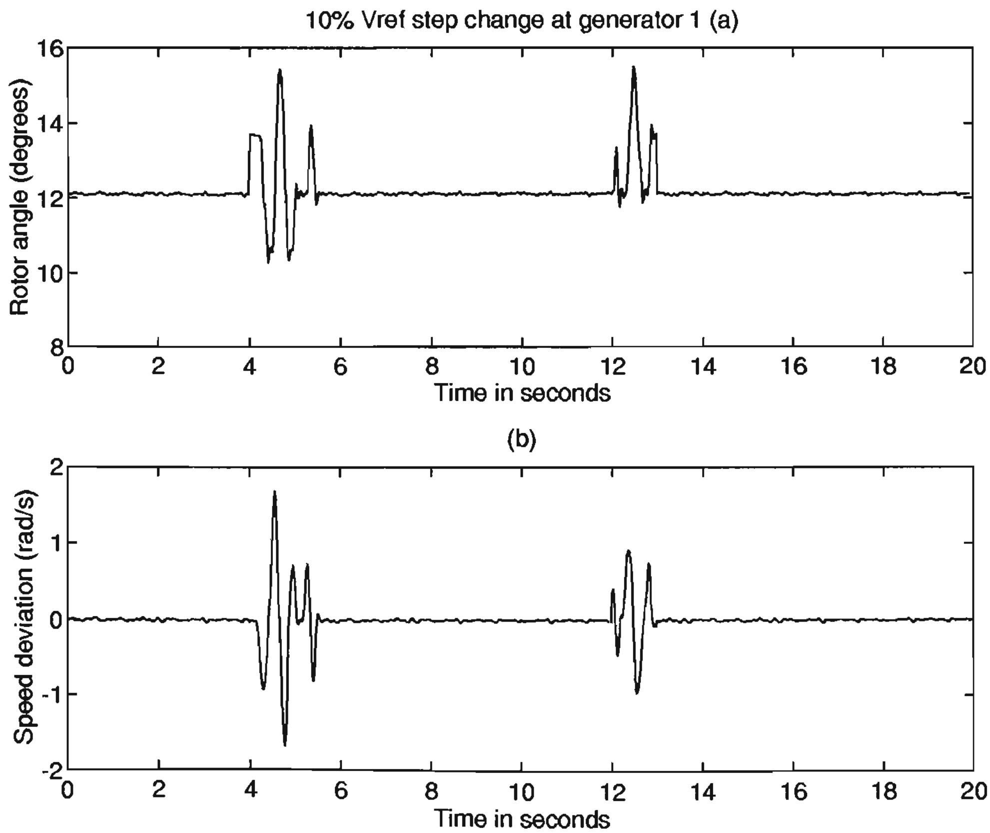

Figure 7.14: Rotor angle and speed deviation for generator 2 corresponding to a 10% step increase in the reference voltage at generator 1 sustained for 7.5 seconds (with the FLBPSS), (a)-rotor angle, (b)-speed deviation

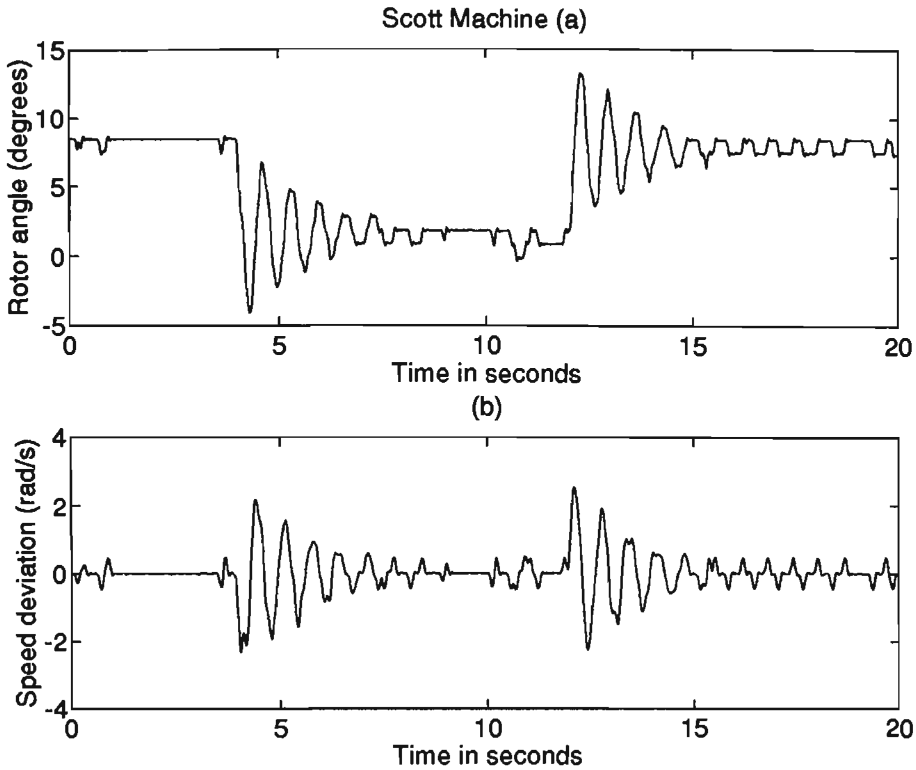

Figure 7.15: Rotor angle and speed deviation for generator 1 corresponding to sudden resistive load change (without the FLBPSS), (a)-rotor angle, (b)-speed deviation

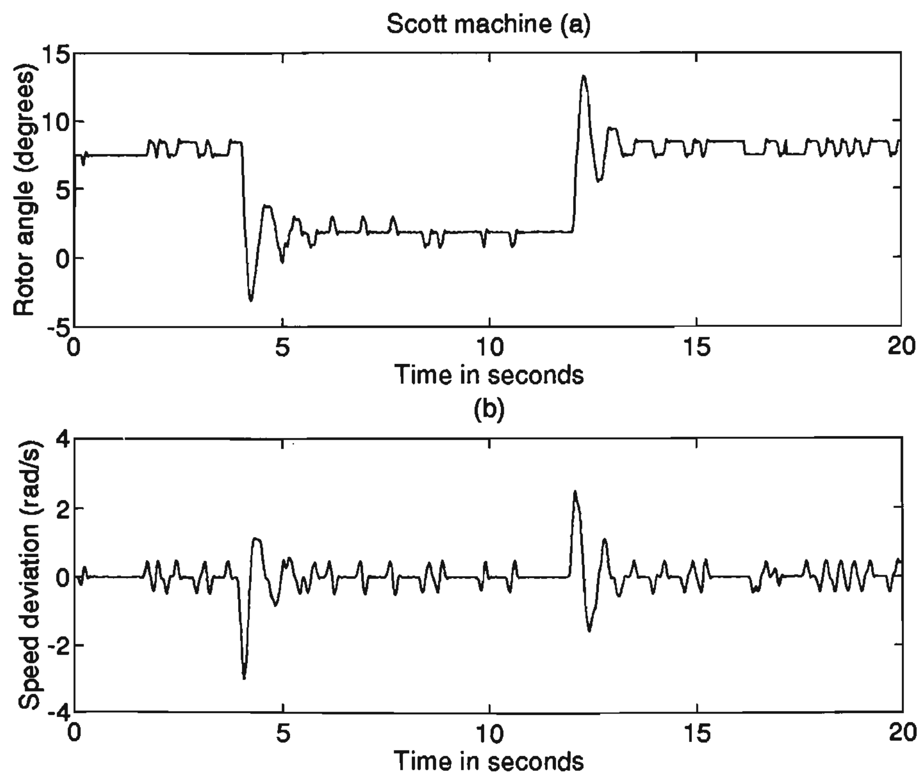

Figure 7.16: Rotor angle and speed deviation for generator 1 corresponding to 3/4 rated sudden resistive load change (with the FLBPSS), (a)-rotor angle, (b)-speed deviation

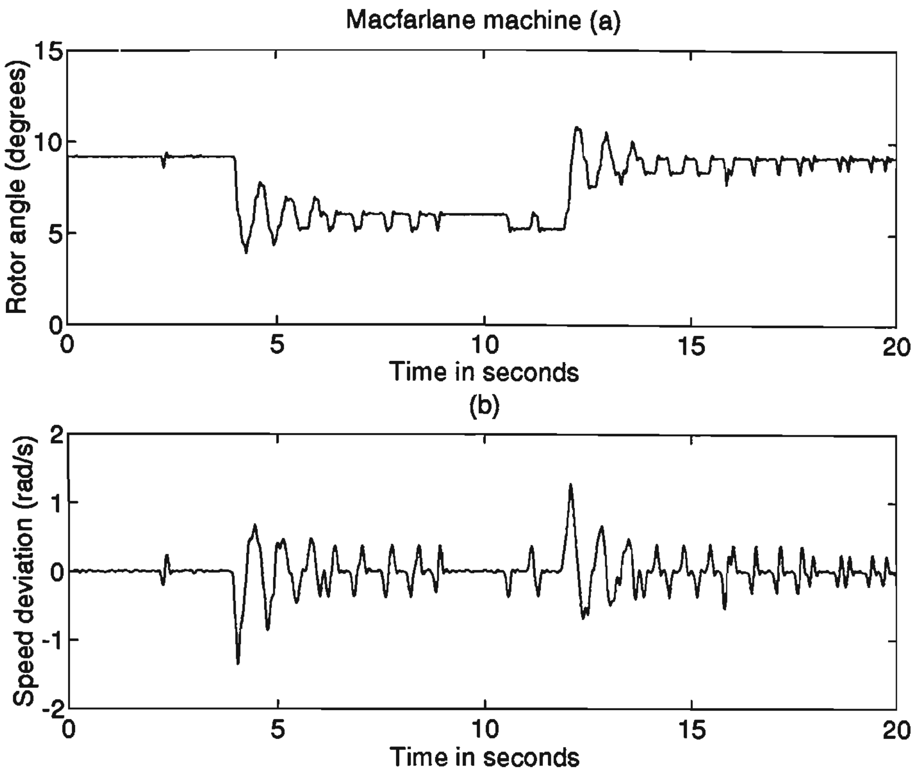

Figure 7.17: Rotor angle and speed deviation for generator 2 corresponding to 3/4 rated sudden resistive load change (without the FLBPSS), (a)-rotor angle, (b)-speed deviation

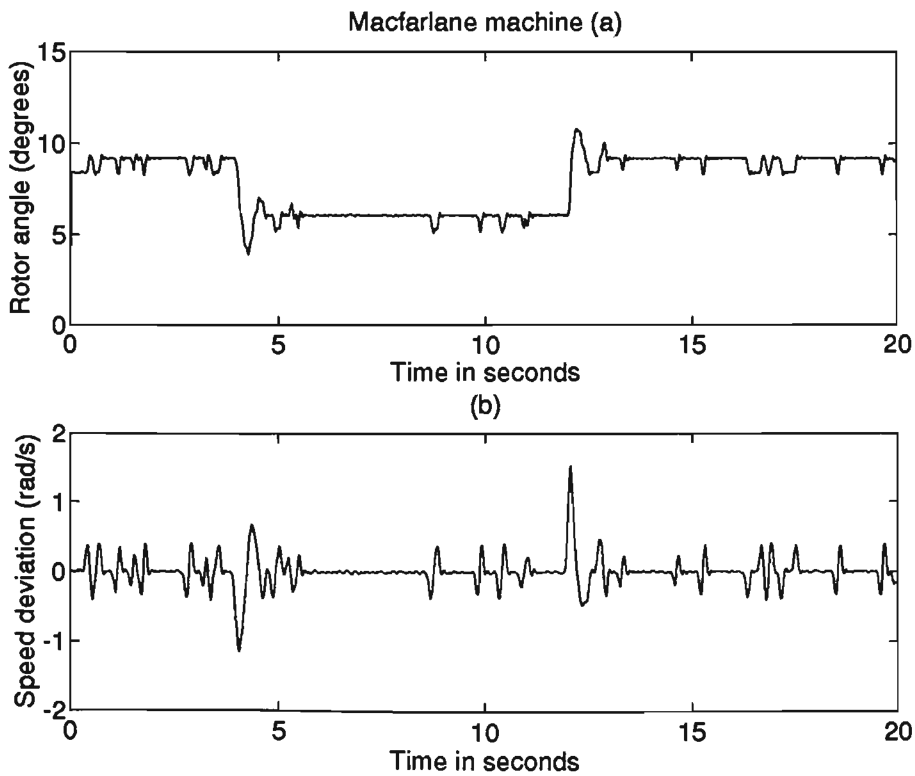

Figure 7.18: Rotor angle and speed deviation for generator 2 corresponding to 3/4 rated sudden resistive load change (with the FLBPSS), (a)-rotor angle, (b)-speed deviation

7.5.3 Test Results Under Different Operating Conditions

The performance of the FLBPSS corresponding to a 10% step change in reference voltage and sudden load change has also been tested under different operating conditions (OC) as shown in Table (7.1). However, only the system response corresponding to resistive load change under operating condition $P1$ is shown here. Figures (7.27)-(7.30) show the rotor angle and speed deviation for both generators corresponding to a 3/4 rated resistive load change under operating condition $P1$. Figures (7.27) and (7.29) show the results without the FLBPSS for generators 1 and 2 respectively. Figures (7.28) and (7.30) show the results with the FLBPSS for generators 1 and 2 respectively. It can be seen that the FLBPSS works well under different operating conditions. Similar test results were also obtained (not shown here) for inductive and capacitive load changes at different operating conditions.

OC	OC0	OC1	OC2
P	$P_1 = 1pu, P_2 = 1pu$	$P_1 = 0.6pu, P_2 = 1pu$	$P_1 = 0.42pu, P_2 = 1pu$
PF	$PF_1 = 0.95,\ PF_2 = 0.85$	$PF_1 = 0.98,\ PF_2 = 0.84$	$PF_1 = 0.707,\ PF_2 = 0.85$

Table 7.1: Operating conditions for two-machine infinite bus power system

7.5.4 Three-phase to Ground Fault

The system response corresponding to a three-phase to ground fault at B (Figure 2.4) sustained for 125 milliseconds under the nominal operating condition are shown in Figures (7.31)-(7.34). Figures (7.31) and (7.33) show the rotor angle and speed deviation without the FLBPSS for generator 1 and 2 respectively. Figures (7.32) and (7.34) demonstrate the rotor angle and speed deviation with the FLBPSS for generators 1 and 2 respectively. Comparing Figures (7.32) and (7.34) with Figures (7.31) and (7.33), it can be seen that the FLBPSS works well when the system was subject to such large disturbances. Similar results were obtained (not shown here) under different operating conditions as listed previously in Table 7.1.

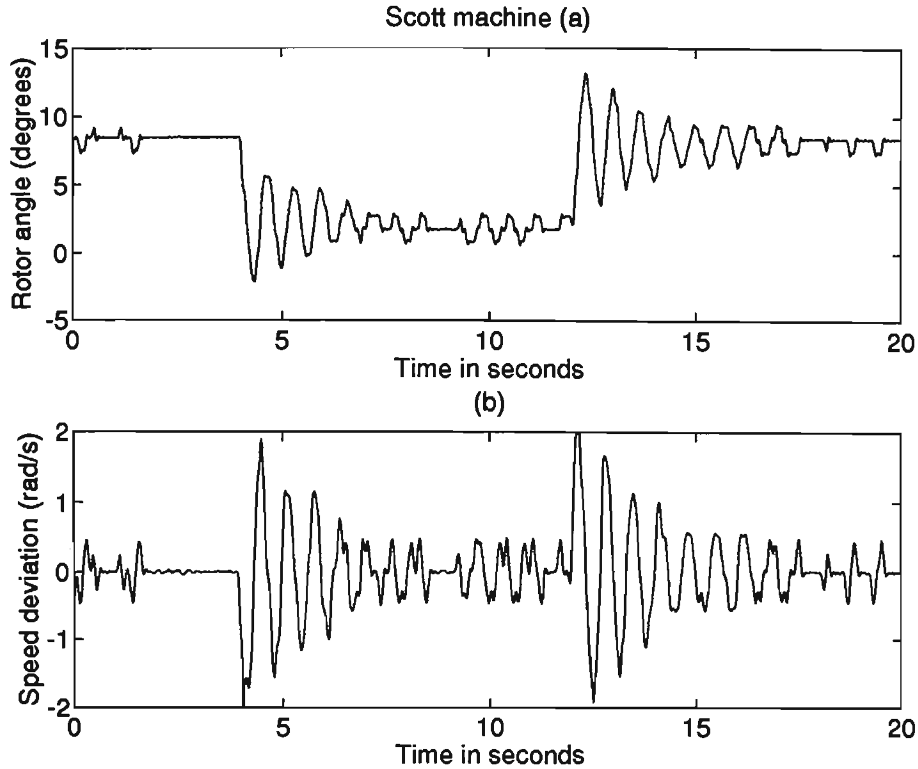

Figure 7.19: Rotor angle and speed deviation for generator 1 corresponding to 3/4 rated sudden inductive load change (without the FLBPSS), (a)-rotor angle, (b)-speed deviation

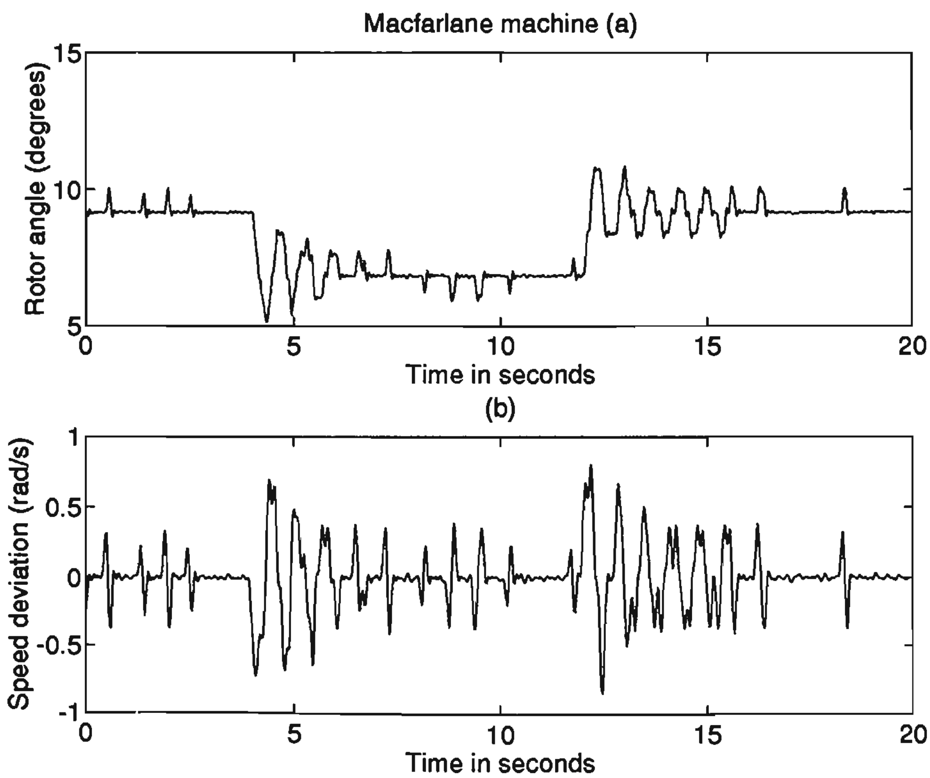

Figure 7.20: Rotor angle and speed deviation for generator 2 corresponding to 3/4 rated sudden inductive load change (without the FLBPSS), (a)-rotor angle, (b)-speed deviation

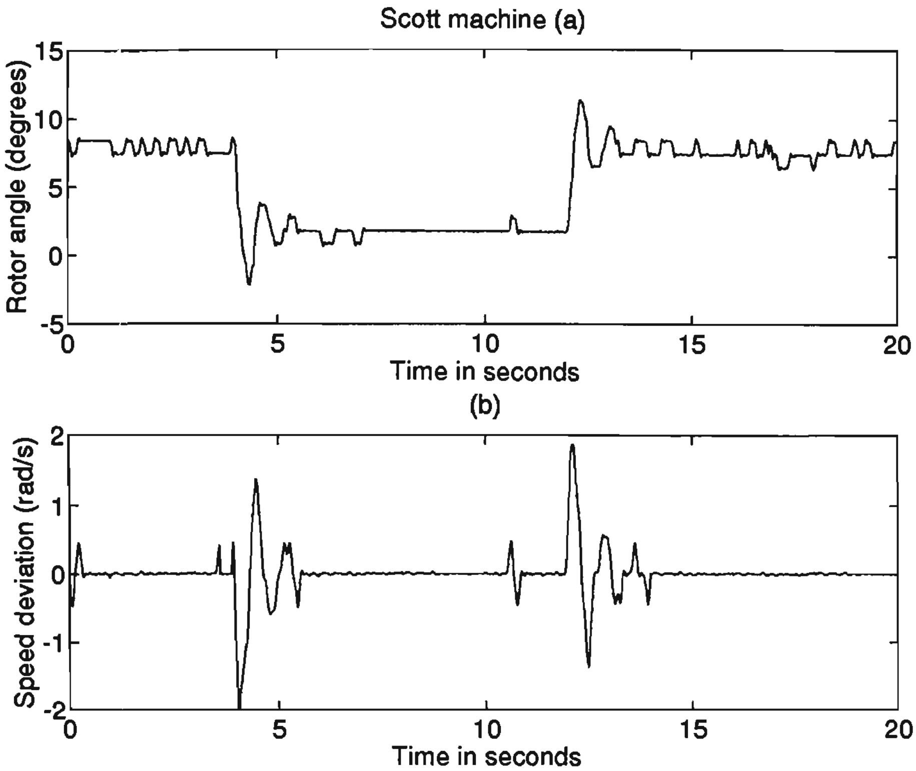

Figure 7.21: Rotor angle and speed deviation for generator 1 corresponding to 3/4 rated sudden inductive load change (with the FLBPSS), (a)-rotor angle, (b)-speed deviation

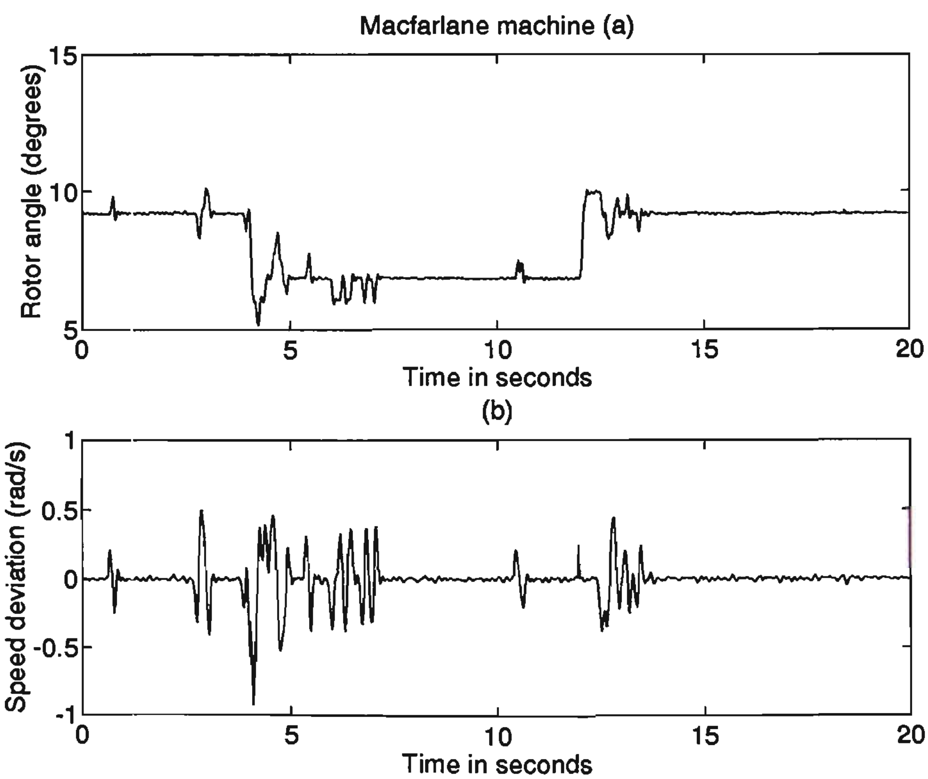

Figure 7.22: Rotor angle and speed deviation for generator 2 corresponding to 3/4 rated sudden inductive load change (with the FLBPSS), (a)-rotor angle, (b)-speed deviation

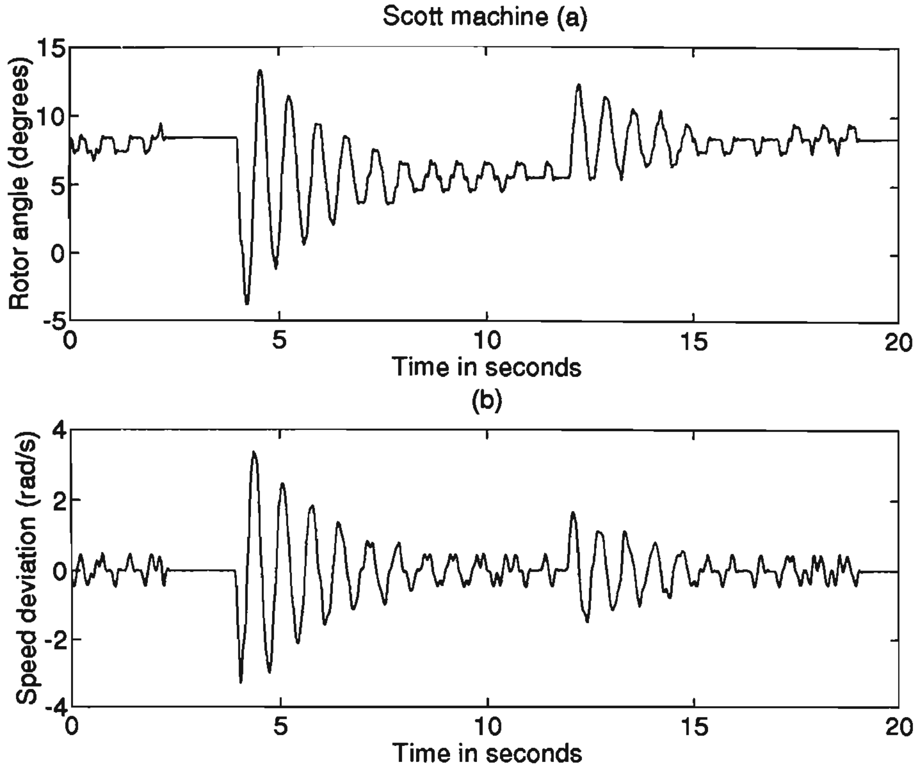

Figure 7.23: Rotor angle and speed deviation for generator 1 corresponding to 3/4 rated sudden capacitive load change (without the FLBPSS), (a)-rotor angle, (b)-speed deviation

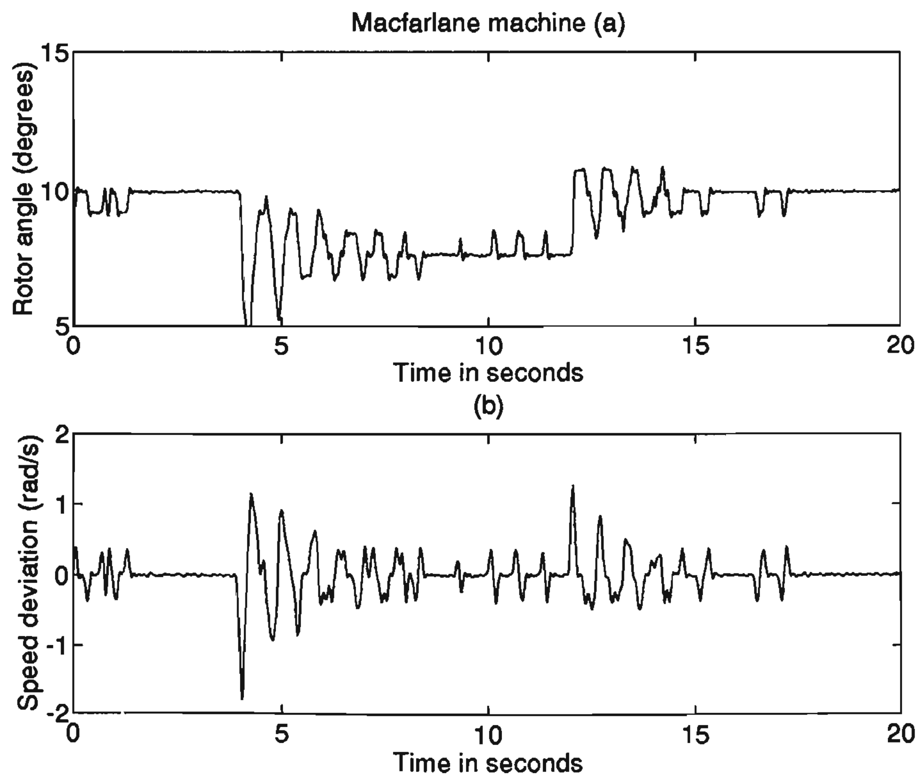

Figure 7.24: Rotor angle and speed deviation for generator 2 corresponding to 3/4 rated sudden capacitive load change (without the FLBPSS), (a)-rotor angle, (b)-speed deviation

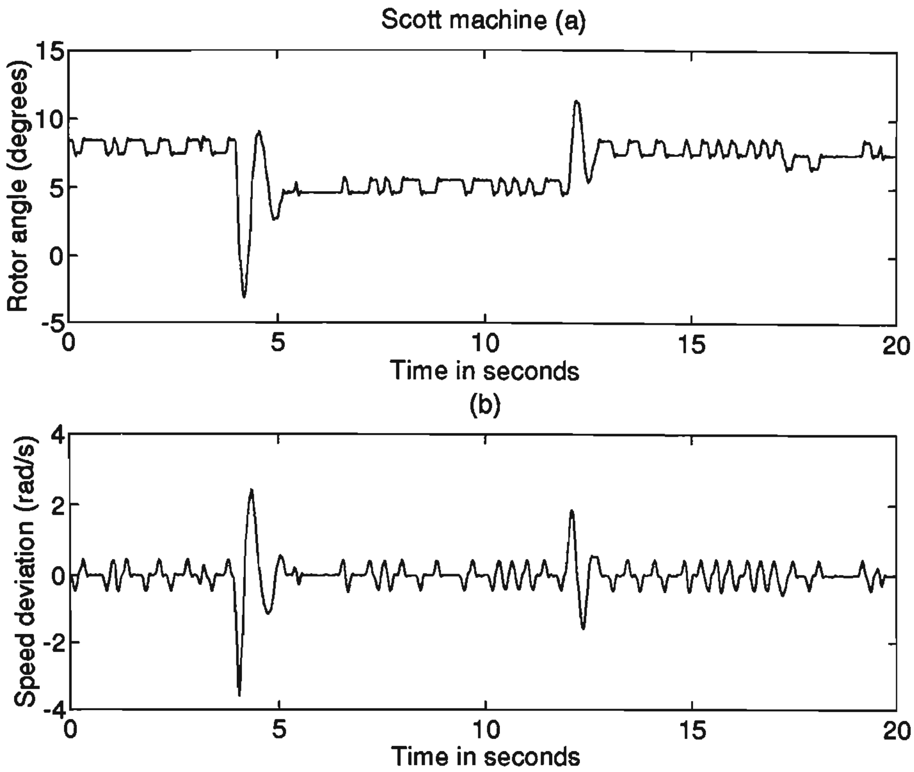

Figure 7.25: Rotor angle and speed deviation for generator 1 corresponding to 3/4 rated sudden capacitive load change (with the FLBPSS), (a)-rotor angle, (b)-speed deviation

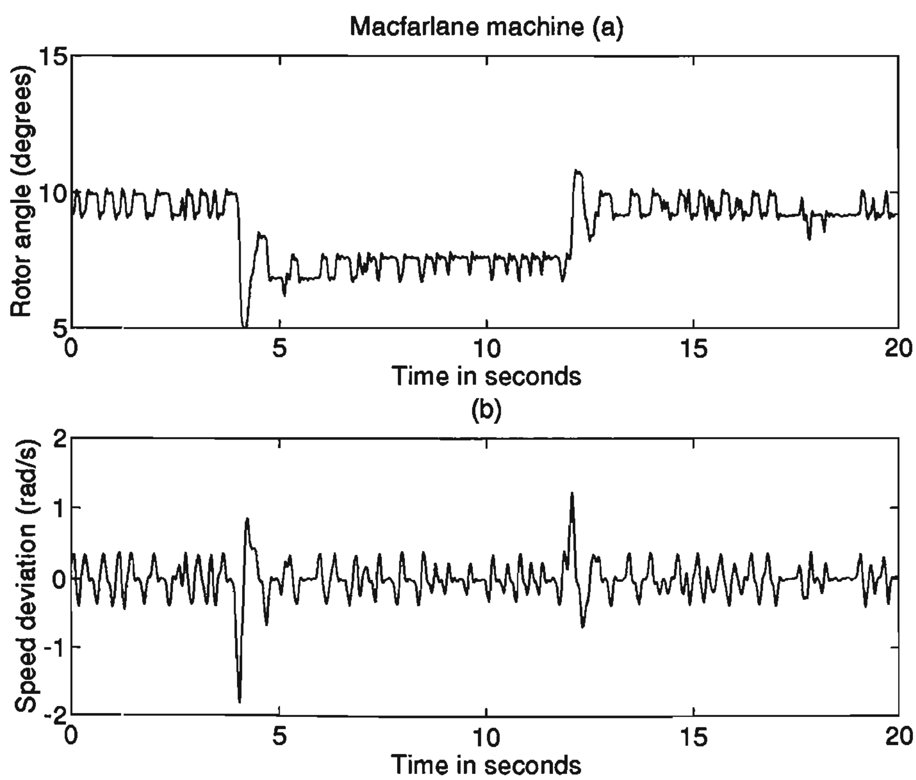

Figure 7.26: Rotor angle and speed deviation for generator 2 corresponding to 3/4 rated sudden capacitive load change (with the FLBPSS), (a)-rotor angle, (b)-speed deviation

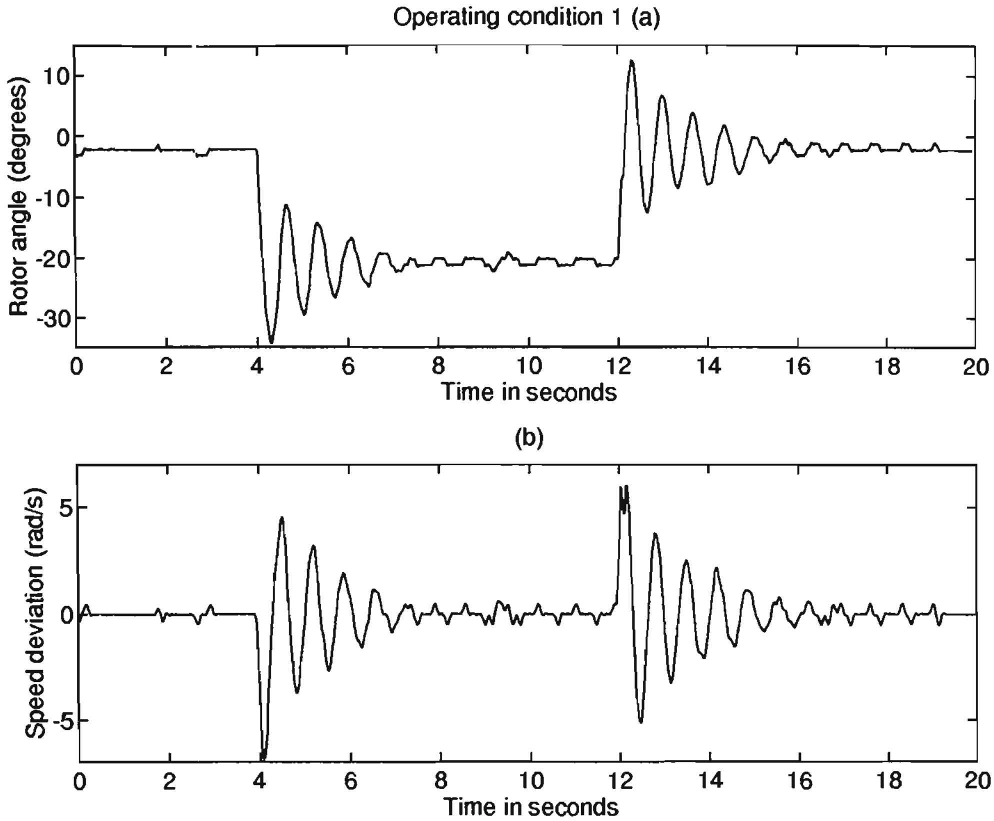

Figure 7.27: Rotor angle and speed deviation for generator 1 corresponding to 3/4 rated sudden resistive load change without the FLBPSS (Operating condition OC1), (a)-rotor angle, (b)-speed deviation

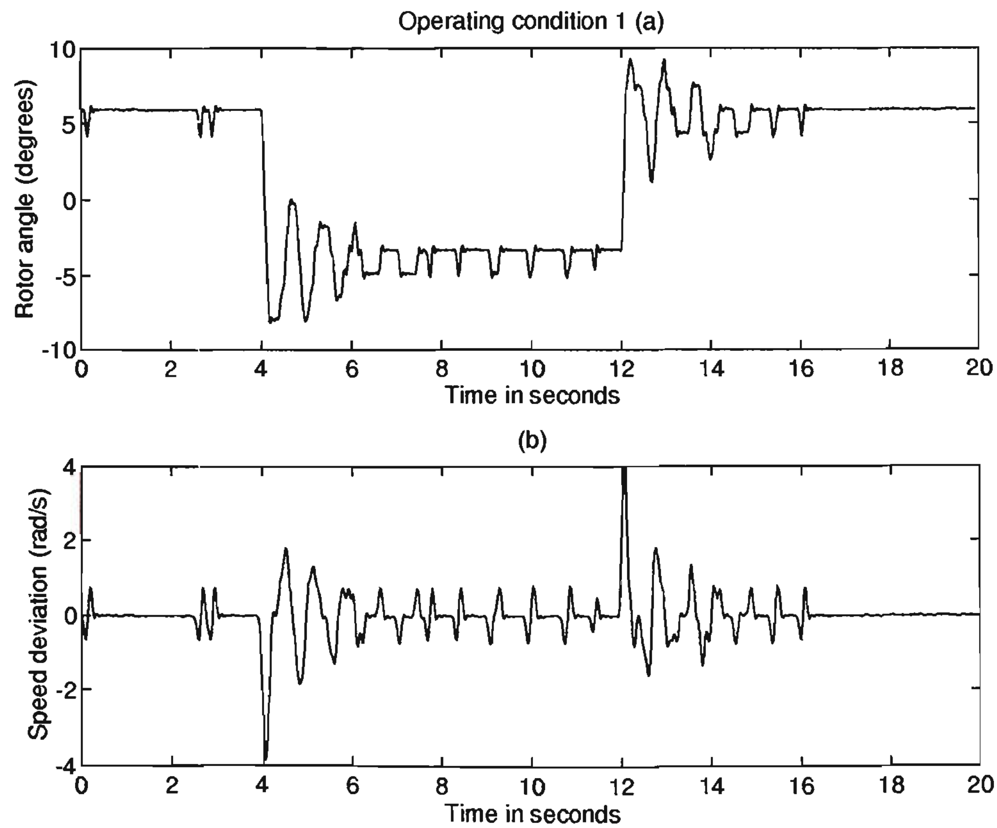

Figure 7.28: Rotor angle and speed deviation for generator 2 corresponding to 3/4 rated sudden resistive load change without the FLBPSS (Operating condition OC1), (a)-rotor angle, (b)-speed deviation

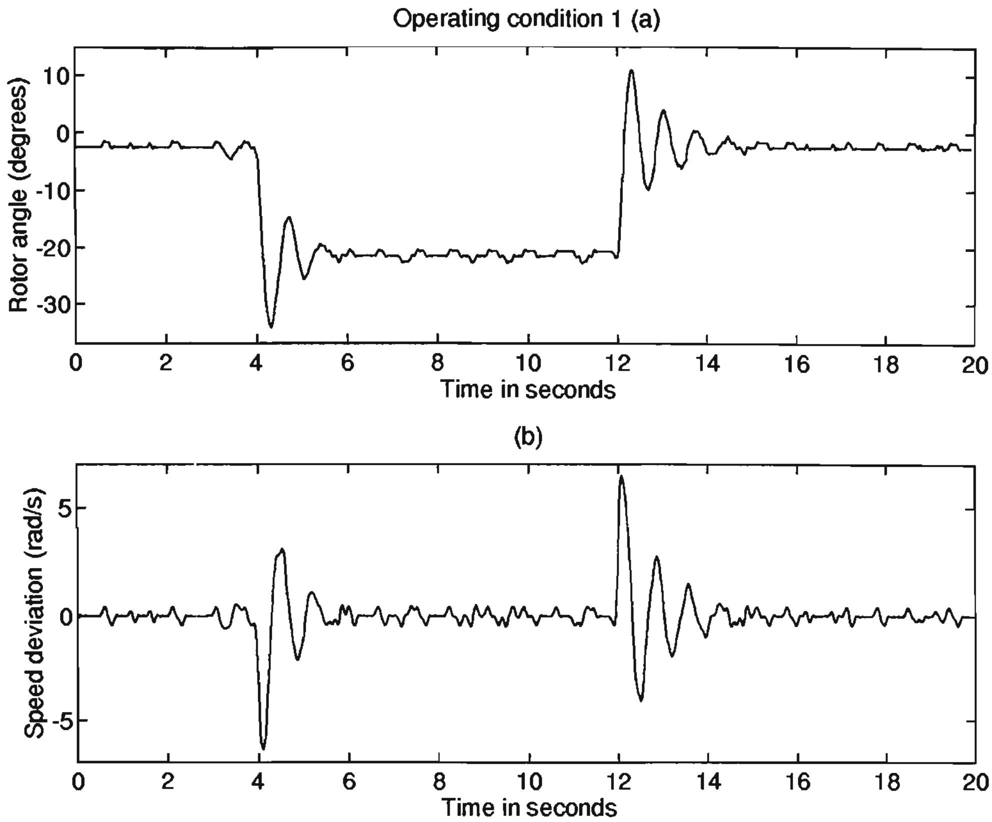

Figure 7.29: Rotor angle and speed deviation for generator 1 corresponding to 3/4 rated sudden resistive load change with the FLBPSS (Operating condition OC1), (a)-rotor angle, (b)-speed deviation

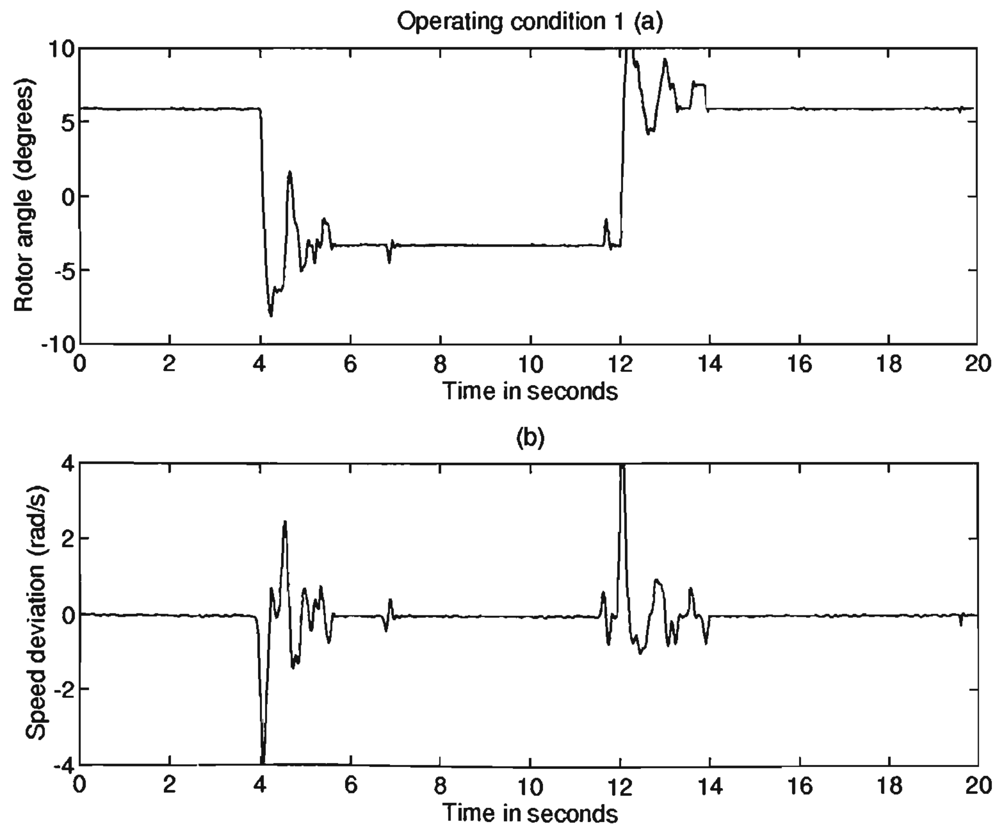

Figure 7.30: Rotor angle and speed deviation for generator 2 corresponding to 3/4 rated sudden resistive load change with the FLBPSS (Operating condition OC1), (a)-rotor angle, (b)-speed deviation

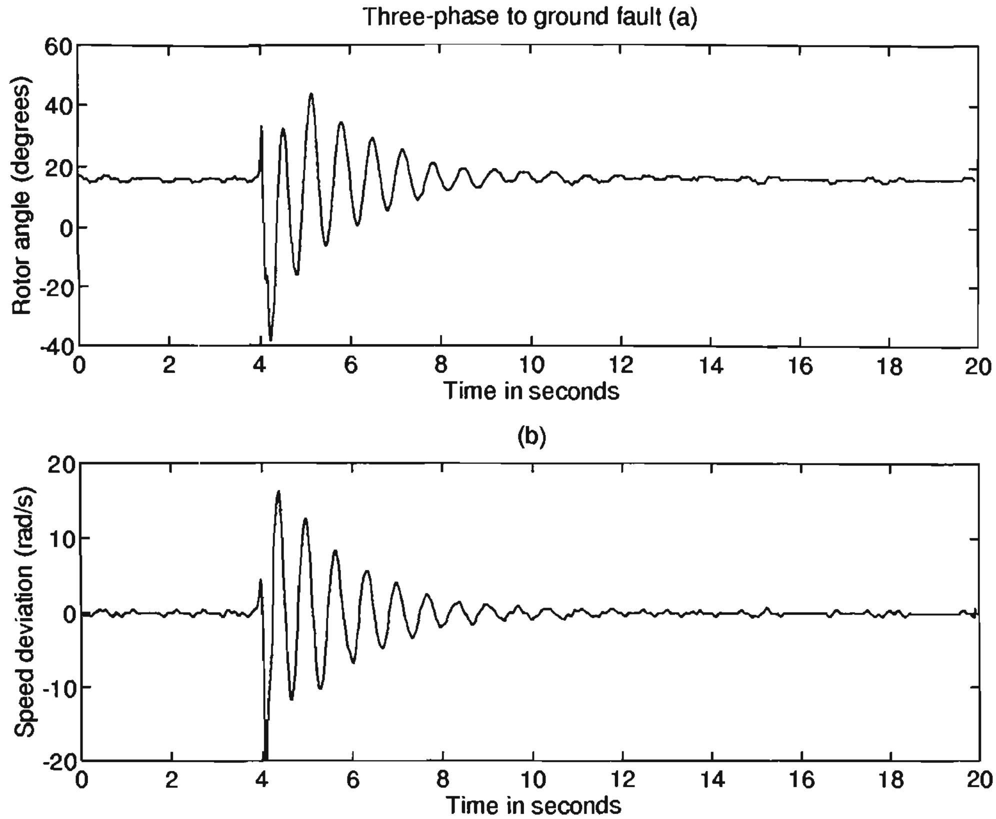

Figure 7.31: Rotor angle and speed deviation for generator 1 corresponding to a three-phase fault at B (Figure 2.4) sustained for 125 milliseconds (without the FLBPSS), (a)-rotor angle, (b)-speed deviation

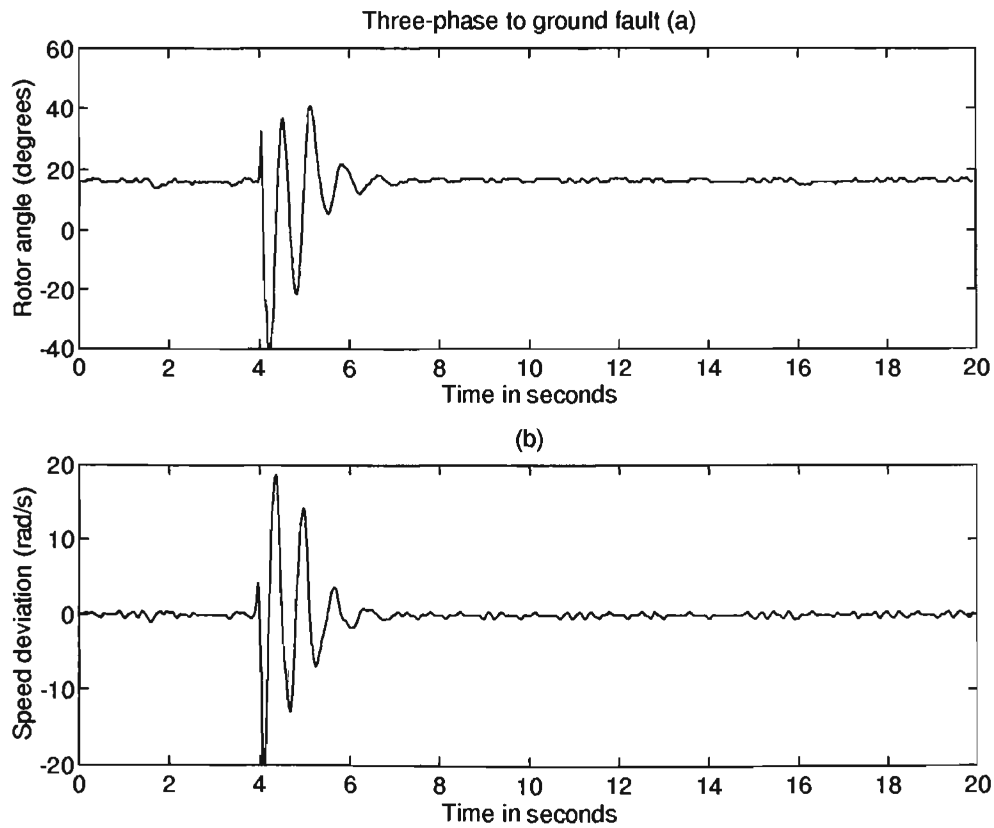

Figure 7.32: Rotor angle and speed deviation for generator 1 corresponding to a three-phase fault at B (Figure 2.4) sustained for 125 milliseconds (with the FLBPSS), (a)-rotor angle, (b)-speed deviation

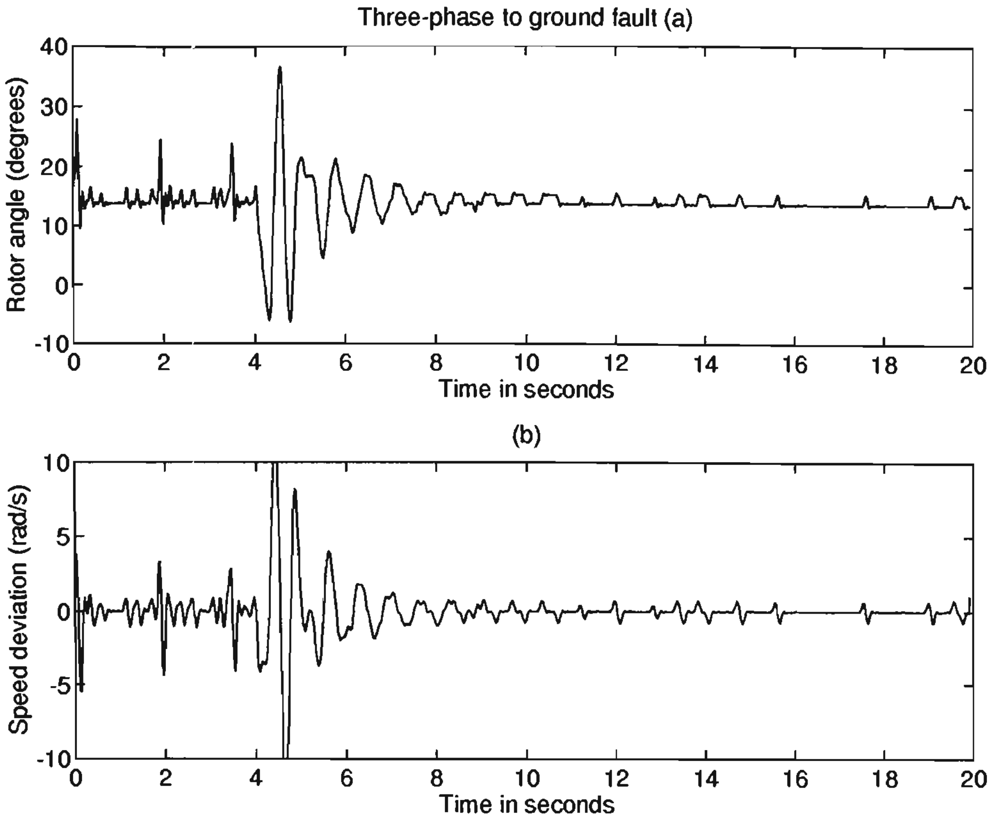

Figure 7.33: Rotor angle and speed deviation for generator 2 corresponding to a three-phase fault at B (Figure 2.4) sustained for 125 milliseconds (without the FLBPSS), (a)-rotor angle, (b)-speed deviation

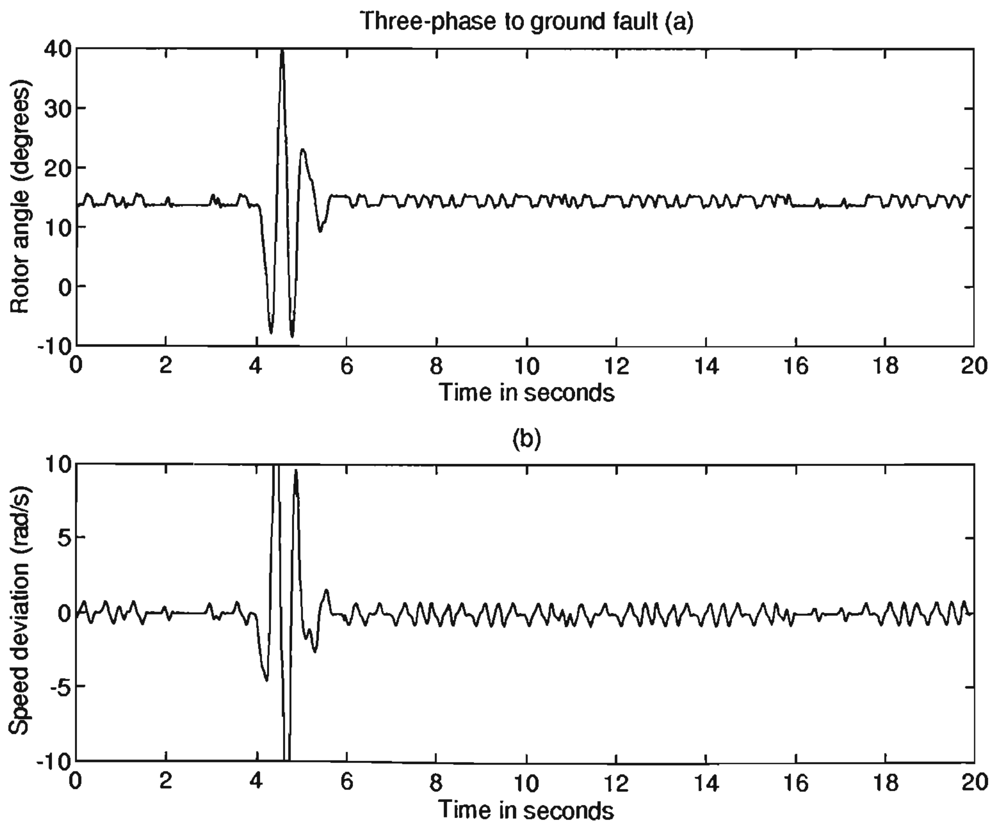

Figure 7.34: Rotor angle and speed deviation for generator 2 corresponding to a three-phase fault at B (Figure 2.4) sustained for 125 milliseconds (with the FLBPSS), (a)-rotor angle, (b)-speed deviation

7.5.5 Transmission Line Loss Between Generators 1 and 2

The oscillation occurred when the system was subject to a transmission line loss between generators 1 and 2. This happens when a power system is subject to a fault and the circuit breaker at each end of the transmission line will trip resulting the transmission line loss. The FLBPSS can also be used to damp out this kind of oscillation. Figures (7.35) and (7.36) show the rotor angle and speed deviation in response to the transmission loss under the nominal operating condition without the FLBPSS for both generators 1 and 2 respectively. Figures (7.37) and (7.38) show the corresponding results with the FLBPSS for generators 1 and 2 respectively. It is obvious from these figures that the oscillation has been damped out very effectively by using the FLBPSS.

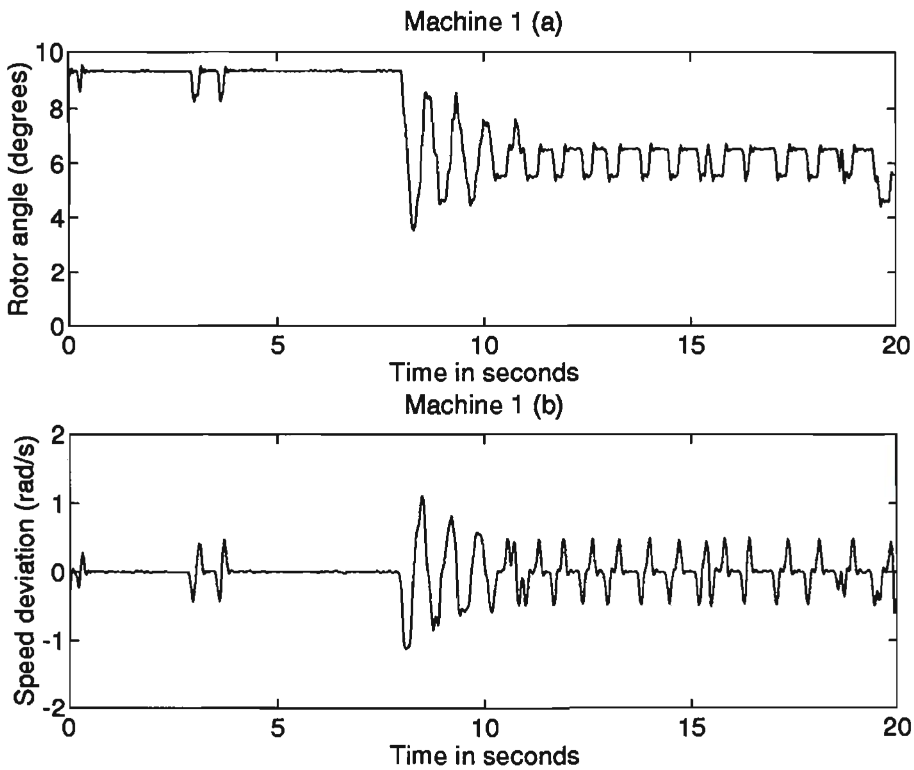

Figure 7.35: Rotor angle and speed deviation for generator 1 corresponding to the loss of the transmission line (without the FLBPSS), (a)-rotor angle, (b)-speed deviation

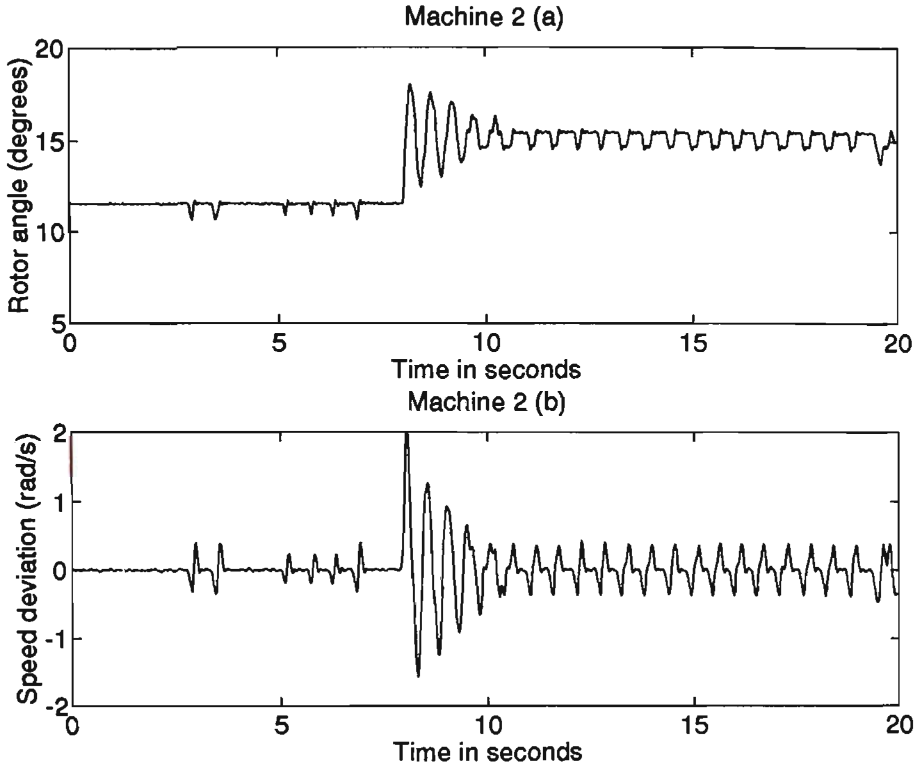

Figure 7.36: Rotor angle and speed deviation for generator 2 corresponding to the loss of the transmission line (without the FLBPSS), (a)-rotor angle, (b)-speed deviation

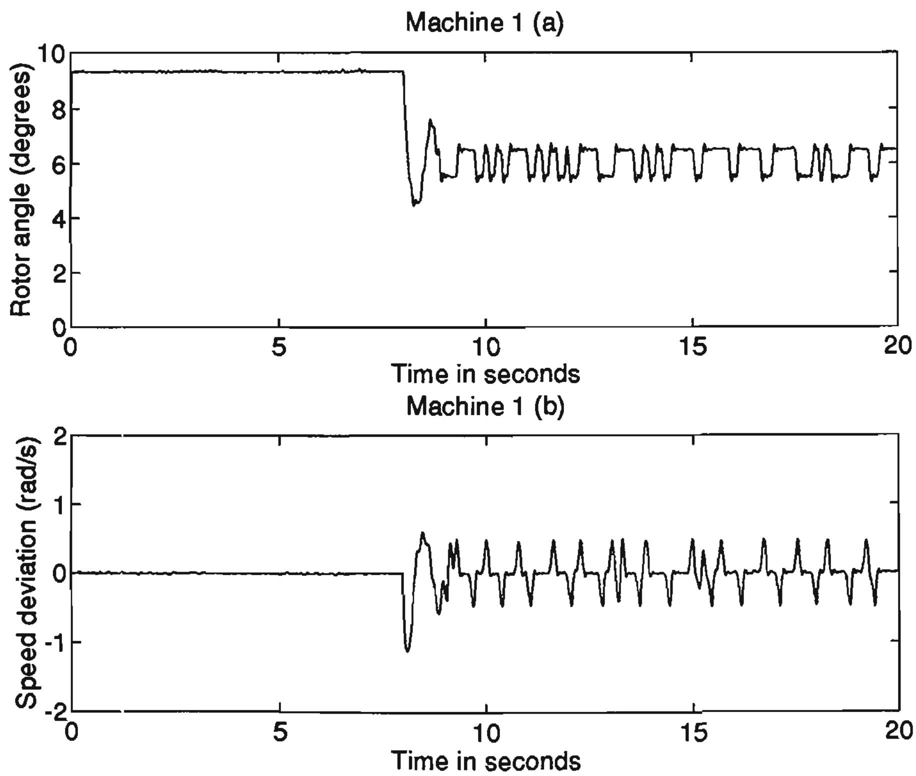

Figure 7.37: Rotor angle and speed deviation for generator 1 corresponding to the loss of the transmission line (with the FLBPSS), (a)-rotor angle, (b)-speed deviation

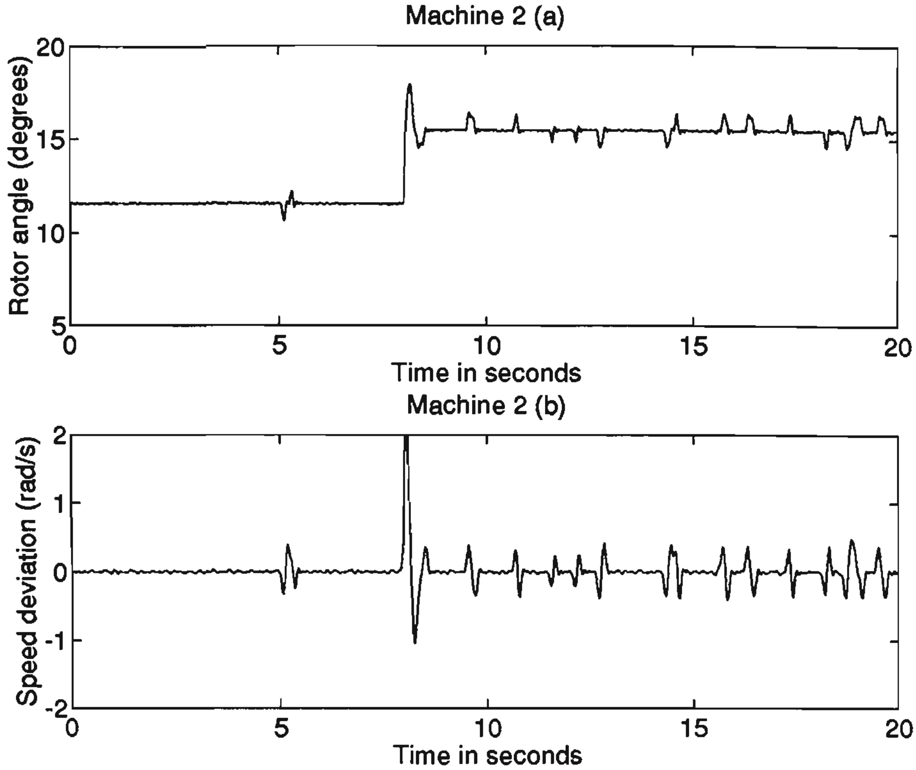

Figure 7.38: Rotor angle and speed deviation for generator 2 corresponding to the loss of the transmission line (with the FLBPSS), (a)-rotor angle, (b)-speed deviation

7.6 Concluding Remarks

In this chapter the merits of the interconnection of electric power systems have been summarised. The design of the AVRs for the two synchronous generators have been introduced. The performance of the designed AVRs have been tested in real time. The test results show that the AVRs control the terminal voltage value according to the reference voltage. The overshoot and settling time all satisfy the IEEE standard for excitation control. The terminal voltages have been kept constant under various sudden load change conditions. The performance of the AVRs is robust against different step changes in loading. Experimental results have also been obtained when the system was subject to a three-phase to ground fault.

The simulation and implementation studies of the optimised FLBPSS have also been carried out for the two-machine infinite bus power system. The simulation test has been demonstrated when a step change in the reference voltage and mechanical torque have been applied to the system. The rotor angle and speed deviation oscillations for both generators have been damped out within one and half cycles although only generator 1 was equipped with the FLBPSS. The implementation test has been carried out under different disturbance and operating conditions. Four different kinds of disturbances such as a 10% step change in the reference voltage, a 3/4 rated load (inductive, capacitive and resistive) change, a three-phase to ground fault and a transmission line loss have been applied to the system in order to test the robustness of the FLBPSS. All the test results reveal that the oscillations resulted from the above mentioned disturbances have been damped out within either one and half to two cycles in the presence of the optimised FLBPSS. The maximum transient deviation has also been reduced substantially. For three-phase to ground fault, it takes a longer time to damp the oscillation out due to the hardware limitation of the control signal. The performance of the FLBPSS has also been tested under different operating conditions.

From the simulation and implementation results, it can be concluded that the FLBPSS works satisfactorily without resetting and tuning of the optimised parameters under different disturbances at various operating conditions for the two-machine infinite bus power system.

Chapter 8

Rules Reduction for the FLC Using Neural Networks

8.1 Introduction

The previously designed Fuzzy Logic Controller (FLC) is not very efficient in comparison with the Fuzzy Logic Based Power System Stabiliser (FLBPSS) because it uses too many rules but provides poorer performance. By using neural network techniques, the rules can be reduced, fine tuned and also the FLC performance can be improved.

Neural networks are trained to give a certain output based on a certain input through the use of learning methods. Generally, a node of a neural network contains an activation level which during training is increased or decreased based on how "close" the node is to the current input being trained for. Training methods are used to change the value of the node based on this "closeness".

In the literature, Neural Networks (NN) are used for learning rules from input/output data. Such an example is given in Kosko [Kosko, 1992] for obtaining rules to stabilise an inverted pendulum. Consider a system which has a simple inverted pendulum free to rotate in the plane on a pivot attached to the cart. A human operator is taking actions in order to keep the pendulum vertical at all times by applying a restoring force $F(t)$ (control signal) to the cart at some discrete time t in response to change in both linear and angular positions $(x(t), \theta(t))$ and velocity $(\dot{x}(t), \dot{\theta}(t))$ of the pendulum. The set of input and output (operator's action) pairs are the data fed into a NN to perform Adaptive Vector Quantisation (AVQ).

The obtained rules in correlation with the predefined membership functions are used to define a fuzzy system for which the control surface is approximately the one used by the human operator in stabilising the pendulum.

TILGen [Tilgen, 1991] is a tool that automatically generates a fuzzy expert system from a set of inputs and required outputs. **TILGen** is a combination of two techniques: a neural network to learn the input-output function described by the set of inputs and outputs, and a technique to decode the neural network to generate the rules for the fuzzy expert system. **TILGen** creates a neural network by partitioning the input space of the fuzzy rule base being generated. This partitioning is based upon the number of input variables and the number of membership functions defined for each variable.

In **TILGen** any one of the three learning algorithms can be adopted: *unsupervised competitive learning, supervised competitive learning, or differential competitive learning.* The methods work by first initialising the **n** nodes of the neural network with the first **n** test vectors. Then, each remaining vector is compared with the **n** nodes and the node (or nodes) which most closely match the input vector are found. These nodes are commonly known as the winning nodes. The nodes are then updated according to the learning method used.

When *unsupervised competitive learning* is used, the winning nodes are rewarded by having their activation levels increased. When *supervised competitive learning* is used, the winning nodes are rewarded by increasing their activation levels and the non-winning nodes are punished by decreasing their activation levels. When *differential competitive learning* is used, the winning nodes are found and the closest winning node is rewarded and the other winning nodes are punished. It should be noted that *unsupervised competitive learning* and *differential competitive learning* are similar in that they do not punish losing nodes; they are only concerned with winning nodes. *Unsupervised competitive learning* and *differential competitive learning* tend to produce similar results and *differential competitive learning* is guaranteed to converge exponentially quickly, while *unsupervised competitive learning* is not guaranteed to converge. The neural networks with *supervised competitive learning* algorithm tend to need more time and information to train.

8.2 Rules Reduction for the FLC Using Neural Networks

In the case when the FLC has been used as power system stabiliser, it is difficult to have a predefined desired control surface. The idea was to approximate the FLC in order to possibly simplify its structure (reduce rules). The input signals which were generated by applying disturbances such as a 20% step change in mechanical torque T_m and a 20% step change in reference voltage V_{ref} to the power system have been applied to the original 49-rule FLC to obtain the output control signal. Thus the input/output pairs were not obtained from a human-based control but from the excitation of the initial FLC. Using this input-output data, the Neural Network facility of **TILGen** has led to a simplified version of the FLC.

System Inputs

TILGen takes input as two files: an input Fuzzy Programming Language (FPL) file and an input data vector file.

The input FPL file must be a properly defined FPL file capable of being loaded by the TILShell [Tilshell, 1991] or run through one of the TIL compilers such as the Fuzzy-C Compiler. A FUZZY object for which TILGen will generate a fuzzy rule base has been defined in this file. A VAR objects (including their membership functions) which will be the inputs and outputs of the FUZZY object and the CONNECT objects which define the input/output relationships between the FUZZY object and the VAR objects have also been defined in the FPL file. The only object which will be modified by TILGen is the FUZZY object. It will have its current contents (if any) replaced by the newly generated rules. The input FPL file for the FLC is listed in Appendix E.1.

The structure of the input data vector file is crucial for the proper execution of TILGen. The structure of the vector file is simply that each line of the vector file must contain one and only one entry for each input and output variable defined in the input FPL file separated by either a comma, space or tab. The entries should be ordered with the input variables in alphabetical order followed by the output variables in alphabetical order. The data vector file contains input variables **aSpeed** and **bAcceleration** and output variable **Control** which was generated by applying disturbances such as a 20% step change in mechanical torque T_m and a 20% step change in reference voltage V_{ref} to the original 49-rule FLC.

In order to guarantee proper training there have to be enough vectors in the vector file. As a rule of thumb, there must be at least twice as many vectors as the number of nodes used in the neural network. The number of nodes in the neural network varies depending upon the number of variables and the number of membership functions defined for each variable. To compute the number of nodes in the neural network, compute the combined product of the number of membership functions for each variable in the system. There are two inputs (speed and acceleration) and one output (stabilising signal) in the system and there are 7 membership functions for both inputs and output. The number of nodes in the neural network is $7 \times 7 \times 7$ or 343 [Tilgen, 1991]. Therefore, 1000 data vectors have been used which is almost three times the number of nodes. The input and output data have been multiplied by 10000 to get large values in order to guarantee proper training.

Executing TILGen to generate fuzzy rule base

When executing TILGen a few command line options have to be specified. Some of the options are explained as follows:

- <u>Specify the learning method</u>

  The differential competitive learning algorithm has been adopted in order to guarantee the convergence and reduce training time.

- Specify the cell threshold

  The cell threshold value can be specified for whether or not to emit a rule based upon how many neurones converge to that point in the input space. The default setting for this value is 5 and range from 1 to 100. This value does not usually have a large effect on the output of the system as the neural network nodes tend to clump into a few areas of the input space. As a result, there are not areas in the input space which only one or two nodes have been trained to. Instead of that there are areas where twenty or more nodes have been trained to. To ensure all areas of the input space containing nodes generate rules, the threshold can be set to one. With the threshold of one, a rule will be generated for an area of the input space when at least one node has been trained to that area. This option works with the *number of winners option* to give the user more control over how many rules are to be generated from TILGen. Setting this value very low and the number of winners very high causes more rules to be generated because more nodes will be rewarded, causing less convergence to take place. The default value 5 has been chosen for this option.

- Specify the number of winners

  The number of winning nodes in the neural network being trained can be specified using this option. How these winning nodes are rewarded varies with the learning method used. If *unsupervised competitive learning* is specified, the **n** winning nodes have their activation levels increased. If *supervised competitive learning* is specified, the **n** winning nodes have their activation levels increased and the losing nodes have their activation levels decreased. If *differential competitive learning* is specified, the closest winning node is rewarded by having its activation level increased and the other **n-1** winning nodes have their activation levels decreased. The default value 3 has been chosen for this option. However, this value can be ranged from 1 to 100.

The generated rule base is shown in Appendix E.2.

The rule base is summarised in Table (8.1).

$\Delta\omega$	$\Delta\dot{\omega}$						
	NB	NM	NS	ZR	PS	PM	PB
PB							
PM			**ZR**	**PM**	**PM**	**PB**	
PS		**NS**	**ZR**	**PS**	**PM**	**PB**	
ZR		**NM**	**NM**	**ZR**	**PM**	**PM**	
NS		**NB**	**NM**	**NS**	**ZR**	**PS**	
NM			**NM**	**NM**	**NS**		
NB			**NB**	**NB**			

Table 8.1: The decision table after learning

The **TILGen** generated 24 rules by using neural network technique. Therefore, the original decision table which contains 49 rules has been simplified.

8.3 Comparison Study

The comparison study between the original 49-rule FLC and the simplified 24-rule FLC presented here were obtained on the single-machine infinite bus power system.

Table (8.2) shows the performance index corresponding to a changes of membership function whole overlap ratio (WOR) in response to a 20% step increase in mechanical torque T_m followed by a 10% step increase in reference voltage V_{ref} and a 10% step decrease in V_{ref} with the original 49-rule FLC and the 24-rule FLC. From Table (8.2), it can be seen that the optimal WOR is 14.29% and the corresponding performance index for the original FLC and the reduced rule FLC are 2.50% and 1.78% respectively. The performance index of the FLC has been improved substantially by using the 24-rule FLC.

Table (8.3) shows the performance index corresponding to different mechanical torque changes with the original FLC and the reduced rule FLC (WOR=14.29%). It can be observed that the performance index has been reduced substantially with the 24-rule FLC.

The dynamic results using this simplified FLC are compared with the initial one as can be observed in Figure (8.1) to (8.4). Figures (8.1) and (8.3) show the results with the original 49-rule FLC. Figures (8.2) and (8.4) show the result with

WOR%	30.95	26.78	24.27	21.95	18.79	15.98	15.12	14.7
49-rule	*4.31*	*3.51*	*2.82*	*2.79*	*2.74*	*2.63*	*2.58*	*2.54*
24-rule	*3.04*	*2.39*	*1.91*	*1.90*	*1.88*	*1.84*	*1.82*	*1.80*
WOR%	14.45	**14.29**	13.48	12.72	11.98	11.27	10.58	9.93
49-rule	*2.52*	**2.50**	*2.53*	*2.56*	*2.59*	*2.63*	*2.67*	*2.71*
24-rule	*1.79*	**1.78**	*1.80*	*1.82*	*1.85*	*1.88*	*1.91*	*1.94*
WOR%	9.3	8.7	8.1	7.6	5.1	3.2		
49-rule	*2.76*	*2.82*	*2.88*	*2.94*	*3.50*	*12.83*		
24-rule	*1.98*	*2.02*	*2.07*	*2.12*	*2.56*	*9.56*		

Table 8.2: The performance index corresponding to changes in WOR (20% step increase in mechanical torque followed by a 10% step increase in the reference voltage sustained for 7.5 seconds)

T_m	original FLC with 49 rules	FLC with 24 rules
0.01pu	8.0347×10^{-4}	4.7945×10^{-4}
0.2 pu	*0.69*	*0.42*
0.5 pu	*5.41*	*3.63*

Table 8.3: The performance index corresponding to different mechanical torque changes

the 24-rule FLC. Figures (8.1) and (8.2) demonstrate the speed deviation and rotor angle corresponding to $0.1pu$ step change in mechanical torque and reference voltage. Figures (8.3) and (8.4) demonstrate the speed deviation and rotor angle corresponding to a $0.2pu$ step change in mechanical torque and reference voltage. It can be seen that the simplified 24-rule FLC gives better performance. The maximum transient deviation of the speed deviation and rotor angle are smaller and the oscillations corresponding to the mechanical torque change are less with the 24-rule FLC.

The explanation for this is that the starting FLC was not shaping an optimal control surface. Some of the cells of the starting FLC are just an extrapolation/interpolation of the cells filled in by experience. The decision table was a complete starting table.

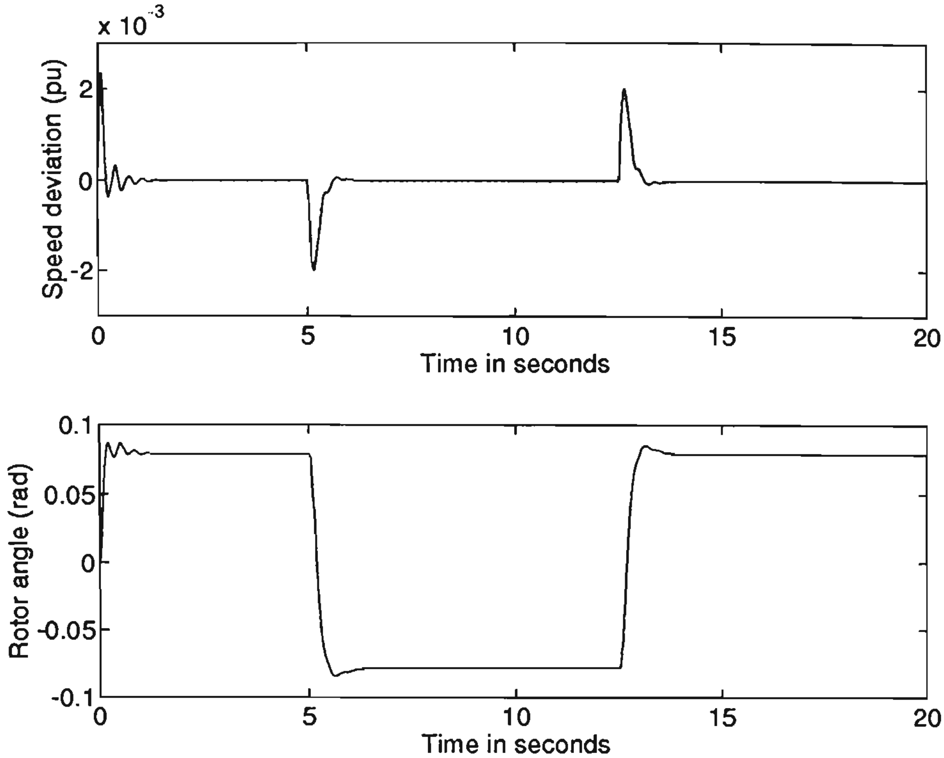

Figure 8.1: Speed deviation and rotor angle corresponding to a 10% step increase in mechanical torque followed by a 10% step increase in the reference voltage sustained for 7.5 seconds with the original 49-rule FLC

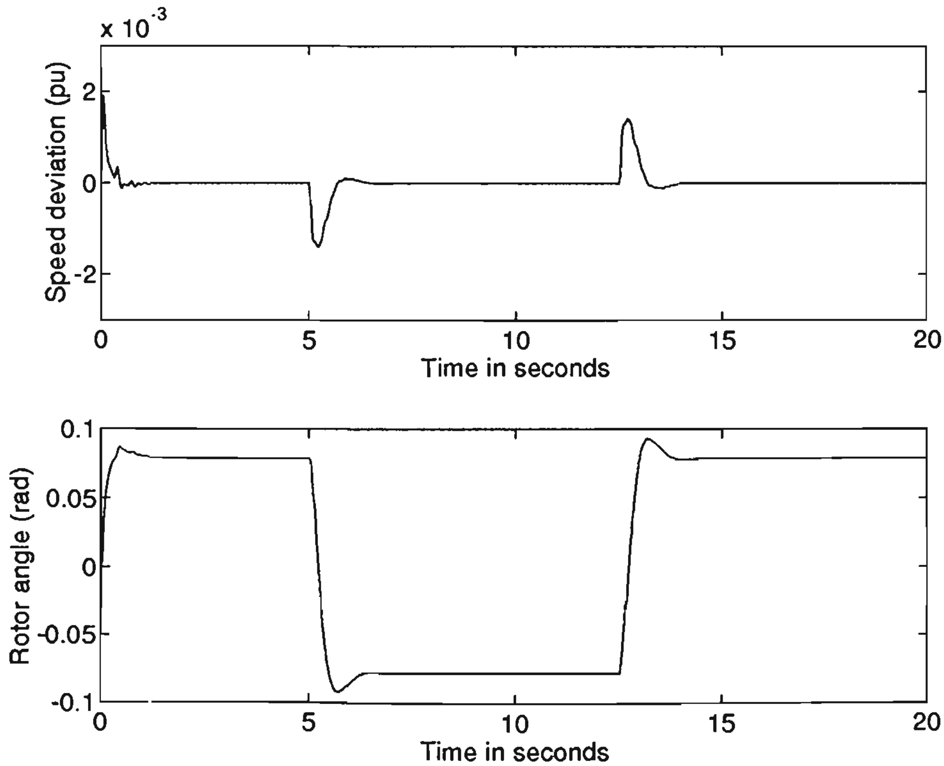

Figure 8.2: Speed deviation and rotor angle corresponding to a 10% step increase in mechanical torque followed by a 10% step increase in the reference voltage sustained for 7.5 seconds with the 24-rule FLC

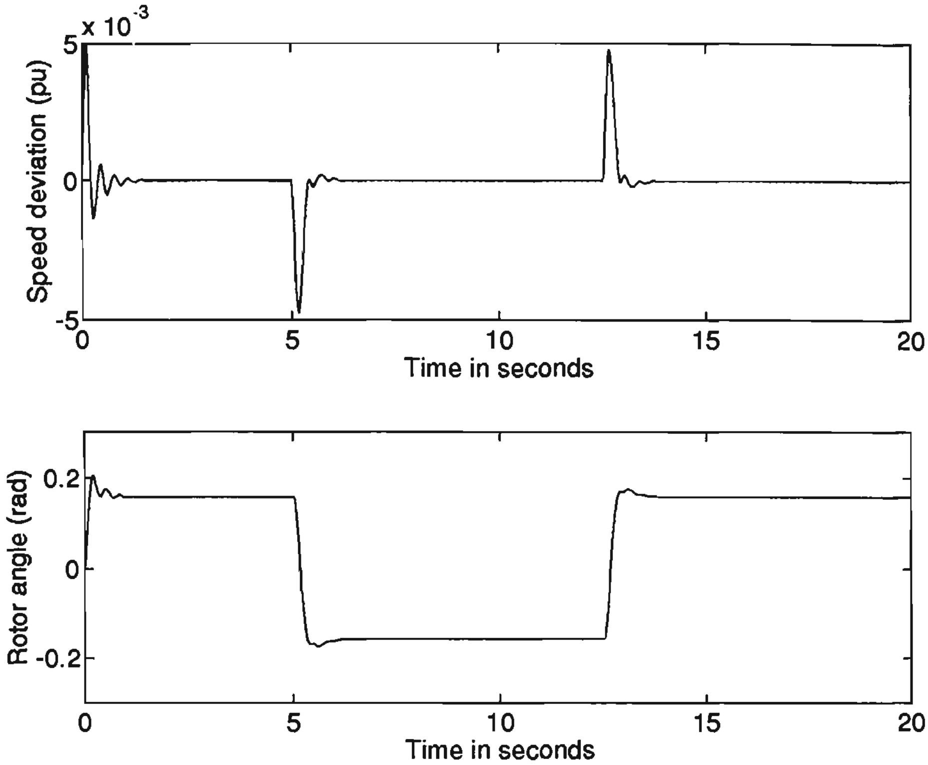

Figure 8.3: Speed deviation and rotor angle corresponding to a 20% step increase in mechanical torque followed by a 20% step increase in the reference voltage sustained for 7.5 seconds with the original 49-rule FLC

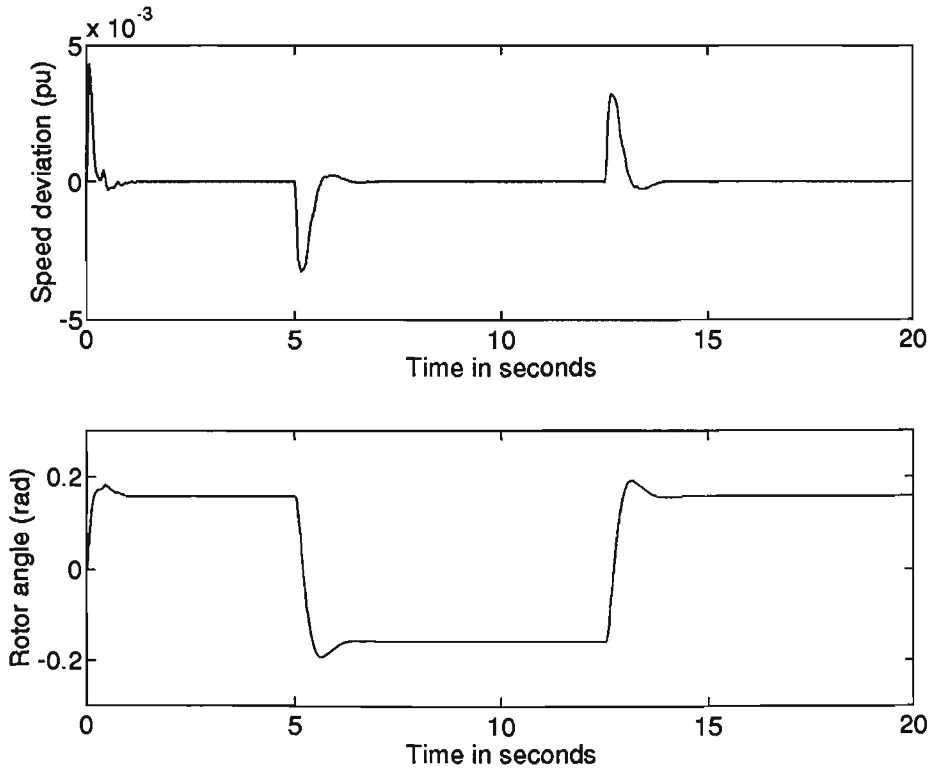

Figure 8.4: Speed deviation and rotor angle corresponding to a 20% step increase in mechanical torque followed by a 20% step increase in the reference voltage sustained for 7.5 seconds with the 24-rule FLC

8.4 Concluding Remarks

TILGen which uses neural network techniques to learn the input-output function described by the set of inputs and outputs, and a technique to decode the neural network to generate the rules for the fuzzy expert system has been employed for rule reduction for the FLC. 24 rules has been generated using *differential competitive learning* when the system is subject to small disturbances. Both the performance index and the dynamic response have been improved substantially with the reduced rule FLC for the dynamic stability study.

Chapter 9

Conclusions

9.1 A Retrospective Overview of the Thesis

In this thesis, research has been conducted on the design, analysis, optimisation, and laboratory evaluation of two types of fuzzy controllers, namely the FLBPSS, and the FLC for power system stabilisation. Robustness and sensitivity analysis of the two fuzzy control schemes have been investigated. In addition, an AVR has been designed using discrete time analytical design method to assist in the assessment of the fuzzy controllers as mentioned above. Neural network techniques have been adopted to simplify the rule base of the second type of fuzzy controller. In particular, the designed AVR and optimised fuzzy controllers have been implemented in real time firstly on a single-machine infinite bus and secondly on a two-machine infinite bus power system.

The development of fuzzy controllers as power system stabilisers is motivated by the fact that a power system is a highly non-linear system, and the design of the most widely used conventional PSS is based on linearised fixed parameter models which are derived from the linearisation of the power system at a given operating point. The gain settings of these conventional PSS are usually determined off-line based on a particular operating condition and fixed in field applications. The use of a conventional PSS will result in shortcomings since the operating point of a power system will change with varying system load. Moreover, drastic changes in system operating conditions will result when the system is subject to a major disturbances such as a three-phase fault. Hence, the best dynamic performance cannot be achieved by a fixed gain PSS under varying operating conditions. The self-tuning and adaptive PSSs have been developed to improve the damping characteristics of a power system over a wide range of operating conditions. In the self-tuning or adaptive PSS, the system model is first identified in real-time using the measured system input and output variables. The gain settings are then computed and adjusted based on the identified system model and the adaptation law. A major disadvantage of the self-tuning or adaptive PSS is that the system model parameters need to be identified in real time which is very time consuming. The situation is worsened by the fact that the self-tuning PSS must be implemented by a microcomputer with limited computational capacity. The need to eliminate the above shortcomings suggests the use of fuzzy control approach which can yield good damping characteristics over a wide range of operating conditions and does not require model identification as the self-tuning PSS does in real time.

In order to carry out an investigation into the design of fuzzy controllers as power system stabilisers, the following four stages are essential:

- analyse the circuit of the single-machine and two-machine infinite bus power system;
- model the non-linear experimental power systems;
- design the AVR;
- evaluate the designed AVR in real time.

The above aspects have been discussed (in Chapter 2 and 3) prior to the design, analysis, optimisation, and also implementation of the fuzzy controllers.

Firstly, the single-machine and two-machine infinite bus power system used in the power laboratory has been introduced. The experimental circuits have been analysed and the generator parameters have been provided.

Secondly, the mathematical model of the single-machine infinite bus power system has been developed. The development of the simplified linear model facilitates the design of the AVR in this chapter. The parameters of the mathematical model for the experimental power system have been derived (see Section 3.2).

Thirdly, the discrete time analytical design method has been analysed under the requirements essential for the design of the AVR. The digital AVR hence has been designed for the single-machine infinite bus power system according to the chosen control law.

Fourthly, the designed AVR has been experimentally verified in real time followed by the theoretical analysis of the AVR. The designed AVR has been tested under the following disturbance condition:

1. 1/2 rated and 3/4 rated inductive step load change;
2. 1/2 rated and 3/4 rated capacitive step load change;
3. 1/2 rated and 3/4 rated resistive step load changes;
4. a 10% step change in reference voltage;
5. a three-phase to ground fault;
6. at various operating conditions with the above disturbances.

The designed AVR performs satisfactorily as the AVR kept the generator output voltage constant under normal operating conditions at various load levels. The dynamic performance satisfy the IEEE standard of excitation control system dynamic performance indices. This is confirmed by both the simulation and real time implementation.

The completion of the above four stages establishes a valid basis for the excitation control on which the fuzzy controllers have been investigated.

The proposed design of two fuzzy control schemes has been investigated (see Chapter 4). The basic structure of a FLC has been described and the design of a FLC as a PSS has been developed. The generator speed $\Delta\omega$ and acceleration $\Delta\dot{\omega}$ have been chosen as the input signals of the FLC. The triangular membership function shape has been chosen for both the input and output signal and the universe of discourse has been specified. A 49-rule decision table has been developed based on the theoretical knowledge. Different defuzzification methods have been introduced and the performance have been compared in terms of memory requirement, speed, etc.

The design of the FLBPSS has been presented and new two non-linear membership functions have been proposed. The resultant stabilising output is computed according to the fuzzy membership functions depending on the speed $\Delta\omega$ and acceleration $\Delta\dot{\omega}$ states of the synchronous generator.

The main features of the FLC and the FLBPSS are:

- the stabilising signal is updated on line depending on the speed $\Delta\omega$ and acceleration $\Delta\dot{\omega}$ of the synchronous generator, and hence provides optimal performance under a wide range of operating conditions;
- the design of the FLC and the FLBPSS does not necessitate the use of the mathematical model of the power system.

In order to optimise the fuzzy control strategy, the following five steps have to be performed (see Chapter 5):

- optimisation of the designed FLC;
- investigation of the optimal parameter settings for the proposed FLBPSS;
- introduction of the STFLBPSS and the optimisation of its parameter settings;
- comparison study between the proposed FLBPSS and the STFLBPSS;
- comparison study between the proposed FLC and the proposed FLBPSS.

Firstly, in order to optimise the designed FLC, the Whole Overlap Ratio (WOR) has been proposed to evaluate the membership function shape for the FLC.

It has been found that the FLC gives best performance when the WOR is approximately from 12% to 15%. Different implication methods, such as the *Mamdani* and *Larsen* methods, and different defuzzification methods, such as *Means of max* and *Centroid*, have also been evaluated by using the performance index. Sensitivity test of the FLC has been carried out to assess the robustness of the FLC by varying the system parameters for ±20% and under various operating conditions for both small and large perturbations.

Secondly, the optimal setting of the FLBPSS parameters has also been evaluated by using the performance index. The optimal settings of the proposed FLBPSS parameters α, β and D_r have been obtained either by applying small or large perturbations. The best value of α, β and D_r chosen for the nominal condition works well with a ±20% change in the nominal parameters. Thus no resetting or tuning of these parameters are needed with deviation of the parameters from the nominal conditions. Although the optimal values for different operating conditions are found to be different, investigation reveals that the optimal values of α, β and D_r obtained at the nominal operating condition works satisfactorily for a wide variation of the operating conditions under both small and large perturbations. The optimal values of α, β and D_r at one optimal point is sub-optimal at the other point with hardly any difference in the quality of the dynamic response.

Thirdly, a STFLBPSS has also been introduced in order to compare with the FLBPSS. The optimal settings of θ, F_a and D_r values have also been explored. It has been found that at any operating point, the optimal values of the above mentioned parameters obtained by applying small perturbations differs from that for large perturbations and vice versa. Considering the system performance under different operating conditions with different perturbations and the system parameter variations, a compromise values of θ, F_a and D_r have been chosen.

Fourthly, comparison study between the proposed FLBPSS and the STFLBPSS has been demonstrated through both the performance index and the dynamic response. Extensive study has been performed when the system is subject to small or large disturbances, variations in the system parameters and under wide variation of the operating conditions. Both the performance index and the dynamic response show that the proposed FLBPSS gives better performance than the STFLBPSS.

Lastly, a comparison study between the proposed FLBPSS and the proposed FLC has also been demonstrated through both the performance index and the dynamic response. Extensive study has been performed when the system is subject to both small and large disturbances, variations in the system parameters and under wide variation of the operating conditions. The performance index of the FLC is 2 times larger than that of the FLBPSS. From the dynamic response, it can be seen that the maximum transient deviation is smaller and the settling time is shorter when the system is equipped with the FLBPSS. Therefore, the FLBPSS has been chosen as the practical PSS for real time implementation.

The implementation of the optimised FLBPSS was tested on a single-machine infinite bus power system (see Chapter 6). The implementation results reveal that:

- the optimised FLBPSS works well when the system is subject to either small (10% step change in the reference voltage) or large (three-phase to ground fault) perturbations;
- the performance of the optimised FLBPSS is robust with different types of step load changes (inductive, capacitive and resistive load);
- the FLBPSS also works satisfactorily under a wide range of operating conditions without tuning or resetting of any parameters of the optimised FLBPSS.

To demonstrate the effectiveness of the FLBPSS for multi-machine power system, the single-machine infinite bus power system has been extended to two-machine infinite bus power system due to the equipment limitation. The AVRs for the two synchronous generators have been designed (see Chapter 7) in order to carry on the research. The performance of the designed AVRs have been tested in real time. The test results show that:

- The AVRs control the terminal voltage value according to the reference voltage;

- The overshoot and settling time both satisfy the IEEE standard for excitation control;

- The terminal voltages have been kept constant under various sudden load change conditions; The performance of the AVRs is robust against different kinds of step change in loading. The AVRs also works satisfactorily when the system was subject to a three-phase to ground fault.

The effectiveness of the proposed FLBPSS for the two-machine infinite bus power system has been demonstrated by both simulation and implementation studies. The simulation test has been evaluated when a step change in the reference voltage and mechanical torque have been applied to the system. The rotor angle and speed deviation oscillations for both machines have been damped out very quickly (within one and half cycles) although only generator 1 was equipped with the FLBPSS. The implementation test has been carried out under different disturbance and operating conditions. Four different kinds of disturbances such as a 10% step change in the reference voltage, a 3/4 rated load (inductive, capacitive and resistive) change, a three-phase to ground fault and a transmission line loss have been applied to the system in order to test the robustness of the FLBPSS. All the test results reveal that the oscillations resulted from the above mentioned disturbances have been damped out within either one and half or two cycles. The maximum transient deviation has also been reduced substantially. For a three-phase to ground fault, it takes a longer time to damp the oscillation out due to the hardware limitation of the control signal. The performance of the FLBPSS has also been tested under different operating conditions.

From the simulation and implementation results, it can be concluded that the FLBPSS works satisfactorily without resetting and tuning of the optimised parameters under different disturbances at various operating conditions for the two-machine infinite bus power system.

In conclusion, the FLBPSS is an appropriate and practical approach for damping single-machine and two-machine infinite bus power system oscillations and improving both the dynamic and transient power system stability.

Finally, neural network techniques have been used to improve the dynamic performance of the original 49-rule FLC (see Chapter 8). 24 rules have been generated when the single-machine infinite bus power system is subject to a step change in mechanical torque and reference voltage. Both the performance index and the dynamic response have been improved with the reduced rule FLC for dynamic stability study.

9.2 Avenues to be Explored in Further Work

The studies reported in this thesis involve the design, optimisation, simulation, and implementation of the fuzzy controllers for power system stabilisation. The following aspects relating to future research into the fuzzy control strategies in the design of power system stabilisers are suggested:

- Mathematically, the self-tuning control algorithm is much more complicated due to parameter identification, state observation and feedback gain computation which require extensive computing power, whereas the fuzzy logic based algorithm is very simple and easy to implement. Comprehensive comparison study of the performance of the self-tuning PSS and the FLBPSS need to be explored in future work.

- An adaptive FLC can be developed with a number of sets of parameters such as *the scaling factors for each variable, the fuzzy set representing the meaning of linguistic values (the Whole Overlap Ratio of the membership functions) and the if-then rules* altered on-line to achieve the optimal performance. The development of the so called self-tuning FLC and self-organising FLC need to be studied in detail in further work.

- Fuzzy if-then rules have been formulated with the predefined membership functions which are needed for calibration using neural network techniques. The performance of the FLC with the generated rules by using input-output data pairs and the defined membership functions has been improved for the dynamic response under small perturbations. However, the 24-rule FLC does not work well when the system is subject to a large disturbance such as a three-phase to ground fault. Therefore, the complete decision table is needed for transient stability studies. In order to improve the performance of the FLC for both small and large perturbations under various operating conditions, neural network learning techniques can be used to produce the mapping rules from the empirical training sets, but the mapping rules in the neural network is not visible and is difficult to understand. It is also difficult to determine and to tune the rules in the FLC since the fuzzy sets does not have learning and adaptation capability. In order to solve these difficulties, the neural networks and the fuzzy sets can be combined to form **Fuzzy Neural Networks (FNN)** which is believed to have considerable potential in improving the performance of the FLC. There are two types of the synthesis of the fuzzy sets and the neural networks:

1. **The Neural Network and the Fuzzy Set:** The fuzzy set and the neural network are used independently in fuzzy control system or either one serves as a preprocessor for the other. For example, the fuzzy set can be used as a supervisor for the neural network in order to improve convergence of learning. The learning rate is determined by using fuzzy rules.

2. **The Neural-like Fuzzy Set:** The neural network uses the fuzzy neurones that are described by fuzzy sets, instead of the non-fuzzy neuron. In this case, antecedents and consequents in the 'if-then" rules are treated as fuzzy sets.

The work of using **FNN** to improve the overall performance of the FLC need to be studied in the future.

- Fuzzy control systems are essentially non-linear systems. For this reason it is difficult to obtain general results on the analysis and design of the fuzzy controller. In the fuzzy control literature, the stability analysis of fuzzy controller is usually done in the context of the following two views of the system under control:

1. Classical non-linear dynamic systems theory: the system under control is a non-fuzzy system, and the fuzzy controller is a particular class of non-linear controller;

2. Dynamic fuzzy systems.

Although the optimised fuzzy controllers work satisfactorily in practice in this research work, mathematical studies of controllability and stability in fuzzy control systems need to be investigated in depth in further work.

- Although the optimised fuzzy controller has been experimentally implemented in the Power Laboratory, the algorithm and methodology need to be implemented in the actual power system in the future.

Appendix A

Mathematical Model of the Synchronous Machine

A.1 Mathematical Model of the Synchronous Machine

In this section a brief introduction is given to the mathematical model of a synchronous machine connected to a very large power system through transmission lines for use in the design of the AVR.

Two models have been developed [Anderson, 1977]:

- Current model, using the currents as state variables;
- Flux linkage model, using the fluxes as state variables.

The synchronous machine under consideration is assumed to have:

- three stator windings sa-fa, sb-fb, and sc-fc;
- one field winding F-F';
- two amortisseur (damper) windings D-D' and Q-Q'.

These six windings are magnetically coupled. The type of the generator used is a salient pole type.

Let the positive directions of stator currents be the directions of leaving the machine terminals. The sign convention of torque is that a positive (driving) torque $T_m(t)$ accelerates the shaft, whereas a positive electrical (retarding or load) torque $T_e(t)$ decelerates the shaft. The definition of the position of the d-axis and q-axis is described in detail in [Anderson, 1977].

For the six-winding salient-pole synchronous generator, it is assumed that:

- *There is no saturation and there is no distributed material in which eddy currents can flow [Adkins, 1975];*
- *The harmonics above second-order can be neglected, thus all the inductances vary sinusoidally with an additional constant term in some cases [Adkins, 1975], [Rafian, 1987];*
- *The machine is operating under balanced conditions [Anderson, 1977].*

In the following equations all quantities are normalised in per unit except that time t is in seconds. The mechanical torque $T_m(t)$ and the electrical torque $T_e(t)$ are normalised on a three-phase base.

A.1.1 Flux Linkage Equations

The flux linkage equation for the six windings are as shown in equation (A.1):

$$\begin{bmatrix} \lambda_a(t) \\ \lambda_b(t) \\ \lambda_c(t) \\ \lambda_F(t) \\ \lambda_D(t) \\ \lambda_Q(t) \end{bmatrix} = \begin{bmatrix} L_{aa} & L_{ab} & L_{ac} & L_{aF} & L_{aD} & L_{aQ} \\ L_{ba} & L_{bb} & L_{bc} & L_{bF} & L_{bD} & L_{bQ} \\ L_{ca} & L_{cb} & L_{cc} & L_{cF} & L_{cD} & L_{cQ} \\ L_{Fa} & L_{Fb} & L_{Fc} & L_{FF} & L_{FD} & L_{FQ} \\ L_{Da} & L_{Db} & L_{Dc} & L_{DF} & L_{DD} & L_{DQ} \\ L_{Qa} & L_{Qb} & L_{Qc} & L_{QF} & L_{QD} & L_{QQ} \end{bmatrix} \begin{bmatrix} i_a(t) \\ i_b(t) \\ i_c(t) \\ i_F(t) \\ i_D(t) \\ i_Q(t) \end{bmatrix} \tag{A.1}$$

where $L_{jk} = \begin{cases} \text{self-inductance} & \text{when } j = k \\ \text{mutual inductance} & \text{when } j \neq k \end{cases}$

and

where $L_{jk} = L_{kj}$ in all cases.

Note that in equation (A.1) lower-case subscripts are used for stator quantities and upper-case subscripts are used for rotor quantities. Most of the inductances in equation (A.1) are functions of the rotor position angle $\theta(t)$. Also observe that nearly all terms in the matrix of equation (A.1) are time-varying, since θ is a function of time. The time varying inductances can be simplified by referring all quantities to a rotor frame of reference through Park's transformation [Anderson, 1977]. After utilising Park's transformation, the flux linkage equation can be expressed in the following equation:

$$\begin{bmatrix} \lambda_0(t) \\ \lambda_d(t) \\ \lambda_q(t) \\ \lambda_F(t) \\ \lambda_D(t) \\ \lambda_Q(t) \end{bmatrix} = \begin{bmatrix} L_0 & 0 & 0 & 0 & 0 & 0 \\ 0 & L_d & 0 & kM_F & kM_D & 0 \\ 0 & 0 & L_q & 0 & 0 & kM_Q \\ 0 & kM_F & 0 & L_F & M_R & 0 \\ 0 & kM_D & 0 & M_R & L_D & 0 \\ 0 & 0 & kM_Q & 0 & 0 & L_Q \end{bmatrix} \begin{bmatrix} i_0(t) \\ i_d(t) \\ i_q(t) \\ i_F(t) \\ i_D(t) \\ i_Q(t) \end{bmatrix} \tag{A.2}$$

where

- λ_d is the flux linkage on the d-axis of the rotor;
- λ_q is the flux linkage on the q-axis of the rotor;
- λ_0 is completely uncoupled from the other circuits;
- M_R is the mutual inductance between windings F and D;
- M_F is the mutual inductance between stator and rotor windings;
- M_D is the mutual inductance between phase windings to damper winding D;
- M_Q is the mutual inductance between phase windings to damper winding Q;
- $k = \sqrt{\frac{3}{2}}$

It can also be observed that the inductance matrix of equation (A.2) is a matrix of constants (all quantities have only one subscript). The advantage of Park's transformation is such that it removes the time-varying coefficients.

A.1.2 Voltage Equations

The generator voltage equations are of the form [Anderson, 1977]:

$$v(t) = \pm\sum ri(t) \pm \sum \dot{\lambda}(t) \tag{A.3}$$

where $\lambda(t)$ is the flux linkage, r is the winding resistance, and $i(t)$ is the current. The matrix equation can be written in equation (A.4):

$$\begin{bmatrix} v_a(t) \\ v_b(t) \\ v_c(t) \\ -v_F(t) \\ 0 \\ 0 \end{bmatrix} = \begin{bmatrix} r_a & 0 & 0 & 0 & 0 & 0 \\ 0 & r_b & 0 & 0 & 0 & 0 \\ 0 & 0 & r_c & 0 & 0 & 0 \\ 0 & 0 & 0 & r_F & 0 & 0 \\ 0 & 0 & 0 & 0 & r_D & 0 \\ 0 & 0 & 0 & 0 & 0 & r_Q \end{bmatrix} \begin{bmatrix} i_a(t) \\ i_b(t) \\ i_c(t) \\ i_F(t) \\ i_D(t) \\ i_Q(t) \end{bmatrix} - \begin{bmatrix} \dot{\lambda}_a(t) \\ \dot{\lambda}_b(t) \\ \dot{\lambda}_c(t) \\ \dot{\lambda}_F(t) \\ \dot{\lambda}_D(t) \\ \dot{\lambda}_Q(t) \end{bmatrix} + \begin{bmatrix} V_n(t) \\ 0 \end{bmatrix} \tag{A.4}$$

For balanced conditions $r = r_a = r_b = r_c$. The equation (A.4) is complicated by the presence of time-varying coefficients in the $\dot{\lambda}(t)$ term, but these terms can be eliminated by applying a Park's transformation to the stator partition. The resulting equation is shown below:

$$
\begin{bmatrix} v_0(t) \\ v_d(t) \\ v_q(t) \\ -v_F(t) \\ 0 \\ 0 \end{bmatrix} = \begin{bmatrix} r & 0 & 0 & 0 & 0 & 0 \\ 0 & r & 0 & 0 & 0 & 0 \\ 0 & 0 & r & 0 & 0 & 0 \\ 0 & 0 & 0 & r_F & 0 & 0 \\ 0 & 0 & 0 & 0 & r_D & 0 \\ 0 & 0 & 0 & 0 & 0 & r_Q \end{bmatrix} \begin{bmatrix} i_o(t) \\ i_d(t) \\ i_q(t) \\ i_F(t) \\ i_D(t) \\ i_Q(t) \end{bmatrix}
- \begin{bmatrix} \dot\lambda_0(t) \\ \dot\lambda_d(t) \\ \dot\lambda_q(t) \\ \dot\lambda_F(t) \\ \dot\lambda_D(t) \\ \dot\lambda_Q(t) \end{bmatrix} + \begin{bmatrix} 0 \\ -\omega(t)\lambda_q(t) \\ \omega(t)\lambda_d(t) \\ 0 \\ 0 \\ 0 \end{bmatrix} - \begin{bmatrix} 3r_n i_o(t) + 3L_n \dot{i}_0(t) \\ 0 \\ 0 \\ 0 \\ 0 \\ 0 \end{bmatrix} \tag{A.5}
$$

For balanced conditions the zero-sequence voltage is zero and equation (A.5) can be written as:

$$
\begin{bmatrix} v_d(t) \\ v_q(t) \\ -v_F(t) \\ 0 \\ 0 \end{bmatrix} = \begin{bmatrix} r & 0 & 0 & 0 & 0 \\ 0 & r & 0 & 0 & 0 \\ 0 & 0 & r_F & 0 & 0 \\ 0 & 0 & 0 & r_D & 0 \\ 0 & 0 & 0 & 0 & r_Q \end{bmatrix} \begin{bmatrix} i_d(t) \\ i_q(t) \\ i_F(t) \\ i_D(t) \\ i_Q(t) \end{bmatrix} - \begin{bmatrix} \dot\lambda_d(t) \\ \dot\lambda_q(t) \\ \dot\lambda_F(t) \\ \dot\lambda_D(t) \\ \dot\lambda_Q(t) \end{bmatrix} + \begin{bmatrix} -\omega(t)\lambda_q(t) \\ \omega(t)\lambda_d(t) \\ 0 \\ 0 \\ 0 \end{bmatrix} \tag{A.6}
$$

A.1.3 Torque and Power Equations

Expressing the total accelerating torque as

$$
T_a(t) = 2H\dot\omega(t) = T_m(t) - T_e(t) - T_d(t) \tag{A.7}
$$

where

- $T_e(t)$ is the electrical torque,

- $T_m(t)$ is the mechanical torque and,
- $T_d(t)$ is the damping torque.

$$T_d(t) = D\omega(t) \tag{A.8}$$

where D is the damping constant.

$$T_e(t) = i_q(t)\lambda_d(t) - i_d(t)\lambda_q(t) \tag{A.9}$$

The electrical power $P_e(t)$ is shown in the following equation:

$$P_e(t) = T_e(t)\omega(t) \tag{A.10}$$

A.1.4 Swing Equation

The swing equation is written as

$$\dot{\delta}(t) = \omega_0\omega(t), \tag{A.11}$$

$$\dot{\omega}(t) = \frac{1}{2H}(T_m(t) - T_e(t) - D\omega(t)) \tag{A.12}$$

where

$$T_m(t) = \frac{P_m(t)}{\omega(t)} \tag{A.13}$$

A.1.5 Load Equation

The external connection of the synchronous generator to the infinite bus can be described by the following equations

$$\delta(t) = \delta_0 + \int_{t_0}^{t}(\omega(t) - \omega_0)dt \tag{A.14}$$

in radians or

$$\dot{\delta}(t) = \omega(t) - 1 \tag{A.15}$$

in pu.

$$v_{0dq}(t) = V_\infty\sqrt{3}\begin{bmatrix} 0 \\ -\sin(\delta(t)-\alpha) \\ \cos(\delta(t)-\alpha) \end{bmatrix} + R_e i_{0dq}(t) + L_e \dot{i}_{0dq}(t) - \omega(t)L_e \begin{bmatrix} 0 \\ -i_q(t) \\ i_d(t) \end{bmatrix} \tag{A.16}$$

Expressing the synchronous machine terminal voltage V_t in rms equivalent variables

$$V_t(t) = \sqrt{V_d(t)^2 + V_q(t)^2} \tag{A.17}$$

where $V_d(t) = v_d(t)/\sqrt{3}$, $V_q(t) = v_q(t)/\sqrt{3}$.

$$I_t(t) = \sqrt{I_d(t)^2 + I_q(t)^2} \tag{A.18}$$

where $I_d(t) = i_d(t)/\sqrt{3}$, $I_q(t) = i_q(t)/\sqrt{3}$.

A.1.6 Formulation of State-Space Equations

The objective is to derive a set of equations describing the synchronous machine in the form of equation (A.19)

$$\dot{x} = f(x, u, t) \tag{A.19}$$

where

- x is a vector of the state variables;
- u is the system driving function;
- f is a set of nonlinear function.

If the equations describing the synchronous machine are linear, equation (A.19) is of the well known form

$$\dot{x} = Ax + Bu \tag{A.20}$$

Examining equation (A.6), it can be seen that this represents a set of first order differential equations. On putting this set in the form of the equation (A.20), it can be noted that equation (A.6) contains flux linkages and currents as variables.

A.1.7 Current Model

From equation (A.2), compute the values of λ and $\dot{\lambda}$. Substituting these results into equation (A.6) to replace the terms in λ and $\dot{\lambda}$ by terms in i and $\dot{i}$ and rearranging

$$\begin{bmatrix} v_d(t) \\ -v_F(t) \\ 0 \\ v_q(t) \\ 0 \end{bmatrix} = \begin{bmatrix} r & 0 & 0 & \omega(t)L_q & \omega(t)kM_Q \\ 0 & r_F & 0 & 0 & 0 \\ 0 & 0 & r_D & 0 & 0 \\ -\omega(t)L_d & -\omega(t)kM_F & -\omega(t)kM_D & r & 0 \\ 0 & 0 & 0 & 0 & r_Q \end{bmatrix} \begin{bmatrix} i_d(t) \\ i_F(t) \\ i_D(t) \\ i_q(t) \\ i_Q(t) \end{bmatrix}$$

$$- \begin{bmatrix} L_d & kM_F & kM_D & 0 & 0 \\ kM_F & L_F & M_R & 0 & 0 \\ kM_D & M_R & L_D & 0 & 0 \\ 0 & 0 & 0 & L_q & kM_Q \\ 0 & 0 & 0 & kM_Q & L_Q \end{bmatrix} \begin{bmatrix} \dot{i}_d(t) \\ \dot{i}_F(t) \\ \dot{i}_D(t) \\ \dot{i}_q(t) \\ \dot{i}_Q(t) \end{bmatrix} \tag{A.21}$$

Using matrix notation, equation (A.21) is written as

$$v(t) = -(R + \omega(t)N)i(t) - L\dot{i}(t) \tag{A.22}$$

If the inverse of the inductance matrix exists, it can be assumed that

$$\dot{i}(t) = -L^{-1}(R+\omega(t)N)i - L^{-1}v(t) \tag{A.23}$$

This equation has the desired state-space form.

From equation (A.2) the flux linkage can be expressed in terms of current

$$\lambda_d(t) = L_d i_d(t) + kM_F i_F(t) + kM_D i_D(t), \qquad \lambda_q(t) = L_q i_q(t) + kM_Q i_Q(t) \tag{A.24}$$

Thus the electrical torque equation can be written as

$$T_e(t) = \begin{bmatrix} L_d i_q(t) & kM_F i_q(t) & kM_D i_q(t) & -L_q i_d(t) & -kM_Q i_d(t) \end{bmatrix} \begin{bmatrix} i_d(t) \\ i_F(t) \\ i_D(t) \\ i_q(t) \\ i_Q(t) \end{bmatrix} \tag{A.25}$$

By substituting equation (A.25) into equation (A.7), the swing equation may be written as

$$\dot{\omega}(t) = \frac{T_m(t)}{2H} + \begin{bmatrix} -\frac{L_d i_q(t)}{2H} & -\frac{kM_F i_q(t)}{2H} & -\frac{kM_D i_q(t)}{2H} & -\frac{L_q i_d(t)}{2H} & -\frac{kM_Q i_d(t)}{2H} & -\frac{D}{2H} \end{bmatrix} \begin{bmatrix} i_d(t) \\ i_F(t) \\ i_D(t) \\ i_q(t) \\ i_Q(t) \\ \omega(t) \end{bmatrix} \tag{A.26}$$

Define $K = \sqrt{3}V_\infty$ and $\gamma(t) = \delta(t) - \alpha$ and let

$$\hat{R} = r + R_e,\ \hat{L}_d = L_d + L_e,\ \hat{L}_q = L_q + L_e \tag{A.27}$$

Incorporating the above equations into equation (A.22), the current model is shown in the following state-space equation:

$$\begin{bmatrix} \dot{i}_d(t) \\ \dot{i}_F(t) \\ \dot{i}_D(t) \\ \dot{i}_q(t) \\ \dot{i}_Q(t) \\ \dot{\omega}(t) \\ \dot{\delta}(t) \end{bmatrix} = \begin{bmatrix} \multicolumn{5}{c}{-\hat{L}^{-1}(\hat{R}+\omega(t)\hat{N})} & & 0 \\ -\frac{L_d i_q(t)}{2H} & -\frac{kM_F i_q(t)}{2H} & -\frac{kM_D i_q(t)}{2H} & -\frac{L_q i_d(t)}{2H} & -\frac{kM_Q i_d(t)}{2H} & -\frac{D}{2H} & 0 \\ 0 & 0 & 0 & 0 & 0 & 1 & 0 \end{bmatrix} \begin{bmatrix} i_d(t) \\ i_F(t) \\ i_D(t) \\ i_q(t) \\ i_Q(t) \\ \omega(t) \\ \delta(t) \end{bmatrix}$$

$$+ \begin{bmatrix} -\hat{L}^{-1} & 0 & \\ & 1 & 0 \\ 0 & 0 & 1 \end{bmatrix} \begin{bmatrix} -K\sin(\gamma(t)) \\ -v_F(t) \\ 0 \\ K\cos(\gamma(t)) \\ 0 \\ \frac{T_m(t)}{2H} \\ -1 \end{bmatrix} \qquad \text{(A.28)}$$

The system described by the above equation is in the state-space form of $\dot{x} = Ax+Bu$ where u contains the system driving functions $v_F(t)$ and $T_m(t)$. The state x^t equal to $[i_d(t)\ i_F(t)\ i_D(t)\ i_q(t)\ i_Q(t)\ \omega(t)\ \delta(t)]$. The loading effect of the transmission line is incorporated in the matrix $\hat{R}$, $\hat{L}$, and $\hat{N}$. The infinite bus voltage V_∞ appears in the term $K\sin(\gamma(t))$ and $K\cos(\gamma(t))$.

Similar procedure can be adopted to derive the flux linkage model [Anderson, 1977].

A.2 Linearisation of the Non-linear Power System Model

In this section the non-linear current power system model derived in Section A.1 is linearised.

For the power system described previously, the non-linearities are mainly characterised by the product non-linearities and the trigonometric non-linearities.

Most methods for the design of power system controllers in the literature are based on linearised models of power systems. Linearisation of the non-linear power system about a steady-state operating point provides information on the small-perturbation dynamic behaviour of the system at the specified operating point. When a power system is subject to a small perturbation, it tends to acquire a new operating state. During the transition between the initial state and the new state the system behaviour is oscillatory. If the two states are such that all the state variables change slightly, the system is operating near the initial state. The initial operating condition may be considered as a quiescent operating condition for the system. The linear equations thus derived are assumed to be valid in a region near the quiescent condition.

A.2.1 Linearisation of the Generator State-Space Current Model

Let the state-space vector x have an initial state x_0 at time $t = t_0$. At the occurrence of a small disturbance, the state will change slightly from their previous values

$$x = x_0 + x_\Delta \tag{A.29}$$

The state-space model is in the form

$$\dot{x} = Ax + Bu \tag{A.30}$$

by substituting equation (A.29) into equation (A.30)

$$\dot{x}_0 + \dot{x}_\Delta = A(x_0)(x_0 + x_\Delta) + B(x_0)u = A(x_0)x_0 + A(x_0)x_\Delta + B(x_0)u \quad \text{(A.31)}$$

since $\dot{x_0} = A(x_0)x_0$, the linearised state-space equation can be obtained as

$$\dot{x}_\Delta = A(x_0)x_\Delta + B(x_0)u \quad \text{(A.32)}$$

The linearised system equation for a synchronous machine (not including the load equation) can be expressed as in equation (A.33):

$$\begin{bmatrix} v_{d\Delta}(t) \\ -v_{F\Delta}(t) \\ 0 \\ v_{q\Delta}(t) \\ 0 \\ T_{m\Delta}(t) \\ 0 \end{bmatrix} = - \begin{bmatrix} r & 0 & 0 & \omega_0 L_q & \omega_0 k M_Q & \lambda_{q0} & 0 \\ 0 & r_F & 0 & 0 & 0 & 0 & 0 \\ 0 & 0 & r_D & 0 & 0 & 0 & 0 \\ -\omega_0 L_q & -\omega_0 k M_F & -\omega_0 k M_D & r & 0 & -\lambda_{d0} & 0 \\ 0 & 0 & 0 & 0 & r_Q & 0 & 0 \\ \lambda_{q0} - L_d i_{q0} & -kM_F i_{q0} & -kM_D i_{q0} & -\lambda_{d0} + L_q i_{d0} & kM_Q i_{d0} & -D & 0 \\ 0 & 0 & 0 & 0 & 0 & -1 & 0 \end{bmatrix}$$
$$\begin{bmatrix} i_{d\Delta}(t) \\ i_{F\Delta}(t) \\ i_{D\Delta}(t) \\ i_{q\Delta}(t) \\ i_{Q\Delta}(t) \\ \omega_\Delta(t) \\ \delta_\Delta(t) \end{bmatrix} - \begin{bmatrix} L_d & kM_F & kM_D & 0 & 0 & 0 & 0 \\ kM_F & L_F & M_R & 0 & 0 & 0 & 0 \\ kM_D & M_R & L_D & 0 & 0 & 0 & 0 \\ 0 & 0 & 0 & L_q & kM_Q & 0 & 0 \\ 0 & 0 & 0 & kM_Q & L_Q & 0 & 0 \\ 0 & 0 & 0 & 0 & 0 & -2H & 0 \\ 0 & 0 & 0 & 0 & 0 & 0 & 1 \end{bmatrix} \begin{bmatrix} \dot{i}_{d\Delta}(t) \\ \dot{i}_{F\Delta}(t) \\ \dot{i}_{D\Delta}(t) \\ \dot{i}_{q\Delta}(t) \\ \dot{i}_{Q\Delta}(t) \\ \dot{\omega}_\Delta(t) \\ \dot{\delta}_\Delta(t) \end{bmatrix} \quad \text{(A.33)}$$

A.2.2 Linearisation of the Load Equation for the Single-machine Infinite Bus Power System

Equation (A.16) is repeated here for convenience:

$$v_d(t) = -K\sin(\delta(t)-\alpha) + R_e i_d(t) + L_e \dot{i}_d(t) + \omega(t) L_e i_q(t),$$

$$v_q(t) = K\cos(\delta(t)-\alpha) + R_e i_q(t) + L_e \dot{i}_q(t) - \omega(t) L_e i_d(t) \tag{A.34}$$

where $K = \sqrt{3}V_\infty$ and α is the angle of $\bar{V}_\infty$.

The linearised load equation is expressed as

$$v_{d\Delta}(t) = -K\cos(\delta_0-\alpha)\delta_\Delta(t) + R_e i_{d\Delta}(t) + \omega_0 L_e i_{q\Delta}(t) + i_{q0} L_e \omega_\Delta(t) + L_e \dot{i}_{d\Delta}(t),$$

$$v_{q\Delta}(t) = -K\sin(\delta_0-\alpha)\delta_\Delta(t) + R_e i_{q\Delta}(t) + L_e \dot{i}_{q\Delta}(t) - \omega_0 L_e i_{d\Delta}(t) - i_{d0}(t) L_e \omega_\Delta(t) \tag{A.35}$$

By substituting and rearranging, the linearised system equation can be obtained as:

$$
\begin{bmatrix} 0 \\ -v_{F\Delta}(t) \\ 0 \\ 0 \\ 0 \\ T_{m\Delta}(t) \\ 0 \end{bmatrix} =
$$

$$
-\begin{bmatrix}
\hat{R} & 0 & 0 & \omega_0 \hat{L}_q & \omega_0 k M_Q & \hat{\lambda}_{q0} & -K\cos(\delta_0-\alpha) \\
0 & r_F & 0 & 0 & 0 & 0 & 0 \\
0 & 0 & r_D & 0 & 0 & 0 & 0 \\
-\omega_0 \hat{L}_q & -\omega_0 k M_F & -\omega_0 k M_D & \hat{R} & 0 & -\hat{\lambda}_{d0} & -K\sin(\delta_0-\alpha) \\
0 & 0 & 0 & 0 & r_Q & 0 & 0 \\
\lambda_{q0} - L_d i_{q0} & -kM_F i_{q0} & -kM_D i_{q0} & -\lambda_{d0} + L_q i_{d0} & kM_Q i_{d0} & -D & 0 \\
0 & 0 & 0 & 0 & 0 & -1 & 0
\end{bmatrix}
$$

$$
\begin{bmatrix} i_{d\Delta}(t) \\ i_{F\Delta}(t) \\ i_{D\Delta}(t) \\ i_{q\Delta}(t) \\ i_{Q\Delta}(t) \\ \omega_\Delta(t) \\ \delta_\Delta(t) \end{bmatrix}
-
\begin{bmatrix}
\hat{L}_d & kM_F & kM_D & 0 & 0 & 0 & 0 \\
kM_F & L_F & M_R & 0 & 0 & 0 & 0 \\
kM_D & M_R & L_D & 0 & 0 & 0 & 0 \\
0 & 0 & 0 & \hat{L}_q & kM_Q & 0 & 0 \\
0 & 0 & 0 & kM_Q & L_Q & 0 & 0 \\
0 & 0 & 0 & 0 & 0 & -2H & 0 \\
0 & 0 & 0 & 0 & 0 & 0 & 1
\end{bmatrix}
\begin{bmatrix} \dot{i}_{d\Delta}(t) \\ \dot{i}_{F\Delta}(t) \\ \dot{i}_{D\Delta}(t) \\ \dot{i}_{q\Delta}(t) \\ \dot{i}_{Q\Delta}(t) \\ \dot{\omega}_\Delta(t) \\ \dot{\delta}_\Delta(t) \end{bmatrix}
\tag{A.36}
$$

Note that the only driving functions in the system equation (A.36) are the field voltage $v_{F\Delta}(t)$ and the mechanical torque $T_{m\Delta}(t)$.

A.3 Simplified Linear Model

A simplified linear model for a synchronous machine connected to an infinite bus through a transmission line having resistance R_e and inductance L_e (or a reactance X_e) can be developed [Hefron, 1952], [DeMello, 1969]. Let the following assumptions be made:

1. *Amortisseur effects are neglected;*
2. *Stator winding resistance is neglected;*
3. *The $\dot{\lambda}_d$ and $\dot{\lambda}_q$ terms in the stator and load voltage equations are neglected compared to the speed voltage terms $\omega\lambda_q$ and $\omega\lambda_d$;*
4. *The terms $\omega\lambda$ in the stator and load voltage equations are assumed to be approximately equal to $\omega_R\lambda$;*
5. *Balanced conditions are assumed and saturation effects are neglected.*

Based on the above assumptions, the simplified linear model can be achieved by using a number of steps which are described below.

Step 1: The E' equation

The field equation are given by

$$v_F(t) = r_F i_F(t) + \dot{\lambda}_F(t), \qquad \lambda_F(t) = L_F i_F(t) + kM_F i_d(t) \tag{A.37}$$

Eliminating $i_F(t)$

$$v_F(t) = \frac{r_F}{L_F}(\lambda_F(t) - kM_F i_d(t)) + \dot{\lambda}_F(t) \tag{A.38}$$

Let $e'_q(t) = \sqrt{3}E'_q(t)$ be the stator EMF proportional to the main winding flux linkage the stator; i.e., $\sqrt{3}E'_q(t) = \omega_R kM_F \lambda_F(t)/L_F$. Also let $E_{FD}(t)$ be the stator EMF that is produced by the field current and corresponds to the field voltage $v_F(t)$; i.e.,

$$\sqrt{3}E_{FD}(t) = \omega_R kM_F v_F(t)/r_F \tag{A.39}$$

Using the above definition and the definition of τ'_{d0}, equation (A.38) can be expressed in the s domain

$$E_{FD} = (1 + \tau'_{d0}s)E'_q - (x_d - x'_d)I_d \tag{A.40}$$

where $I_d = i_d/\sqrt{3}$.

Using the above definition for E'_q, the second equation in (A.37) can be arranged as follows

$$E'_q(t) = \omega_R k M_F i_F(t)/\sqrt{3} + (x_d - x'_d)I_d(t) = E(t) + (x_d - x'_d)I_d(t) \quad (A.41)$$

From the voltage equation and the assumptions made in the simplified model, voltage v_d and v_q for infinite bus loading can be computed

$$\begin{aligned} v_d(t) &= -\omega_R L_q i_q(t) = -\sqrt{3}V_\infty \sin(\delta(t) - \alpha) + R_e i_d(t) + \omega_R L_e i_q(t) \\ v_q(t) &= \omega_R L_d i_d(t) + \omega_R k M_F i_F(t) = \sqrt{3}V_\infty \cos(\delta(t) - \alpha) + R_e i_q(t) - \omega_R L_e i_d(t) \end{aligned} \quad (A.42)$$

Linearising equation (A.42),

$$\begin{aligned} 0 &= -R_e i_{q\Delta}(t) + (x_d + X_e)i_{d\Delta}(t) + \omega_R k M_F i_{F\Delta}(t) + [K \sin(\delta_0 - \alpha)]\delta_\Delta(t) \\ 0 &= -R_e i_{d\Delta}(t) - (x_q + X_e)i_{q\Delta}(t) + [K \cos(\delta_0 - \alpha)]\delta_\Delta(t) \end{aligned} \quad (A.43)$$

where $K = \sqrt{3}V_\infty$ and V_∞ is the infinite bus voltage to neutral.

Rearranging equation (A.41) and equation (A.43),

$$\begin{aligned} -(x'_d + X_e)I_{d\Delta}(t) + R_e I_{q\Delta}(t) &= E'_{q\Delta}(t) + [V_\infty \sin(\delta_0 - \alpha)]\delta_\Delta(t) \\ R_e I_{d\Delta}(t) + (x_q + X_e)I_{q\Delta}(t) &= [V_\infty \cos(\delta_0 - \alpha)]\delta_\Delta(t) \end{aligned} \quad (A.44)$$

Solving equation (A.44) for $I_{d\Delta}(t)$ and $I_{q\Delta}(t)$

$$\begin{bmatrix} I_{d\Delta}(t) \\ I_{q\Delta}(t) \end{bmatrix} = K_I \begin{bmatrix} -(x_q + X_e) & R_e \cos(\delta_0 - \alpha) - (x_q + X_e)\sin(\delta_0 - \alpha) \\ R_e & (x'_d + X_e)\cos(\delta_0 - \alpha) + R_e \sin(\delta_0 - \alpha) \end{bmatrix} \begin{bmatrix} E'_{q\Delta}(t) \\ V_\infty \delta_\Delta(t) \end{bmatrix} \quad (A.45)$$

where

$$K_I = \frac{1}{{R_e}^2 + (x_q + X_e)(x'_d + X_e)} \tag{A.46}$$

Substituting I_d into an incremental version of equation (A.40) to compute

$$E_{FD} = (1/K_3 + \tau'_{d0}s)E'_{q\Delta} + K_4\delta_\Delta \tag{A.47}$$

where K_3 and K_4 are defined as follows:

$$K_3 = \frac{1}{[1 + K_I(x_d - x'_d)(x_q + X_e)]} \tag{A.48}$$

$$K_4 = V_\infty K_I(x_d - x'_d)[(x_q + X_e)\sin(\delta_0 - \alpha) - R_e\cos(\delta_0 - \alpha)] \tag{A.49}$$

where K_3 is an impedance factor that takes into account the loading effect of the external impedance. K_4 is related to the demagnetizing effect of a change in the rotor angle; i.e.,

$$K_4 = \frac{1}{K_3}\frac{E'_q}{\delta_\Delta}|_{E_{FD}=constant} \tag{A.50}$$

From equations (A.47), (A.48) and (A.49), the following s domain relation can be derived

$$E'_{q\Delta} = \frac{K_3}{1 + K_3\tau'_{d0}s}E_{FD\Delta} - \frac{K_3K_4}{1 + K_3\tau'_{d0}s}\delta_\Delta \tag{A.51}$$

Step 2: Electrical torque equation

The pu electrical torque $T_e(t)$ is numerically equal to the three-phase power. Therefore,

$$T_e(t) = \frac{1}{3}(v_d(t)i_d(t) + v_q(t)i_q(t)) \tag{A.52}$$

Under the assumptions used in this model

$$V_d(t) = -x_q I_q(t), \quad V_q(t) = x_d I_d(t) + \omega_R k M_F i_F(t)/\sqrt{3} \tag{A.53}$$

Using equation (A.41) in the second equation of equation (A.42),

$$V_d(t) = -x_q I_q(t), \quad V_q(t) = x'_d I_d(t) + E'_q(t) \tag{A.54}$$

From equation (A.54) and equation (A.52)

$$T_e(t) = [E'_q(t) - (x_q - x'_d)I_d(t)]I_q(t) \tag{A.55}$$

Linearising equation (A.55)

$$\begin{aligned} T_{e\Delta}(t) &= I_{q0}E'_{q\Delta}(t) + [E'_{q0} - (x_q - x'_d)I_{d0}]I_{q\Delta}(t) - (x_q - x'_d)I_{q0}I_{d\Delta}(t) \\ &= I_{q0}E'_{q\Delta}(t) + E_{qa0}I_{q\Delta}(t) - (x_q - x'_d)I_{q0}I_{d\Delta}(t) \end{aligned} \tag{A.56}$$

where $E_{qa}(t) = E(t) + (x_d - x_q)I_d(t)$ with E taken from equation (A.41) to write the initial condition

$$\begin{aligned} E_{qa0} &= E_0 + (x_d - x_q)I_{d0} \\ &= E'_{q0} - (x_d - x'_d)I_{d0} + (x_d - x_q)I_{d0} \\ &= E'_{q0} - (x_q - x'_d)I_{d0} \end{aligned} \tag{A.57}$$

The incremental torque can be computed by substituting equation (A.45) and equation (A.46) into equation (A.56)

$$T_{e\Delta}(t) = K_I V_\infty \{E_{qa0}[R_e \sin(\delta_0 - \alpha) + (x'_d + X_e)\cos(\delta_0 - \alpha)] +$$
$$I_{q0}(x_q - x'_d)[(x_q + X_e)\sin(\delta_0 - \alpha) - R_e \cos(\delta_0 - \alpha)]\}\delta_\Delta(t) +$$
$$K_I\{I_{q0}[{R_e}^2 + (x_q + X_e)^2] + E_{qa0}R_e\}E'_{q\Delta}(t) \equiv K_1\delta_\Delta(t) + K_2E'_{q\Delta}(t) \quad (A.58)$$

Where K_1 is the change in electrical torque for a small change in rotor angle at constant d-axis flux linkage.

$$K_1 = \frac{T_{e\Delta}(t)}{\delta_\Delta(t)}|_{E'_q = E'_{q0}}$$
$$= K_I V_\infty \{E_{q0}[R_e \sin(\delta_0 - \alpha) + (x'_d + X_e)\cos(\delta_0 - \alpha)] +$$
$$(i_{q0}/\sqrt{3})(x_q - x'_d)[(x_q + X_e)\sin(\delta_0 - \alpha) - R_e\cos(\delta_0 - \alpha)]\} \quad (A.59)$$

K_2 is the change in electrical torque for a small change in d-axis flux linkage at constant rotor angle.

$$K_2 = \frac{T_{e\Delta}(t)}{E'_{q\Delta}(t)}|_{\delta=\delta_0} = K_I\{R_eE_{q0} + (i_{q0}/\sqrt{3})[{R_e}^2 + (x_q + X_e)^2]\} \quad (A.60)$$

Step 3: Terminal voltage equation

The synchronous machine terminal voltage $V_t(t)$ is given by equation (A.17). This equation is linearised to obtain

$$V_{t\Delta}(t) = (V_{d0}/V_{t0})V_{d\Delta}(t) + (V_{q0}/V_{t0})V_{q\Delta}(t) \quad (A.61)$$

Substituting equation (A.54) in equation (A.61),

$$V_{t\Delta}(t) = -(V_{d0}/V_{t0})x_q I_{q\Delta}(t) + (V_{q0}/V_{t0})(x'_d I_{d\Delta}(t) + E'_{q\Delta}(t)) \quad (A.62)$$

Substituting for $I_{q\Delta}(t)$ and $I_{d\Delta}(t)$ from equation (A.45),

$$\begin{aligned} V_{t\Delta}(t) = \{ & (K_I V_\infty x'_d V_{q0}/V_{t0})[R_e \cos(\delta_0 - \alpha) - (x_q + X_e)\sin(\delta_0 - \alpha)] \\ & - (K_I V_\infty x_q V_{d0}/V_{t0})[(x'_d + X_e)\cos(\delta_0 - \alpha) + R_e \sin(\delta_0 - \alpha)]\}\delta_\Delta(t) \\ & + \{(V_{q0}/V_{t0})[1 - K_I x'_d(x_q + X_e)] - (V_{d0}/V_{t0})K_I x_q R_e\}E'_{q\Delta}(t) \\ & \equiv K_5\delta_\Delta(t) + K_6 E'_{q\Delta}(t) \quad (A.63) \end{aligned}$$

K_5 is the change in the terminal voltage $V_t(t)$ for a small change in rotor angle at constant d-axis flux linkage.

$$\begin{aligned} K_5 = \frac{V_{t\Delta}(t)}{\delta_\Delta(t)}|_{E'_q=E'_{q0}} = \{ & (K_I V_\infty x'_d v_{q0}/\sqrt{3}V_{t0})[R_e \cos(\delta_0 - \alpha) - (x_q + X_e)\sin(\delta_0 - \alpha)] \\ & - (K_I V_\infty x_q v_{d0}(\sqrt{3}V_{t0})[(x'_d + X_e)\cos(\delta_0 - \alpha) - R_e \sin(\delta_0 - \alpha)]\} \quad (A.64) \end{aligned}$$

K_6 is the change in the terminal voltage $V_t(t)$ for a small change in the d-axis flux linkage at constant rotor angle.

$$K_6 = \frac{V_{t\Delta}(t)}{E'_{q\Delta}(t)}|_{\delta=\delta_0} =$$

$$\{(K_I V_\infty x'_d v_{q0}/\sqrt{3}V_{t0})\{(v_{q0}/\sqrt{3}V_{t0})[1 - K_I X'_d(X_q + X_e)] - (v_{d0}/\sqrt{3}V_{t0})K_I X_q R_e\} \quad (A.65)$$

This model is a substantial improvement over the classical model since it accounts for the demagnetizing effects of the armature reaction through the change in $E_{q\Delta}{}'(t)$ due to change in $\delta_\Delta(t)$.

Appendix B

Introduction to Fuzzy Set Theory

B.1 Fuzzy Sets and Terminology

A fuzzy set is an extension of a crisp set. Fuzzy sets allow partial membership. An element may partially belong to a set.

In a crisp set membership of an element u in a set F is described by a characteristic function $\mu_F(u)$, where

$$\mu_F(u) = \begin{cases} 1 & \text{if } x \in F \\ 0 & \text{if } x \notin F \end{cases} \tag{B.1}$$

Let U be a collection of objects whose generic elements are denoted by u, which could be discrete or continuous, U is called the *Universe of Discourse.*

Fuzzy Set

A fuzzy set F in a universe of discourse U is characterised by a membership function μ_F which takes values in the interval [0,1] namely, $\mu_F : U \to [0,1]$. A fuzzy set may be viewed as a generalisation of the concept of an ordinary crisp set whose membership function takes only two values $\{0,1\}$. Thus a fuzzy set F in U may be represented as a set of ordered pairs of a generic element u and its grade of membership function $\mu_F(u)$:

$$F = \{(u, \mu_F(u) \mid u \in U\} \tag{B.2}$$

When U is continuous, a fuzzy set F can be written concisely as

$$F = \int_u \mu_F(u)/u \tag{B.3}$$

When U is discrete, a fuzzy set F can be represented as

$$F = \sum_{i=1}^{n} \mu_F(u_i)/u_i \tag{B.4}$$

It should be noted that the positive (+) sign in the summation in equation (B.4) denotes the union rather than the arithmetic sum.

Support, Crossover Point and Fuzzy Singleton:

The *support* of a fuzzy set F is the crisp set of all points u in U such that $\mu_F(u) > 0$. In particular, the element u in U at which $\mu_F = 0.5$, is called the *crossover point* and a fuzzy set whose support is a single point in U with $\mu_F = 1.0$ is referred to as *fuzzy singleton*.

α-cut of a Fuzzy Set F:

To exhibit an element $u \in U$ that typically belongs to a fuzzy set F, it may be demanded that its membership value to be greater than some threshold $\alpha \in [0, 1]$. The ordinary set of such elements is the α-cut F_α of F,

$$F_\alpha = \{u \in U, \mu_F(u) \geq \alpha\} \tag{B.5}$$

One also define the strong α-cut as:

$$F_{\bar{\alpha}} = \{u \in U, \mu_F(u) > \alpha\} \tag{B.6}$$

Height of a Fuzzy Set:

By a height of a fuzzy set, $height(F)$, it means a supremum of its membership function

$$height(F) = \sup_{u \in U} \mu_F(u) \tag{B.7}$$

If $height(F) = 1$, the set F is called a normalised fuzzy set.

Fuzzy Number:

A fuzzy number F in a continuous universe U is a fuzzy set F in U which is normal and convex, i.e.,

$$\begin{aligned} &\max_{u \in U} \mu_F(u) = 1 && \text{(normal)} \\ &\mu_F(\lambda u_1 + (1-\lambda)u_2) \geq \min(\mu_F(u_1), \mu_F(u_2)), \quad u_1, u_2 \in U, \lambda \in [0,1] && \text{(convex)} \end{aligned} \tag{B.8}$$

B.2 Fuzzy Set Theoretical Operations

Let A and B be two fuzzy sets in U with membership functions μ_A and μ_B, respectively. The membership function is the crucial components of a fuzzy set. Therefore, the set theoretical operations of union, intersection and complement, etc., for fuzzy sets are defined via their membership functions.

- **Union (OR)**:

  The membership function $\mu_{A\cup B}$ of the union $A \cup B$ is pointwise defined for all $u \in U$ by

  $$\mu_{A\cup B}(u) = \max\{\mu_A(u), \mu_B(u)\} \tag{B.9}$$

- **Intersection (AND)**:

  The membership function $\mu_{A\cap B}$ of the intersection $A \cap B$ is pointwise defined for all $u \in U$ by

$$\mu_{A\cap B}(u) = min\{\mu_A(u), \mu_B(u)\} \tag{B.10}$$

- **Complement (NOT):**

The membership function $\mu_{\bar{A}}$ of the complement of a fuzzy set A is pointwise defined for all $u \in U$ by

$$\mu_{\bar{A}}(u) = 1 - \mu_A(u) \tag{B.11}$$

- **Cartesian Product:**

If $A_1, \cdots, A_n$ are fuzzy sets in $U_1, \cdots, U_n$, respectively, the Cartesian product of $A_1, \cdots, A_n$ is a fuzzy set in the product space $U_1 \times \cdots \times U_n$ with the membership function

$$\mu_{A_1\times\cdots\times A_n}(u_1, u_2, \cdots, u_n) = min\{\mu_{A_1}(u_1), \cdots, \mu_{A_n}(u_n)\} \tag{B.12}$$

or

$$\mu_{A_1\times\cdots\times A_n}(u_1, u_2, \cdots, u_n) = \mu_{A_1}(u_1) \cdot \mu_{A_2}(u_2) \cdots \mu_{A_n}(u_n) \tag{B.13}$$

- **Triangular Norms or T-norms:**

The triangular norm or t-norm $*$ is a two-place function $[0,1] \times [0,1]$ to $[0,1]$, i.e., $*$: $[0,1] \times [0,1] \to [0,1]$ which includes intersection, algebraic product, bounded product, and drastic product. The greatest triangular norm is the intersection and the least one is the drastic product. The operations associated with triangular norms are defined for all $x, y \in [0,1]$ by:

intersection:	$xty = x \cap y = min\{x, y\}$
algebraic product:	$xty = x \cdot y = xy$
bounded product:	$xty = x \odot y = max\{0, x + y - 1\}$

drastic product:

$$xty = x\dot{\cap}y = \begin{cases} x & \text{if } y = 1 \\ y & \text{if } x = 1 \\ 0 & \text{if } x, y < 1 \end{cases} \tag{B.14}$$

Triangular norms are employed for defining conjunctions in approximate reasoning.

- **Triangular Co-Norms or S-norms:**

The triangular co-norm or s-norm $\dot{+}$ is a two-place function from $[0,1] \times [0,1]$ to $[0,1]$, i.e., $\dot{+}$: $[0,1] \times [0,1]$ to $[0,1]$ which includes union, algebraic sum, bounded sum, drastic sum and disjoint sum. The operations associated with triangular co-norms are defined for all $x, y \in [0,1]$ by:

union: $xsy{=}x \cup y = max\{x, y\}$

algebraic sum: $xsy{=}x\hat{+}y = x + y - xy$

bounded sum: $xsy{=}x \oplus y = min\{1, x + y\}$

drastic sum: $xsy{=}x \uplus y = \begin{cases} x & \text{if } y = 0 \\ y & \text{if } x = 0 \\ 1 & \text{if } x, y > 0 \end{cases}$

disjoint sum:

$$xsy = x \bigtriangleup y = max\{min\{x, 1 - y\}, min\{1 - x, y\}\} \tag{B.15}$$

The triangular norms are employed for defining conjunctions in approximate reasoning, while the triangular co-norms serve the same role for disjunctions. A fuzzy control rule, "if x is A and y is B", is represented by a fuzzy implication function and is denoted by $A \to B$, where A and B are fuzzy sets in universes U and V with membership functions μ_A and μ_B, respectively.

- **Fuzzy Conjunction:**

The fuzzy conjunction is defined for all $u \in U$ and $v \in V$ by

$$A \to B = A \times B = \int_{U \times V} \mu_A(u) * \mu_B(v)/(u, v) \tag{B.16}$$

where $*$ is an operator representing a triangular norm or t-norm.

- **Fuzzy Disjunction**:

The fuzzy disjunction is defined for all $u \in U$ and $v \in V$ by

$$A \rightarrow B = A \times B = \int_{U \times V} \mu_A(u) \dot{+} \mu_B(v)/(u,v) \tag{B.17}$$

where $\dot{+}$ is an operator representing a triangular co-norm or s-norm.

B.3 Linguistic Variables and Linguistic Hedges

- **Linguistic Variables**

Fuzzy sets provide a systematic means for dealing with uncertain and imprecise notions. Of particular significance in control systems is the use of linguistic variables, which may be considered as a variable whose value is a fuzzy number or as a variable whose values are defined in linguistic terms.

A linguistic variable is characterised by a quintuple $(x, T(x), U, G, M)$ in which x is the name of variable; $T(x)$ is the term set of x, that is, the set of names of linguistic values of x with each value being a fuzzy number defined on U; G is a syntactic rule for generating the names of values of x; and M is a semantic rule for associating with each value its meaning. For example, if *speed* is interpreted as a linguistic variable, then its term set T(speed) could be

T(speed)=slow, moderate, fast, very slow, more or less fast, $\cdots$

where each term in T(speed) is characterised by a fuzzy set in a universe of discourse U=[0,100]. It might be interpreted "slow" as "a speed below about 40 kmph," "moderate" as "a speed close to 55 kmph," and "fast" as "a speed above about 70 kmph." These terms can be characterised as fuzzy sets with their membership functions.

- **Linguistic Hedges**

A major reason behind using fuzzy logic in control engineering is the use of qualitative linguistic expressions favoured by human experts and operators such as *very* small and *rather* big. The purpose of the hedges such as *very*, *more or less* etc. is to generate a larger set of values for a linguistic variable from a small collection of primary terms through the processes of intensifier or concentration, dilation and normalisation.

- **Concentration (CON(F))**:

The concentration operation concentrates fuzzy elements by reducing in higher grades of the membership function more than that in lower grades membership function. This operation and the following ones of dilation, intensification and normalisation have no counterpart in ordinary set operations. A common concentration operator is:

$$\mu_{CON(F)}(u) = (\mu_F(u))^2 \tag{B.18}$$

The concentration operator can be used to roughly approximate the effect of the linguistic modifier *very*. That is, for some fuzzy set F

$$Very \quad F = F^2 = CON(F) \tag{B.19}$$

The result of applying the operator *very* on a fuzzy label *big* is a new fuzzy label *very big*.

- **Dilation (DIL(F))**:

$$\mu_{DIL(F)}(u) = (\mu_F(u))^{0.5} \tag{B.20}$$

The dilation operation dilates fuzzy elements by increasing the lower grades of membership function more than that in higher grades of membership function. It performs the inverse operation to concentration for these choices of powers 2 and 0.5. The dilation operator is roughly approximated by the linguistic modifier *More or Less*. Thus for any fuzzy set F

$$More\ \ or\ \ Less\ \ F = F^{0.5} = DIL(F) \tag{B.21}$$

- **Intensification (INT(F)):**

$$\mu_{INT(F)}(u) = \begin{cases} 2(\mu_F(u))^2 & \text{for } 0 \leq \mu_F(u) \leq 0.5 \\ 1 - 2(1 - \mu_F(u))^2 & \text{for } 0.5 < \mu_F(u) \leq 1 \end{cases} \tag{B.22}$$

The INT operation is like the contrast intensification of a picture. The intensification raises the membership function grade of those elements within the crossover points and reduces the membership grade of those outside the crossover points.

- **Normalisation (NORM(F)):**

$$\mu_{NORM(F)}(u) = \mu_F(u)/max\{\mu_F(u)\} \tag{B.23}$$

where the *max* function returns the maximum membership function for all elements u. If the membership function is < 1, then all membership functions will be increased. If the $max = 1$, then the membership functions are unchanged.

B.4 Fuzzy Inference and Composition

- **Fuzzy Relation:**

In control systems, relationships are defined between systems inputs and outputs. In fuzzy systems, these relationships or mappings are between fuzzy variables defined on different universe of discourse through the fuzzy conditional statement or linguistic implication which links the conditional or antecedent set with the consequent or output set. An n-ary fuzzy relation R is a fuzzy set in $U_1 \times \cdots \times U_n$ and is expressed as

$$R_{U_1\times\cdots\times U_n} = \{((u_1,\cdots,u_n),\mu_R(u_1,\cdots,u_n)) \mid (u_1,\cdots,u_n)\in U_1\times\cdots\times U_n\} \tag{B.24}$$

A broad class of models for logical connectives (union and intersection) is formed by triangular norms.

- **Fuzzy Relation Projection**

  Given a fuzzy set $A \in U, B \in V$, and a fuzzy relation R defined by $A \to B$, with associated membership function $\mu_R(u,v)$; then A is A^R, where A^R is the projection of the binary relation R on the domain of A defined by:

$$\mu_{A^R}(u) = \sup_{v\in V} \mu_R(u,v), \qquad u\in U, v\in V \tag{B.25}$$

- **Fuzzy Composition**

  To adequately represent any dynamic process or to provide control, several rules in the form of conditional statements or production rules are required. It is impractical to have a rule for every possible situation, therefore use is made of the compositional rule of inference which allows rules to be used in situations not normally covered. This important rule may be viewed as a combination of the fuzzy conjunctive and projection rules.

- **Max-Min Composition**:

  If R and S are fuzzy relations in $U\times V$ and $V\times W$, respectively, the composition of R and S is a fuzzy relation denoted by $R\circ S$ and is defined by

$$R\circ S = \{[(u,w), \vee(\mu_R(u,v)\wedge\mu_s(v,w))], u\in U, v\in V, w\in W\} \tag{B.26}$$

  where $\vee$ and $\wedge$ denote **max** and **min** respectively.

- **Sup-Star Composition**:

If R and S are fuzzy relations in $U \times V$ and $V \times W$, respectively, the composition of R and S is a fuzzy relation denoted by $R \circ S$ and is defined by

$$R \circ S = \{[(u, w), sup(\mu_R(u, v) * \mu_s(v, w))], u \in U, v \in V, w \in W\} \tag{B.27}$$

where $*$ could be any operator in the class of triangular norms, namely, minimum, algebraic product, bounded product, or drastic product. In addition to these basic operations, there are other operations that are used in the representation of linguistic hedges.

- **Fuzzy Implication–Representing the Meaning of If-then Rules:**

In general, a fuzzy control rule is a fuzzy relation which is expressed as a fuzzy implication. Fuzzy implication may be defined in many ways and it may be expressed as a fuzzy implication function. There are nearly 40 distinct fuzzy implication functions described in the literature. In general, they can be classified into three main categories: the fuzzy conjunction, the fuzzy disjunction and the fuzzy implication. The former two which were described previously bear a close relationship to a fuzzy Cartesian product. In fuzzy logic and approximate reasoning, there are five families of fuzzy implication functions in use. These implication functions can be shown as follows:

1. Material implication: $A \rightarrow B = (not\ A)\dot{+}B$
2. Propositional calculus: $A \rightarrow B = (not\ A)\dot{+}(A * B)$
3. Extended propositional calculus: $A \rightarrow B = (not\ A \times not\ B)\dot{+}B$
4. Generalisation of modus ponens: $A \rightarrow B = sup\{c \in [0, 1], A * c \leq B\}$
5. Generalisation of modus tollens: $A \rightarrow B = inf\{t \in [0, 1], B\dot{+}t \leq A\}$

Based on these definitions, many fuzzy implication functions may be generated by utilising the triangular norms and co-norms.

Mamdani's mini-operation rule of fuzzy implication:

$$R_m = A \times B = \int_{U \times V} \mu_A(u) \wedge \mu_B(v)/(u, v). \tag{B.28}$$

Larsen's algebraic product operation rule of fuzzy implication:

$$R_l = A \times B = \int_{U \times V} \mu_A(u)\mu_B(v)/(u,v). \tag{B.29}$$

Selecting the s-bounded sum operator (see s-norm definition) in the material implication rule leads to Zadeh's arithmetic rule of fuzzy implication:

$$R_{Z_a} = (not\ A \times V) \oplus (U \times B) = \int_{U \times V} 1 \wedge (1 - \mu_A(u) + \mu_B(v))/(u,v) \tag{B.30}$$

Also if the union operator is used in the material implication rule, the Boolean fuzzy implication follows:

$$R_B = (not\ A \times V) \cup (U \times B) = \int_{U \times V} (1 - \mu_A(u)) \vee (\mu_B(v))/(u,v) \tag{B.31}$$

The fuzzy propositional implication, utilising the intersection and union operators leads to Zadeh's *max-min* rule of implication:

$$R_{Z_m} = (A \times B) \cup (not\ A \times V) = \int_{U \times V} (\mu_A(u) \wedge \mu_B(v)) \vee (1 - \mu_A(u))/(u,v) \tag{B.32}$$

The generalisation of modus ponens (GMP) with bounded product leads to the standard sequence fuzzy implication:

$$R_s = A \times V \to U \times B = \int_{U \times V} (\mu_A(u) > \mu_B(v))/(u,v) \tag{B.33}$$

where

$$\mu_A(u) > \mu_B(v) = \begin{cases} 1 & \text{if } \mu_A(u) \leq \mu_B(v) \\ 0 & \text{if } \mu_A(u) \geq \mu_B(v) \end{cases} \tag{B.34}$$

If instead, the algebraic product is used for GMP, Goguen's fuzzy implication follows:

$$R_G = A \times V \rightarrow U \times B = \int_{U \times V} (\mu_A(u) \gg \mu_B(v))/(u,v) \qquad \text{(B.35)}$$

where

$$\mu_A(u) \gg \mu_B(v) = \begin{cases} 1 & \text{if } \mu_A(u) \leq \mu_B(v) \\ \frac{\mu_B(u)}{\mu_A(v)} & \text{if } \mu_A(u) > \mu_B(v) \end{cases} \qquad \text{(B.36)}$$

B.5 Fuzzy Logic and Approximate Reasoning

Approximate reasoning is the best-known form of fuzzy logic and covers a variety of inference rules whose premises contain fuzzy propositions. Inference in approximate reasoning is in sharp contrast to inference in classical logic–in the former the consequence of a given set of fuzzy propositions depends on the meaning attached to these fuzzy propositions. Thus, inference in approximate reasoning is computation with fuzzy sets that represent the meaning of a certain set of fuzzy propositions. For example, given the membership functions of μ_A and μ_R, representing the meaning of a fuzzy proposition "X is A" and the meaning of a fuzzy conditional "if X is A then Y is B," the membership function representing the meaning of the conclusion " Y is B " can be computed.

- **Inference Rules**

  In approximate reasoning, two inference rules are of major importance, i.e., the *compositional rule of inference* and the *generalised modus ponens.* The first rule uses a fuzzy relation to represent explicitly the connection between two fuzzy propositions, the second uses an *if-then* rule that implicitly represents a fuzzy relation. The generalised modus ponens has the symbolic inference scheme

$$S_1 \text{ is } Q_1,$$
$$\text{if } S_1 \text{ is } P_1 \text{ then } S_2 \text{ is } P_2,$$

$$\clubsuit\ S_2 \text{ is } Q_2;$$

where S_1 and S_2 are symbolic names for objects, and P_1, P_2, Q_1 and Q_2 are objects properties.

The *compositional rule of inference* can be considered to be a special case of the generalised modus ponens. Its general symbolic form is

$$S_1 \text{ is } Q_1,$$
$$S_1\ R\ S_2,$$
$$\clubsuit\ S_2 \text{ is } Q_2;$$

where $S_1\ R\ S_2$ reads as "S_1 is in relation R to S_2" and its meaning is represented as a fuzzy relation μ_R. Hence, instead of the *if-then* rule, there is a fuzzy relation R.

- **Sup-Star Compositional Rule of Inference**:

If R is a fuzzy relation in $U \times V$, and x is a fuzzy set in U, then the *sup-star compositional rule of inference* asserts that the fuzzy set y in V induced by x is given by

$$y = x \circ R \tag{B.37}$$

where $x \circ R$ is the sup-star composition of x and R. If the star represents the minimum operator, then this definition reduces to Zadeh's compositional rule of inference [Zadeh, 1973].

Appendix C

The Whole Overlap Ratio (WOR)

C.1 The WOR for Linear Membership Functions

The proposed index of the Whole Overlap Ratio:

$$WOR = \frac{\int_{-\infty}^{\infty} MIN(\mu_1(x), \mu_2(x))dx}{\int_{-\infty}^{\infty} MAX(\mu_1(x), \mu_2(x))dx} \tag{C.1}$$

The expression for two adjacent linear membership functions $\mu_1(x)$ and $\mu_2(x)$ are:

$$\mu_1(x) = 1 - abs(\frac{x - m_1}{\delta}) \tag{C.2}$$

$$\mu_2(x) = 1 - abs(\frac{x - m_2}{\delta}) \tag{C.3}$$

This can be shown in Figure (C.1).

The maximum height h of the intersection area is:

$$h = \frac{\frac{m_1+m_2}{2} - (m_2 + \delta)}{\delta} = 1 - \frac{m_2 - m_1}{2\delta} \tag{C.4}$$

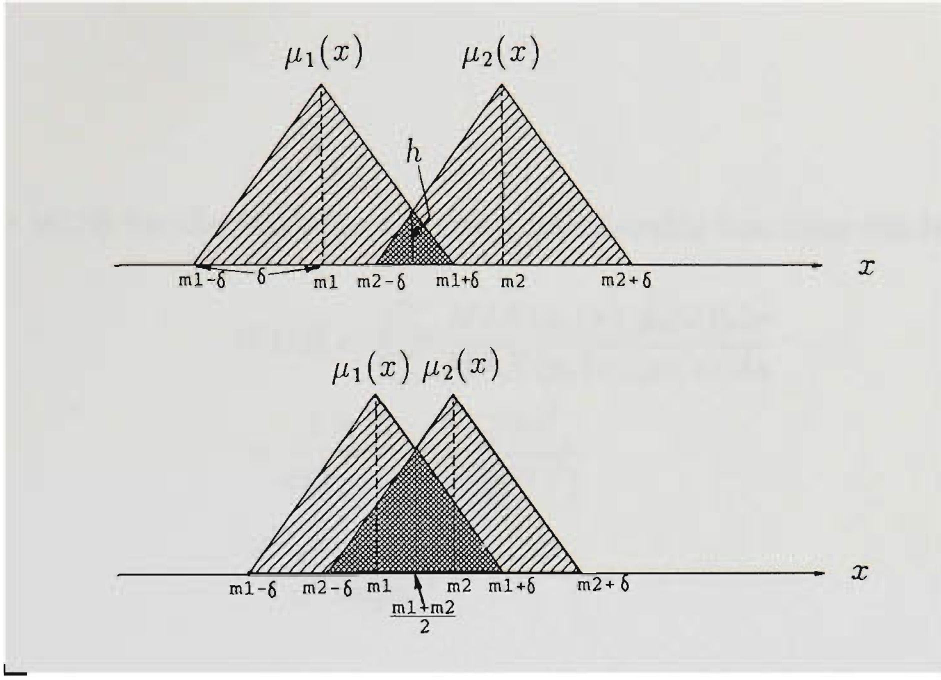

Figure C.1: Two adjacent linear membership functions

For the intersection area:

$$
\begin{aligned}
&\int_{-\infty}^{\infty} MIN(\mu_1(x), \mu_2(x))dx \\
&= \frac{1}{2} \times h \times (m_1 + m_2 + 2\delta) \\
&= \frac{1}{2} \times (1 - \frac{m_2 - m_1}{2\delta})(m_1 - m_2 + 2\delta) \\
&= \delta \times (1 - \frac{m_2 - m_1}{2\delta})^2
\end{aligned}
\tag{C.5}
$$

For the whole area:

$$
\begin{aligned}
&\int_{-\infty}^{\infty} MAX(\mu_1(x), \mu_2(x))dx \\
&= \frac{1}{2} \times 2\delta \times 1 + \frac{1}{2} \times 2\delta \times 1 - \int_{-\infty}^{\infty} min(\mu_1(x), \mu_2(x))dx \\
&= 2\delta - \delta \times (1 - \frac{m_2 - m_1}{2\delta})^2 \\
&= \delta(2 - (1 - \frac{m_2 - m_1}{2\delta})^2)
\end{aligned}
$$

(C.6)

The WOR for the two adjacent linear membership functions can be derived as:

$$
\begin{aligned}
WOR &= \frac{\int_{-\infty}^{\infty} MIN(\mu_1(x), \mu_2(x))dx}{\int_{-\infty}^{\infty} MAX(\mu_1(x), \mu_2(x))dx} \\
&= \frac{\delta \times (1 - \frac{m_2-m_1}{2\delta})^2}{\delta(2 - (1 - \frac{m_2-m_1}{2\delta})^2)} \\
&= \frac{1}{\frac{2}{(1-\frac{m_2-m_1}{2\delta})^2} - 1}
\end{aligned}
\tag{C.7}
$$

C.2 The WOR for Quadratic Membership Functions

The expression for two adjacent quadratic membership functions $\mu_1(x)$ and $\mu_2(x)$ are:

$$\mu_1(x) = 1 - (\frac{x - m_1}{\delta})^2 \tag{C.8}$$

$$\mu_2(x) = 1 - (\frac{x - m_2}{\delta})^2 \tag{C.9}$$

This can be shown in Figure (C.2).

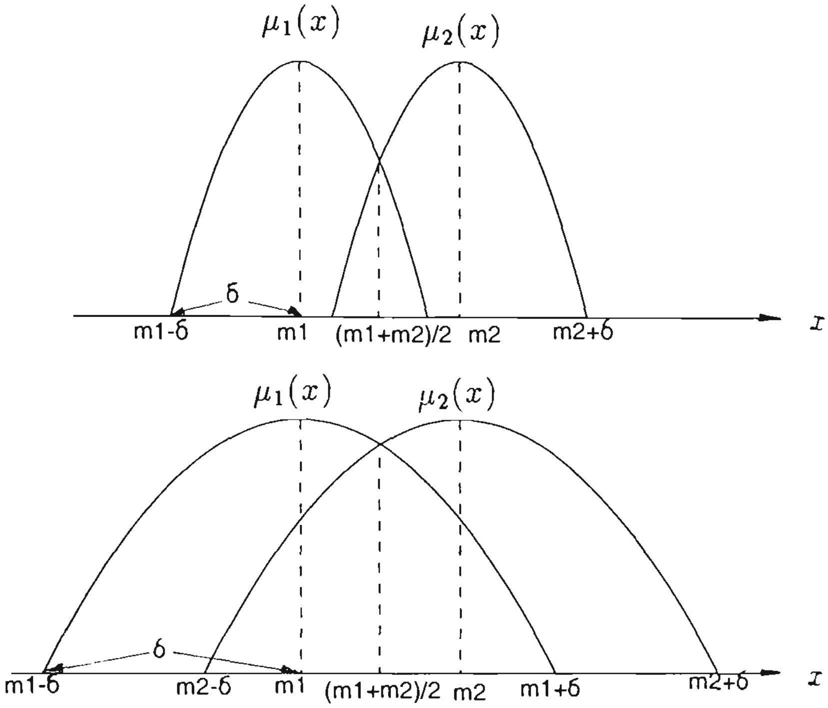

Figure C.2: Two adjacent quadratic membership functions

For the intersection area:

$$
\begin{aligned}
&\int_{-\infty}^{\infty} MIN(\mu_1(x), \mu_2(x))dx \\
&= 2 \times \int_{m_2-\delta}^{\frac{m_1+m_2}{2}} (1 - (\frac{x - m_2}{\delta})^2)dx \\
&= 2 \times \int_{-1}^{\frac{m_1-m_2}{2\delta}} (1 - y^2)\delta dy \\
&= 2 \times \delta \times (\frac{1}{3} \times (\frac{m_2 - m_1}{2\delta})^3 - \frac{m_2 - m_1}{2\delta} + \frac{2}{3})
\end{aligned}
\qquad (C.10)
$$

For the whole area:

$$
\begin{aligned}
&\int_{-\infty}^{\infty} MAX(\mu_1(x),\mu_2(x))dx \\
&= 2 \times \int_{\frac{m_1+m_2}{2}}^{m_2+\delta} (1-(\frac{x-m_2}{\delta})^2)dx \\
&= 2 \times \int_{\frac{m_1-m_2}{2\delta}}^{1} (1-y^2)\delta dy \\
&= 2 \times \delta \times (1-\frac{1}{3} \times (\frac{m_2-m_1}{2\delta})^3 + \frac{m_2-m_1}{2\delta} - \frac{1}{3})
\end{aligned}
\tag{C.11}
$$

The WOR for the two adjacent quadratic membership functions can be derived as:

$$
\begin{aligned}
WOR &= \frac{\int_{-\infty}^{\infty} MIN(\mu_1(x),\mu_2(x))dx}{\int_{-\infty}^{\infty} MAX(\mu_1(x),\mu_2(x))dx} \\
&= \frac{2 \times \delta \times (\frac{1}{3} \times (\frac{m_2-m_1}{2\delta})^3 - \frac{m_2-m_1}{2\delta} + \frac{2}{3})}{2 \times \delta \times (1-\frac{1}{3} \times (\frac{m_2-m_1}{2\delta})^3 + \frac{m_2-m_1}{2\delta} - \frac{1}{3})} \\
&= \frac{(\frac{1}{3} \times (\frac{m_2-m_1}{2\delta})^3 - \frac{m_2-m_1}{2\delta} + \frac{2}{3})}{(1-\frac{1}{3} \times (\frac{m_2-m_1}{2\delta})^3 + \frac{m_2-m_1}{2\delta} - \frac{1}{3})} \\
&= \frac{\frac{2}{3} - \frac{m_2-m_1}{2\delta} + \frac{1}{3}(\frac{m_2-m_1}{2\delta})^3}{\frac{2}{3} + \frac{m_2-m_1}{2\delta} - \frac{1}{3}(\frac{m_2-m_1}{2\delta})^3}
\end{aligned}
\tag{C.12}
$$

C.3 The WOR for Gaussian Membership Functions

The expression for two adjacent Gaussian (exponential) membership functions $\mu_1(x)$ and $\mu_2(x)$ are:

$$\mu_1(x) = e^{-(\frac{x-m_1}{\delta})^2} \tag{C.13}$$

$$\mu_2(x) = e^{-(\frac{x-m_2}{\delta})^2} \tag{C.14}$$

This can be shown in Figure (C.3).

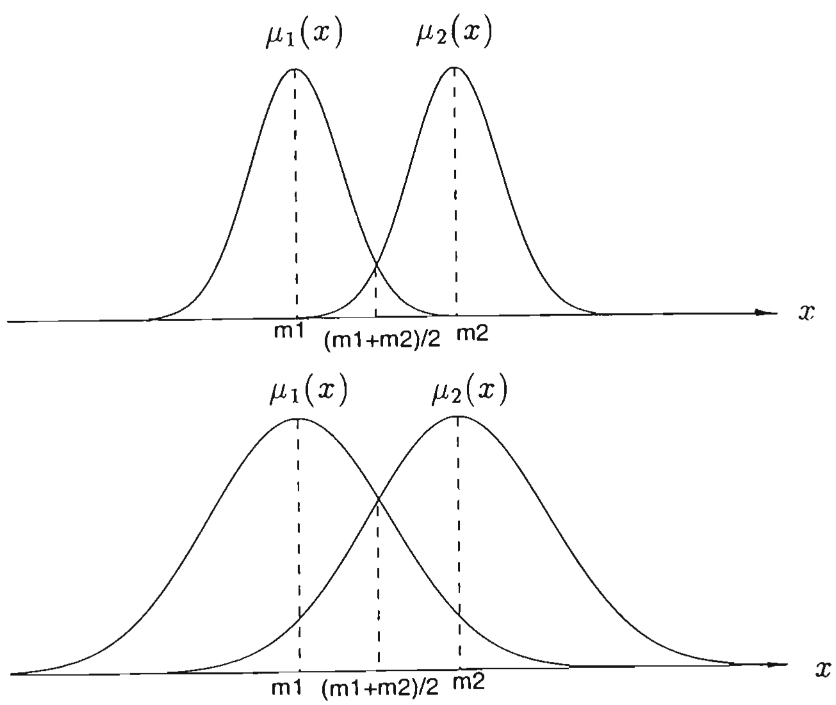

Figure C.3: Two adjacent exponential membership functions

$$M(x) = \int_{-\infty}^{x} e^{-(\frac{t-m}{\delta})^2} dt = \delta\sqrt{\pi} F(\frac{\sqrt{2}}{\delta}(x-m)) \tag{C.15}$$

For the intersection area:

$$\begin{aligned}
&\int_{-\infty}^{\infty} MIN(\mu_1(x), \mu_2(x))dx \\
&= 2 \times \int_{-\infty}^{\frac{m_1+m_2}{2}} e^{-(\frac{t-m_2}{\delta})^2} dt \\
&= 2 \times M_1(\frac{m_1+m_2}{2}) \\
&= 2 \times \delta \times \sqrt{\pi} F(\frac{\sqrt{2}}{\delta} \times \frac{m_1-m_2}{2}) \\
&= 2 \times \delta \times \sqrt{\pi} F(\sqrt{2} \times \frac{m_1-m_2}{2\delta})
\end{aligned} \tag{C.16}$$

For the whole area:

$$\begin{aligned}
&\int_{-\infty}^{\infty} MAX(\mu_1(x), \mu_2(x))dx \\
&= 2 \times \int_{-\infty}^{\frac{m_1+m_2}{2}} e^{-(\frac{t-m_1}{\delta}^2} dt \\
&= 2 \times \delta \times \sqrt{\pi} F(\sqrt{2} \times \frac{m_2-m_1}{2\delta})
\end{aligned} \tag{C.17}$$

The WOR for the two adjacent Gaussian membership functions can be derived as:

$$\begin{aligned}
WOR &= \frac{\int_{-\infty}^{\infty} MIN(\mu_1(x), \mu_2(x))dx}{\int_{-\infty}^{\infty} MAX(\mu_1(x), \mu_2(x))dx} \\
&= \frac{F(\sqrt{2} \times \frac{m_1 - m_2}{2\delta})}{F(\sqrt{2} \times \frac{m_2 - m_1}{2\delta})} \\
&= \frac{1 - F(\sqrt{2} \times \frac{m_2 - m_1}{2\delta})}{F(\sqrt{2} \times \frac{m_2 - m_1}{2\delta})} \\
&= \frac{1}{F(\sqrt{2} \times \frac{m_2 - m_1}{2\delta})} - 1
\end{aligned} \tag{C.18}$$

Appendix D

Mathematical Model for Multi-machine Power System

D.1 Statement of the Problem

The equations will be developed here is in the case where the loads are to be represented by constant impedances. The objective is to give a mathematical description of the multi-machine system with the load constraints included [Anderson, 1977].

For multi-machine system, each machine is described mathematically by a set of equations of the form

$$\dot{x} = f(x, v, T_m, t) \tag{D.1}$$

where x is a vector of state variables, v is a vector of voltages, and T_m is the mechanical torque. The dimension of the vector x depends on the model used. The order of x ranges from seventh order for the full model to second order for the classical model where only ω and δ are retained as the state variables.

For machine i the phasors $\bar{V}_i$ and $\bar{I}_i$ can be defined as

$$\bar{V}_i = V_{qi} + jV_{di} \qquad \bar{I}_i = I_{qi} + jI_{di} \tag{D.2}$$

where

$$V_{qi} \triangleq v_{qi}/\sqrt{3} \qquad V_{di} \triangleq v_{di}/\sqrt{3} \qquad I_{qi} \triangleq i_{qi}/\sqrt{3} \qquad I_{di} \triangleq i_{di}/\sqrt{3} \qquad \text{(D.3)}$$

and where the axis q_i is taken as the phasor reference in each case. Then the complex vectors $\bar{V}$ and $\bar{I}$ can be defined by

$$\bar{V} \triangleq \begin{bmatrix} V_{q1} + jV_{d1} \\ V_{q2} + jV_{d2} \\ \cdots \\ V_{qn} + jV_{dn} \end{bmatrix} = \begin{bmatrix} \bar{V}_1 \\ \bar{V}_2 \\ \cdots \\ \bar{V}_n \end{bmatrix} \qquad \bar{I} \triangleq \begin{bmatrix} I_{q1} + jI_{d1} \\ I_{q2} + jI_{d2} \\ \cdots \\ I_{qn} + jI_{dn} \end{bmatrix} = \begin{bmatrix} \bar{I}_1 \\ \bar{I}_2 \\ \cdots \\ \bar{I}_n \end{bmatrix} \qquad \text{(D.4)}$$

The voltage $\bar{V}_i$ and the current $\bar{I}_i$ are reffered to the q and d axes of machine i. In other words the different voltages and currents are expressed in terms of different reference frames. At steady state these currents and voltages can be represented by phasors to a common reference frame. To distinguish these phasors defined by (D.2), the symbols $\hat{I}_i$ and $\hat{V}_i$, $i = 1, 2 \cdots, n$ will be used to designate the use of a common frame of reference.

Similarly, the matrices $\hat{I}_i$ and $\hat{V}_i$ can be formed. From the network steady state equation

$$\hat{I} = \bar{Y}\hat{V} \qquad \text{(D.5)}$$

where

$$\hat{I} \triangleq \begin{bmatrix} \hat{I}_1 \\ \hat{I}_2 \\ \cdots \\ \hat{I}_n \end{bmatrix} \qquad \hat{V} \triangleq \begin{bmatrix} \hat{V}_1 \\ \hat{V}_2 \\ \cdots \\ \hat{V}_n \end{bmatrix} \qquad \text{(D.6)}$$

and $\bar{Y}$ is the short circuit admittance matrix of the network.

D.2 Conversion to a Common Reference Frame

To obtain general network relationships, it is desirable to express the various branch quantities to the same reference. Let us assume that we want to convert the phasor $\bar{V}_i = V_{qi} + jV_{di}$ to the common reference frame (moving at synchronous speed). Let the same voltage, expressed in the new notation, be $\hat{V}_i = V_{Qi} + jV_{Di}$ as shown in Figure (D.1)

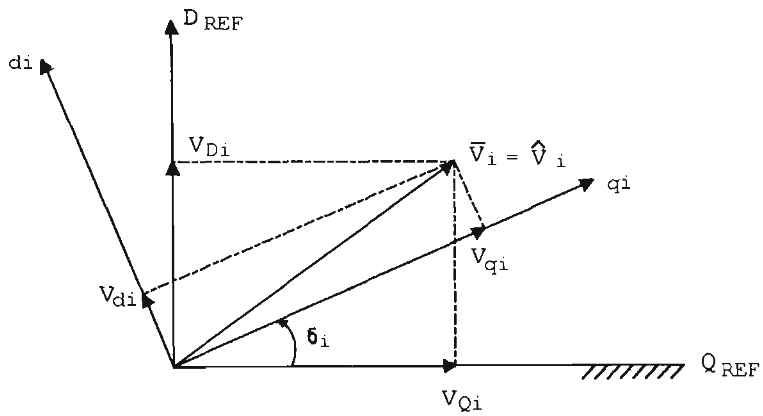

Figure D.1: Two frames of reference for phasor quantities for a voltage V_i

From Figure (D.1) it can be seen that

$$V_{Qi} + jV_{Di} = (V_{qi}cos\delta_i - V_{di}sin\delta_i) + j(V_{qi}sin\delta_i + V_{di}cos\delta_i)$$

$$or \qquad \hat{V}_i = \bar{V}_i e^{j\delta_i} \tag{D.7}$$

Convert network branch voltage drop equation to the system reference frame by using (D.7)

$$\hat{V}_k e^{-j\delta_i} = \bar{Z}_k \hat{I}_k e^{-j\delta_i}$$

$$or \qquad \hat{V}_k = \bar{Z}_k \hat{I}_k \qquad k = 1, 2, \cdots, b \tag{D.8}$$

Where b is the number of the network branches and impedance matrix $\bar{Z}_k$ is calculated based on rated angular speed.

Equation (D.8) can be expressed in matrix form

$$\hat{V}_b = \bar{z}_b \hat{I}_b \tag{D.9}$$

Where the subscript b is used to indicate a branch matrix. The inverse of the primitive branch matrix $\bar{Z}_b$ exists and is denoted by $\bar{Y}_b$, thus

$$\hat{I}_b = \bar{y}_b \hat{V}_b \tag{D.10}$$

Equation (D.10) is expressed in terms of the primitive admittance matrix of a passive network. From network theory the node incidence matrix A can be constructed which is used to convert (D.10) into a nodal admittance equation

$$\hat{I} = (A^t \bar{y}_b A)\hat{V} \triangleq \bar{Y}\hat{V} \tag{D.11}$$

Where $\bar{Y}$ is the matrix of short circuit driving point and transfer admittances and
$A = [a_{pq}] = 1$ if current in branch p leaves node q
$A = [a_{pq}] = -1$ if current in branch p enters node q
$A = [a_{pq}] = 0$ if branch p is not connected to node q
with $p = 1, 2, \cdots, b$ and $q = 1, 2, \cdots, n$.

Since $\bar{Y}^{-1} = \bar{Z}$ exists,

$$\hat{V} = \bar{Y}^{-1}\hat{I} = \bar{Z}\hat{I} \tag{D.12}$$

Where $\bar{Z}$ is the matrix of the open circuit driving point and transfer impedances of the network.

D.3 Conversion of Machine Coordinates to System Reference

Consider a voltage v_{abci} at node i. The Park's transformation can be applied to this voltage to obtain v_{dqi}. From (D.2) this voltage can be expressed in phasor notation as $\bar{V}_i$, using the rotor of machine i as reference. It can also be expressed to the system reference as $\hat{V}_i$, using the transformation of equation (D.7). Equation (D.7) can be generalised to include all the nodes. Let

$$T = \begin{bmatrix} e^{j\delta_1} & 0 & \cdots & 0 \\ 0 & e^{j\delta_2} & \cdots & 0 \\ \cdots & \cdots & \cdots & \cdots \\ 0 & 0 & \cdots & e^{j\delta_n} \end{bmatrix} \qquad \hat{V} = \begin{bmatrix} V_{Q1} + jV_{D1} \\ V_{Q2} + jV_{D2} \\ \cdots \\ V_{Qn} + jV_{Dn} \end{bmatrix} \qquad \bar{V} = \begin{bmatrix} V_{q1} + jV_{d1} \\ V_{q2} + jV_{d2} \\ \cdots \\ V_{qn} + jV_{dn} \end{bmatrix} \tag{D.13}$$

Then

$$\hat{V} = T\bar{V} \tag{D.14}$$

Thus T is a transformation that transforms the d and q quantities of all machines to the system frame, which is a common frame moving at synchronous speed. The transformation T is orthogonal, i.e.,

$$T^{-1} = T^* \tag{D.15}$$

Therefore, from equation (D.14) and equation (D.15)

$$\bar{V} = T * \hat{V} \tag{D.16}$$

Similarly for the node currents we get

$$\hat{I} = T\bar{I} \qquad \bar{I} = T * \hat{I} \tag{D.17}$$

The relation between machine currents and voltages is:

$$T\bar{I} = \bar{Y}T\bar{V} \tag{D.18}$$

Premultiplying equation (D.18) by T^{-1}

$$\bar{I} = T^{-1}\bar{Y}T\bar{V} = \bar{M}\bar{V} \tag{D.19}$$

Where

$$\bar{M} \triangleq (T^{-1}\bar{Y}T) \tag{D.20}$$

and if $\bar{M}^{-1}$ exists,

$$\bar{V} = (T^{-1}\bar{Y}T)^{-1}\bar{I} = (T^{-1}\bar{Z}T)\bar{I} \tag{D.21}$$

For a three-machine system, the matrix $\bar{Y}$ of the network is of the form

$$\bar{Y} = \begin{bmatrix} Y_{11}e^{j\theta_{11}} & Y_{12}e^{j\theta_{12}} & Y_{13}e^{j\theta_{13}} \\ Y_{21}e^{j\theta_{21}} & Y_{22}e^{j\theta_{22}} & Y_{23}e^{j\theta_{23}} \\ Y_{31}e^{j\theta_{31}} & Y_{32}e^{j\theta_{32}} & Y_{33}e^{j\theta_{33}} \end{bmatrix} \tag{D.22}$$

$$T = \begin{bmatrix} e^{j\delta_1} & 0 & 0 \\ 0 & e^{j\frac{\delta}{2}} & 0 \\ 0 & 0 & e^{j\delta_3} \end{bmatrix} \qquad T^{-1} = \begin{bmatrix} e^{-j\delta_1} & 0 & 0 \\ 0 & e^{-j\delta_2} & 0 \\ 0 & 0 & e^{-j\delta_3} \end{bmatrix} \tag{D.23}$$

$$\bar{Y}T = \begin{bmatrix} Y_{11}e^{j(\theta_{11}+\delta_1)} & Y_{12}e^{j(\theta_{12}+\delta_2)} & Y_{13}e^{j(\theta_{13}+\delta_3)} \\ Y_{21}e^{j(\theta_{21}+\delta_1)} & Y_{22}e^{j(\theta_{22}+\delta_2)} & Y_{23}e^{j(\theta_{23}+\delta_3)} \\ Y_{31}e^{j(\theta_{31}+\delta_1)} & Y_{32}e^{j(\theta_{32}+\delta_2)} & Y_{33}e^{j(\theta_{33}+\delta_3)} \end{bmatrix} \tag{D.24}$$

$$T^{-1}\bar{Y}T \triangleq \bar{M} = \begin{bmatrix} Y_{11}e^{j\theta_{11}} & Y_{12}e^{j(\theta_{12}-\delta_{12})} & Y_{13}e^{j(\theta_{13}-\delta_{13})} \\ Y_{21}e^{j(\theta_{21}-\delta_{21})} & Y_{22}e^{j\theta_{22}} & Y_{23}e^{j(\theta_{23}-\delta_{23})} \\ Y_{31}e^{j(\theta_{31}-\delta_{31})} & Y_{32}e^{j(\theta_{32}-\delta_{32})} & Y_{33}e^{j\theta_{33}} \end{bmatrix} \quad (D.25)$$

D.4 Linearised Model for the Network

From equation (D.14) $\hat{V} = T\bar{V}$, where T is defined by equation (D.23) and $\bar{V}$ and $\hat{V}$ are defined by equations (D.4), (D.6) and also from (D.19) $\bar{I} = \bar{M}\bar{V}$, where $\bar{M}$ is given by equation (D.20). Linearising equation (D.19)

$$\bar{I}_{\Delta} = \bar{M}_0\bar{V}_{\Delta} + \bar{M}_{\Delta}\bar{V}_0 \quad (D.26)$$

Where $\bar{M}_0$ is evaluated at the initial angles $\delta_{io}, i = 1, 2, \cdots, n$, and $\bar{V}_0$ is the initial value of the vector $\bar{V}$. Let $\delta_i = \delta_{io} + \delta_{i\Delta}$. Then the matrix $\bar{M}$ becomes

$$\bar{M} := \begin{bmatrix} Y_{11}e^{j\theta_{11}} & Y_{12}e^{j(\theta_{12}-\delta_{120}-\delta_{12\Delta})} & Y_{13}e^{j(\theta_{13}-\delta_{130}-\delta_{13\Delta})} \\ Y_{21}e^{j(\theta_{21}-\delta_{210}-\delta_{21\Delta})} & Y_{22}e^{j\theta_{22}} & Y_{23}e^{j(\theta_{23}-\delta_{230}-\delta_{23\Delta})} \\ Y_{31}e^{j(\theta_{31}-\delta_{310}-\delta_{31\Delta})} & Y_{32}e^{j(\theta_{32}-\delta_{320}-\delta_{32\Delta})} & Y_{33}e^{j\theta_{33}} \end{bmatrix} \quad (D.27)$$

The general term $\bar{m}_{ij}$ of the matrix $\bar{M}$ is of the form$Y_{ij}e^{j(\theta_{ij}-\delta_{ij0}-\delta_{ij\Delta})}$, thus

$$\bar{m}_{ij} = Y_{ij}e^{j(\theta_{ij}-\delta_{ij0})}e^{-j\delta_{ij\Delta}} \quad (D.28)$$

using the relation $\delta_{ij\Delta} \cong 1, sin\delta_{ij\Delta} \cong \delta_{ij\Delta}$, the general term can be obtained:

$$\bar{m}_{ij} \cong Y_{ij}e^{j(\theta_{ij}-\delta_{ij0})}(1 - j\delta_{ij\Delta}) \quad (D.29)$$

The general term in $\bar{M}_\Delta$ is given by

$$\bar{m}_{ij\Delta} \cong -jY_{ij}e^{j(\theta_{ij}-\delta_{ij0})}\delta_{ij\Delta} \tag{D.30}$$

$$\bar{M}_\Delta \bar{V}_0 =$$

$$-j\begin{bmatrix} 0 & Y_{12}e^{j(\theta_{12}-\delta_{120})}\delta_{12\Delta} & Y_{13}e^{j(\theta_{13}-\delta_{130})}\delta_{13\Delta} \\ Y_{21}e^{j(\theta_{21}-\delta_{210})}\delta_{21\Delta} & 0 & Y_{23}e^{j(\theta_{23}-\delta_{230})}\delta_{23\Delta} \\ Y_{31}e^{j(\theta_{31}-\delta_{310})}\delta_{31\Delta} & Y_{32}e^{j(\theta_{32}-\delta_{320})}\delta_{32\Delta} & 0 \end{bmatrix}\begin{bmatrix}\bar{V}_{10}\\ \bar{V}_{20}\\ \bar{V}_{30}\end{bmatrix} \tag{D.31}$$

$$\bar{M}_\Delta \bar{V}_0 = -j\begin{bmatrix} \sum_{k=1}^{3} Y_{1k}e^{j(\theta_{1k}-\delta_{1k0})}\bar{V}_{k0}\delta_{1k\Delta} \\ \sum_{k=1}^{3} Y_{2k}e^{j(\theta_{2k}-\delta_{2k0})}\bar{V}_{k0}\delta_{2k\Delta} \\ \sum_{k=1}^{3} Y_{3k}e^{j(\theta_{3k}-\delta_{3k0})}\bar{V}_{k0}\delta_{3k\Delta} \end{bmatrix} \tag{D.32}$$

and the linearised equation (D.27) becomes

$$\begin{bmatrix} I_{1\Delta}\\ I_{2\Delta}\\ I_{3\Delta}\end{bmatrix} = \begin{bmatrix} Y_{11}e^{j\theta_{11}} & Y_{12}e^{j(\theta_{12}-\delta_{120})} & Y_{13}e^{j(\theta_{13}-\delta_{130})} \\ Y_{21}e^{j(\theta_{21}-\delta_{210})} & Y_{22}e^{j\theta_{22}} & Y_{23}e^{j(\theta_{23}-\delta_{230})} \\ Y_{31}e^{j(\theta_{31}-\delta_{310})} & Y_{32}e^{j(\theta_{32}-\delta_{320})} & Y_{33}e^{j\theta_{33}} \end{bmatrix}\begin{bmatrix}\bar{V}_{10}\\ \bar{V}_{20}\\ \bar{V}_{30}\end{bmatrix}$$
$$-j\begin{bmatrix} \sum_{k=1}^{3} Y_{1k}e^{j(\theta_{1k}-\delta_{1k0})}\bar{V}_{k0}\delta_{1k\Delta} \\ \sum_{k=1}^{3} Y_{2k}e^{j(\theta_{2k}-\delta_{2k0})}\bar{V}_{k0}\delta_{2k\Delta} \\ \sum_{k=1}^{3} Y_{3k}e^{j(\theta_{3k}-\delta_{3k0})}\bar{V}_{k0}\delta_{3k\Delta} \end{bmatrix} \tag{D.33}$$

Let $T = T_0 + T_\Delta$ to compute

$$T_\Delta = jT_0\delta_\Delta \qquad \delta_\Delta \stackrel{\Delta}{=} diag(\delta_{1\Delta}, \delta_{2\Delta}, \delta_{3\Delta}) \tag{D.34}$$

$$\bar{M}_\Delta = -j({T_0}^{-1}\delta_\Delta\bar{Y}T_0 - {T_0}^{-1}\bar{Y}T_0\delta_\Delta) \tag{D.35}$$

$$T_0{}^{-1}\bar{Y}T_0\delta_\Delta = \begin{bmatrix} Y_{11}e^{j\theta_{11}} & Y_{12}e^{j(\theta_{12}-\delta_{120})} & Y_{13}e^{j(\theta_{13}-\delta_{130})} \\ Y_{21}e^{j(\theta_{21}-\delta_{210})} & Y_{22}e^{j\theta_{22}} & Y_{23}e^{j(\theta_{23}-\delta_{230})} \\ Y_{31}e^{j(\theta_{31}-\delta_{310})} & Y_{32}e^{j(\theta_{32}-\delta_{320})} & Y_{33}e^{j\theta_{33}} \end{bmatrix} \begin{bmatrix} \delta_{1\Delta} & 0 & 0 \\ 0 & \delta_{2\Delta} & 0 \\ 0 & 0 & \delta_{3\Delta} \end{bmatrix}$$
$$= \bar{M}_0\delta_\Delta \tag{D.36}$$

$$T_0{}^{-1}\delta_\Delta\bar{Y}T_0 = \begin{bmatrix} Y_{11}e^{j\theta_{11}}\delta_{1\Delta} & Y_{12}e^{j(\theta_{12}-\delta_{120})}\delta_{1\Delta} & Y_{13}e^{j(\theta_{13}-\delta_{130})}\delta_{1\Delta} \\ Y_{21}e^{j(\theta_{21}-\delta_{210})}\delta_{2\Delta} & Y_{22}e^{j\theta_{22}}\delta_{2\Delta} & Y_{23}e^{j(\theta_{23}-\delta_{230})}\delta_{2\Delta} \\ Y_{31}e^{j(\theta_{31}-\delta_{310})}\delta_{3\Delta} & Y_{32}e^{j(\theta_{32}-\delta_{320})}\delta_{3\Delta} & Y_{33}e^{j\theta_{33}}\delta_{3\Delta} \end{bmatrix}$$
$$= \delta_\Delta\bar{M}_0 \tag{D.37}$$

$$\bar{M}_\Delta = -j[\delta_\Delta\bar{M}_0 - \bar{M}_0\delta_\Delta] \tag{D.38}$$

$$\bar{I}_\Delta = \bar{M}_0\bar{V}_\Delta - j[\delta_\Delta\bar{M}_0 - \bar{M}_0\delta_\Delta]\bar{V}_0 \tag{D.39}$$

$$\begin{bmatrix} I_{1\Delta} \\ I_{2\Delta} \\ I_{3\Delta} \end{bmatrix} =$$

$$\begin{bmatrix} Y_{11}e^{j\theta_{11}} & Y_{12}e^{j(\theta_{12}-\delta_{120})} & Y_{13}e^{j(\theta_{13}-\delta_{130})} & -j\bar{V}'_{20}Y_{12}e^{j(\theta_{12}-\delta_{120})} & -j\bar{V}'_{30}Y_{13}e^{j(\theta_{13}-\delta_{130})} & 0 \\ Y_{21}e^{j(\theta_{21}-\delta_{210})} & Y_{22}e^{j\theta_{22}} & Y_{23}e^{j(\theta_{23}-\delta_{230})} & j\bar{V}'_{10}Y_{21}e^{j(\theta_{21}-\delta_{210})} & 0 & -j\bar{V}'_{30}Y_{23}e^{j(\theta_{23}-\delta_{230})} \\ Y_{31}e^{j(\theta_{31}-\delta_{310})} & Y_{32}e^{j(\theta_{32}-\delta_{320})} & Y_{33}e^{j\theta_{33}} & 0 & j\bar{V}'_{10}Y_{31}e^{j(\theta_{31}-\delta_{310})} & j\bar{V}'_{20}Y_{32}e^{j(\theta_{32}-\delta_{320})} \end{bmatrix}$$

$$\begin{bmatrix} \bar{V}'_{1\Delta} \\ \bar{V}'_{2\Delta} \\ \bar{V}'_{3\Delta} \\ \delta_{12\Delta} \\ \delta_{13\Delta} \\ \delta_{23\Delta} \end{bmatrix} \qquad \text{(D.40)}$$

D.5 Generator Equations

Generator 2 and 3 (two-axis model) (the subscript Δ is omitted, generator 1 has been treated as infinite bus in this case)

$$\tau'_{q0i}\dot{E}_{di}{}' = -E'_{di} - (x_{qi} - x'_{di})I_{qi}$$

$$\tau'_{d0i}\dot{E}_{qi}{}' = -E_{FDi} - E'_{qi} + (x_{di} - x'_{di})I_{di}$$

$$\tau_{ji}\dot{\omega}_i = T_{mi} - D_i\omega_i - I_{di0}E'_{di} - I_{qi0}E'_{qi} - E'_{di0}I_{di} - E'_{qi0}I_{qi}$$

$$\dot{\delta}_{1i} = \omega_1 - \omega_i, \quad i = 2, 3 \qquad \text{(D.41)}$$

Appendix E

The Input FPL File and the Generated Rule Base

E.1 The Input FPL File

```
PROJECT FLC
VAR aSpeed
    TYPE float
    MIN -100
    MAX 100
    MEMBER NB
    POINTS -100,1, -75, 1, -50,0
    END
    MEMBER NM
    POINTS -75,0, -50, 1, -25, 0
    END
    MEMBER NS
    POINTS -50,0, -25, 1, 0, 0
    END
    MEMBER Z
    POINTS -25,0, 0, 1, 25, 0
```

```
    END
    MEMBER PS
    POINTS 0,0, 25, 1, 50, 0
    END
    MEMBER PM
    POINTS 25,0, 50, 1, 75, 0
    END
    MEMBER PB
    POINTS 50,0, 75, 1, 100,1
    END
END
END /* Speed definition */
VAR bAcceleration
    TYPE float
    MIN -1500
    MAX 1500
    MEMBER NB
    POINTS -1500,1, -1125, 1, -750,0
    END
    MEMBER NM
    POINTS -1125,0, -750, 1, -375, 0
    END
    MEMBER NS
    POINTS -750,0, -375, 1, 0, 0
    END
    MEMBER Z
    POINTS -375,0, 0, 1, 375, 0
    END
    MEMBER PS
    POINTS 0,0, 375, 1, 750, 0
    END
    MEMBER PM
```

```
    POINTS 375,0, 750, 1, 1125, 0
    END
    MEMBER PB
    POINTS 750,0, 1125, 1, 1500,1
    END
END
END /* Acceleration definition */
VAR Control
    TYPE float
    MIN -800
    MAX 800
    MEMBER NB
    POINTS -800,1, -600, 1, -400,0
    END
    MEMBER NM
    POINTS -600,0, -400, 1, -200, 0
    END
    MEMBER NS
    POINTS -400,0, -200, 1, 0, 0
    END
    MEMBER Z
    POINTS -200,0, 0, 1, 200, 0
    END
    MEMBER PS
    POINTS 0,0, 200, 1, 400, 0
    END
    MEMBER PM
    POINTS 200,0, 400, 1, 600, 0
    END
    MEMBER PB
    POINTS 400,0, 600, 1, 800,1
    END
```

```
END
END /* Control signal definition */
FUZZY FLC-control
END /* Fuzzy rule base definition */
CONNECT
    FROM aSpeed
    To FLC-control
END
CONNECT
    FROM bAcceleration
    To FLC-control
END
CONNECT
    FROM FLC-control
    To Control
END
END /* of PROJECT FLC definition * /
```

E.2 The Generated Rule Base

```
RULE Rule0000
     OPTIONS
     ENABLE="ON"
     END
     IF (aSpeed IS NB) AND (bAcceleration IS NS) THEN
        Control=NB
END
RULE Rule0001
     OPTIONS
     ENABLE="ON"
```

```
        END
        IF (aSpeed IS NB) AND (bAcceleration IS Z) THEN
            Control=NB
END
RULE Rule0002
        OPTIONS
        ENABLE="ON"
        END
        IF (aSpeed IS NM) AND (bAcceleration IS NS) THEN
            Control=NM
END
RULE Rule0003
        OPTIONS
        ENABLE="ON"
        END
        IF (aSpeed IS NM) AND (bAcceleration IS Z) THEN
            Control=NM
END
RULE Rule0004
        OPTIONS
        ENABLE="ON"
        END
        IF (aSpeed IS NM) AND (bAcceleration IS PS) THEN
            Control=NS
END
RULE Rule0005
        OPTIONS
        ENABLE="ON"
        END
        IF (aSpeed IS NS) AND (bAcceleration IS NM) THEN
            Control=NB
END
```

```
RULE Rule0006
        OPTIONS
        ENABLE="ON"
        END
        IF (aSpeed IS NS) AND (bAcceleration IS NS) THEN
            Control=NM
END
RULE Rule0007
        OPTIONS
        ENABLE="ON"
        END
        IF (aSpeed IS NS) AND (bAcceleration IS Z) THEN
            Control=NS
END
RULE Rule0008
        OPTIONS
        ENABLE="ON"
        END
        IF (aSpeed IS NS) AND (bAcceleration IS PS) THEN
            Control=Z
END
RULE Rule0009
        OPTIONS
        ENABLE="ON"
        END
        IF (aSpeed IS NS) AND (bAcceleration IS PM) THEN
            Control=PS
END
RULE Rule0010
        OPTIONS
        ENABLE="ON"
        END
```

```
        IF (aSpeed IS Z) AND (bAcceleration IS NM) THEN
            Control=NM
END
RULE Rule0011
        OPTIONS
        ENABLE="ON"
        END
        IF (aSpeed IS Z) AND (bAcceleration IS NS) THEN
            Control=NM
END
RULE Rule0012
        OPTIONS
        ENABLE="ON"
        END
        IF (aSpeed IS Z) AND (bAcceleration IS Z) THEN
            Control=Z
END
RULE Rule0013
        OPTIONS
        ENABLE="ON"
        END
        IF (aSpeed IS Z) AND (bAcceleration IS PS) THEN
            Control=PM
END
RULE Rule0014
        OPTIONS
        ENABLE="ON"
        END
        IF (aSpeed IS Z) AND (bAcceleration IS PM) THEN
            Control=PM
END
RULE Rule0015
```

```
        OPTIONS
        ENABLE="ON"
        END
        IF (aSpeed IS PS) AND (bAcceleration IS NM) THEN
            Control=NS
END
RULE Rule0016
        OPTIONS
        ENABLE="ON"
        END
        IF (aSpeed IS PS) AND (bAcceleration IS NS) THEN
            Control=Z
END
RULE Rule0017
        OPTIONS
        ENABLE="ON"
        END
        IF (aSpeed IS PS) AND (bAcceleration IS Z) THEN
            Control=PS
END
RULE Rule0018
        OPTIONS
        ENABLE="ON"
        END
        IF (aSpeed IS PS) AND (bAcceleration IS PS) THEN
            Control=PM
END
RULE Rule0019
        OPTIONS
        ENABLE="ON"
        END
        IF (aSpeed IS PS) AND (bAcceleration IS PM) THEN
```

```
        Control=PB
END
RULE Rule0020
    OPTIONS
    ENABLE="ON"
    END
    IF (aSpeed IS PM) AND (bAcceleration IS NS) THEN
        Control=Z
END
RULE Rule0021
    OPTIONS
    ENABLE="ON"
    END
    IF (aSpeed IS PM) AND (bAcceleration IS Z) THEN
        Control=PM
END
RULE Rule0022
    OPTIONS
    ENABLE="ON"
    END
    IF (aSpeed IS PM) AND (bAcceleration IS PS) THEN
        Control=PM
END
RULE Rule0023
    OPTIONS
    ENABLE="ON"
    END
    IF (aSpeed IS PM) AND (bAcceleration IS PM) THEN
        Control=PB
END
```

Appendix F

Bibliography

Bibliography

[Adkins, 1975] Adkins,B., "*The general theory of alternating current machines: application to practical problems*", Chapman and Hall, London,1975.

[Anderson, 1977] Anderson,P.M. and Fouad,A.A. "*Power System Control and Stability*". Iowa State University Press, Ames, Iowa, 1977.

[Arnautovic, 1987] Arnautovic, D., and Medanic, J., "Design of Decentralized Multivariable Excitation Controllers in Multimachine Power Systems by Projective Controls. " *IEEE Transactions on Energy Conversion, Vol. EC-2, No.4, pp. 598-604*, 1987.

[Astrom, 1986] Astrom, K., Anton, J.G., and Arzen, K.E., "Expert Control", *Automatica, Vol. 13, pp. 277-286*, 1986.

[Baldwin, 1980] Baldwin, J.F., and Pilsworth, B.W., "Axiomatic Approach to Implication for Approximate Reasoning with Fuzzy Logic, " *Fuzzy Sets Syst., Vol. 3, pp. 193-219*, 1980.

[Bayne, 1977] Bayne,J.P., Lee,D.C., and Watson, W., "A Power System Stabilizer for Thermal Units Based on Derivation of Accelerating Power", *IEEE Trans. Power Apparatus and Systems, PAS-96, No.6, pp.1777-1783*, November/December 1977.

[Bollinger, 1975] Bollinger, K., Laha, A., Hamilton, R. and Harras, T. "Power Stabilizer Design Using Root Locus Methods ". *IEEE Transactions on Power Apparatus Systems, Vol. PAS-94, No.5, pp.1484-1488*, September/October 1975.

[Bollinger, 1990] Bollinger, K.E., and Gu, W., "A Comparison of Rotor Damping from Adaptive and Conventional PSS in a Multi-machine Power System", *IEEE Trans. Energy Conversion, EC-5(3), pp. 453-461*, September 1990.

[Bolden, 1982] Bolden, R.L., Walace, P.J., and Grainger, A.W. "Considerations in the Improvement of System Damping on the South East Australian Interconnected System ". *CIGRE paper 31-05*, 1975.

[Byerly, 1967] Byerly, R.T., Skooglund, J.W., and Keay, F.W. "Control of generator excitation for improved power system stability". *Proc. Am. Power Conf. 29, pp.1011-1022*, 1967.

[Chalam, 1987] Chalam, V.V., *Adaptive Control Systems-Techniques and Applications*, Marcel Dekker Inc., New York and Basel, 1987.

[Chan, 1983] Chan, W.C. and Hsu, Y.Y. " An Optimal Variable Structure Stabilizer for Power System Stabilization ". *IEEE Trans. on Power Apparatus and Systems, Vol. PAS-102, No.6, pp. 1738-1746*, June 1983.

[Chandra, 1987] Chandra, A., Malik, O.P., and Hope, G.S., "A Self-tuning Controller for the Control of Multi-machine Power Systems", *IEEE/PES 1987 Summer Meeting, 87 SM 452-6 PWRS*, July 1987.

[Chandra, 1988] Chandra, A., Malik, O.P., and Hope, G.S. "A self-tuning Controller for the control of Multi-machine Power Systems ", *IEEE Trans. on Power Systems, Vol.3, No.3, pp. 1065-1071*, August 1988.

[Cheng, 1986a] Cheng, S.J., Chow, Y.S., Malik, O.P., and Hope, G.S. " An Adaptive Synchronous Machine Stabilizer". *IEEE Trans. PWRS-1(3), pp. 101-109*, 1986

[Cheng, 1986b] Cheng, S.J., Malik, O.P. and Hope, G.S. "Self-tuning Stabiliser for a Multimachine Power System ". *IEE Proceedings Vol. 133, Pt. C, No.4, pp. 176-185*, May 1986.

[Cheng, 1988] Cheng, S.J., Malik, O.P., and Hope, G.S., "Damping of Multi-modal Oscillations in Power Systems Using a Dual-rate Adaptive Stabilizer", *IEEE Trans. Power Systems, PWRS-3(1), pp.101-108*, February 1988.

[Chow, 1989] Chow, J.H. and Sanchez-Gasca, J.J. "Pole-placement Designs of Power System Stabilizers ". *IEEE Transactions on Power Systems, Vol.4, No.1, pp.271-277*, February 1989.

[Concordia, 1944] Concordia,C. "Steady state stability of synchronous machines as affected by voltage regulator characteristics", *AIEE Trans. PAS-63, pp.215-220*, 1944.

[Crarg, 1950] Crarg S.B. "Long distance power transmission". *AIEE Trans. (Pt.2), pp.834-844*, 1950.

[Crusca, 1991] Crusca, F., and Aldeen, M. "Multivariable Frequency-domain Techniques for the Systematic Design of Stabilizers for Large-Scale Power Systems". *IEEE Transactions on Power Systems, Vol.6, No.3, pp.1133-1139*, August 1991.

[Dandeno, 1968] Dandeno, P.L., Karas, A.N., $M_c clymont$, K.R., and Watson, W. "Effect of high speed rectifier excitation systems on generator stability limites". *IEEE Trans. PAS-87, pp.190-201*, 1968.

[DeMello, 1969] DeMello, F.P., and Concordia, C. "Concepts of synchronous machine stability as affected by excitation control". *IEEE Trans. PAS-88, pp.316-329*, 1969.

[DeMello, 1978] DeMello,F.P.,Hannett,L.N.,and Undrill, J.M., "Practical Approaches to Supplementary Stabilizing from Accelerating Power ", *IEEE Trans. Power Apparatus and Systems, PAS-97, No.5, pp.1515-1522*, September/October 1978.

[DeMello, 1982] DeMello, F.P., Hannett, L.N., Parkinson, D.W., and Czuba, J.S. "A Power System Stabilizer Design Using Digital Control ". *IEEE Transactions on Power System Apparatus and Systems, Vol. PAS-101, No.8, pp.2860-2868*, August 1982.

[Driankov, 1993] Driankov, D., Hellendoorn, H., and Reinfrank, M., *An Introduction to Fuzzy Control*, Springer-Verlag Berlin Heidelberg, 1993.

[Efsfathiou, 1988] Efsfathiou, J., "Expert Systems, Fuzzy Logic and Rule Based Control Explained at last", *Trans. Inst. MC. Vol.10, No 4, pp.198-206*, 1988.

[Ellis, 1966] Ellis, H.M., Hardy, J.E., Blythe, A.L., and Skooglund, J.W. "Dynamic stability of the Peace River transmission system. *IEEE Trans. PAS-85, pp. 586-600*, 1966.

[El-sherbiny, 1971] El-sherbiny, M.K., and Fouad, A. " Digital Analysis of Excitation Control for Interconnected Systems". *IEEE Trans., Vol. PAS-90, No.2, pp.441-447*, March/April 1971.

[El-sherbiny, 1973] El-sherbiny, M.K., and Mehta, D.M. " Dynamic System Stability, Part I-Investigation of the Effect of Different Loading and Excitation Systems ". *IEEE Trans., PAS-92, pp.1538-1546*, September/October 1973.

[Fan, 1990] Fan, J.Y., Ortmeyer, T.H., and Mukundan, R., "Power System Stability Improvement with Multivariable Self-tuning Control", *IEEE Trans. Power Systems, PWRS-5(1), pp.227-234*, February 1990.

[Flming, 1981] Fleming, R.J., Parvatisam, K. "Selection of Parameters of Stabilisers in Multimachine Power Systems ". *IEEE Trans. Vol. PAS-100, No.5, pp.2329-2333*, 1981.

[Fujitec, 1988] Fujitec, F., "FLEX-8800 Series Elevator Group Control System,"*Fujitec Co., Ltd., Osaka, Japan*, 1988.

[Fukuda, 1992] Fukuda, T., and Shibata, T. "Theory and Applications of Neural Networks for Industrial Control Systems". *IEEE Transactions on Industrial Electronics, Vol. 39, No. 6, pp. 472-489*, December 1992.

[Gerheart, 1971] Gerheart, A.D., Hilllesland, Jr,T., Luini, J.F., and Rockfield, Jr, M.L. "Power system stabilizer: Field Testing and Digital Simulation". *IEEE Trans, PAS-90, pp. 2095-2100*, 1971.

[Ghandakly, 1987a] Ghandakly, A., and Kronegger, P. " Digital Controller Design Method for Synchronous Generator Excitation and Stabilizer Systems, Part I: Methodology and Computer Simulation ". *IEEE Transactions on Power Systems ". Vol. PWS-2, No.3, pp.633-637*, August 1987.

[Ghandakly, 1987b] Ghandakly, A., and Kronegger, P. " Digital Controller Design Method for Synchronous Generator Excitation and Stabilizer Systems, Part II:" Hardware/Software Design and Implementation Results ". *IEEE Transactions on Power Systems ". Vol. PWS-2, No.3, pp.638-644*, August 1987.

[Ghandakly, 1990] Ghandakly, A., and Idowu, P., "Design of a Model Reference Adaptive Stabilizer for the Exciter and Governor Loops of Power Generators", *IEEE Trans. Power Systems, PWRS-5(3), pp.887-893*, August 1990.

[Ghosh, 1984] Ghosh, A., Ledwich, G., Malik, O.P., and Hope, G.S. "Power System Stabilizer Based on Adaptive Control Techniques". *IEEE Trans. Power Apparatus and Systems, PAS-103, pp.1983-1989*, August 1984.

[Ghosh,1985] Ghosh, A., Ledwich, G., Hope, G.S., and Malik, O.P., "Power System Stabilizer for Large Disturbances", *IEE Proc., 132, Pt. C(1), pp.14-19*, January 1985.

[Gibbard, 1991] Gibbard, Michael J. "Robust Design of Fixed Parameter Power System Stabilizers Over a Wide Range of Operating Conditions " *IEEE Transactions on Power Systems, Vol.6, No.2, pp.794-800*, May 1991.

[Gu, 1989] Gu, W., and Bollinger, K.E., " A Self-tuning Power System Stabilizer for Wide-range Synchronous Generator Operation", *IEEE Trans. Power Systems, PWRS-4(3), pp. 1191-1199*, August 1989.

[Gupta, 1977] Gupta, M.M., Saridis, G.N., and Gaines, B.R., *Fuzzy Automata and Decision Processes*, New York, North-Holland Inc. (eds), 1977.

[Hanson, 1968] Hanson, O.W., Goodwin, C.J., and Dandeno, P.L. "Influence of excitation and speed control parameters in stabilizing intersystem oscillations". *IEEE Trans. PAS-87, pp. 1306-1313*, 1968.

[Harris, 1985] Harris, C.J., and Billings, S.A., *Self-Tuning and Adaptive Control: Theory and Applications.* Peter Peregrinus, Stevenage, 2nd Edition, 1985.

[Harris, 1989a] Harris, C.J., and Moore, C.G., "Intelligent Identification and Control for Autonomous Guided Vehicles Using Adaptive Fuzzy Based Algorithms", *Eng. Applic. of AI, Vol.2, pp. 267-285*, 1989.

[Harris, 1989b] Harris, C.J., and Moore, C.G., "Fuzzy Adaptive Controllers with PID Fine Control", *MARDI Research Rept. No.13, Southampton University, Aero and Astro Dept. 17p*, 1989.

[Hassan, 1991] Hassan, M.A.M, Malik, O.P., and Hope, G.S. "A Fuzzy Logic Based Stabilizer for a Synchronous Machine ". *IEEE Trans. on Energy Conversion, Vol.6, No.3, pp. 407-413*, 1991.

[Hassan, 1992] Hassan, M.A.M., Malik, O.P., and Hope, G.S.:'A Fuzzy Logic Based Self-Tuned Power System Stabilizer', *Third International Conference on Power System Monitoring and Control (Conference Publ. No. 336) pp.146-151*, 1992.

[Hassan, 1993a] Hassan, M.A.M., Malik, O.P. " Laboratory Evaluation and Test Results for Rule-based and Fuzzy Logic-based Power System Stabilizers: A Comparative Study ". *IEE Intelligent Systems Engineering, Vol.2, No.1, pp.52-60*, Spring 1993.

[Hassan, 1993b] Hassan, M.A.M., and Malik, O.P., "Implementation and Laboratory Test Results for a Fuzzy Logic Based Self-tuned Power System Stabilizer", *IEEE Transactions on Energy Conversion, Vol. 8, No. 2, pp.221-228*, 1993.

[Hayes, 1973] Hayes, D.R., and Craythorn, G.E. "Modelling and Testing of Valley Steam Plant Supplemental Excitation Control System". *IEEE Trans. PAS-92*, pp. 464-470, 1973.

[Heffron, 1952] Heffron, W.G., Phillips, R.A., "Effect of modern amplidyne voltage regulators on underexcited operation of large turbine generators ", *AIEE*

Transactions on Power Apparatus and Systems, Vol. PAS-71, pp. 692-697, August 1952.

[Hiyama, 1989] Hiyama, T. "Application of Rule-based Stabilizing Controller to Electrical Power System". *IEE Proc. C, Vol.136, No.3, pp.175-181*, 1989.

[Hiyama, 1990] Hiyama, T."Rule-Based Stabilizer for Multi-Machine Power System". *IEEE Trans. on Power Systems, Vol.5,No.2,pp. 403-411*, 1990.

[Hiyama, 1991] Hiyama, T., and Sameshima, T. "Fuzzy Logic Control Scheme for On-line Stabilization of Multimachine Power System". *Fuzzy Sets and Systems 39, pp. 181-194*, 1991.

[Hsu, 1983] Hsu, Y.Y., Chan, W.C., " Stabilization of Power Systems Using Variable Structure Stabilizer ". *J. Ele. Pow. Sys. Res, Vol.6, No.2*, April, 1983.

[Hsu, 1986] Hsu, Y.Y., Chan, W.C., "Application of Sliding Modes to Digital Power System Stabilizer Design", *Electr. Mach. Power Syst., Vol.11, pp.171-184*, 1986.

[Hsu, 1987] Hsu, Y.Y., and Liou, K.L. "Design of Self-tuning PID Power System Stabilizer for Synchronous Generator". *IEEE Trans., EC-2, pp.343-348*, 1987.

[Hsu, 1990] Hsu, Y. Cheng, C. "Design of Fuzzy Power System Stabilisers for Multimachine Power Systems". *IEE Proc. C, Vol.137, No.3, pp. 233-238*,May 1990.

[Ibrahim, 1989a] Ibrahim, A.S., Hogg, B.W., and Sharaf, M.M., " Self-tuning Controllers for Turbogenerator Excitation and Governing Systems", *IEE Proc., 136, Pt. D(5), pp.238-251*, September 1989.

[Ibrahim, 1989b] Ibrahim, A.S., Hogg, B.W., and Sharaf, M.M., " Self-tuning Automatic Voltage Regulators for a Synchronous Generator", *IEE Proc., 136, Pt. D(5), pp.252-260*, September 1989.

[IEEE, 1978] IEEE Power Generation Committee of IEEE Power Engineering Society, *An American National Standard IEEE Guide for Identification, Test-*

ing, and Evaluation of the Dynamic Performance of Excitation Control Systems, The Institute of Electrical and Electronics Engineers, Inc., 1978.

[Itoh, 1987] Itoh, O., Gotoh, K., Nakayama, T., and Takamizawa, S., " Application of Fuzzy Control to Activated Sludge Process, " Proc. 2nd IFSA Congress, Tokyo, Japan, pp.282-285, July 1987.

[Kanniah, 1984a] Kanniah, J., Malik, O.P., and Hope, G.S. "Microprocessor Based Universal Regulator Using Dual Rate Sampling". *IEEE Trans. on Industrial Electronics, Vol. IE-31, No.4, pp.306-312*, November 1984.

[Kanniah, 1984b] Kanniah, J., Malik, O.P., and Hope, G.S. " Excitation Control of Synchronous Generators Using Adaptive Regulators Part I-Theory and Simulation Results " *IEEE Transactions on Power Apparatus and Systems, Vol. PAS-103, No.5, pp. 897-903*, May 1984.

[Kanniah, 1984c] Kanniah, J., Malik, O.P., and Hope, G.S. " Excitation Control of Synchronous Generators Using Adaptive Regulators Part II-Implementation and test results" *IEEE Transactions on Power Apparatus and Systems, Vol. PAS-103, No.5, pp. 904-910*, May 1984.

[Kasai, 1988] Kasai, Y., and Morimoto, Y., "Electronically Controlled Continuously Variable Transmission, " *Proc Int. Congress on Transportation Electronics, Dearborn, MI*, 1988.

[Keay, 1971] Keay, F.W., South, W.H., "Design of a Power System Stabilizer Sensing Frequency Deviation ", *IEEE Transactions on Power Apparatus and Systems, Vol. PAS-90, pp.705-713*, March/April 1971.

[Kickert, 1976] Kickert, W.J.M., and Van Nauta Lemke, H.R., "Application of a Fuzzy Control in a Warm Water Plant", *Automatica, Vol.12, pp.301-308*, 1976.

[Klein, 1991] Klein, M., Roger, G.J., and Kundur, P. "A Fundamental Study of Inter-area Oscillations in Power Systems ". *IEEE Transactions on Power Systems, Vol.6, No.3, pp.914-921*, August 1991.

[Klopfenstein, 1971] Klopfenstein, A. "Experience with system stability controls on the generation of the southern California Edison Co." *IEEE Trans. PAS-90, pp. 698-706*, 1971.

[Kosko, 1986] Kosko, B., "Differential Hebbian Learning," *Proceedings American Institute of Physics: Neural Networks for Computing, pp. 277-282*, April, 1986.

[Kosko, 1992] Kosko, Bart. *Neural Networks and Fuzzy Systems: A Dynamical Systems Approach To Machine Intelligence.* Prentice Hall, Englewood Cliffs, 1992.

[Kundur, 1989] Kundur, P., Klein, M., Rogers, G.J., and Zywno, M.S. "Application of Power System Stabilisers for enhancement of Overall Power System Stability", *IEEE Transactions on Power Systems, Vol.4, No.2, pp.614-624*, 1989.

[Larsen, 1980] Larsen, P.M., "Industrial Applications of Fuzzy Logic Control",*Int. J. Man Machine Studies, Vol.12, pp.3-10*, 1980.

[Larsen, 1981] Larsen, E.V., and Swann, D.A. "Applying Power System Stabilizers". *IEEE Trans. PAS-100, pp. 3017-3046*, 1981.

[Laughton, 1966] Laughton, M.A. "Matrix Analysis of Dynamic Stability in Synchronous Multimachine Systems", *PROC. IEE, Vol. 113, No. 2, pp.325-336*, February 1966.

[Ledwich, 1979] Ledwich, G., "Adaptive Excitation Control", *IEE Proc., 126(3): pp.249-253*, March 1979.

[Lee, 1981] Lee, D.C., Beaulieu, R.E., and Service, J.R.R., " A Power System Stabilizer Using Speed and Electrical Power Inputs-Design and Field Experience", *IEEE Trans. Power Appratus and Systems, PAS-100, No.9, pp.4151-4157*, September 1981.

[Lee, 1990a] Lee, C.C., "Fuzzy Logic in Control Systems: Fuzzy Logic Controller-Part I",*IEEE Trans. Syst.Man Cybern., Vol.SMC-20,No.2 pp. 404-418*, 1990.

[Lee, 1990b] Lee, C.C., "Fuzzy Logic in Control Systems: Fuzzy Logic Controller-Part II",*IEEE Trans. Syst.Man Cybern., Vol.SMC-20,No.2 pp. 419-435*, 1990.

[Lim, 1989] Lim, C.M. "A self-tuning stabiliser for Excitation or Governor Control of Power Systems ". *IEEE Transactions on Energy Conversion, Vol.4, No.2, pp.152-159*, June 1989.

[Lim, 1990] Lim, C.M., and Hiyama, T., "Self-tuning Control Scheme for Stability Enhancement of Multimachine POwer Systems", *IEE Proc., 137, Pt. C(4), pp.269-275*, July 1990.

[Lim, 1992] Lim, C.M., and Hiyama, T., "A New Fuzzy Logic Control Scheme for Stability Enhancement of Power Systems", *Asia-Pacific Engineering Journal (Part A), Vol.2, No. 1 pp. 63-84*, 1992.

[Lim, 1993] Lim, C.M., Hiyama, T., "Comparison Study Between A Fuzzy Logic Stabiliser and A Self-tuning Stabiliser ". *Computers in Industry, Elsevier Science Publisher, 21, pp. 199-215*, 1993.

[Lim, 1990] Lim, M., and Takefuji, Y., "Implementing Fuzzy Rule-Based Systems on Silicon Chips," *IEEE Expert 5, pp.31-45*, 1990.

[Maiers, 1985] Maiers, J., and Sherif, Y.S., "Application of Fuzzy Set Theory," *IEEE Trans. Syst. Man Cybern. SMC-15, PP.175-189*, 1985.

[Mamdani, 1975] Mamdani, E.H., and Assilian, S., "An experiment in linguistic synthesis with a fuzzy logic controller". *Inter. J. Man-Mach. Studies 7. pp. 1-13*, 1975.

[Mamdani, 1986] Mamdani, E.H., and Efstathiou, H.J., *Expert Systems and Optimisation in Process Control*, Unicorn series, Technical Press, Aldershot, 1986.

[Manzoul, 1992] Manzoul, M.A., and Jayabharathi, D., "Fuzzy Controllers on FPGA," *Proc. IEEE International Conf. on Fuzzy Systems, San Diego, CA, pp.348-353*, March 1992.

[Mao, 1990a] Mao, C., Prakash, K.S., Malik, O.P., Hope, G.S., and Fan, J., " Implementation and Laboratory Test Results for an Adaptive Power System Stabilizer Based on Linear Optimal Control", *IEEE/PES 1990 Summer Meeting, 90 SM 427-5 EC*, July 1990.

[Mao, 1990b] Mao, C., Malik, O.P., Hope, G.S., and Fan, J., " An Adaptive Generator Excitation Controller Based On Linear Optimal Control", *IEEE/PES 1990 Summer Meeting, 90 SM 425-9, EC*, July 1990.

[Mao, 1992] Mao, C.X., Malik, O.P., and Hope, G.S. "Studies of Real-time Adaptive Optimal Excitation Controller and Adaptive Optimal Power System Stabilizer". *IEEE Transactions on Energy Conversion, Vol.7, No.3, pp.598-605*, September 1992.

[Matsuki, 1991] Matsuki, J., and Okada, T., "Design and Test of Fuzzy Controller for Power System Stabilization ", *IFAC Computer Aided Design in Control Systems, Swansea, UK, pp.405-410*, 1991.

[Motorola Inc., 1992] Motorola Inc., Fuzzy Logic Educational Program, Center for Emerging Computer Technologies, 1992.

[Norum, 1993] Norum, W.E., and Bollinger, K.E., "Lab and Field Tests of a Self-tuning Power System Stabilizer", *IEEE Trans. Energy Conversion, Vol. 8, No. 3, pp. 476-483*, September 1993.

[Ogata, 1987] Ogata, K., *Discrete-time Control Systems*, Prentice-Hall, Inc.. Englewood Cliffs, New Jersey, 1987.

[Ostojic, 1990] Ostojic, D., and Kovacevic, B., "On the Eigenvalue Control of Electromechanical Oscillations by Adaptive Power System Stabilizer", *IEEE Trans. Power Systems, PWRS-5(4), pp.1118-1126*, November 1990.

[Pahalawaththa, 1991] Pahalawaththa, N.C., Hope, G.S., and Malik, O.P., "MIMO Self-tuning Power System Stabilizer", *Int. J. Control, 54(4), pp.815-829*, October 1991.

[Pedrycz, 1989] Pedrycz, Witold. *Fuzzy Control and Fuzzy Systems*, Research Studies Press LTD, Jhon Wiley and Son's INC. 1989.

[Pierre, 1987] Pierre, D.A., "A Perspective on Adaptive Control of Power Systems", *IEEE Trans. Power Systems, PWRS-2(2), pp.387-396*, May 1987.

[Procyk, 1979] Procyk, T.J., and Mamdani, E.H., "A Linguistic Self-organizing Process Controller", *Automatica, Vol. 15, No. 1, pp.15-30,* 1979.

[Rafian, 1987] Rafian,M., "Real-time power system simulation", *IEE Proc., 134, Pt.C(3): pp.206-223*, May 1987.

[Reznik and Shi, 1993] Reznik, L., and Shi, J. "Simulation Study of the Choice of a Membership Function Model for Control Applications", *The 2nd International Conference on Modelling and Simulation, Melbourne, Australia, Vol.1, pp.209-217*, 12-14 July 1993.

[Romero, 1986] Romero, D.R., and Heydt, G.T., "An Adaptive Excitation System Controller in a Stochastic Enviroment", *IEEE Trans. Power Systems, PWRS-1(1), pp.168-175*, February 1986.

[Runtz, 1973] Runtz, K.J., et al. "Digital Control Scheme for a Generating Unit". *IEEE Trans. PAS-92, pp. 478-483*, 1973.

[Schleif, 1966] Schleif, F.R., and White, J.H. "Damping for the northwest-southwest tieline oscillations-An analog study". *IEEE Trans. PAS-85, pp. 1239-1247*, 1966.

[Schleif, 1967] Schleif, F.R., Martin, G.E., and Angell, R.R. "Damping of system oscillations with a hydrogenerating unit". *IEEE Trans. PAS-86, pp. 438-442*, 1967.

[Schleif, 1968] Schleif, F.R., Hunkins, H.D., Martin, G.E., and Hatten, E.E. "Excitation control to improve power line stability". *IEEE Trans. PAS-87, pp. 1426-1434*, 1968.

[Schleif, 1969] Schleif, F.R., Hunkins, H.D., Hattan, E.E., and Gish, W.B. "Control of rotating exciters for power system damping: Pilot applications and experience". *IEEE Trans. PAS-88, pp. 1259-1266*, 1969.

[Seifi, 1990] Seifi, H., Hughes, F.M., and Shuttleworth, R., "Adaptive Power System Stabilizer Using a Bang-bang Pole-placement Strategy", *Int. J. Control, 51(1), pp.33-50]*, January 1990.

[Sen Gupta, 1985] Sen Gupta, D.P., Narahari, N.G., Boyd, I., and Hogg, B.W., "An Adaptive Power-System Stabiliser which Cancels the Negtive Damping Torque of a Synchronous Generator", *IEE Proc., 132, Pt. C(3), pp.109-117*, May 1985.

[Sheirah, 1979] Sheirah, M.A.H., Malik, O.P., and Hope, G.S., "A Self-tuning Automatic Voltage Regulator", *Electric Power Systems Research, 2(3): pp.199-213*, November 1979.

[Shier, 1968] Shier, R.M., and Blythe, A.L. "Field tests of dynamic stability using a stabilizing signal and computer program verification".*IEEE Trans. PAS-87, pp.315-322*, 1968.

[Sugeno, 1984] Sugeno, M., and Murakami, K., "An Experimental Study on Fuzzy Parking Control Using a Model Car", *Proc. of the 23rd IEEE Conf. on Decision and Control, Las Vegas*, 1984.

[Sugeno, 1985a] Sugeno, M., *Industrial Applications of Fuzzy Control*, Amsterdam, New York, 1985a.

[Sugeno, 1985b] Sugeno, M., "An introductory survey of fuzzy control ". *Information sci. 36, pp. 59-83*, 1985b.

[Takagi, 1983] Takagi, T., and Sugeno, M., "Derivation of Fuzzy Control Rules from Human Operators Control Actions", *Proc IFAC Symp. Fuzzy Info. Know. Represent. and Decision Anayl. France. pp.55-60*, 1983.

[Tang, 1987] Tang, K.L., and Mulholland, R.J., "Comparing Fuzzy Logic with Classical Controller Designs ", *IEEE Trans., SMC-17, pp. 1085-1087*, 1987.

[Tilgen, 1991] Tilgen User's Manual, Togai Infralogic Inc. 1991.

[Tilshell, 1991] Tilshell+ User's Manual, Togai Infralogic Inc. 1991.

[Trankle, 1985] Trankle, T.L., and Markosian, L.Z., "An Expert System for Control System Design", *Proc. IEE 2nd Int. Conf. Control, Cambrige UK, pp.495-499*, 1985.

[Tuma, 1979] Tuma, J.J., *Engineering Mathematics Handbook*, McGraw-Hill Book Company, Second, Enlarged and Revised Edition, 1979.

[Ula, 1992] Ula, A.H.M.S., and Hasan, Abul R. "Design and Implementation of A Personal Computer Based Automatic Voltage Regulator For a Synchronous Generator ". *IEEE Transactions on Energy Conversion, Vol.7, No.1, pp.125-131*, March 1992.

[Vaahedi, 1986] Vaahedi, E., Noble, A.D., and Macdonald, D.C., "Generator On-line State Estimation and Optimal Control: Laboratory Implementation and Prospects for Development ", *IEEE Transactions on Energy Conversion, Vol. EC-1, No.3, pp.55-60*, 1986.

[Wang, 1992] Wang, L.X., and Mendel, J.M., "Generating Fuzzy Rules by Learning from Examples", *IEEE Transactions on Systems, Man, and Cybernetics, Vol. 22, No. 6, pp.1414-1427*, November/December 1992.

[Warchol, 1971] Warchol, E.J., Schleif, F.R., Gish, W.B., and Church, J.R. "Alinement and modeling of Hanford Excitation Control for System Damping". *IEEE Trans. PAS-90, pp.714-724*, 1971.

[Wood, 1984] Wood, A.J., and Wollenberg, B.F., *Power Generation, Operation and Control*, John Wiley and Sons, 1984.

[Wu, 1986] Wu, C.J., and Hsu, Y.Y. "Self-tuning excitation control for synchronous machine". *IEEE Trans. AES-22, pp. 389-394*, 1986.

[Wu, 1988] Wu, Chi-Jui, Hsu, Yuan-Yih. "Design of Self-tuning PID Power System Stabilizer for Multimachine Power Systems ". *IEEE Transactions on Power Systems, Vol.3, No.3, pp.1059-1064*, August 1988.

[Wu, 1988] Wu, Q.H., and Hogg, B.W., "Robust Self-tuning Regulator for a Synchronous Generator", *IEE Proc., 135, Pt. D (6), pp. 463-473*, November 1988.

[Wu, 1990] Wu, Q.H., and Hogg, B.W., "Self-tuning Control for Turbogenerators in Multi-machine Power Systems", *IEE Proc., 137, Pt. C(2), pp.146-158*, March 1990.

[Wu, 1991] Wu, Q.H., and Hogg, B.W., "Laboratory Evaluation of Adaptive Controllers for Synchronous Generators", *Automatica, 27(5),pp.845-852*, September 1991.

[Xia, 1983] Xia, D., and Heydt, G.T., "Self-tuning Controller for Generator Excitation Control",*IEEE Trans. Power Apparatus and Systems, PAS-102(6), pp.1877-1885*, June 1983.

[Yagishita, 1985] Yagishita, O., Itoh, O., and Sugeno, M., "Application of Fuzzy Reasoning to the Water Purification Process", *Industrial Application of Fuzzy Control, Sugeno, M., Ed. Amsterdam: North-Holland, pp. 19-40*, 1985.

[Yamakawa, 1986a] Yamakawa, T., "High Speed Fuzzy Controller Hardware System", *Proc. 2nd Fuzzy System Symp., Japan, pp.122-130*, 1986.

[Yamakawa, 1986b] Yamakawa, T., and Miki, T., "The Current Mode Fuzzy Logic Integrated Circuits Fabricated by the Standard CMOS Process ", *IEEE Trans. Computer, Vol. C-35, No. 2, pp. 161-167*, 1986.

[Yamakawa, 1987a] Yamakawa, T., "Fuzzy Controller Hardware System", *Proc. 2nd IFSA Congress, Tokyo, Japan*, July 1987.

[Yamakawa, 1987b] Yamakawa, T., "A Simple Fuzzy Computer Hardware System Employing Min and Max Operations–A Challenge to 6th Generation Computer," *Proc. 2nd IFSA Congress, Tokyo, Japan*, July 1987.

[Yamakawa, 1987c] Yamakawa, T., "Fuzzy Hardware Systems of Tomorrow in Approximate Reasoning in Intelligent Systems," *Decision and Control, eds. Sanchez, E., and Zadeh, L.A., pp.1-20, New York, Pergamon*, 1987.

[Yamakawa, 1988] Yamakawa, T., "Fuzzy Microprocessors-Rule Chip and Defuzzifier Chip ", *Int. Workshop on Fuzzy System Applications, Iizuka, Japan, pp.51-52*, August 1988.

[Yasunobu, 1983] Yasunobu, S., Miyamoto, S., and Ihara, H., "Fuzzy Control for Automatic Train Operation System," *Proc. 4th IFAC/IFIP/IFORS Int. Congress on Control in Transportation Systems, Baden*, April 1983.

[Yasunobu, 1985] Yasunobu, S., and Miyamoto, S., "Automatic Train Operation by Predictive Fuzzy Control", *Industrial Application of Fuzzy Control, Sugeno, M., Ed. Amsterdam: North-Holland, pp. 1-18*, 1985.

[Yasunobu, 1986] Yasunobu, S., and Hasegawa, T., "Evaluation of an Automatic Container Crane Operation System Based on Predictive Fuzzy Control", *Control Theory Adv. Technol, Vol. 2, No. 3, pp.419-432*, 1986.

[Yu, 1971] Yu, Y.N., Moussa, H.A.M., "Optimal Power System Stabilization through Excitation and/or Governor Control ". *IEEE Transactions on Power Apparatus and Systems, Vol. PAS-90, pp. 1166-1173*, 1971.

[Yu, 1983] Yu, Y.N., *Electric Power System Dynamics.* Academic Press, 1983.

[Zadeh, 1965] Zadeh, L.A., "Fuzzy sets". *Information and Control 8, pp. 338-353*, 1965.

[Zadeh, 1973] Zadeh, L.A., "Outline of a New Approach to the Analysis Complex Systems and Decision Processes ". *IEEE Trans. Syst. Man Cybern., Vol. SMC-3, pp. 28-44,* 1973.

[Zadeh, 1988] Zadeh, L.A., "Fuzzy Logic", *IEEE Comput. 21, pp.83-92*, 1988.

[Zimmermann, 1990] Zimmermann, H.J. *Fuzzy Set Theory and Its Applications.* Kluwer-Nijhoff Publishing Company, 1990.

Appendix G

Turbo Pascal Source Code For Single-Machine Infinite Bus Power System

```
Program response(Input,Output);
uses crt,dos,auxinout,dt2801,scrnplt5;



Const
        dtconv=204.8;
        number_points=800;
        norm_color=red;
        chan=0;
        chan1=1;
        chan2=2;
        chan3=3;
        chan4=4;
        alt_color=cyan;
        console : boolean = false;
        print : boolean = true;
        car_ret = ^M;
        NormalTimer=0; {Constants for interrupt}
        OneMillisecond=1179;
        TenMillisecond=11790;
        TimerInt=$08;
        type
              line_string=string[70];
              output_array=array[1..number_points] of real;
              string19=string[19];
Var
{ Variables for main program }
      v_out:output_array;
      control_array,power_array,speed_array:output_array;
      angle_array,angle1_array,time_array:output_array;
      inerror,outerror:array [1..2] of byte;
      op_dev : text;
```

```
    repeatprocess,first_time,returnmenu,quit_f :boolean;
    voltage,current,voltage1,uk,uk_1,plant_output,control_output, uf,uf_1 :real;
    plus,rnum,xmax,ymin,ymax,sample_time,timer,power_facter :real;
    plant_input,plant_input1,ref,error_signal,umax,umin,e_array_1,e_array : real;
    angle,angle_0,angle_1,op,op_1,ip,angle_old,angular_speed_1,angular_speed :real;
    pss,pss_1,pss_2,pss_3,speed,speed_1,a_speed,a_speed_1,a_speed_2,a_speed_3:real;
    number_waits,wait,temp,index,IDX,IDY,da_data,da_data1,i,ad_data,count :integer;
    ad_data1,ad_data2,ad_data3 :integer;
    uk_2,uk_3,uk_4,uk_5,uk_6,uk_7,uk_8,uk_9,uk_10,uk_11,uk_12 :real;
    e,e_1,e_2,e_3,e_4,e_5,e_6,e_7,e_8,e_9,e_10,e_11,e_12, angular_speed1 :real;
    ask,kb_char,reply :char;
    Dr,Dk,Gk,Us,Pk,Usmax,acce,theta,x,y,power_voltage,power_current,power_angle :real;
    op_6,op_5, op_4,op_3,op_2,ip_6,ip_5,ip_4,ip_3,ip_2,ip_1,: real;
    uf_4,uf_3,uf_2: real;
    plant_input4,plant_input3,plant_input2 :real;
    anguspeed,anguspeed_1,anguspeed_2,anguspeed_3,anguspeed_4: real;
    speed_4,speed_3,speed_2:real;
    outf :text;
    Clicks: Word; { For interrupt Procedure}
    OldVector: Pointer;
    key: Char;
{.PA}
{***********************Procedure for Interrupt *********************}
Procedure TimerClick ;Interrupt;
Var
    Regs: Registers;
Begin
      Inc(Clicks);
      port[$20]:=$20;
End;
Procedure SetTimerPeriod (N : Word);
Var
```

```
    A:Integer;
Begin
      port[$43]:=$36;
      Inc(A);
      Port[$40]:=Lo (N);
      Inc(A);
      Port[$40]:=Hi (N);
End;
Procedure InitTimer;
Begin
      GetIntVec(TimerInt,OldVector);
      SetIntVec(TimerInt,@TimerClick);
      SetTimerPeriod (OneMilliSecond);
      Clicks:=0;
End;
Procedure RestoreTimer;
Begin
      SetTimerPeriod (NormalTimer);
      SetIntVec(TimerInt,Oldvector);
End;
{ ************ Read Analog Voltage From Specified Channel ************* }
Procedure ad_read;
var
    ad_data,ad_data1,ad_data2,ad_data3,m,status,gain,dummy:integer;
    ad_data4,chan,chan1,chan2,chan3,chan4: integer;
begin
      chan:=0;
      chan1:=1;
      chan2:=2;
      chan3:=3;
      chan4:=4;
      gain:=0;
```

```
    dummy:=0;
    adstp;
    rdadi(gain,chan,ad_data,status); {channel 0 terminal voltage}
    rdadi(gain,chan1,ad_data1,status); {channel 1 rotor angle}
    rdadi(gain,chan2,ad_data2,status); {channel 2 voltage}
    rdadi(gain,chan3,ad_data3,status); {channel 3 current}
    rdadi(gain,chan4,ad_data4,status); {channel 4 power angle}
    voltage:=ad_data/204.8; {convert digital voltage to analoge}
    plant_output:=voltage/5; {convert to refence voltage, (400v:5v)}
    ip:=ad_data1/204.8;
    op:=1.627*op_1-1.89031*op_2+1.07761*op_3-0.46637*op_4+0.08469*op_5
    -0.0123*op_6+0.0550073*(ip+1.0491*ip_1+2.19433*ip_2+2.05156*ip_3
    +2.19433*ip_4+1.0491*ip_5+1*ip_6);
    op_6:=op_5;
    op_5:=op_4;
    op_4:=op_3; {use 6th order Chebyshev_I filter to filter from angle signal}
    op_3:=op_2;
    op_2:=op_1;
    op_1:=op;
    ip_6:=ip_5;
    ip_5:=ip_4;
    ip_4:=ip_3;
    ip_3:=ip_2;
    ip_2:=ip_1;
    ip_1:=ip;
    angle:=op;
    speed:=(angle-angle_1)/(0.025*314);{calculate speed from measured rotor angle}
    angle_1:=angle;
    power_voltage:=ad_data2/204.8;
    power_current:=ad_data3/204.8; {convert digital current to analogue}
    power_angle:=ad_data4/204.8;
end;
```

```
{**************Fuzzy Logic Based Power System Stabiliser ****************}
Procedure pssf;
begin
    Dr:=2:
    Usmax:=0.4;
    anguspeed:=1.0586*anguspeed_1-0.98622*anguspeed_2+0.389485*anguspeed_3
    -0.0789937*anguspeed_4+0.0385299*(speed+4*speed_1+6*speed_2
    +4*speed_3+speed_4);
    anguspeed_4:=anguspeed_3;
    {use 4th order Chebyshev_I filter to filter noise from angle signal}
    anguspeed_3:=anguspeed_2;
    anguspeed_2:=anguspeed_1;
    anguspeed_1:=anguspeed;
    speed_4:=speed_3;
    speed_3:=speed_2;
    speed_2:=speed_1;
    speed_1:=speed;
    angular_speed:=anguspeed;
    acce:=(angular_speed-angular_speed_1)/0.025; {calculate acceleration signal}
    Dk:=sqrt(angular_speed*angular_speed+acce*acce);
    if Dk≤Dr then Gk:=Dk/Dr
                  else Gk:=1;
    angular_speed_1:=angular_speed;
    x:=angular_speed;
    y:=acce;
    if x=0 then x:=0.0000001;
    if x≥0 then
                if y≥0 then theta:=arctan(y/x)
                else theta:=2*3.1415926+arctan(y/x);
    if x<0 then theta:=3.1415926+arctan(y/x);
    if theta≤1.658 then Pk:=0;
    if theta≤1.91986 then
```

```
                        if theta>1.658 then
                        Pk:=7.2951*(theta-1.658)*(theta-1.658);
    if theta≤2.18166 then
                        if theta>1.91986 then
                        Pk:=1-7.2951*(theta-2.18166)*(theta-2.18166);
    if theta≤4.7996 then
                       if theta>2.18166 then Pk:=1;
    if theta≤5.06145 then
                        if theta>4.7996 then
                        Pk:=1-7.2951*(theta-4.7996)*(theta-4.7996);
    if theta≤5.32325 then
                        if theta>5.06145 then
                        Pk:=7.2951*(theta-5.32325)*(theta-5.32325);
    if theta>5.32325 then Pk:=0;
    Us:=Gk*Usmax*(1-2*Pk);
    pss:=Us;
end;
{******************** Automatic Voltage Regulator ********************}
Procedure controller;
begin
    error_signal:=ref+pss-plant_output;
    e:=error_signal;
    plant_input:=(0.1467*uk_1)+(0.1304*uk_2)+(0.1160*uk_3)+(0.1031*uk_4)
    +(0.0917*uk_5)+(0.0815*uk_6)+(0.0725*uk_7)+(0.0644*uk_8)
    +(0.0573*uk_9)+(0.0509*uk_10)+(0.0453*uk_11)+(0.0402*uk_12)
    +50*((5.0586*e)+(0*e_1)+(0*e_2)+(0*e_3)+(0*e_4)
    +(0*e_5)+(0*e_6)+(0*e_7)+(0*e_8)+(0*e_9)
    +(0*e_10)+(0*e_11)+(-1.2345*e_12));
    uk:=plant_input;
    uk_12:=uk_11;
    uk_11:=uk_10;
    uk_10:=uk_9;
```

```
        uk_9:=uk_8;
        uk_8:=uk_7;
        uk_7:=uk_6;
        uk_6:=uk_5;
        uk_5:=uk_4;
        uk_4:=uk_3;
        uk_3:=uk_2;
        uk_2:=uk_1;
        uk_1:=uk;
        e_12:=e_11;
        e_11:=e_10;
        e_10:=e_9;
        e_9:=e_8;
        e_8:=e_7;
        e_7:=e_6;
        e_6:=e_5;
        e_5:=e_4;
        e_4:=e_3;
        e_3:=e_2;
        e_2:=e_1;
        e_1:=e;
        if(uk≥9.9) then uk:=9.9; {DT2801 A/D and D/A converter limit 10}
        if(uk≤-9.9)then uk:=-9.9;
end;
{ **************Output an Analog Voltage on Specified Channel **************}
Procedure da_write;
var
     chan,dummy,status :integer;
begin
        chan:=0;
        control_output:=uk*204.8;
        da_data:=round(control_output); {convert analog to digital}
```

```
        wrdai(chan,da_data,dummy,status);
end;
Procedure da_write1;
var
     chan1,dummy,status :integer;
begin
        chan1:=1;
        for i:=1 to 10 do
            begin
            plus:=5*204.8;
            da_data1:=round(plus);
            wrdai(chan1,da_data1,dummy,status);
            end;
end;
Procedure da_write0;
var
     chan1,dummy,status :integer;
begin
        chan1:=1;
        for i:=1 to 10 do
            begin
            plus:=0*204.8;
            da_data1:=round(plus);
            wrdai(chan1,da_data1,dummy,status);
            end;
end;
{******************************** Scale ********************************}
Procedure testr;
var
    xply,rtmp:real;
    icnt:integer;
begin
```

```
    icnt:=0;
    xply:=0.1;
    while rnum>0.001 do
    begin
        rnum:=rnum*xply;
        icnt:=icnt+1;
    end;
    rtmp:=0.001;
    if(rnum>0.0001)then rtmp:=0.0002;
    if(rnum>0.0002)then rtmp:=0.00025;
    if(rnum>0.00025)then rtmp:=0.0005;
    if(rnum>0.0005)then rtmp:=0.001;
    if(icnt>0) then
            begin
                for index:=1 to icnt do
                rtmp:=rtmp/xply;
                rnum:=rtmp;
            end
            else
            rnum:=rtmp;
end; {testr}
{****************************************************************}
Procedure graphresults;
begin
    clearplotdata;
    plotlabel('time (sec)','plant output','System Response');
    plotdata(time_array,v_out,number_points,curve);
    plotdata(time_array,control_array,number_points,curve);
    plotdata(time_array,angle_array,number_points,curve);
    plotdata(time_array,power_array,number_points,curve);
    plotdata(time_array,speed_array,number_points,curve);
    plotgraph;
```

```
end;
Procedure hardcopy;
var
    xfactor,yfactor,scalex,scaley,adds,increment:real;
    ix,iy,increm,itemp,ixtk,yup,ydn,ilim,ixof,iyof,i,xx,yy:integer;
    iyy :integer;
    xact,yact :real;
    iend:char;
    com1:text;
begin
    assignaux(com1,0,$E7);
    rewrite(com1);
    xfactor:=9000/xmax; {scale factor for Hp}
    yfactor:=7000/(ymax-ymin);
    ix:=1000; {seems good place for origin}
    iy:=1000-round(ymin*yfactor);
    scalex:=800/xfactor; {find scale value for 2cm}
    rnum:=scalex; { get nice number for scale}
    testr;
    scalex:=rnum;
    scaley:=800/yfactor;
    rnum:=scaley;
    testr;
    scaley:=rnum;
    writeln(com1,'IN;SP1;PAPU',ix,',',iy,';'); {start plotter}
    increm:=400; { 1 cm ticks}
    itemp:=ix;
    ixtk:=0;
    repeat
        writeln(com1,'PRPD',increm,',0,XT;'); {plot x axis with ticks}
        itemp:=itemp+increm;
        ixtk:=ixtk+1;
```

```
until (itemp≥9300);
itemp:=iy;
yup:=0;
writeln(com1,'PAPU',ix,',',iy,';'); { return pen to origin}
repeat
    writeln(com1,'PRPD0,',increm,'YT;'); { positive y axis now}
    itemp:=itemp+increm;
    yup:=yup+1;
until (itemp≥7500);
writeln(com1,'PAPU',ix,',',iy,';');
itemp:=iy;
ydn:=0;
increm:=-400;
repeat
    writeln(com1,'PRPD0,',increm,'YT;'); {negative y axis}
    itemp:=itemp+increm;
    ydn:=ydn+1;
until (itemp≤2000);
iend:=char(3);
xact:=scalex;
yact:=scaley;
writeln(com1,'PAPU',ix,',',iy,';SI;DI0,1;'); {start printing scale}
iyof:=iy-720;
increm:=800;
ilim:=round(ixtk/2 -1);
if (ixtk>2) then
begin
    for i:=1 to ilim do
    begin
        ixof:=ix+(i*increm)+40;
        writeln(com1,'PAPU',ixof,',',iyof,';LB',xact:4:2,iend);
        xact:=xact+scalex;
```

```
        end;
    end;
    ixof:=ix-750;
    writeln(com1,'DI1,0;');
    ilim:=round(yup/2);
    if (yup>2)then
    begin
        for i:=1 to ilim do
        begin
            iyof:=(increm*i)+iy-40;
            writeln(com1,'PAPU',ixof,',',iyof,';LB',yact:4:2,iend);
            yact:=yact+scaley;
        end;
    end;
    yact:=-scaley;
    ilim:=round(ydn/2);
    if (ydn>2)then
    begin
        for i:=1 to ilim do
        begin
            iyof:=iy-(increm*i)-40;
            writeln(com1,'PAPU',ixof,',',iyof,';LB',yact:4:2,iend);
            yact:=yact-scaley;
        end;
    end;
    writeln(com1,'PAPU',ixof,',',iy,';LB 0.00',iend);
    writeln(com1,'PAPU5000,7000;
        LB SYSTEM RESPONSE WITH AVR AND PSS',iend);
    iyy:=iy+round(800/scaley*v_out[1]);
    writeln(com1,'SP2;PAPU',ix,',',iyy);
    for i:=1 to number_points do
    begin
```

```
        xx:=ix+round(800/scalex * time_array[i]);
        yy:=iy+round(800/scaley * v_out[i]);
        writeln(com1,'PAPD',xx,',',yy,';');
        increment:=increment+adds;
    end;
    iyy:=iy+round(800/scaley*control_array[1]);
    writeln(com1,'SP3;PAPU',ix,',',iyy);
    for i:=1 to number_points do
    begin
        xx:=ix+round(800/scalex * time_array[i]);
        yy:=iy+round(800/scaley * control_array[i]);
        writeln(com1,'PAPD',xx,',',yy,';');
        increment:=increment+adds;
    end;
    iyy:=iy+round(800/scaley*angle_array[1]);
    writeln(com1,'SP4;PAPU',ix,',',iyy);
    for i:=1 to number_points do
    begin
        xx:=ix+round(800/scalex * time_array[i]);
        yy:=iy+round(800/scaley * angle_array[i]);
        writeln(com1,'PAPD',xx,',',yy,';');
        increment:=increment+adds;
    end;
    iyy:=iy+round(800/scaley*power_array[1]);
    writeln(com1,'SP4;PAPU',ix,',',iyy);
    for i:=1 to number_points do
    begin
        xx:=ix+round(800/scalex * time_array[i]);
        yy:=iy+round(800/scaley * power_array[i]);
        writeln(com1,'PAPD',xx,',',yy,';');
        increment:=increment+adds;
    end;
```

```
    writeln(com1,'IN;PU,SP0;');
    close(com1);
end;
{*************************** Display Instructions *******************}
Procedure display_insts;
begin
    clrscr;
    textcolor(lightgray);
    gotoxy(20,5);write('<<<<<<        >>>>>>');
    gotoxy(20,6);write('<<<<<<        >>>>>>');
    gotoxy(20,7);write('<<<<<<        >>>>>>');
    gotoxy(28,5);
    textcolor(lightgreen);write('MEASUREMENT OF STEP RESPONSE');
    textcolor(green);
    gotoxy(28,7);write('Set_up Instructions for IBM');
    if first_time then
    begin
        textcolor(alt_color);
        gotoxy(20,12);write('[1]');
        textcolor(norm_color);
        write('connect system output to A/D channel 0,1 and 2');
        gotoxy(20,15);
        textcolor(alt_color);write('[2]');
        textcolor(norm_color);
        write(' connect D/A channel 0 to plant input');
        gotoxy(20,18);
        textcolor(alt_color);write('[3]');
        textcolor(norm_color);
        write(' press ENTER key to continue....');
        repeat
            kb_char:=readkey;
        until kb_char = car_ret;
```

```
            first_time := false;
        end;
        textcolor(yellow);
        clrscr;
        gotoxy(17,8);write('Sample time is 25 milliseconds ');
        gotoxy(17,10);
        write('Enter reference -> ');
        readln(ref);
        repeat
        gotoxy(17,18);
        write('Enter final time of plot, minimum is 5 secs -> ');
        readln(xmax);
        until xmax≥5.0 ;
        clrscr;
        gotoxy(15,17);writeln('WAIT - Response being measured ...');
        gotoxy(15,19);
        writeln('Press any key to perform sudden load change and collect data...');
end;
{display_insts}
{***************************Set Menu *****************************}
Procedure read_menu;
var
    kb_char : char;
begin
        repeatprocess := false;
        returnmenu := false;
        repeat
                kb_char:=readkey;
                kb_char := upcase(kb_char);
        until kb_char in ['G','Q','R','H'];
        case kb_char of
        'H': begin
```

```
                hardcopy;
                returnmenu := true;
                end;
        'R': repeatprocess := true;
        'Q': begin
                clrscr;
                end;
        'G': begin
                graphresults;
                clrscr;
                returnmenu := true;
                end;
        end;
end;
Procedure output_menu;
begin
        textcolor(lightgray);
        gotoxy(20,5);write('<<<<<< OUTPUT MENU >>>>>>');
        textcolor(red);
        gotoxy(20,8);write('G');textcolor(green);write('raph of results on screen');
        textcolor(red);
        gotoxy(20,10);write('H');textcolor(green);write('ardcopy of plot');
        textcolor(red);
        gotoxy(20,12);write('S');textcolor(green);write('creen listing of graph data');
        textcolor(red);
        gotoxy(20,14);write('P');textcolor(green);write('rinter listing of graph data');
        textcolor(red);
        gotoxy(20,16);write('R');textcolor(green);write('epeat test Procedure');
        textcolor(red);
        gotoxy(20,18);write('Q');textcolor(green);write('uit resp.com program');
        textcolor(lightgray);
        gotoxy(20,21); write('Enter highlighted letter option...');
```

```
        read_menu;
        textcolor(norm_color);
end;
{************************* Main Program *************************}
var
    status,dummy :integer;
Begin
        clrscr;
        writeln('Please wait for a while ...');
        delay(5000);
        InitTimer;
        assign(outf,'c:/tp/vflpss.shi');
        rewrite(outf);
        first_time := true;
        xmax :=5;
        repeat
                clrscr;
                ref:=0;
                ip_6:=0; ip_5:=0; ip_4:=0; ip_3:=0; ip_2:=0; ip:=0;
                op_6:=0; op_5:=0; op_4:=0; op_3:=0; op_2:=0; op_1:=0; op:=0;
                uf_4:=0;uf_3:=0;uf_2:=0;uf_1:=0;
                plant_input4:=0;plant_input3:=0;plant_input2:=0;plant_input1:=0;
                error_signal:=0;voltage:=0;
                speed:=0; speed_1:=0; speed_2:=0;speed_3:=0;speed_4:=0;
                anguspeed:=0; anguspeed_1:=0;anguspeed_2:=0;anguspeed_3:=0;
                anguspeed_4:=0; angular_speed:=0; angular_speed_1:=0;
                a_speed:=0; a_speed_1:=0; a_speed_2:=0; a_speed_3:=0;
                angle:=0; angle_0:=0; angle_1:=1;
                pss:=0; pss_1:=0; pss_2:=0; pss_3:=0;
                power_voltage:=0; power_current:=0; power_angle:=0;
                for i:=1 to number_points do
                begin
```

```
                v_out[i]:=0;
                control_array[i]:=0;
                angle_array[i]:=0;
                angle1_array[i]:=0;
                power_array[i]:=0;
                time_array[i]:=0;
                speed_array[i]:=0;
            end;
            uf:=0; uf_1:=0;
            plant_input1:=0;
            uk:=0; uk_1:=0; uk_2:=0; uk_3:=0; uk_4:=0; uk_5:=0; uk_6:=0;
            uk_7:=0; uk_8:=0; uk_9:=0; uk_10:=0; uk_11:=0; uk_12:=0;
            e:=0; e_1:=0; e_2:=0; e_3:=0; e_4:=0; e_5:=0; e_6:=0;
            e_7:=0; e_8:=0; e_9:=0; e_10:=0; e_11:=0; e_12:=0;
            acce:=0;
            angular_speed:=0; angular_speed_1:=0;
            Dr:=0; Dk:=0; Gk:=0; Us:=0; Pk:=0;
            theta:=0; x:=0; y:=0; plant_output:=0;
    display_insts;
    if clicks≥25 then
    begin
        Clicks:=0;
        ad_read;
        pssf;
        controller;
        da_write;
    end;
    repeat
    if clicks≥25 then
            clicks:=0;
            ad_read;
            pssf;
```

```
                    controller;
                    da_write;
        end;
        until keypressed;
        if clicks≥25 then
        begin
                clicks:=0;
                ad_read;
                pssf;
                controller;
                da_write;
                v_out[1]:=plant_output*5;
                power_facter:=cos(power_angle*3.14159/18);
                power_array[1]:=(3*power_current*power_voltage*power_facter)/10;
                control_array[1]:=uk;
                angle_array[1]:=angle;
                speed_array[1]:=angular_speed;
                time_array[1]:=0;
        end;
        for i:=2 to 200 do
            begin
                    repeat until clicks≥25;
                    clicks:=0;
                    ad_read;
                    pssf;
                    controller;
                    da_write;
                    v_out[i]:=plant_output*5;
                    power_facter:=cos(power_angle*3.14159/18);
                    power_array[i]:=(3*power_current*power_voltage*power_facter)/10;
                    control_array[i]:=uk;
                    angle_array[i]:=angle;
```

```
            speed_array[i]:=angular_speed;
            time_array[i]:=0.025+time_array[i-1];
    end;
da_write1; {produce signal to operate the relay}
for i:=201 to 500 do
    begin
            repeat until clicks≥25;
            clicks:=0;
            ad_read;
            pssf;
            controller;
            da_write;
            v_out[i]:=plant_output*5;
            power_facter:=cos(power_angle*3.14159/18);
            power_array[i]:=(3*power_current*power_voltage*power_facter)/10;
            control_array[i]:=uk;
            angle_array[i]:=angle;
            speed_array[i]:=angular_speed;
            time_array[i]:=0.025+time_array[i-1];
    end;
da_write0;
for i:=501 to number_points do
    begin
            repeat until clicks≥25;
            clicks:=0;
            ad_read;
            pssf;
            controller;
            da_write;
            v_out[i]:=plant_output*5;
            power_facter:=cos(power_angle*3.14159/18);
            power_array[i]:=(3*power_current*power_voltage*power_facter)/10;
```

```
                control_array[i]:=uk;
                angle_array[i]:=angle;
                speed_array[i]:=angular_speed;
                time_array[i]:=0.025+time_array[i-1];
        end;
    for i:=1 to 200 do
        begin
                repeat until clicks≥25;
                clicks:=0;
                ad_read;
                pssf;
                controller;
                da_write;
        end;
    RestoreTimer;
    for i:=1 to number_points do
        begin
                writeln(outf,time_array[i],' ',v_out[i],' ',control_array[i],' ',
                power_array[i],' ',angle_array[i],' ',speed_array[i]);
        end;
    ymax:=10;
    ymin:=-4;
    for index:=1 to number_points do
        begin
                if v_out[index]>ymax then ymax:=v_out[index];
                if v_out[index]<ymin then ymin:=v_out[index];
                if control_array[index]>ymax then
                ymax:=control_array[index];
                if control_array[index]<ymin then
                ymin:=control_array[index];
                if angle1_array[index]>ymax then
                ymax:=angle1_array[index];
```

```
            if angle1_array[index]<ymin then
            ymin:=angle1_array[index];
        end;
    if ymin>0 then ymin:=-4;
    repeatprocess := false;
    returnmenu := false;
    repeat
        clrscr;
        output_menu;
    until not returnmenu;
    until not repeatprocess;
    close(outf);
    RestoreTimer;
end.
```